

VOLUME 16 / September 2021

detritus

Multidisciplinary Journal for Waste Resources & Residues

Editor in Chief:
RAFFAELLO COSSU

detritusjournal.com

an official journal of:

iwwg
international waste working group


CISA



ISSN 2611-4135 / ISBN 9788862650779
DETRITUS - Multidisciplinary Journal for Waste Resources & Residues

Detritus is indexed in:

- Emerging Sources Citation Index (ESCI), Clarivate Analytics, Web of Science
- Scopus, Elsevier
- DOAJ Directory of Open Access Journals
- Google Scholar

Partner Universities:

- Faculty of Agriculture and Environmental Sciences, University of Rostock, Germany
- Waste Science & Technology, Department of Civil, Environmental and Natural Resources Engineering, Luleå University of Technology, Sweden
- School of Environment, Tsinghua University, Beijing, Cina
- Polytechnic Department of Engineering and Architecture, University of Udine, Italy

© 2021 CISA Publisher. All rights Reserved

The journal contents are available on the official website: www.detritusjournal.com

Open access articles under CC BY-NC-ND license (<http://creativecommons.org/licenses/by-nc-nd/4.0/>)

Legal head office: Cisa Publisher - Eurowaste Srl, Via Beato Pellegrino 23, 35137 Padova - Italy / www.cisapublisher.com

Graphics and layout: Elena Cossu, Anna Artuso - Studio Arcoplan, Padova / studio@arcoplan.it

Printed by Cleup, Padova, Italy

Front page photo credits: 'Your waste is their responsibility...' courtesy of Prabha Jayesh Patel, India - Waste to Photo 2015 / Sardinia Symposium

For subscription to printed version, advertising or other commercial opportunities please contact the Administration Office at administration@eurowaste.it

Papers should be submitted online at <https://mc04.manuscriptcentral.com/detritusjournal>

Instructions to authors may be found at <https://detritusjournal.com/guide-for-authors/>

For any enquiries and information please contact the Editorial Office at editorialoffice@detritusjournal.com

Registered at the Court of Padova on March 13, 2018 with No. 2457

www.detritusjournal.com

VOLUME 16 / September 2021

detrītus

Multidisciplinary Journal for Waste Resources & Residues

Editor in Chief:

RAFFAELLO COSSU

detrītusjournal.com

an official journal of:

iwwg
international waste working group


CISA



Detritus - Multidisciplinary Journal for Waste Resources and Residues - is aimed at extending the "waste" concept by opening up the field to other waste-related disciplines (e.g. earth science, applied microbiology, environmental science, architecture, art, law, etc.) welcoming strategic, review and opinion papers. **Detritus is indexed in Emerging Sources Citation Index (ESCI) Web of Science, Scopus, Elsevier, DOAJ Directory of Open Access Journals and Google Scholar.** Detritus is an official journal of IWWG (International Waste Working Group), a non-profit organisation established in 2002 to serve as a forum for the scientific and professional community and to respond to a need for the international promotion and dissemination of new developments in the waste management industry.

EDITOR-IN-CHIEF:

Raffaello Cossu, University of Padova, Italy
E-mail: raffaello.cossu@unipd.it

ASSOCIATE EDITORS:

Damià Barcelo, ICRA Catalan Institute for Water Research, Spain
E-mail: damia.barcelo@idaea.csic.es

Jutta Gutberlet, University of Victoria, Canada
E-mail: gutber@uvic.ca

Pierre Hennebert, INERIS, France
E-mail: pierre.hennebert@ineris.fr

Ole Hjelmar, Danish Waste Solutions ApS
E-mail: oh@danws.dk

Uta Krogmann, Rutgers University, USA
E-mail: krogmann@rutgers.edu

Anders Lagerkvist, Lulea University of Technology, Sweden
E-mail: anders.lagerkvist@ltu.se

Michael Nelles, University of Rostock, Germany
E-mail: michael.nelles@uni-rostock.de

Abdul-Sattar Nizami, King Abdulaziz University, Saudi Arabia
E-mail: nizami_pk@yahoo.com

Mohamed Osmani, Loughborough University, United Kingdom
E-mail: m.osmani@lboro.ac.uk

Alessandra Poletti, University of Rome "La Sapienza", Italy
E-mail: alessandra.poletti@uniroma1.it

Marco Ritzkowski, TuTech Innovation GmbH, Germany
E-mail: m.ritzkowski@tuhh.de

Howard Robinson, Phoenix Engineering, United Kingdom
E-mail: howardrRobinson@phoenix-engineers.co.uk

Rainer Stegmann, TuTech Innovation GmbH, Germany
E-mail: stegmann@tuhh.de

Ian Williams, University of Southampton, United Kingdom
E-mail: i.d.Williams@soton.ac.uk

Jonathan Wong, Hong Kong Baptist University, Hong Kong
E-mail: jwcwong@hkbu.edu.hk

Haoran Yuan, Guang Zhou Institute of Energy Conversion, Chinese Academy of Sciences, China
E-mail: yuanhr@ms.giec.ac.cn

Liangtong Tony Zhan, Zhejiang University, China
E-mail: zhanlt@zju.edu.cn

Christian Zurbrugg, Eawag/Sandec, Switzerland
E-mail: christian.zurbrugg@eawag.ch

EDITORIAL OFFICE:

Giacomo Gallinaro, Eurowaste Srl, Italy
E-mail: editorialoffice@detritusjournal.com

MANAGING EDITORS:

Maria Cristina Lavagnolo, University of Padova, Italy
Info from the global world
E-mail: mariacristina.lavagnolo@unipd.it

Alberto Pivato, University of Padova, Italy
Research to industry and industry to research
E-mail: alberto.pivato@unipd.it

Alberto Pivato, University of Padova, Italy
Claire Gwinnett, Staffordshire University, United Kingdom
George Varghese, NIT Calicut, Kozhikode, India
Environmental Forensic
E-mail: alberto.pivato@unipd.it, c.gwinnett@staffs.ac.uk, gkv@nitc.ac.in

Roberto Raga, University of Padova, Italy
Books Review
E-mail: roberto.raga@unipd.it

Marco Ritzkowski, TuTech Innovation GmbH, Germany
New projects
E-mail: m.ritzkowski@tuhh.de

Rainer Stegmann, TuTech Innovations GmbH, Germany
Detritus & Art
E-mail: stegmann@tuhh.de

EDITORIAL ADVISORY BOARD:

Mohammad Alamgir, Khulna University of Engineering & Technology, Bangladesh

Luca Alibardi, Cranfield University, United Kingdom

Sven Andersson, Babcock & Wilcox Vølund AB, Sweden

Andreas Bartl, Vienna University of Technology, Austria

Luciano Butti, B&P Avvocati, Italy

Dezhen Chen, Tongji University, China

Christophe Cord'Homme, CNIM Group, France

Hervé Corvellec, Lund University, Sweden

Frederic Coulon, Cranfield University, United Kingdom

Francesco Di Maria, University of Perugia, Italy

Lisa Doeland, Radboud University Nijmegen, The Netherlands

Marco Frey, Sant'Anna School of Advance Studies, Italy

Dieter Gerten, Potsdam Institute for Climate Impact Research and Humboldt University of Berlin, Germany

Apostolos Giannis, Nanyang Technological University, Singapore

Ketil Haarstad, Norwegian Institute for Bioeconomy, Norway

Jianguo Liu, Tsinghua University, China

Weisheng Lu, University of Hong Kong, Hong Kong

Wenjing Lu, Tsinghua University, China

Claudio Fernando Mahler, COPPE/UFRJ, Brazil

Sandeep Panda, Süleyman Demirel University, Turkey

Marco Ragazzi, University of Trento, Italy

Jörg Römbke, ECT GmbH, Germany

Silvia Serranti, University Roma La Sapienza, Italy

Natalia Sliusar, Perm National Research Polytechnic University, Russia

Elisabeth Tilley, University of Malawi, Malawi

Giuseppe Tipaldo, University of Turin, Italy

Evangelos Voudrias, Democritus University of Thrace, Greece

Casta Zecena, Universidad de San Carlos de Guatemala, Guatemala

Editorial

A NEW DISCIPLINE: WASTE PREVENTION MANAGEMENT

We live in challenging times: climate change, with vast fires, flooding, droughts, hurricanes, coronavirus pandemics, difficult political situations and now also limited resources resulting in reduced production in the construction sector and car industry. Economies need more raw materials for their steadily increasing production. Wood, steel, plastics, and other materials are becoming scarce. Prices for soya, palm oil, wood, sand, and steel have increased significantly due to reduced availability on the world market. This lack has been caused by a series of reasons, such as increased production "after" coronavirus, worldwide competition, supply chains, and availability of natural resources. This situation highlights how vulnerable industry is, and that the times of abundant availability are over. The situation of the rare earth elements Gallium (Semiconductors), Germanium (Optical Fibres), Indium (flat screens) and Hafnium (Superalloys), which are becoming depleted and are not replaceable (<https://goldengates.de/de/ratgeber/rohstoffknappheit-2021/>) is particularly critical.

It is time to do more with regards to resource saving and substituting rare materials, otherwise our quality of life will change significantly. I think we are approaching a tipping point. Although we have known about the endlessness of resources for a long time, to date very little action has been taken.

Circular Economy

A popular opinion maintains that the application of Circular Economy (CE) and other approaches such as Zero Waste and Cradle to Cradle solves all waste management problems. We all have seen the closed circle that graphically describes the CE. People may get the impression that material use is unlimited, producing little or no residues for disposal. I do not intend to question the CE, but it is essential to look at what is actually behind it.

Until now, the CE has not heralded the necessary breakthrough in waste reduction: waste production globally has not changed much (Simon and Holm, 2018). The worldwide average waste production amounts to 1.2 kg/Pers./d and - as predicted by the World Bank - will reach 1.42 kg/Pers./d in 2025. Even in Germany, with relatively high recycling rates, waste production remains almost constant. Statistics report high recycling rates for different countries, and Germany often sees itself as the waste recycling champion. However, on looking more closely at these rates, how the data are collected and which measures count as recycling, the situation is rather different. In Germany for example, separately collected packaging waste that enters a

recycling plant counts as recycled. I would estimate that 20%-30% of the material is not recyclable (think of particle sizes < 40 mm); these residues are mainly thermally utilized. It should be taken into account that, in general, municipal waste (MSW) incinerators have an energy efficiency for electricity production of < 20%.

Parts of used electronics (most no longer functional), clothing, separately collected plastic waste and paper are shipped to Africa, Asia, and other non-European areas and enter statistics as recycled. I am very skeptical as to the recycling efficiency for the different materials in the receiving countries, without any control (see also Bartl, 2014; 2020).

Waste statistics

What should we look at when scrutinizing waste recycling statistics? In Germany for example, official material recycling rates for separately collected glass (2016: 85.5%), paper (2018: around 76 %) and plastic (2017: 46.7 %) - <https://www.umweltbundesamt.de> - are relatively high, but one has to take into account separate waste material collection rates between 50%-70% (<https://www.bmu.de>). For plastic, actual material recycling lies between 23% and 32%. Reutilization cycles for paper and plastic are limited to 5-7 times, i.e., for new - mainly low quality- paper production, approx. 28% virgin material has to be added (www.altpapier.ch).

It is a widespread opinion that metals can be recycled endlessly. However, the presence of numerous alloys will modify the original metal quality, which limits the recycling of certain metals. Trace elements that improve metal characteristics can often not be recovered during thermochemical reprocessing because they stay in the slag or remain in the metal. Reck et al. (2012) presented the results of Markov chain modelling, "which shows that a unit of the common metals iron, copper, or nickel is only reused two or three times before being lost gainsaying metals being repeatedly recyclable" the notion of a consequent approach can save certain industries from timely collapsing due to a lack of resources".

In the majority of cases, recycling is actually a down-cycling of resources, and statistical data of material recycling rates do not indicate the quality of the recycled product. The products from material recycling are frequently of a low value, although improvements may be gained by means of more detailed separation, such as into different types of plastics. Material recycling rates for electrical and electronic waste are pretty low. Following the recovery of compounds with high values such as gold, copper and oth-

er metals, the plastic parts are often energetically used in metal smelters, cement kilns, and waste incinerators. Statistics frequently fail to distinguish between energy and material recovery.

I should also like to discuss another aspect: the general opinion that recycling only makes sense if profitable. This opinion is one of the reasons why large amounts of recycled plastic are thermally treated. We need a new approach and take natural resource savings as a benchmark; costs are substantial, but they should not control recycling. This approach is comparable with climate change, where all necessary interventions must be undertaken.

Waste prevention

Why do I mention all this? Although efficient separate collection and mechanical separation techniques are available, the material recycling rates and quality of products are generally relatively low. Recycling as practiced today has reached its limits, and therefore, other forms of waste avoidance should be fostered to save more resources. This approach is vital for humankind to avoid the onset of a significant economic recession with increasing global pollution.

Waste prevention "... takes place before products or materials are identified or recognised as waste" (OECD, 2000). Waste prevention is part of waste minimization. The latter encompasses prevention and or reduction of waste at the source, improving the quality of the generated waste, such as lowering the hazardous element, and encouraging reuse, recycling and recovery.

When waste recycling is carried out, this implies that waste has been produced and requires some form of treatment. In the case of avoidance, no waste is produced (primary avoidance).

Recycling activities should be validated, with a particular focus on waste avoidance (i.e. material avoidance, MA, = resource saving). As a consequence, we should validate recycling measures by calculating the number of saved resources. The same should be applied to refund systems.

$$WA\% = MA\% = M\% - \frac{M\%}{n} \quad (1)$$

WA: avoided waste (%); MA: avoided material (%); M: original material (=100%); n: number of reuses and recycling loops,

when n=1, avoidance = 0

The degree of waste avoidance can be calculated using equation 1: e.g. using a cup eight times means that the material saving rate is 87.5% compared to single use cups.

We need to bear in mind that all recycled materials will ultimately become waste destined for disposal (Cossu et al, 2020; Matasci et al., 2021). According to the Lavoisier law, no materials are lost, but are only transformed. According to the second law of thermodynamics, entropy increases with each utilization and recycling step; actually, I set entropy up with diffusive pollution i.e. producing non-recoverable waste.

In the official WM hierarchy, waste avoidance assumes the highest priority. Numerous regulations to this regard have already been issued, including mainly recommendations with general targets.

However, to foster waste avoidance, regulations, tax-

es, and raising awareness amongst the private, public and commercial sectors is necessary: cleaner production, material saving and reuse, refund and leasing systems, change of habits, digitalization, and development of products that are easier to recycle. The necessary measures are known to us all, but need to be implemented on a large scale on a routine basis. Many technical, social, economic and logistical aspects need to be taken into account, together with their effects on emissions, used resources and consumption of energy. The use of these tools becomes rather complex due to their frequently interrelated nature. Life cycle assessment (LCA) may help to validate these processes and measures to a certain extent, although some modifications may be required as a significant consideration of resource consumption. A new tailor-made model should be developed for waste recycling and prevention to clarify their relationships and provide transparency. Responsible and effective waste minimization concepts can accordingly be developed on this basis and achieve individual measures.

Worldwide, numerous systems, concepts and activities of waste avoidance are already in place (Umweltbundesamt, Germany, <https://www.uba.de/uba-info-medien/4043.html>). An essential goal of recycling in several countries is the diversion of waste from landfills (Zero Waste Landfilling - Zaman et al., 2013), although new priorities should be identified and consideration given to the fact that a sink for the final sustainable deposit of residues from CE are likely to be required (Cossu and Stegmann, 2019; Cossu et al., 2020).

Used products back to producer and extended producer responsibility (EPR)

Avoidance and recycling concepts for all end-use products such as electrical and electronic devices, textiles, furniture, plastic, and metal household products should be further developed.

The author supports a waste avoidance strategy, where "all" used products that the owner wishes to dispose of should be returned to the producer to reuse the entire product, parts or materials. For this purpose, factories should implement new product lines for the processing of used products into "recycled products" (exchange products). For materials that the producer cannot sensibly recycle as a second option, external recycling should be considered. The remaining non-useable product residues may end up as energy sources in MSW incinerators or industrial plants; alternatively, these residues will need to be safely landfilled. The producer must also assume responsibility for the remaining residues at their final destination.

Today, in most cases, the manufacturing industry uses third-party companies to recycle materials from their discarded products, e.g., cars. By these means, the producer is not obliged to accept responsibility for their products once they become waste. It is fundamental therefore that the producer be directly encharged with the task of recycling their used products to ensure that the company has an invested interest in saving resources and designing and manufacturing their products to fulfil the established recycling targets. Accordingly, only products complying with

the required recycling/reuse targets and identifying the final destination of non-useable residues would be able to enter the market.

The Government should be called upon to emanate regulations and - dependent on the product group - reuse and recycling goals. To a certain extent, similar prescriptions exist for material recycling for cars, electrical and electronic products (WEEE directive) and perhaps others, but are currently lacking for product or product parts reuse and recycling. The EU should amend their regulations to comprise resource minimization of "all" products. Only the implementation of a targeted approach would save certain industries from an untimely collapse due to lack of resources.

How can this concept be implemented?

Companies often claim that their products are recycled, although the amount of product and/or material recovery is relatively low. A recycling logo on a product may be misleading because it does not inform us as to the extent and quality of recycled materials.

To provide for a greater transparency over material avoidance, I propose the introduction of the Product-Material-Avoidance Index (PMAI). The EU-Regulation 2010/30/EU has introduced an energy label on electrical household products that shows qualitatively electrical efficacy for household devices (i.e. tumble dryers). By further developing such a label to document material and product parts avoidance rates, companies would need to ensure the reuse and recycling of their products. The Product-Material-Avoidance Index, PMAI provides details relating to reduction of use of virgin materials and substitution of product parts. The PMAI would relate to a specific product line, such as computers or refrigerators.

Actual material avoidance rates should be calculated by considering the number of reuses (equation 1). When products or parts of these consist of recycled components (e.g. a pump in a washing machine), the manufacturer should determine the percentage of avoided product parts. Different green color intensities distinguish between various product components (e.g., machine parts, electronic devices, casing), reused or recycled. The length of the bar shows recovery percentages for each category (Figure 1).

But how can the quality of the recycled materials be described? As a first approach, the author proposes three quality categories: up-cycling, recycling and down-cycling. These categories are related to different intensities of the blue color. The number of recycled materials in the three types is marked as a percentage of the total material used. This approach can be further detailed for the different kinds of materials as copper, plastic, etc. Red indicates there is no material avoidance i.e., single-use products.

If a producer claims that the detergent bottle consists of 100% recycled plastic, the limited reuse potential of plastic material – let's say seven times - reduces the actual material avoidance rate to 86% (equation 1), i.e. the green bar becomes a bit shorter. The label on a refrigerator may indicate that the casing consists of recycled material (steel) (yellow bar up to 90%) and if – let's assume - the electrical pump is reused once more, the green bar extends to 50%.

We are well aware that the problem lies in the details, and a similar system should probably start first with home utilities using a pragmatic, not over-detailed approach. This concept should be further developed and tested for practical application – standardization of the procedure using a model is vital.

Social impact

The options presented here aimed at increasing both product and material avoidance and, at the same time, waste production, are mainly of a technical and organizational nature. The implementation of this or similar concepts implies an inherent need for acceptance by and support from society, with politics being called upon to implement the regulatory frame for the private, industrial and commercial sectors. New waste avoidance concepts will result in fewer single-use products, less fast fashion, more second-hand products, and more recyclable-friendly designs. Subsequent to the required modification of production processes, job profiles may change. Since there are no visible short-term benefits but rather potential disadvantages for society, it is essential to convince people of the necessity of such a new concept.

Why should people buy products made partly from reused materials and product parts? First of all, legislators will establish a framework implicating the reuse of materials and mechanical and electrical components for each product line (e.g. washing machine) so that all competitors produce under the same conditions. In buying secondary products, incentives may be represented by lower prices with the same guarantee.

Companies' "green" image will become more and more important in achieving better sales performance and higher ratings on the stock market (<https://youmatter.world/en/responsible-companies-perform-better-on-the-stock-market/>). A recent trend highlights how more people are investing in companies that care about the environment, producing "green" technologies and saving energy and material resources.

The main challenges for producers will lie in the design and production of products using a minimal material and energy input and the reintegration of the returned used products in their production processes. Digitalization, artificial intelligence and robots may significantly support and innovate the necessary actions. New jobs will consequently be created; the unfailling Yin (阴) and the Yang (阳).

A recent example may be observed in the presentation of a BMW concept car "iVision Circular", which the producer claims consists of 100% recycled and recyclable materials. This study shows that, on a general level, this can be achieved, although BMW claims that such a car will not be available on the market before 2040 (Hamburger Abendblatt 18.9.2021). Hopefully, in the meantime, more and more parts will be substituted by recycled and recyclable materials. Increasing pressure to foster this will need to be applied by the public, the scientific field and politics.

The provision of education and information are fundamental, with all educational institutions playing a highly important role of responsibility. Numerous activities are already in the pipeline, starting from Kindergarten, where

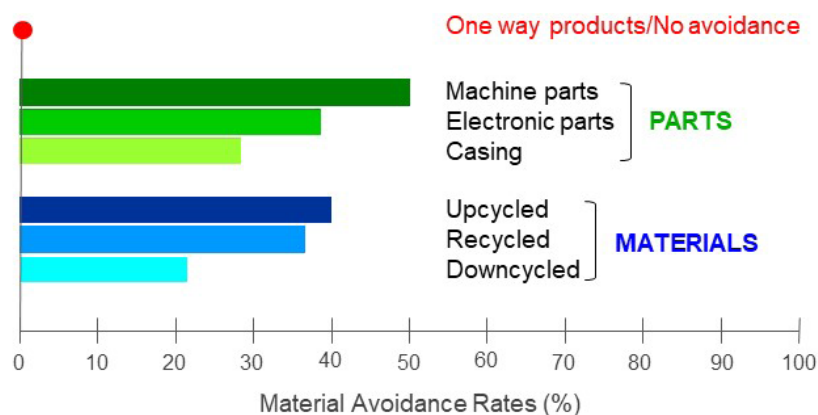


FIGURE 1: Proposal for a product label indicating the quantity and quality of avoided material used. Material avoidance rates could be calculated according to equation (1).

kids learn by playing to preserve our environment (de Feo et al., 2019). More compulsory courses on environment and sustainability should be scheduled in all disciplines taught in schools and universities as a kind of "General Studies" (Stegmann, 2018).

As has become apparent during the Coronavirus crisis, the media play a role of the utmost importance, with a wide range of media constantly presenting scientifically correct information. An identical approach should also be applied to foster waste avoidance.

Conclusions

A number of individual and commercial recycling initiatives have already been implemented: second-hand shops have become more popular on the internet; we see more detailed collections of used materials and products. Waste avoidance includes the use of less packaging and prohibiting plastic materials and products. Other initiatives include car-sharing, increased use of bicycles, opposing fast fashion. In addition, many private organizations are actively fighting for global change. These "germ cells" are essential to spread and actively support material and waste avoidance concepts.

The author keenly promotes of an intensified waste minimization by proposing practical ways and procedures to achieve increased waste prevention. Together with the stakeholders, the scientific community needs to develop new ideas and further develop waste avoidance concepts in theory and practice. Material and waste prevention should be viewed as a new scientific discipline referred to as "Resource Prevention Management" - borne by a great variety of technical and social disciplines requiring close cooperation with industry. Bartl, 2020 provides a graph illustrating a high publication rate of scientific papers on CE with increasing tendency but very low constant publications on waste prevention. This neglected discipline should encourage us to perform more targeted research in the field and adequate funding should be made available.

In the future, major cultural and social changes should be expected. There will be less food waste as more people tend to eat outside the house or to order food deliveries.

Due to digitalization, there will be less paper consumption. The increasing use of robots may open up new production processes and resource recovery procedures. More products will be purchased online, and there will be a tendency towards product leasing and home offices. All these aspects should be investigated in detail in the new scientific discipline of Resource Prevention Management.

Rainer Stegmann
Hamburg University of Technology, Hamburg, Germany
stegmann@tuhh.de

REFERENCES

- Bartl, A., (2014). Moving from recycling to waste prevention: a review of barriers and enables Waste Management & Research Vol. 32(9), doi:10.1177/0734242X14541986
- Bartl, A., (2020). The circular economy package of the European Union: are new paths being taken or is it an old story? Detritus (12), 12–17. doi: 10.31025/2611-4135/2020.13991
- Cossu, R., Grossule, V., Lavagnolo, M. C. (2020). What about residues from circular economy and role of landfilling? Detritus, (9), 1–3. doi:10.31025/2611-4135/2020.13920
- Cossu, R., Stegmann, R. (2019). Solid waste Landfilling, Concepts, Processes, Technologies, Elsevier Publisher, ISBN: 9780128183366
- De Feo, G., Faiella, F. (2019). Waste management and education: from kindergarten to higher education, Proceedings Sardinia 2019, CISA Publisher, ISBN: 9788862650144
- Matasci, C., Gauch, M., & Boeni, H. (2021). How to increase circularity in the Swiss economy? Detritus (14), 25–31. doi: 10.31025/2611-4135/2021.14057
- OECD, (2000). Strategic waste prevention- Working Party on Pollution Prevention and Control Environment directorate environment policy committee . Reference Manual, ENV/ EPOC/ PPC(2000)5/FINAL . [https://www.oecd.org/officialdocuments/publicdisplaydocumentpdf/?doclanguage=en&cote=env/epoc/ppc\(2000\)5/final](https://www.oecd.org/officialdocuments/publicdisplaydocumentpdf/?doclanguage=en&cote=env/epoc/ppc(2000)5/final) (visited on the 20.09.2021)
- Reck, B.K., and Graedel, T.E. (2012). Challenges in Metal Recycling Science 337, 690 doi:10.1126/science.1217501
- Simon, F.-G., and Holm, O. (2018). Resources from recycling and urban mining: limits and prospects. Detritus, (2), 24. doi:10.31025/2611-4135/2018.13665
- Stegmann, R., (2018). Thinking from the End, 7th International Symposium on Energy from Biomass and Waste, VENICE 2018, CISA Publisher, Padova. ISBN: 9788862650137
- Zaman, A.U., Lehman, S. (2013). The "zero waste index": a performance measurement tool for waste management systems in a "zero waste city", Journal of Cleaner Production, 50, 123- 132, doi:10.1016/j.jclepro.2012.11.041

WASTE HAZARD PROPERTIES HP 4 'IRRITANT' AND HP 8 'CORROSIVE' BY PH, ACID/BASE BUFFER CAPACITY AND ACID/BASE CONCENTRATION

Pierre Hennebert *

Ineris (French National Institute for Industrial Environment and Risks), BP 2, F-60550 Verneuil-en-Halatte, France

Article Info:

Received:
5 March 2021
Revised:
7 June 2021
Accepted:
2 August 2021
Available online:
30 September 2021

Keywords:

Hazard property
Reference method
Product
CLP
H314
H315
H318
H319

ABSTRACT

European "Technical Recommendations" have proposed, with the use of substance concentrations, the use of a pH (≤ 2 or ≥ 11.5) to classify waste for the hazard properties HP4 'Irritant' and HP8 'Corrosive'. The document add unfortunately that the buffer capacity must be "not low" to classify as hazardous. Buffer capacity refers to a 2018 UK classification guide referring to the 'corrosive' level of a method proposed in 1988 for substances and preparations but not retained in EU regulations, but well in its Guidance. The product method uses the pH unclearly associated or not to a 1% concentration. The different methods of classifying products and wastes in terms of corrosivity or irritation are expressed as acid/base concentration and compared. The "corrosive" level of 1988 corresponds to an average strong acid/base concentration $\geq 14.4\%$, i.e. 14 times less severe than CLP (acid/base concentration $\geq 0.44-0.15\%$ for pH only or $\geq 1\%$ for pH and concentration). The "pH only" method corresponds to the lowest concentration of acid/base and is the most severe. These methods were applied to five hazardous alkaline wastes (pH ≥ 11.5). The "pH only" method is the only that classifies all waste in accordance with the European List of Waste. To avoid innovation and divergence between products and waste, it seems preferable to use the product regulations "pH only" or eventually "pH and concentration" for HP4 and HP8. Fortunately, the elimination of the danger HP 4 and HP 8 from acidic or alkaline waste can be obtained by neutralization, including for alkaline wastes with CO_2 .

1. INTRODUCTION

The waste hazard properties HP 4 'Irritant' and HP 8 'Corrosive' are assessed by concentrations of substances classified with hazard statement codes H314 1A or 1B or 1C, H315, H318 and H319, and the corresponding concentration limits (EU 2014). Further, European technical guidelines have recently also proposed the use of pH (≤ 2 or ≥ 11.5) and of acid / base buffer capacity to classify waste for the properties HP 4 and HP 8, "where the waste is not 'Irritant' as a result of the known substances and some substances are still unknown" (EU 2018). The buffer capacity limit is not given. However, it is suggested to refer to a classification guide from the United Kingdom (UK 2018), referring to a method proposed by the soap and detergent industry for substances and mixtures in the UK in 1988 (Young et al. 1988, 1994).

The UK soap and detergent industry developed a method for substances and mixtures, whose irritant or corrosive action through the skin is caused by acidity (pH ≤ 4) or alkalinity (pH ≥ 10) associated with a significant buffer

capacity. This combination of pH and buffering capacity is adjusted in order to correspond to experimental data of the two reference methods of that time (i.e. by calculation with the "R" system and by animal test), and to expert evaluations. This method classifies substances and mixtures into three levels: unclassified, irritant (low level) and corrosive (high level). The original method proposed in 1988 is presented and discussed using the raw data from the original publication.

The later European Regulation for the classification, labelling and packaging of substances and mixtures in Europe (CLP 2008) uses the United Nations Global Harmonized System, thus referring to the hazard statements codes "H" of substances and other classification methods by calculation. Additionally, when the substances are not known in the mixture, mixtures are classified for hazard as "Skin corrosives (category 1)" and "Serious eye damage (category 1)", if the pH is ≤ 2 or ≥ 11.5 , and the acid or base concentration is $\geq 1\%$. The classification of Young et al. (1988) has not been directly included in the CLP but is proposed in the Guidance of the CLP (ECHA 2017).

* Corresponding author:
Pierre Hennebert
email: pierre.hennebert@ineris.fr

As mentioned above, a communication from the European Commission (Technical Recommendations, EU 2018) suggests combining the pH limits of ≤ 2 and ≥ 11.5 of CLP combined with the "non-low" buffer capacity of waste (waste then classified as hazardous HP 8 'Corrosive') or "low" (waste then classified non-hazardous HP 4, but can be classified HP 4), according to the aforementioned UK Guide. The threshold for buffer capacity between non-low and low values is not indicated, but it is suggested to refer to the UK guide, i.e. to the "corrosive" limit set by the Young's classification.

In this paper, the Technical Recommendations (with some hypotheses) are expressed in terms of pH and acid or base concentration (rather than a combination of pH and buffer capacity) and are compared to the CLP Regulation. Five wastes are classified in the two systems and compared. The question of the reference method for the comparison of conventional classification methods, as for HP 14 'Ecotoxic' by list of waste, by calculation and by test, is discussed.

In supplementary information, (i) a simple method for determining the concentration of strong acid or base of a waste, (ii) the classification of lime, (iii) the harmonised classification of the main acids and bases that can be present in waste, and (iv) a list of acids and bases with their pKa are proposed.

2. MATERIAL AND METHODS

2.1 The classification by composition in substances of products (EU 2008) and waste (EU 2014)

The classification of substances and mixtures (called here "products") for Corrosion and Irritancy by composition in substances (CLP 2008) is done by route (eye / skin) and intensity in the route (irritation / corrosion). On the contrary, wastes are classified by intensity: low intensity HP 4 (route: skin and eye) and high intensity HP 8 (route: skin) (Table 1). There is no categories correspondence. The only matching calculation rule is highlighted in blue in the table. It can be useful to have gradual HP 8 "strong" and HP 4 "weak" with the same hazard statement codes (the only case in

the HPs) for the management of hazardous waste by the risk, here graduated.

2.2 Classification rules by pH, buffer capacity, and acid or base concentration limits (skin and eye corrosion and irritation)

For products, there are additional rules of pH and acid / base concentration for non-additives substances (CLP 2008, Table 3.2.4): the generic concentration limits of ingredients of a mixture for which the additivity approach does not apply, that trigger classification of the mixture as corrosive/irritant to skin are: Acid with $\text{pH} \leq 2$, concentration $\geq 1\%$ (Category 1), and Base with $\text{pH} \geq 11.5$, concentration $\geq 1\%$ (Category 1). The same system applies for eye exposure. It is not clear (including in the Guidance – ECHA 2017) if the pH and concentration conditions have to be fulfilled simultaneously (AND) or not (OR).

For wastes, the Commission Communication on technical recommendations concerning the classification of waste (EU 2018) proposes a flowchart for the classification of waste according to HP 4 and HP 8 which is based firstly on the knowledge of the substances of the waste, then secondly on taking into account the pH (≤ 2 and ≥ 11.5) and the buffering capacity, and thirdly, the performance of in vitro tests:

Where the waste is not 'Irritant' as a result of the known substances and some substances are still unknown, the pH value of the waste should be used for assessment (Figure 10). A waste with a $\text{pH} \leq 2$ or ≥ 11.5 should generally be considered HP 8 Corrosive unless both:

- an acid or alkali reserve test suggests that the classification as 'Corrosive' is not warranted, and
- further in vitro testing, or existing human experience and animal data from single or repeated exposure has confirmed that classification as neither 'Irritant'/'Corrosive' applies.

But the Figure 14 (p 107) of that document add unfortunately that the buffer capacity must be "not low" to

TABLE 1: Classification of substances and mixtures ("products") and waste by hazard statement of substances and calculation. The only matching rule is highlighted.

Category (Severity) → Route of exposure ↓	Hazard Statement Codes		PRODUCTS	Hazard classes of mixtures	
	High level Cat. 1	Low level Cat. 2		High level	Low level
Dermal	H314 Skin Corr. 1A, 1B, 1C	H315 Skin irrit. 2	→	« Skin corrosion» $\sum \text{H314 1A} \geq 5\%$ $\sum \text{H314 1A, 1B} \geq 5\%$ $\sum \text{H314 1A, 1B, 1C} \geq 5\%$	« Skin irritation» H 314 1A,1B, 1C $\geq 1\%$ but < 5%. $\sum [10*(\text{H314 1A, 1B, 1C}) + \text{H315}] \geq 10\%$
Eye	H318 Eye dam. 1	H319 Eye irrit. 2	→	« Serious eye damage» $\sum (\text{H314 1A, 1B, 1C} + \text{H318}) \geq 3\%$	« Eye irritation» $\sum [(10*\text{H314 1A, 1B, 1C}) + \text{H315} + (10*\text{H318}) + \text{H 319}] \geq 10\%$
WASTE	↓	↓			
Waste Hazard Property	HP 8 'Corrosive' $\sum \text{H314 1A, 1B, 1C} \geq 5\%$	HP 4 'Irritant' $\sum \text{H314 1A} \geq 1\%$ $\sum \text{H318} \geq 10\%$ $\sum (\text{H315 and H319}) \geq 20\%$			

classify as hazardous. The buffer capacity refers to the UK Guide, citing Young et al. (1988). There is no concentration limit of buffer capacity indicated in this European document.

Negative conditions should be avoided in classification wording since they are more difficult to understand and to implement. We understand the conditions mentioned above as:

- if $\text{pH} \leq 2$ or ≥ 11.5 , the waste is classified HP 8;
- if $\text{pH} \leq 2$ or ≥ 11.5 AND the buffer capacity is low AND a biotest is negative, the waste is NOT classified HP 8;
- if $\text{pH} \geq 2$ or ≤ 11.5 , the waste is NOT classified HP 8.

A recent study has shown that there is no solution with biological tests up till now (Concawe, 2020), so that option will not be studied here. Even more, concentration limits to assess the result of tests are nor proposed neither validated by comparison with a reference method for waste. Some possible outdated options can be found

in OECD (1981). The above conditions can then be re-phrased as:

- if $\text{pH} \leq 2$ or ≥ 11.5 , the waste is classified HP 8;
- if $\text{pH} \leq 2$ or ≥ 11.5 AND the buffer capacity is high, the waste is classified HP 8;
- if $\text{pH} \geq 2$ and ≤ 11.5 , the waste is NOT classified HP 8.

How the first two parallel conditions inter-relate? That question will be clarified in this paper (Table 2).

The buffer capacity is a measure of the concentration of dissociated acid or base in the mixture at a given pH, by titration to a given pH. In this document, the « acid alkali reserve » of Young et al. is converted in buffer capacity (BC): 1 unit Acid Alkaline Reserve AAR = 1 g NaOH/100 g = 0.25 mol H⁺ or OH⁻/kg = 0.25 BC (mol/kg). The buffer capacity is measured by titration with a strong base or a strong acid, up to a given pH. Young et al. chose pH 4 for the acid domain and pH 10 for the alkaline domain. It is considered that there is no irritancy or corrosiveness by acidity or al-

TABLE 2: Classification of substances and mixtures (“products”) and waste by pH, acid/base concentration, and acid/base buffer capacity.

Hazard	Domain	Conditions to be fulfilled simultaneously		
		pH	Concentration	Buffer capacity (mol H ⁺ or OH ⁻ /kg)
Products (CLP 2008)				
Skin corrosion, Severe eye damage (high level)	Acid	≤ 2	AND? OR? $\geq 1\%$	-
	Alkaline	≥ 11.5	AND? OR? $\geq 1\%$	-
Products (ECHA Guidance 2017 3.3.3.2.1.1.)				
Skin corrosion, Severe eye damage (high level)	Acid	≤ 2	-	-
	Alkaline	≥ 11.5	-	-
Waste (EC 2018)				
HP 8 ‘Corrosive’	Acid	≤ 2	-	AND « Not low » as in UK 2018
	Alkaline	≥ 11.5	-	AND « Not low » as in UK 2018
HP 4 ‘Irritant’	Acid	≤ 2	-	→ classify by HP 8
	Alkaline	≥ 11.5	-	→ classify by HP 8
Waste (UK 2018)				
HP 8 ‘Corrosive’	Acid	≤ 2	-	AND $\text{pH} - 1/3 \text{BC}_{\text{pH}4} \leq -0.5$ (high level of Young)
	Alkaline	≥ 11.5	-	AND $\text{pH} + 1/3 \text{BC}_{\text{pH}10} \geq 14.5$ (high level of Young)
HP 4 ‘Irritant’	Acid	≤ 2	-	→ classify by HP 8
	Alkaline	≥ 11.5	-	→ classify by HP 8
Products (Young et al. 1988)				
Expression in buffer capacity*:				
Skin corrosive (high level)	Acid	≤ 4	-	$\text{pH} - 1/3 \text{BC}_{\text{pH}4} \leq -0.5$
	Alkaline	≥ 10	-	$\text{pH} + 1/3 \text{BC}_{\text{pH}10} \geq 14.5$
Skin irritant (low level)	Acid	≤ 4	-	$\text{pH} - 2/3 \text{BC}_{\text{pH}4} \leq 1$
	Alkaline	≥ 10	-	$\text{pH} + 2/3 \text{BC}_{\text{pH}10} \geq 13$
Original expression in acid-alkaline ratio AAR*				
Skin corrosive (high level)	Acid	≤ 4	-	$\text{pH} - 1/12 \text{AAR}_{\text{pH}4} \leq -0.5$
	Alkaline	≥ 10	-	$\text{pH} + 1/12 \text{AAR}_{\text{pH}10} \geq 14.5$
Skin irritant (low level)	Acid	≤ 4	-	$\text{pH} - 2/12 \text{AAR}_{\text{pH}4} \leq 1$
	Alkaline	≥ 10	-	$\text{pH} + 2/12 \text{AAR}_{\text{pH}10} \geq 13$

* Buffer capacity BC (mol H⁺ or OH⁻ / kg) = 4 x Acid Alkaline Ratio AAR (g NaOH / 100 g) (one unit AAR = 1 g NaOH / 100 g = 10 g NaOH / kg = 0.25 mol OH⁻ / kg = ¼ unit BC)

kalinity between pH 4 and pH 10. It should be noted that these pHs are not the ones chosen for classification by the CLP and for waste.

2.3 Determination of the concentration limits of the pH and buffer capacity method by the soap and detergents industry of UK

Numerous substances and mixtures were classified according to the two reference methods at that time: substance properties and concentration (with the previous "risk phrase R" system and their concentration limits of the Dangerous Preparation Directive EEC 1967), and animal test (rabbit eye damages). Their pH and buffer capacity were also measured. Empirical concentration limits combining pH and buffer capacity were then adjusted to the reference classification data (Figure 1). The obtained correspondence or correlation with the two reference methods is convincing (Figure 2).

2.4 Reference method for the assessment of the buffer capacity classification method, and expression of the pH and the BC in strong acid/base concentration

Classifications are conventional and can always be discussed as they set punctual limits to continuous variables. New classification systems can be built in line with refer-

ence system(s). On the issue of the reference method when building a new classification system, Jung et al. (1988) adjusted empirically their concentration limits to the reference methods of their time by concentration and by animal tests. For the waste hazard property HP 14, concentration limits are proposed for ecotoxicological tests (without pH adjustment) by matching with classification by the European list of waste of absolute non-hazardous (with control of chemical composition) and hazardous waste (Hennebert 2018). The question is similar here. To assess the Young method, we chose as reference method the CLP because it is in fact the Global Harmonised System for chemicals of the United Nations and has been built by a high-level global expertise in toxicology.

In order to compare methods, their expression must be harmonised. The pH, the acid and base concentration, and the buffer capacity are functions of each other. The correspondences are easily calculated under the assumption that all the acid or the base of the product or the waste is in solution in the suspension in water used for the measurement of the pH and the titration of the buffer capacity, or equivalently the acids and bases are "strong". For $\text{pH} \leq 2$ and ≥ 11.5 , the acids and bases are always "strong". A list of acids and bases with their pKa (the pH at which they are 50% dissociated) is given in the supplementary information section. From the pH to the concentration, the normal concentration of acid or base in the 10 l leachate per kg solid waste is equal to or greater than $\log(-\text{pH}) = \log(-2)$ for acids and $\log(-\text{pOH}) = \log(-2.5)$ for bases. The result in normal concentration is expressed per kg waste. From the BC to the concentration, the BC (mol H^+ or OH^-/kg) is a normal concentration. The normal concentration is multiplied by the mass of one equivalent (the molar mass divided by the number of equivalent) to obtain a weight concentration. These calculations have been done with 3 strong acids and 3 strong bases. CaO dissolves only partly at $\text{pH} > 12$ and more precise calculations were done with Minteq (free reference software supported by USEPA). The calculated concentration levels are lower than the maximum solubilities in water at 25°C (Minteq V3 calculations, not shown), excepted for the case of lime $\text{Ca}(\text{OH})_2$. In the acid domain, the buffer capacity of HNO_3 , HCl , H_2SO_4 (mean 44.4 g/mol H^+) is 44.4 g/kg or 4.44% w/w for 1 mol H^+/kg . In the alkaline domain, the buffer capacity of NaOH , KOH , $\text{Ca}(\text{OH})_2$ (mean 49.5 g/mol OH^-) (use of Minteq V3 for partial dissolution of $\text{Ca}(\text{OH})_2$) is 49.5 g/kg or 4.95% w/w for 1 mol OH^-/kg . The mean BC of acids and bases is 46.9 g/kg = 4.69% w/w for 1 mol H^+ or OH^-/kg .

3. RESULTS

3.1 Comparison of the acid/base concentration proposed for waste classification (EU 2018) and for products (CLP 2018)

The buffer capacity (BC) and its relationship with the pH of Young – UK Guide– EU Recommendations are expressed in concentration of strong acids and bases (Table 3, Figure 3). Reversely, the acid and base concentrations of the CLP can be expressed in pH (with a solid-to-liquid ratio of 10 l/kg for solids, as in the leaching standard EN 12457-

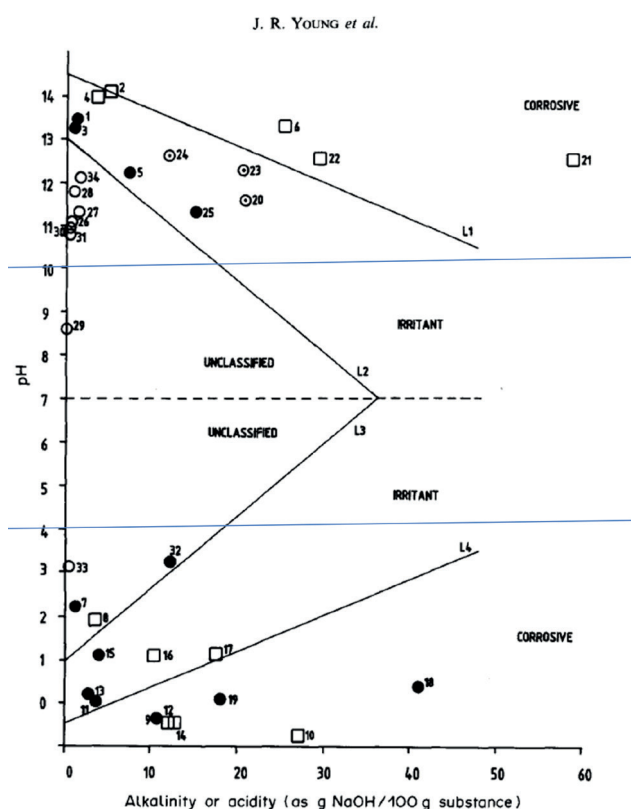


FIGURE 1: Buffer capacity and pH of 34 substances, classification by the R regulation of 1967 (black balls: irritant, white squares: corrosive), and proposed pH and buffering capacity limits (black straight lines) (Young et al. 1988). Non-classifying limits of $\text{pH} = 4$ and $\text{pH} = 10$ are added as blue vertical lines – the labels "irritant" should move to the left and to the right.

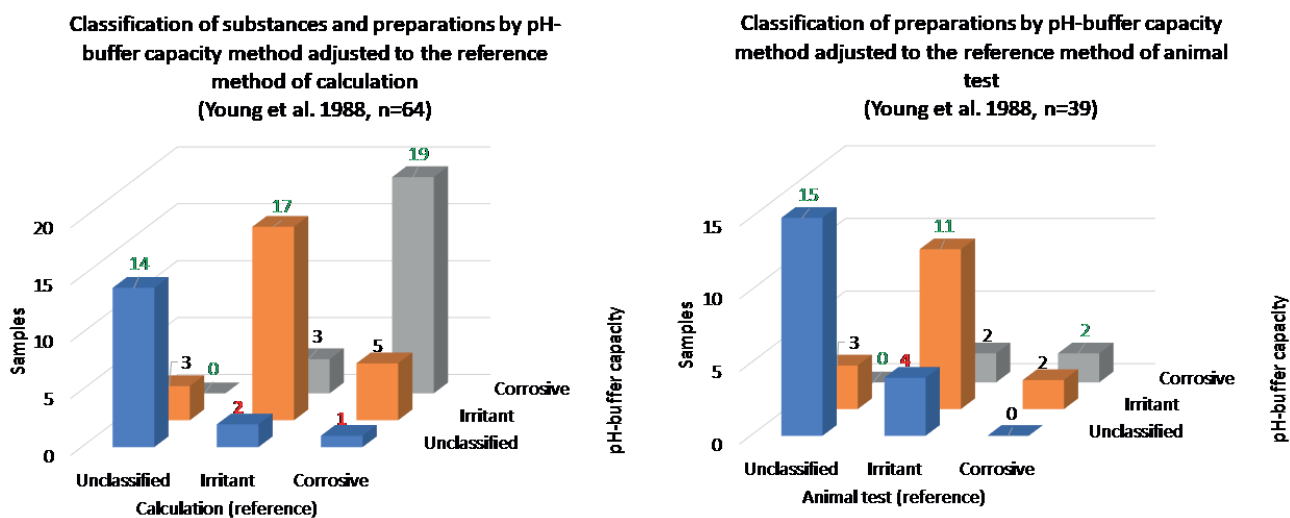


FIGURE 2: Correspondence between two reference methods and the adjusted pH-buffer capacity of substances and mixtures (recalculated from Young et al. 1988). The number of samples of each category is labelled.

2) and buffer capacity. The 'irritant domains' of Young are not used in the recommended waste classification and are not presented in the table. The 'corrosive domains' of Young corresponds to BCs > 3 mol/kg, by the presence of strong acids and bases), to a concentration of strong acids $\geq 15.2\%$ and a concentration of strong base $\geq 13.6\%$, and to the pHs ≤ 0.5 or ≥ 13.1 . The mean concentration of acid and bases is 14.4%.

The waste classification conditions for HP 8:

- if $\text{pH} \leq 2$ or ≥ 11.5 , the waste is classified HP 8;
- if $\text{pH} \leq 2$ or ≥ 11.5 AND the buffer capacity is high, the waste is classified HP 8;
- if $\text{pH} \geq 2$ and ≤ 11.5 , the waste is NOT classified HP 8 by the pH.

Can then be rephrased as:

- if $\text{pH} \leq 2$ or ≥ 11.5 , the waste is classified HP 8;
- if $2 \leq \text{pH} \leq 11.5$, the waste is NOT classified for HP 8 by the pH (and the buffer capacity).

Named here "classification by pH only (BC de facto fulfilled)" since the condition of BC is always fulfilled when the conditions of pH are fulfilled, these re-expressed calculation rules have the important advantages of (i) chemical consistency, (ii) non-divergence between waste and product classification, and (iii) simplicity.

3.2 Comparison of the acid/base concentration proposed for waste classification (EU 2018) and the harmonised classification of strong acids and bases (CLP 2018)

The detailed hazard statements of the acids and bases that can be found in waste are given in Supplementary Information, with a list of pKa and pKb of numerous acids and bases (the pH with 50% dissociation of the acid and base). For three common strong acids and base, the hazard statement code, the waste hazard calculation, and the concentration limit are presented in Table 4. The concentration limits for the waste HPs are 1% for HNO_3 , H_2SO_4 , NaOH and KOH, 5% for HCl, and 10% for $\text{CaO}/\text{Ca}(\text{OH})_2$. It

TABLE 3: The pH, the acid/base concentration, and the buffer capacity (BC) for the classification of products (skin corrosion, severe eye damage) and the recommended classification of waste for the hazard property HP 8 'Corrosive'. Yellow: classification rule, orange: calculated corresponding pH, concentration and BC.

Classification	Domain	Rules (yellow)			Corresponding calculated pH, concentration and BC for direct comparison		
		pH	Concentration limit (data)	BC mol/kg	pH 10 l/kg	Concentration limit	BC mol/kg (up to pH 4 or down to pH 10)
Products CLP High level	Acid	≤ 2		Undefined	≤ 2	$\geq 0.44\%$	≥ 0.10
	Alkaline	≥ 11.5		Undefined	≥ 11.5	$\geq 0.15\%$	≥ 0.03
Products CLP High level	Acid		$\geq 1\%$	Undefined		$\geq 1\%$	≥ 0.21
	Alkaline		$\geq 1\%$	Undefined		$\geq 1\%$	≥ 0.23
Product Young 1988 Corrosive	Acid	≤ 4	Undefined	$\text{pH} - 1/3$ $\text{BC}_{\text{pH4}} \leq -0.5$	≤ 0.5	$\geq 15.2\%$	≥ 3.06
Waste Recommended UK 2018 HP 8 Recommended EU 2018 HP 8	Alkaline	≥ 10	Undefined	$\text{pH} + 1/3$ $\text{BC}_{\text{pH10}} \geq 14.5$	$\geq 13.1^*$	$\geq 13.6\%$	≥ 3.05

* Note: NaOH, KOH = pH 13.5, Ca(OH)2 (partial dissolution) = pH 12.4, mean pH = 13.1

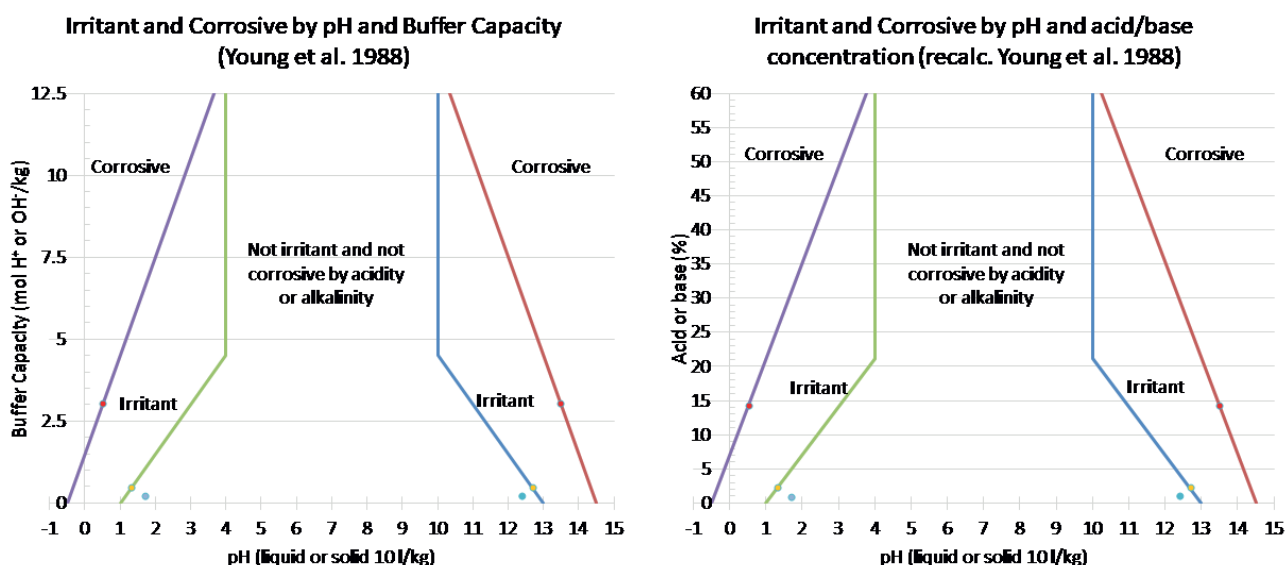


FIGURE 3: The pH - buffer capacity domain of irritancy and corrosiveness of Young et al. 1988, expressed in buffer capacity (left) and acid/base concentration (right). The blue points correspond to the classification of products in the CLP, and the yellow and red points to classification as irritant and corrosive by Young et al. (1988).

should be noted that these substances (excepted CaO and Ca(OH)₂) have specific concentration limits in the product CLP regulation (with graduated concentrations and hazard statements, the lowest being for HNO₃ and H₂SO₄ 5%, HCl 10%, NaOH and KOH 0.5%) (see supplementary information). The specific concentration limits of substances do not apply to waste. In summary, all these concentrations are lower than the 14.4% suggested by Young et al. (1988) and proposed to be used in waste classification (EU 2018), the latest being here also less severe.

3.3 Correspondence of classification with the CLP and the EU Technical Recommendations for 5 wastes

The pH (L/S = 10 l/kg) and the buffer capacity of five alkaline waste (fly ashes and air pollution control residues) have been measured. The buffer capacity is converted into base concentration using 0.044 kg acid/equivalent, as explained above. These wastes were classified by (i) the product or waste method by pH only (BC de facto fulfilled) (CLP 2008) and (ii) by pH and concentration of 1% (CLP 2008), and (iii) by the Technical Recommendations for waste classification (EU 2018) (Table 5, Figure 4). The two last classification systems correspond for low and high pHs and BCs (sample 1 and 3, 4, 5), but not for the intermediate pH and BC (sample 2).

The classification with pH only (BC de facto fulfilled) classifies all waste HP 8. pH and 1% concentration system is less severe (sample 1 is not classified hazardous). The BC system is the less severe (samples 1 and 2 are not classified hazardous). It should be noted that the air pollution control residues are classified as “absolute hazardous” in the European List of Waste. The classification with the pH only (BC de facto fulfilled) match with that reference method.

3.4 Correspondence of the different classification systems for irritancy and corrosiveness

The chronology and the correspondences and differences of the systems that were used and are used are presented in Figure 5. The proposed system for waste uses a concentration of 14% of acid or base, which is an obvious discrepancy (very highly less severe) between products and waste, not favourable to the smooth flow between waste status and product status that should exist in the circular economy. In order not to innovate and create a new divergence between products and waste, it seems preferable to use the product regulation for waste classification for HP 4 and HP 8.

Classifying waste with a concentration of acid or base > 1% or lower with the “pH only” rule rather than 14% as hazardous is a supplementary burden for their management.

TABLE 4: Concentration limit of strong acids and bases by the harmonised classification of substances of the CLP and the classification rules for HP 4 and HP 8.

Acid domain	Alkaline domain	Hazard statement code	Waste Hazard property, classification rule and concentration limit	Lowest Concentration limit for hazardous waste
HNO ₃ , H ₂ SO ₄	NaOH, KOH	H314 1A	HP 4 A: $\sum H314\ 1A \geq 1\%$ HP 8 A: $\sum H314 \geq 5\%$	HP 4: 1%
HCl		H314 1B	HP 8 A: $\sum H314 \geq 5\%$	HP 8: 5%
	CaO, Ca(OH) ₂	H318 H315	HP 4 B: $\sum H318 \geq 10\%$ HP 4 C: $\sum H315$ and $H319 \geq 20\%$	HP 4: 10%

TABLE 5: Analyses and classification of 5 waste (fly ashes, air pollution control residues) with the waste pH system, the product system and the proposed BC waste system (BC = buffer capacity).

Sample	Analyses		Calculated strong base concentration corresponding to the measured BC (0.044 kg/eq)	Waste classification by pH (EU Recommendations 2018) or Product classification by pH (CLP 2008, ECHA 2017) = classification by pH only (BC de facto fulfilled)	Product classification by pH AND 1% concentration (CLP 2008)	Classification by pH AND pH+BC high limit (UK guide 2018 suggested in EU Recommendations 2018)
	Initial pH	BC _{pH10} (mol/kg)				
1	11.7	0.05	0.2%	HP 8	Unclassified	Unclassified
2	12.4	0.7	3.1%	HP 8	Skin corrosion, Severe eye damage (high level)	Unclassified
3	12.6	7.1	31.5%	HP 8	Skin corrosion, Severe eye damage (high level)	HP 8
4	12.6	8.7	38.5%	HP 8	Skin corrosion, Severe eye damage (high level)	HP 8
5	12.8	7.4	32.9%	HP 8	Skin corrosion, Severe eye damage (high level)	HP 8

Fortunately, the elimination of the hazardous nature HP 4 and HP 8 from acid or alkaline waste can be obtained by neutralization (possibly by waste of the other acid/alkali domain), as done in specialised hazardous waste management facilities, before stabilisation/solidification and landfilling in dedicated landfills. Neutralisation of acid waste or alkaline waste is not done to dilute the hazardous concentration and to change the classification and the management of the waste to a lower demanding level, but well to destroy the hazard, as well as incineration for organic substances.

Another option for alkaline waste is the (natural) carbonation by atmospheric CO₂ in presence of soluble calcium, to precipitate the carbonate of the liquid phase to the solid phase and decrease the pH potentially up to the pH 8.5 (the pH of limestone in water) if the alkaline metals Na and K are washed out. This beneficial process is used for instance for the “maturation” of bottom ash from house-

hold waste incineration and the carbonation of red mud from alumina production.

4. CONCLUSIONS

The product system is not clear between two options: pH ≤ 2 or ≥ 11.5 OR concentration ≥ 1% (with a corresponding concentration of strong acid and base of 0.44 and 0.15%, respectively), or pH ≤ 2 or ≥ 11.5 AND concentration ≥ 1% (with a corresponding pH ≤ 1.7 or ≥ 12.4). It should be made clear what is the official option.

The “irritant” low level of Young's classification (1988, 1994), not proposed in the UK guide and EU recommendations, corresponds to pH ≤ 1.3 and ≥ 12.7, and average concentrations of acid and base ≥ 2.3%, which is a classification approach half as severe as the CLP.

The “corrosive” high level of Young et al. proposed for waste classification as a second compulsory condition (EU 2018) corresponds on average with 3 strong acids (HCl, HNO₃ and H₂SO₄) and 3 strong bases (NaOH, KOH and Ca(OH)₂) to pH ≤ 0.5 and ≥ 13.5, respectively, and at an average to an acid and base concentrations ≥ 14.4%. Therefore, Young's classification is very much less severe than the product's system CLP: much more acid or base is necessary to be hazardous. That condition in the “Technical Recommendations” should be withdrawn.

These propositions have been applied to five air pollution control residues (pH ≥ 11.5) which have been analysed and classified according to the different rules. These wastes are “absolute hazardous” in the European list of waste. The only method that classifies the five waste as HP 8 is the simplest one: pH ≤ 2 or ≥ 11.5. Addition of the requirement of a “not low” buffer capacity (corresponding to a concentration ≥ 14.4%) do not classify as hazardous two of the five wastes.

In order not to innovate and create a new divergence between products and waste (as observed in one of the five wastes studied), it seems preferable to use the simple product first option: pH ≤ 2 or ≥ 11.5.

Elimination of the hazardous nature HP 4 and HP 8 from acid or alkaline waste can be obtained by neutralization (possibly by other waste in specialised waste treat-

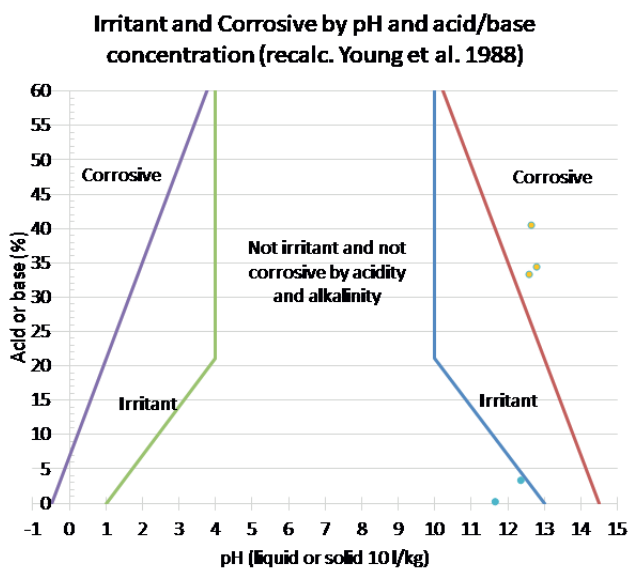


FIGURE 4: pH and base concentration of 5 wastes in the proposed classification system for waste (EU 2018).

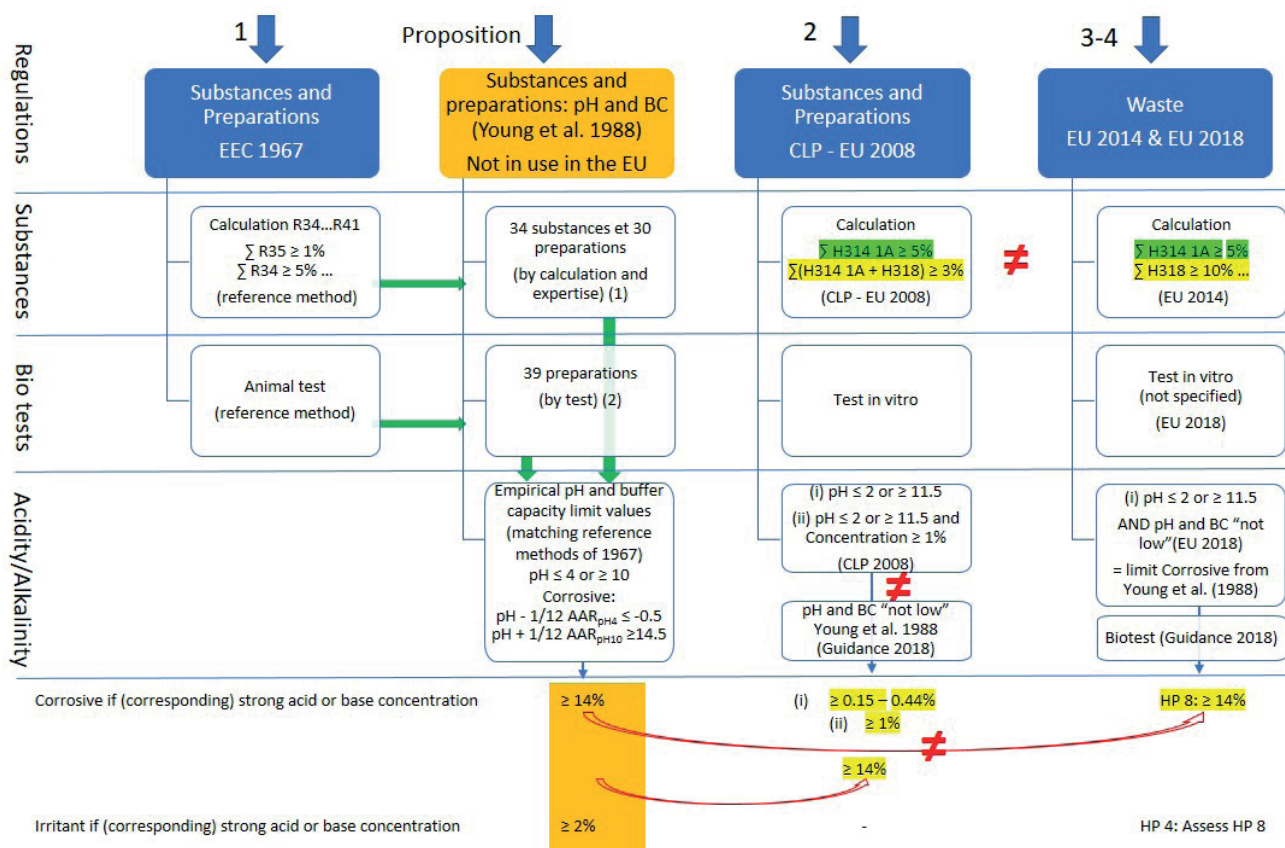


FIGURE 5: Regulations on corrosive and irritating for the skin and eyes products and waste. BC = buffer capacity. Large blue arrows: regulations in chronological order; green arrows: reference method and laboratory data used by Young et al. to derive pH-BC relationships; AAR: acid alkaline ratio, an old expression of buffer capacity; ≠: differences; green highlight: concordance; yellow highlight: differences.

ment facilities), including for alkaline waste by (natural) carbonation by atmospheric CO₂. This beneficial process is used for instance for the "maturation" of bottom ash from household waste incineration and the carbonation of red mud from alumina production.

A simple method determining the strong acid or base concentration of a waste is proposed in supplementary information.

ACKNOWLEDGMENTS

This work has been funded by the Ministry for Ecologic Transition (France) and Ineris.

REFERENCES

Concawe 2020. Literature Review: Effects-Based Analysis for Soils, Risk Management and Waste Disposal; Report no. 16/20, prepared by Marks, B., Leverett, D. and Bishop, I., August 2020.

ECHA European Chemical Agency 2017. Guidance on the Application of CLP Criteria. Reference: ECHA-17-G-21-EN. 647 pp. doi: 10.2823/124801

EEC 1967. Council Directive 67/548/EEC of 27 June 1967 on the approximation of laws, regulations and administrative provisions relating to the classification, packaging and labelling of dangerous substances.

EN 12457-2:2002. Characterization of waste – Compliance test for leaching of granular waste materials and sludges – Part 2: One stage batch test at a liquid to solid ratio of 10 l/kg for materials with particle size below 4 mm (without or with size reduction). CEN, Belgium.

EU 2008. CLP Regulation (EC) No 1272/2008 of the European Parliament and of the Council of 16 December 2008, on classification, labelling and packaging of substances and mixtures, amending and repealing Directives 67/548/EEC and 1999/45/EC, and amending Regulation (EC) No 1907/2006.

EU 2014a. Commission Decision 2014/955/EU of 18 December 2014, amending Decision 2000/532/EC on the list of waste pursuant to Directive 2008/98/EC of the European Parliament and of the Council.

EU 2014b. Commission Regulation (EU) No 1357/2014 of 18 December 2014, amending Annex III to Directive 2008/98/EC of the European Parliament and of the Council on waste and repealing certain Directives.

EU 2017. Regulation (EU) No 2017/997 of 8 June 2017, amending Annex III to Directive 2008/98/EC of the European Parliament and of the Council as regards the hazardous property HP 14 'Ecotoxic'.

EU 2018. European Commission; Commission notice on technical guidance on the classification of waste, 2018/C 124/01. 134 p. [https://eur-lex.europa.eu/legal-content/EN/TXT/PDF/?uri=CELEX:52018XC0409\(01\)&from=EN](https://eur-lex.europa.eu/legal-content/EN/TXT/PDF/?uri=CELEX:52018XC0409(01)&from=EN)

Hennebert P. 2018. Proposal of concentration limits for determining the hazard property HP 14 for waste using ecotoxicological tests. Waste Management 74, April 2018, 74-85.

OECD 1981. Acute dermal irritation/corrosion. In OECD Guidelines for Testing of Chemicals. Section 4, No. 404. OECD, Paris.

OECD 2013. 122. Guideline for testing of chemicals; Determination of pH, acidity and alkalinity. July 26th 2013 <https://www.oecd-ilibrary.org/docserver/9789264203693-fr.pdf?expires=1576835995&id=id&accname=guest&checksum=6F22D-76DD6A0C307DF01282660F4FC40> . https://www.oecd-ilibrary.org/environment/essai-n-122-determination-du-ph-de-l-acidite-de-l-alkalinite_9789264203693-fr

UK 2018. Natural Resources Wales, Scottish Environment Protection Agency (SEPA), Northern Ireland Environment Agency (NIEA), Environment Agency. Waste Classification: Guidance on the classification and assessment of waste (1st Edition v1.1). May 2018. 181 p.

Young J R, How M J, Walker A P and Worth W M. 1988. Classification as corrosive or irritant to skin of preparations containing acidic or alkaline substances, without testing on animals. Toxic. In Vitro, Vol 2, No 1, pp. 19-26

Young J.R., How M.J. 1994. Product classification as corrosive or irritant by measuring pH and acid/alkali reserve. B. In Vitro Approaches, I. Physico-chemical Methods, Method BI-1. In Alternative Methods in Toxicology vol. 10 - In Vitro Skin Toxicology: Irritation, Phototoxicity, Sensitization, eds. A.Rougier, A.M. Goldberg and H.I Maibach, Mary Ann Liebert, Inc. pp. 23-27.

1. SUPPLEMENTARY INFORMATION

1.1 Proposal for a method measuring the concentration of strong acid or strong base in a waste

A method for products is described in OECD (2013). For waste, using classical waste methods, the concentration and identification of strong acids or bases can be done as follows:

1. Measurement of the pH of liquid waste or of a suspension in water of solid waste at 10 litres / kg of dry matter (EN 12457-2, without liquid / solid separation) after 1 h of equilibration;
2. If the pH ≤ 2 or ≥ 11.5 , measure the buffering capacity of the liquid waste or of the suspension of solid waste by titration with a base up to pH 4 or a strong acid up to pH 10, with 48 h. balancing (EN 14997 leaching at different pH, used in titration mode up to pH 4 or pH 10).
3. Preparation of a leachate (EN 12457-2 with liquid / solid separation) on a separate sample and measurement of pH, electrical conductivity, TOC, anions and leachable cations.

The quantity (in equivalent) of strong acid or strong base of the sample is equal to the buffering capacity of the sample up to pH 4 or pH 10. The nature of the acid (s) and bases is determined by the majority anions and cations measured in the leachate. The amount in acid or base equivalent is then expressed as a substance concentration, using the molecular weight and the number of acid or alkali equivalents of the substance (s) identified.

In a simplified mode (without determining the acid or the base):

1. Measure the pH
2. Measure the buffering capacity
3. Express the buffering capacity in concentration of acid or base by multiplying by the mass of an equivalent of acid or base chosen (1 mol H⁺ or OH⁻ / kg \approx 4.5% acid or base)
4. This approach does not give information on substances (with their specific approach like lime) and will not be available.

1.2 Special case of lime

1.2.1 Hazard statements for quicklime and slaked lime (self-classification) and (EC Technical Recommendations 2018)

The presence of free lime (quick or slaked) results in a pH of around 12.5. Quicklime and slaked lime are not classified by the CLP regulation. The data for self-classification are as follows (Table SI 6).

Waste containing 10% lime will therefore be classified HP 4 Irritant 'and waste containing 20% lime will be classified HP 4 'Irritant ' and HP 5 'Harmful - Single target organ toxicity / aspiration toxicity'.

Note: Absolute "non-hazardous" entries in the European list of wastes containing lime should not be reclassified by composition, such as steel mill slags.

1.3 Classification of main acids and bases (CLP)

The table shows the harmonized classification of strong acids and strong bases that may be present in the waste. The last column gives for information the specific concentration limits in preparations and substances, which do not apply to the classification of waste. For the same substance in a preparation, the hazard statements depend on the concentrations.

TABLE SI 6: Properties of quicklime and hydrated lime according to the registrants in the registration dossier with ECHA and classification rules and concentration limits applicable to waste.

International Chemical Identification	CAS No	Hazard Class and Category Code(s)	Hazard Statement Code(s)	Source	Concentration limits Waste 2014
calcium oxide	1305-78-8	Eye Dam. 1 Skin Irrit. 2 STOT SE 3 respiration	H318 H315 H335	https://echa.europa.eu/brief-profile/-/briefprofile/100.013.763	HP 4 Irritant: \sum H318 \geq 10% HP 4 Irritant: \sum (H315 H319) \geq 20% HP 5 STOT: max H335 \geq 20%
calcium dihydroxide	1305-62-0	Eye Dam. 1 Skin Irrit. 2 STOT SE 3	H318 H315 H335	https://echa.europa.eu/brief-profile/-/briefprofile/100.013.762	HP 4 Irritant: \sum H318 \geq 10% HP 4 Irritant: \sum (H315 H319) \geq 20% HP 5 STOT: max H335 \geq 20%

STOT = single target organ toxicity/aspiration toxicity

There is no harmonized classification for magnesium oxide, hydroxide and carbonate. By default, the hazard statements of the corresponding calcium species could be used (Table SI 7).

1.4 List of acids and bases and pKa and pKb

The pKa is the pH to which 50% of the acid or base is dissociated, or the pH of which the concentration of the acid form equals the concentration of the conjugate base. The basics of chemistry tell us that:

$$K_a = [A^-] [H^+] / HA$$

$$[H^+] = K_a [HA] / [A^-]$$

$$pK_a = \log [A^-] + \log [H^+] - \log [HA]$$

$$pH = \log [A^-] - \log [HA] - pK_a$$

The colors correspond to the extended pH ranges of one unit (acid / conjugate base ratio = 1/10, i.e. one logarithmic unit) (Table SI 8).

TABLE SI 7: Specific concentration limits in preparations and mixtures (harmonized classification of substances, CLP 2008).

Index No	International Chemical Identification	EC No	CAS No	Hazard Class and Category Code(s)	Hazard Statement Code(s)	Specific Conc. Limits, M-factors
017-002-01-X	hydrochloric acid ... %	231-595-7		STOT SE 3 Skin Corr. 1B	H335 H314	Skin Corr. 1B; H314: C ≥ 25% Skin Irrit. 2; H315: 10 % ≤ C < 25% Eye Irrit. 2; H319: 10 % ≤ C < 25% STOT SE 3; H335: C ≥ 10%
009-003-00-1	hydrofluoric acid ... %	231-634-8	7664-39-3	Acute Tox. 1 Acute Tox. 2 * Acute Tox. 2 * Skin Corr. 1A	H310 H330 H300 H314	Skin Corr. 1A; H314: C ≥ 7% Skin Corr. 1B; H314: 1 % ≤ C < 7% Eye Irrit. 2; H319: 0,1 % ≤ C < 1%
007-004-00-1	nitric acid ...%	231-714-2	7697-37-2	Ox. Liq. 2 Skin Corr. 1A	H272 H314	Ox. Liq. 2; H272: C ≥ 99% Ox. Liq. 3; H272: 65% ≤ C < 99% Skin Corr. 1A; H314: C ≥ 20% Skin Corr. 1B; H314: 5% ≤ C < 20%
015-011-00-6	phosphoric acid ... %, orthophosphoric acid ... %	231-633-2	7664-38-2	Skin Corr. 1B	H314	Skin Corr. 1B; H314: C ≥ 25% Skin Irrit. 2; H315: 10 % ≤ C < 25% Eye Irrit. 2; H319: 10 % ≤ C < 25%
016-020-00-8	sulphuric acid ... %	231-639-5	7664-93-9	Skin Corr. 1A	H314	Skin Corr. 1A; H314: C ≥ 15% Skin Irrit. 2; H315: 5% ≤ C < 15% Eye Irrit. 2; H319: 5% ≤ C < 15%
007-001-01-2	ammonia%	215-647-6	1336-21-6	Skin Corr. 1B Aquatic Acute 1	H314 H400	STOT SE 3; H335: C ≥ 5%
011-002-00-6	sodium hydroxide; caustic soda	215-185-5	1310-73-2	Skin Corr. 1A	H314	Skin Corr. 1A; H314: C ≥ 5% Skin Corr. 1B; H314: 2% ≤ C < 5% Skin Irrit. 2; H315: 0,5 % ≤ C < 2% Eye Irrit. 2; H319: 0,5% ≤ C < 2%
011-005-00-2	sodium carbonate	207-838-8	497-19-8	Eye Irrit. 2	H319	
019-002-00-8	potassium hydroxide; caustic potash	215-181-3	1310-58-3	Acute Tox. 4 * Skin Corr. 1A	H302 H314	Skin Corr. 1A; H314: C ≥ 5% Skin Corr. 1B; H314: 2% ≤ C < 5% Skin Irrit. 2; H315: 0,5% ≤ C < 2% Eye Irrit. 2; H319: 0,5% ≤ C < 2%

TABLE SI 8: XX

Acid	Conjugated base	pKa	Domain pH ≤ 2 or ≥ 11.5 (CLP), domain ≤ 4 or ≥ 10 (Young et al. 1988)	Note
HI	I-	-11		Those acids should be considered for HP 4 and HP 8
HBr	Br-	-9		
HClO4	ClO4-	-8		
HCl	Cl-	-7		
H2SO4	HSO4-	-3		
HN03	NO3-	-1.64		
H2CrO4	HCrO4-	-1		
H3PO2	H2PO2-	1.1		
H2C2O4	HC2O4-	1.2		
H3PO3	H2PO3-	1.8		
HSO4-	SO4--	1.9		
			pH 2	
H3PO4	H2PO4-	2.1		
H3AsO4	H2SO4-	2.2		
HF	F-	3.2		Those acids should be considered for HP 4 and HP 8
HNO2	NO2-	3.4		
HCOOH	COOH-	3.8		
			pH 4	
C6H5COOH	C6H5COO-	4.2		
CH3COOH	CH3COO-	4.75		
CH3CH2COOH	CH3CH2COO-	4.9		
H2PO3-	HPO3--	6.2		
H2CO3	HCO3-	6.33		
HCrO4-	CrO4--	6.5		
H2AsO4-	HAsO4--	7		Those acids should be considered for HP 4 and HP 8
H2S	HS-	7		
H2PO4-	HPO4--	7.2		
NH4+	NH3	9.2		
HCN	CN-	9.3		
H3AsO3	H2ASO3-	9.5		
H2SiO3	HSiO3-	9.9		
			pH 10	
C6H5OH	C5H5O-	10		
HCO3- *	CO3--	10.33		
			pH 11.5	Those bases should be considered for HP 4 and HP 8
HAsO4--	AsO4--	11.5		
Ca(OH)+ **	Ca++ + OH-	11.57		
HPO4--	PO4--	11.9		
Ca(OH)2 **	Ca(OH)+ + OH-	12.63		
HS-	S-	13		
NaOH	Na+ + OH-	14.56		
KOH	K+ + OH-	14.7		

* Na2CO3 saturated in deionised water = pH 11.42 (Minteq V3 calculation)
 ** Ca(OH)2 (Portlandite) saturated in deionised water = pH 12.44 (Minteq V3 calculation)

THE SUBSTITUTION OF REGULATED BROMINATED FLAME RETARDANTS IN PLASTIC PRODUCTS AND WASTE AND THE DECLARED PROPERTIES OF THE SUBSTITUTES IN REACH

Pierre Hennebert *

Ineris (French National Institute for Industrial Environment and Risks), BP 2, F-60550 Verneuil-en-Halatte, France

Article Info:

Received:
26 February 2021
Revised:
9 July 2021
Accepted:
23 August 2021
Available online:
30 September 2021

Keywords:

Total bromine
Brominated flame retardants
Substitution
Classification
Registration

ABSTRACT

Plastics containing brominated flame retardants (BFR) currently contain both “legacy” regulated and non-regulated BFR (R-BFRs and NR-BFRs), as evidenced by the increasingly lower correspondence over time between total bromine and R-BFRs content. The portion of substitutive NR-BFR present in the plastics and their toxicity and ecotoxicity properties are documented. Data relating to plastics and foam present in electrical and electronic equipment (EEE), waste EEE, vehicles, textiles and upholstery, toys, leisure and sports equipment show how 88% of plastic waste contains bromine from NR-BFRs. BFR substances mentioned in the catalogs of the three main producers (Albemarle, ICL, Lanxess) and BFR on the official used list of 418 plastic additives in the EU were gathered and the toxic and ecotoxic properties of these compounds as listed in their ECHA registration dossier were compiled. Fifty-five preparations using 34 NR-BFRs substances, including polymers and blends, were found. Seventeen of these substances featured an incomplete dossier, 12 were equipped with a complete dossier, whilst 11 substances (including 2 ill-defined blends) should be reassessed. Eight substances have been notified for assessment by the ECHA as persistent, bioaccumulative and toxic, or as endocrine disruptors, including decabromodiphenylethane; 3 substances display functional concentrations (the concentration of additives that retards flame) exceeding the concentration limits classifying a waste as hazardous but are “reactive” (they bind to the polymer). The technical limit of 2 000 mg total Br/kg indicated for further recycling (EN 50625-3-1) relates to all brominated substances and is relevant in the sorting of all poorly classified new substances.

1. INTRODUCTION

Some plastic constituents of products include flame retardant compounds to protect the users against fire: electrical and electronic equipment, automotive and transport vehicles, construction piping and insulating material, furniture foams and upholstery, professional textiles, and many others. They are used in functional concentrations ranging from 3 to 15% w/w, with up to 30% tetrabromobisphenol A in epoxy resins (Haarman et al. 2020). Animals and people are exposed. For instance, Brominated flame retardants (BFRs), including polybrominated diphenyl ethers (PBDEs), 1,2-bis (2,4,6-tribromophenoxy) ethane (BTBPE), decabromodiphenyl ethane (DBDPE), and polybrominated biphenyls (PBBs) were found in children’s toys purchased from South China, but it accounts for a small proportion of their daily BFR exposure (Cheng SJ et al. 2009). Lower use of flame retardants with the same fire protection are considered (Charbonnet et al. 2020). While many of the toxic FRs

have been eliminated and replaced by other FRs, existing products containing toxic or potentially toxic chemical FRs will remain in use for decades, and new products containing these and similar chemicals will permeate the environment. When such products reach the end of their useful life, proper disposal methods are needed to avoid health and ecological risks (Lucas et al., 2018).

Low concentrations of bromine and (regulated R- or non-regulated NR-) brominated flame retardants (ineffective for flame retardancy) are also found in plastics due to improper recycling, showing that a circular economy must be controlled to avoid looping unwanted substances (Hennebert 2020).

Brominated flame retardants (BFRs) are numerous. So far, the regulated BFRs (R-BFRs), according to the Regulations 2004/850/EC on Persistent Organic Pollutants (POPs) and 2008/98/EC, are:

- Polybromobiphenyls (PBBs – hexabromobiphenyl 50

* Corresponding author:
Pierre Hennebert
email: pierre.hennebert@ineris.fr

mg/kg);

- Polybromodiphenylethers (PBDEs - mainly decabromodiphenylether decaBDE – sum 4-, 5-, 6-, 7-, 10-BDE 1 000 mg/kg);
- Hexabromocyclododecane (HBCDD 1 000 mg/kg) and
- Tetrabromobisphenol A (TBBPA 2 500 mg/kg).

Currently, PBBs are no longer found in plastic waste. For some years, PBDEs were largely replaced by decabromodiphenylethane: the substitution is now complete since the inclusion of decaBDE in the POPs list in 2019. DecaBDE still has exemption in the Stockholm Convention including certain EEE and is still produced and used. TBBPA is used in polyester and polycarbonate resins, typically for electrical and electronic equipment, and HBCDD was used up to 2014 in Europe but is still produced in China and is found only in expanded or extruded polystyrene. Most of HBCDD containing insulation used in construction the last 40 years is still in use and will end the next 50 or even 100 years in construction and demolition waste polymers.

The recycling of the plastics must start with a separation of the plastic pieces/shreds with these R-BFRs that have a concentration above the concentration limit. Sorting of these plastics is performed by surrogate methods: atomic density (by X-ray transmission) or solid density (by flotation). A technical specification of the European standardization committee set the limit of 2,000 mg Br/kg as the maximum content for recycling (EN 50625-3-1). If legacy additives are removed and destructed safely, a recycling technology provides a method to manage such waste streams in an environmentally friendly and economically feasible manner. Therefore, it is important that either recyclers commit and adopt the concept of decontamination, by sorting or solvent based technologies (Wagner and Schlummer 2020).

Brominated plastics now contain both “legacy” regulated and non-regulated BFRs, as is evidenced by the increasingly lower correspondence, with time, between total bromine and R-BFRs content (Haarman et al. 2020). Therefore the question arise to what extent is the part of the substitutive BFR in plastics? And what are the toxicity and ecotoxicity properties of these substitutes? As substitution is going faster than classification and regulation, and as substances with similar structure are used (for instance decabromodiphenylethane replacing decabromodiphenylether), all these new BFRs should be investigated and their properties assessed and published to avoid regrettable substitutes (Fantke et al. 2015). This paper investigates the substitutes’ declared chemical properties on human health and the environment in ECHA registration dossier.

2. MATERIAL AND METHODS

2.1 Assessment on R-BFRs and NR-BFRs in WEEE plastic

The substituting NR-BFRs are not measured during routine quality control. Nevertheless, they can be assessed by the difference between total bromine and the bromine from regulated BFRs (R-BFRs), which are routinely measured. Sample preparation of plastic shreds is done according to

EN 15002. Total bromine is measured by ionic chromatography after combustion in an oxygen bomb. The R-BFRs are measure according to EN 62321-6.

Data from plastics and foam for electrical and electronic equipment (EEE), EEE waste, vehicles, textiles and upholstery, toys, leisure and sports equipment have been gathered, with detailed various origin (Hennebert 2020). Probably, the oldest wastes are cathode ray tubes (CRT), produced about 30 years ago. Some samples are individual particles or articles, and others are composite samples with or without “enough” particles to be representative of the waste lot to be characterized (Hennebert 2019, Hennebert and Beggio 2021, Beggio and Hennebert 2021). Here, the representativity of the laboratory sample is not a challenge, since only paired data (R-BFRs and Br) have been used, measured on the same particle/article or laboratory sample (after pre-treatment). The mean stoichiometric Br concentration in the different R-BFRs is 76% w/w. DecaBDE, by far the most present R-BFRs, has a mean Br concentration of 83% w/w. The corresponding reverse ratios R-BFRs/Br are 1.31 and 1.20, respectively.

2.2 Approach to compile the list of BFRs and source information on REACH properties

The BFR substances mentioned in the catalogs of the three main producers in industrial countries (Albemarle, ICL, Lanxess) were listed and their declared chemical properties on human health and the environment, as stated in their European ECHA registration dossier (<https://echa.europa.eu/information-on-chemicals>), were gathered. The large production in China (> 50% of all BFRs) has not been documented. The 9 brominated flame retardants from the list of the 418 “Plastic Additives Initiative” (a common list by ECHA and industry of additives used in quantity more than 100 tons per year in the EU) presently used in the EU (<https://echa.europa.eu/mapping-exercise-plastic-additives-initiative#table>) have also been used.

3. RESULTS AND DISCUSSION

3.1 Monitoring of the share of R-BFR and NR-BFRs in WEEE plastic

For clarity, all the measured R-BFRs are summed. As explained, in practice, PBBs are not found, decaBDE is dominant in the PBDEs (>90% R-BFRs), HBCDD is present in expanded EPS (and not mixed with the other R-BFRs), and TBBPA is sometimes present. In these data, not all the R-BFRs were measured for all the samples, but PBDEs and especially decaBDE have always been measured. Total bromine has been measured by XRF for particles or articles, or after shredding, combustion in an oxygen bomb and ionic chromatography for the composite samples. R-BFRs have been measured by standardized chromatographic methods (Figure 1, Table 1).

The stoichiometric ratio R-BFRs/Br is 1.31 for all R-BFRs, and for decaBDE it is 1.20. Considering sampling and analytical variability, this range can be extended [1;1.5] (vertical lines in Figure 2). Only 8% of the plastics have a concentration of R-BFRs between 1 and 1.5 times the concentration of bromine in this set of data. 88% of plastic waste contains bromine from BFR(s) other than the reg-

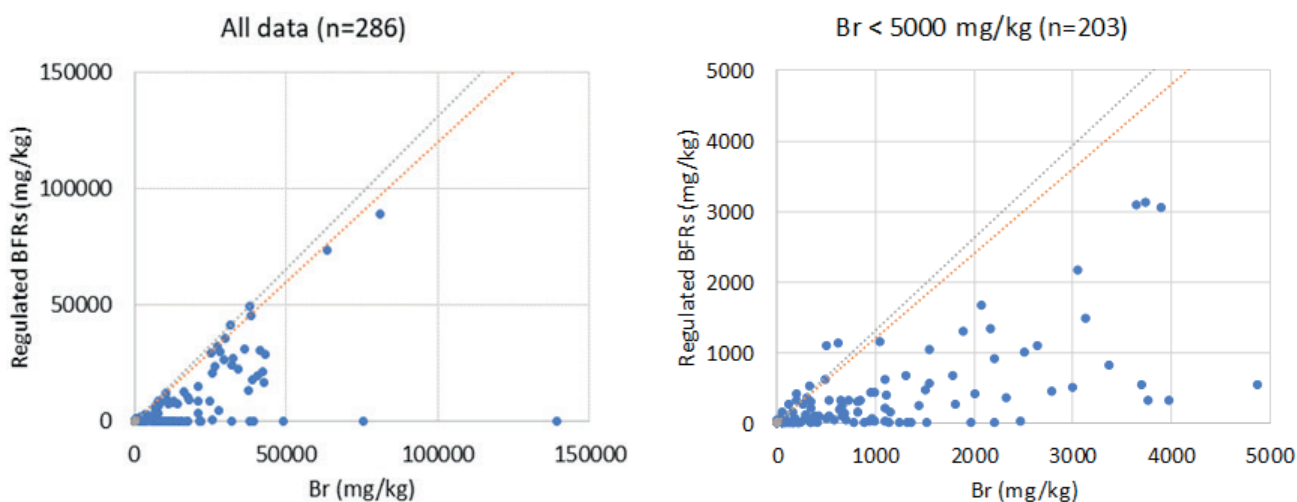


FIGURE 1: Regulated brominated flame retardants (R-BFRs) as a function of total bromine content (left) and the same data with Br ≤ 5,000 mg/kg (right), with stoichiometric ratio R-BFRs/Br of 1.20 w/w (orange line) and 1.31 w/w (grey line).

ulated ones. Only 4% of the data have a concentration of R-BFRs greater than 1.5 times the concentration of Br (with maximum R-BFRs = 1 135 mg/kg). This discrepancy is due mainly to sample preparation (i.e. the test portions of 1 gram that is used for Br and for R-BFRs measurement do not have the same composition), and secondarily to analytical variability (CVanalysis of R-BFRs = 13%, Hennebert 2019).

3.2 REACH evaluation status and hazard information of NR-BFRs substitutes

55 preparations using 34 BFR substances (other than the regulated ones) can be found in the catalogs of the three main producers, consulted in November 2019, and in the list of 418 additives. A summary is presented in Table 2 and Figure 3 and will be discussed first. Detailed results per substance are presented in Table 3.

The 2 R-BFRs and 7 NR-BFRs declared in the list of 418 additives actually used in the EU is presented in Table 4. It is not explained on the ECHA site why the two R-BFRs HBCDD and DecaBDE are included. The initiative started in 2016 and the excel file was published in 2019. The 7 NR-BFRs are included in Group 3 or Group 4 of the list established from the producer's catalog (Table 3). The correspondence is presented in the second column of Table 4.

Some substances (frequently proprietary) have no CAS number and hence no dossier can be found in the ECHA site (called here Group 1). Three of these substances are declared as not registered for sale in Europe. Another group of substances has a CAS number but has not been

declared to ECHA and has no dossier (Group 2). Another group of substances has a CAS number and a dossier, but no hazard statement codes (HSC) (Group 3). Most of their registration dossier items are just filled in as "information non available – n.a.". A fourth group of substances has a CAS number, a more complete dossier, and a HSC (Group 4). The groups are the following (Table 3):

- **Group 1:** 10 substances have no CAS number and no dossier in ECHA, among which 3 substances are not registered for sale in Europe and thus logically without

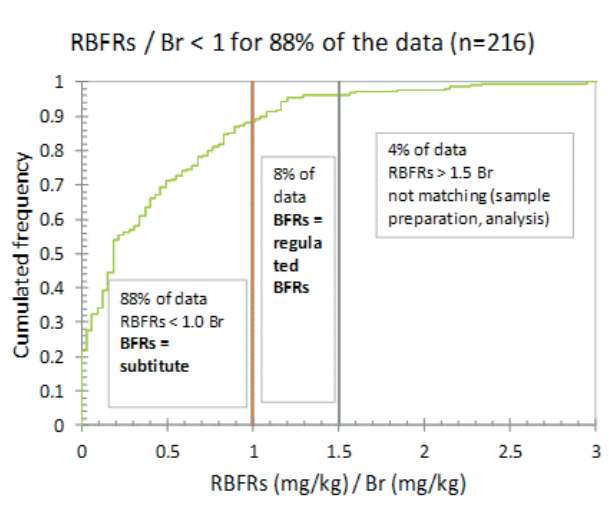


FIGURE 2: Distribution of individual R-BFRs/Br ratio (only data > LOQ) with practical R-BFRs/Br ratio including sampling and an analysis variability of 1 (orange) and 1.5 (grey)..

TABLE 1: Distributions of Br, R-BFRs and R-BFRs / Br ratio (CV coefficient of variation = relative standard deviation = standard deviation/mean).

Parameter	Unit	n	Minimum	Median	Mean	Maximum	Standard deviation	CV
Br	mg/kg	286	<10	596	7196	139000	14962	2.08
Sum R-FBRs	mg/kg	286	<10	18	3483	89200	10258	2.95
R-BFRs / Br	-	216	0.00	0.20	0.41	2.97	0.50	1.21

TABLE 2: Summary of the classification of substitutes of regulated brominated flame retardants (R-BFRs) in the REACH registration dossiers (PBT list = PBT evaluation list, ED list = ED evaluation list).

Preparations and substances	n	CAS #	n	Classification (by notifiers)	n	Classified for HP of waste (CL = concentration limit for hazardous waste)	Notifications (by ECHA)	n	Group name in this paper
Preparations (3 main producers)	55								
Substances	34	No	10*						1
		Yes	24	No dossier in ECHA site	2				2
				Dossier in ECHA site, no Hazard Statement in the dossier	10		PBT list, PBT and ED list, ED list	3+1+2****	3
				Classified with HSC	12	CL 0.1%: 2 substances** CL 0.25%: 2 substances** CL 10%: 1 substance CL 20%: 4 substances CL 25%: 2 substances no HP: 1 substance	PBT list, PBT list and ED list	1+1****	4

* Including 3 proprietary substances not registered for sale in Europe

** The 3 substances with a concentration limit for hazardous waste below the functional concentration are a reactive intermediate for high molecular weight flame retardants and will normally not be found as separate substances in plastics but are linked to the polymer matrix: dibromo neopentyl glycol (CAS 36483-57-5), tribromo neopentyl alcohol (same CAS 36483-57-5) for PU foam, and 2,4,6-tribromophenol (CAS 118-79-6) for epoxides, respectively.

*** PBT list: 2,4,6-Tris (2,4,6-tribromophenoxy) -1,3,5 triazine (CAS 25713-60-4); brominated flame retardant, aromatic, combined with an imide structure (CAS 32588-76-4); decabromodiphenyl ethane (CAS 84852-53-9). The PBT and ED list: 1,3-dibromo-5-(2-[3,5-dibromo-4-(2,3-dibromopropoxy)phenyl]propan-2-yl)-2-(2,3-dibromopropoxy)benzene (CAS 21850-44-2), ED list: 1,1'-(isopropylidene)bis[3,5-dibromo-4-(2,3-dibromo-2-methylpropoxy)benzene] (CAS 97416-84-7), 2,2-bis(bromomethyl)propane-1,3-diol (CAS 3296-90-0)

**** PBT list: 2,4,6-tribromophenol (CAS 118-79-6), PBT+ED list: 2,2',6,6'-tetrabromo-4,4'-isopropylidenediphenol (CAS 79-94-7)

CAS number = Chemical Abstracts Service number

HP = hazard property of waste

HSC = hazard statement code

PBT list = "under evaluation as persistent, bioaccumulative and toxic" by ECHA

ED list = "being assessed as an endocrine disruptor" by ECHA.

a dossier, 4 substances are declared as polymeric or an end-capped polymer (that have not been declared in the REACH system) and one substance is in pellet form (decabromodiphenylethane, the classical substitute

of banned decabromodiphenylether, which has a CAS number and a dossier, and is further detailed in Group 3). The remaining 2 substances are "Blend brominated flame retardant, diol, phosphate ester" and "Blend brominated flame retardant, halogen, phosphorus". Mixtures have not been declared, but their substances have. It is not known if the unnamed individual substances of these blends are registered;

- **Group 2:** 2 substances that have a CAS number but no dossier. These substances are polymers or building blocks for a polymer, that have not been declared in the REACH system;
- **Group 3:** 10 substances that have a CAS number and a dossier but without hazard statements and therefore not classified. The ECHA has, however, placed 6 of these substances on the PBT and/or ED list ("under evaluation as persistent, bioaccumulative and toxic" and "being assessed as an endocrine disruptor"). The most common result of these re-evaluations is that the substances are assessed as hazardous, and that the registration dossier must be modified. 3 other substances are polymers or building blocks for a polymer;
- **Group 4:** 12 substances among which 2 polymers, 2 salts of bromide Br- (potassium and ammonium), 4 tetrabromo phthalic derivatives, 2 brominated pentyl alcohols (5 carbons) and 1 bromophenol (6 carbons). The ECHA has, however, placed 2 of these substances (decabromodiphenylethane: PBT evaluation list; 2,2',6,6'-tetrabromo-4,4'-isopropylidenediphenol: PBT evaluation list + ED evaluation list).

Registration of BFRs other than POP-regulated BFRs
(55 preparations, 34 substances)

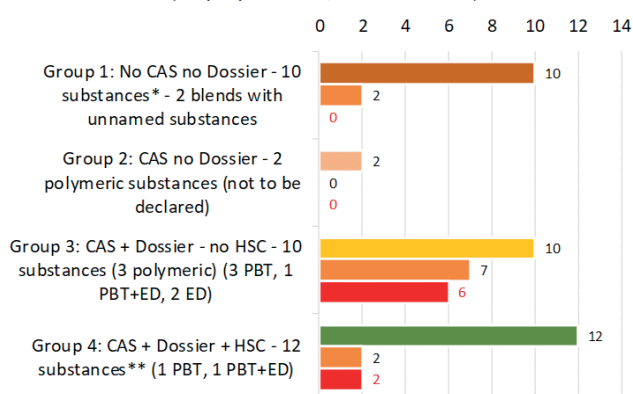


FIGURE 3: Classification of substitutes of regulated brominated flame retardants (R-BFRs) in the REACH registration dossier of ECHA. For each group: first bar: total number of substances; second bar: number of substances to assess or re-assess; third bar: number of substances under assessment by ECHA. (CAS = CAS number, Dossier = dossier in ECHA site, HSC = presence of hazard statement code of the substance, PBT = "under evaluation as persistent, bioaccumulative and toxic" by ECHA, ED = "being assessed as an endocrine disruptor" by ECHA). Notes: *3 substances not for sale in Europe, 4 polymeric, 1 physical form; ** 3 substances with functional concentration > hazardous concentration for waste.

TABLE 3: Substitutes of regulated brominated flame retardants (R-BFRs) as found in the catalogs of the three main producers, CAS number, formula, and their classification in ECHA REACH registration dossiers by the notifiers, ECHA notifications, presence of a Brief Profile (BP), hazard statement codes, corresponding concentration limit for classification as hazardous waste, lowest concentration limit and hazard property of the lowest concentration limit (HP 4 = irritant, HP 5 = toxic, HP 7 = carcinogenic, HP 11 = mutagenic, HP 14 = ecotoxic). Substances to re-evaluate are red coloured cells.

Group and Substances	Name/Note	CAS No	Formula	ECHA (Classification)	ECHA Notifications	BP	Hazard Statement Code, Concentration Limit (Waste Hazard Property)	Lowest CL	HP of lowest CL
GROUP 1 Substances: No CAS (10)									
Decabromodiphenyl ethane pellet form		No		ND					
Brominated Epoxy Polymer		No	-	ND					
Brominated polymeric flame retardant	-	No	-	ND					
End Capped Brominated Epoxy 1		No	-	ND					
Tetrabromobenzoate ester composition	(not registered for sale in Europe)	No	-	ND					
Tetrabromophthalate diol blend	(not registered for sale in Europe)	No	-	ND					
Tetrabromophthalic anhydride derivative	(not registered for sale in Europe)	No	-	ND					
Blend of brominated polystyrene and polyester		No		ND					
Blend brominated flame retardant, diol, phosphate ester		No		ND					
Blend brominated flame retardant, halogen, phosphorus		No		ND					
GROUP 2 Substances: No dossier (2)									
Brominated Butadiene/Styrene Block Copolymer		1195978-93-8	-	ND					
Poly pentabromobenzyl acrylate		59447-57-3	-	ND					
GROUP 3 Substances: No Hazard Statement (10)									
2,4,6-Tris (2,4,6-tribromophenoxy) -1,3,5 triazine		25713-60-4	C ₂₁ H ₆ Br ₉ N ₃ O ₃	No HSC	PBT list	Yes			
Brominated flame retardant, aromatic, combined with an imide structure		32588-76-4	C ₁₈ H ₆ Br ₆ N ₂ O ₄	No HSC	PBT list	Yes			
Decabromodiphenyl ethane	Ethylene-1,2-bis(pentabromophenyl); 1,1'-(ethane-1,2-diyl)bis[pentabromobenzene]	84852-53-9	C ₁₄ H ₄ Br ₁₀	No HSC	PBT list	Yes			
1,3-dibromo-5-(2-[3,5-dibromo-4-(2,3-dibromopropoxy)phenyl]propan-2-yl)-2-(2,3-dibromopropoxy)benzene		21850-44-2	C ₂₁ H ₂₀ Br ₈ O ₂	No HSC	PBT list. ED list.	Yes			
Brominated epoxy flame retardant	Pratherm EC 20	135229-48-0	-	No HSC					
Tris[3-bromo-2,2-bis(bromomethyl)propyl] phosphate		19186-97-1	C ₁₅ H ₂₄ Br ₉ O ₄ P	No HSC		Yes			
Carbonic dichloride, polymer with 4,4'-(1-methylethylidene) bis[2,6-dibromophenol], bis(2,4,6-tribromophenyl) ester	Phenoxy-terminated carbonate oligomer of Tetrabromobisphenol A	71342-77-3	-	No HSC					
Carbonic dichloride, polymer with 4,4'-(1-methylethylidene) bis[2,6-dibromophenol] and phenol	Phenoxy-terminated carbonate oligomer of Tetrabromobisphenol A	94334-64-2	-	No HSC					
1,1'-(isopropylidene)bis[3,5-dibromo-4-(2,3-dibromo-2-methylpropoxy)benzene]	Group 3; hot in catalog but in additives list	97416-84-7	C ₂₃ H ₂₄ Br ₈ O ₂	No HSC	ED list	Yes			

Group and Substances	Name/Note	CAS No	Formula	ECHA (Classification)	ECHA Notifications	BP	Hazard Statement Code, Concentration Limit (Waste Hazard Property)	Lowest CL	HP of lowest CL
2,2-bis(bromomethyl)propane-1,3-diol	Group 3; not in catalog but in additives list	3296-90-0	C ₂₃ H ₂₄ Br ₈ O ₂	No HSC	ED list	Yes			
GROUP 4 Substances: with Hazard Statement Code(s) (12)									
Dibromo neopentyl glycol		36483-57-5	C ₅ H ₁₀ Br ₂ O ₂	H302 H315 H319 H335 H340 1B H341 H350 1B H351 H373 H413		Yes	H302 25% (HP 6) H315 H319 20% (HP 4) H335 20% (HP 5) H340 0.1% (HP 11) H341 1% (HP 11) H350 0.1% (HP 7) H351 1% (HP 7) H373 - (no HP) H413 25% (HP 14)	0.10%	HP 7 HP 11
Tribromo neopentyl alcohol	2,2-dimethylpropan-1-ol, tribromo derivative	36483-57-5	C ₅ H ₉ Br ₃ O	H302 H319 H340 1B H341 H350 1B H412		Yes	H302 25% (HP 6) H315 H319 20% (HP 4) H340 0.1% (HP 11) H341 1% (HP 11) H350 0.1% (HP 7) H412 25% (HP 14)	0.10%	HP 7 HP 11
2,4,6-tribromophenol		118-79-6	C ₆ H ₃ Br ₃ O	H301 H302 H312 H315 H317 H319 H332 H335 H400 H410 H411	PBT list	Yes	H301 5% (HP 6) H302 25% (HP 6) H312 55% (HP 6) H315 H319 20% (HP 4) H332 22.5% (HP 6) H335 20% (HP 5) H400 25% (HP 14) H410 0.25% (HP 14) H411 25% (HP 14)	0.25%	HP 14 (H410)
Potassium bromide		7758-02-3	BrK	H315 H318 H319 H335 H336 H373 H412		Yes	H315+H319 20% (HP 4) H318 10% (HP 4) H335 20% (HP 5) H336 - (no HP) H373 10% (HP 5) H412 25% (HP 14)	10%	HP 4 HP 5
Ammonium bromide		12124-97-9	BrH ₄ N	H315 H319 H335		Yes	H315+H319 20% (HP 4) H335 20% (HP 5)	20%	HP 4 HP 5
Bis(2-ethylhexyl) tetrabromophthalate	Tetrabromophthalate ester	26040-51-7	C ₂₄ H ₃₄ Br ₄ O ₄	H319			H315+H319 20% (HP 4)	20%	HP 4
Brominated Epoxy Oligomery	Tetrabromobisphenol A diglycidyl ether, Brominated Epoxy Polymer	68928-70-1	-	H315 H319			H315+H319 20% (HP 4)	20%	HP 4
Brominated Polystyrene, acrylate copolymer	Benzene, ethenyl-, homopolymer, brominated	88497-56-7	-	H319			H315+H319 20% (HP 4)	20%	HP 4
2-(2-hydroxyethoxy)ethyl 2-hydroxypropyl 3,4,5,6-tetrabromophthalate	Tetrabromophthalate diol, Tetrabromophthalate diol	20566-35-2	C ₁₅ H ₁₆ Br ₄ O ₇	H412		Yes	H412 25% (HP 14)	25%	HP 14 (H412)
Reaction products of tetrabromophthalic anhydride with 2,2'-oxydiethanol and methyloxirane		77098-07-8	-	H412		Yes	H412 25% (HP 14)	25%	HP 14 (H412)
Tetrabromophthalic anhydride		632-79-1	C ₈ Br ₄ O ₃	H317		Yes	H317 - (no HP)	no CL	no HP
2,2',6,6'-tetrabromo-4,4'-isopropylidenediphenol	Group 4; not in catalog	79-94-7	C ₁₅ H ₁₂ Br ₄ O ₂	H400 H410	PBT list, ED list, ED	Yes	H400 25% (HP 14) H410 0.25% (HP 14)	0.25%	HP 14 (H410)

BP = Brief Profile on ECHA site (a summary document on properties and classification of the substance)

ED list = "Under assessment as Endocrine Disrupting"

HSC = hazard statement code

ND = no dossier

PBT list = "Under assessment as Persistent, Bioaccumulative and Toxic"

(HP 14 calculated without multiplying "M-factors")

TABLE 4: Brominated flame retardants (BFRs) declared in the list of 418 plastic additives actually used in the EU.

Group and Substances	Name/Note	CAS No	Formula	ECHA (Classification)	ECHA Notifications	BP	Hazard Statement Code, Concentration Limit (Waste Hazard Property)	Lowest CL	HP of lowest CL
Hexabromocyclododecane	Not in the scope of this paper	25637-99-4			POP+others	Yes			
Bis(pentabromophenyl) ether	Not in the scope of this paper	1163-19-5			POP+others	Yes			
2,4,6-tris(2,4,6-tribromophenoxy)-1,3,5-triazine	Group 3; in catalog	426-040-2 (No CAS number in the file)	C ₂₁ H ₆ Br ₉ N ₃ O ₃	No HSC	PBT	Yes			
1,1'-(ethane-1,2-diyl)bis[pentabromobenzene]	Group 3; in catalog	84852-53-9	C ₁₄ H ₄ Br ₁₀	No HSC	PBT	Yes			
N,N'-ethylenebis(3,4,5,6-tetrabromophthalimide)	Group 3; in catalog	32588-76-4	C ₁₈ H ₄ Br ₈ N ₂ O ₄	No HSC	PBT	Yes			
1,1'-(isopropylidene)bis[3,5-dibromo-4-(2,3-dibromopropoxy)benzene]	Group 3; in catalog	21850-44-2	C ₂₁ H ₂₀ Br ₈ O ₂	No HSC	PBT, ED	Yes			
1,1'-(isopropylidene)bis[3,5-dibromo-4-(2,3-dibromo-2-methylpropoxy)benzene]	Group 3; not in catalog	97416-84-7	C ₂₃ H ₂₄ Br ₈ O ₂	No HSC	ED	Yes			
2,2-bis(bromomethyl)propane-1,3-diol	Group 3; not in catalog	3296-90-0	C ₂₃ H ₂₄ Br ₈ O ₂	No HSC	ED	Yes			
2,2',6,6'-tetrabromo-4,4'-isopropylidenediphenol	Group 4; not in catalog	79-94-7	C ₁₅ H ₁₂ Br ₄ O ₂	H400 H410	PBT, ED	Yes	H400 25% (HP 14) H410 0.25% (HP 14)	0.25%	HP 14 (H410)

BP = Brief Profile on ECHA site (a summary document on properties and classification of the substance)

ED list = "Under assessment as Endocrine Disrupting"

HSC = hazard statement code

PBT list = "Under assessment as Persistent, Bioaccumulative and Toxic"

(HP 14 calculated without multiplying "M-factors")

The substances for which the dossier must be completed, or which are reassessed (according to the REACH regulation), are: the substances of 2 blends of Group 1, 7 substances (6 with ECHA notification) of Group 3, and 2 substances (with ECHA notification) of Group 4. Since there are mixtures, the total substances used that have to be assessed is 11 (or more depending on the composition of the 2 blends) out of 34, of which 8 are notified by the ECHA.

The classification of product plastics incorporating these additives (according to the CLP) is beyond the scope of this study. For the simpler waste classification, the functional concentration of the additives in the plastics (recommended in the technical specifications) can be compared to the concentration that renders a waste hazardous (according to the waste regulations of EU 2014 and EU 2017).

In detail for the 12 classified substances (Table 3, Group 4), the number of substances, the concentration limits and the hazardous properties (for waste) are:

- 2 with 0.1% (for HP 7 'Carcinogenic' and HP 11 'Toxic for reproduction');
- 2 with 0.25% (HP 14 'Ecotoxic' chronic "high level");
- 1 with 10% (HP 4 'Irritant' and HP 5 'Toxic');
- with 20% (HP 4 and / or HP 5), and
- 3 with 25% (HP 14 'Ecotoxic' acute).

The two substances with a concentration limit of 0.1% are neopentyl tribromo alcohol [H350 0.1% (HP 7), H340 0.1% (HP 11), H341 1% (HP 11)] and dibromo neopentyl

glycol [H350 0.1% (HP 7), H351 1% (HP 7), H341 1% (HP 11)]. The substances with a concentration limit of 0.25% are 2,4,6 tribromophenol and 2,2',6,6'-tetrabromo-4,4'-isopropylidenediphenol [0.25% H410 (HP 14)]. According to their producer, the first three substances are used as a reactive intermediate for high molecular weight flame retardants, especially for rigid and flexible PU foam (the first two) and for the capping of brominated epoxides (the latter) (Table 5). These substances should normally not be found as separate substances in plastics but linked to the polymer matrix.

The 5 substances from the producer's catalog with ECHA notifications of assessment are presented in Table 6 with the information from their producer. Four substances are declared "additive" (they are miscible with the polymer but remain extractable and quantifiable) and they have 14 to 21 carbons. One substance (tribromophenol) is "reactive" (it will bind to the polymer and will not be found as a separate substance in a laboratory analysis) and has 6 carbons. Decabromodiphenylethane, the substitute of decabromodiphenylether, present in the catalog of the three producers, and widely used today, is declared without hazard statement codes, but is under assessment in the PBT evaluation list of the ECHA.

To conclude, out of a total of 34 substances, 2 blends do not have a CAS number and dossier (Group 1), 7 substances have a CAS number and a dossier but are without any hazard statement (Group 3), among which 6 are under assessment by the ECHA, and 12 have a CAS number, a dossier and a hazard statement (Group 4), among which

TABLE 5: Producer information on NR-BFRs with functional concentration greater than the concentration limit that renders a waste hazardous.

Substance	Name	Abbreviation / Brand Name	Brand Name 2 - Note	CAS No	Formula	Category
Dibromoneopentyl glycol		FR-522	FR-522, is a reactive, dibromoneopentyl glycol, flame retardant, containing 60% aliphatic bromine. Thermosetting polyester resins formulated with FR-522 have high chemical and flame resistance, minimal thermal discoloration and excellent light stability. The high bromine content of FR-522 and its ready reaction into polyurethanes make it suitable for use in rigid polyurethane foams...	36483-57-5	C ₅ H ₁₀ Br ₂ O ₂	Reactive
Tribromoneopentyl alcohol	2,2-dimethylpropan-1-ol, tribromo derivative	FR-513	FR-513 is a reactive flame retardant containing 73% aliphatic bromine. As tribromoneopentyl alcohol it combines a high bromine content with exceptional stability, and is particularly suitable where thermal, hydrolytic and light stability are required. FR-513 high solubility in polyurethane systems increases effectiveness as a reactive flame retardant for polyurethanes...	36483-57-5	C ₅ H ₃ Br ₃ O	Reactive
2,4,6-tribromophenol		FR-613	FR-613 is a reactive flame retardant with a high content of aromatic bromine, used mainly as an intermediate for high molecular weight flame retardants. It is also an effective fungicide and wood preservative. ...	118-79-6	C ₆ H ₃ Br ₃ O	Reactive

2 are under assessment by the ECHA. Eleven substances or more (due to the use of two blends) are re-assessed or could be re-evaluated in the future, and eventually restricted. The 7 non-POP NR-BFRs on the official list of plastic additives are currently being re-evaluated by the ECHA (3 PBT, 2 ED, 2 PBT + ED) (Table 4).

4. CONCLUSIONS

The regulated R-BFRs have been logically substituted by other non-regulated NR-BFRs. In this numerous data set, 88% of the product and waste samples contain BFR(s) other than the regulated ones.

The European Chemical Agency (ECHA) dossiers of these substances show that:

- 12 substances have no dossier (including polymers that must not be declared, and 3 substances not for sale in Europe);
- 10 substances have a dossier without hazard statements and are therefore not classified: The ECHA has, however, placed 6 of these substances on the PBT evaluation list (“under evaluation as persistent, bioaccumulative and toxic”) and the ED evaluation list (“being assessed as an endocrine disruptor”);
- 12 substances have a dossier and hazard statements (including 3 polymeric substances); however, the ECHA has placed 2 of these substances on the PBT evaluation list and ED evaluation list;
- The 3 substances that have a functional concentration (the concentration of additives that retards flame) greater than the concentration limits classifying a waste as hazardous, are declared as “reactive”: they will bind to the polymer during their use and will not be independent substances anymore;
- The 7 non-POP NR-BFRs on the official list of plastic additives are currently being re-evaluated by ECHA (3 PBT, 2 ED, 2 PBT + ED).

As substitution is going faster than classification and regulation, and as homologous substances are used (for instance decabromodiphenylethane / decabromodipheny-

lether), all these new NR-BFRs should be investigated and their properties on human health and the environment assessed and published, as already done for some, with the European Chemicals Agency (ECHA).

Total bromine is a relevant surrogate indicator of the presence of total BFR(s) in plastic waste, even if the brominated substances are not known and the new substances are currently not monitored for most samples. The technical limit of 2,000 mg Br/kg as the maximum content for further recycling (EN 50625-3-1) takes into account all brominated substances regulated and not yet regulated, and therefore limits the recycling of BFRs that are not currently properly registered. Similar work should be done on phosphorus substitutes.

ACKNOWLEDGMENTS

This work has been supported by INERIS and by the Ministry for Ecologic Transition, France

REFERENCES

- Albemarle 2018. Fire Safety Solutions – Product Selector Guide. <https://www.albemarle.com/businesses/bromine-specialties/fire-safety-solutions>. Product information sheets consulted December 2020.
- Beggio G, Hennebert P. 2021. Sampling and sub-sampling of granular waste: Part 2 - Size of a representative sample in terms of number of particles with different distributions of particle concentration and particle size. Submitted to Detritus.
- Charbonnet J, Weber R, Blum A (2020) Flammability standards for furniture, building insulation and electronics: Benefit and risk. *Emerging Contaminants* 6, 432-441, <https://doi.org/10.1016/j.emcon.2020.05.002>
- Chemtura Great Lakes Solution - Great Lakes Solution 2017. LANXESS Bromine Solutions. Flame retardants product guide. Consulted January 2018. Product information sheets consulted December 2020. http://add.lanxess.com/fileadmin/user_upload/Flame_Retardants_product_guide_04-2017.pdf
- Chen SJ, Ma YJ, Wang J, Chen D, Luo XJ, Mai BX. Brominated flame retardants in children's toys: concentration, composition, and children's exposure and risk assessment. *Environ Sci Technol*. 2009 Jun 1;43(11):4200-6. doi: 10.1021/es9004834.
- EN 50625-3-1:2015 Requirements for the collection, logistics and treatment of WEEE - Part 3-1: Specification relating to depollution - General. CENELEC, Brussels, Belgium.

TABLE 6: Producer information on NR-BFRs with ECHA notifications.

Substance	Abbreviation / Brand Name	Brand Name 2 - Note	CAS No	Formula	ECHA Notifications	Category
2,4,6-Tris (2,4,6-tribromophenoxy) -1,3,5 triazine	FR-245	FR-245 is a proprietary, additive flame retardant. The combination of aromatic bromine and cyanurate provides high FR efficiency and good thermal stability. A major use of FR-245 is in ABS and HIPS. FR-245 combines good UV, impact and flow properties...	25713-60-4	C ₂₁ H ₆ Br ₉ N ₃ O ₃	PBT evaluation list	Additive
Brominated flame retardant, aromatic, combined with an imide structure	SAYTEX® BT-93 Bromine-based flame retardant for electronic enclosures, electrical components, films, and textiles that require the highest degree of UV stability (light yellow powder form). SAYTEX® BT-93W Bromine-based flame retardant for electronic enclosures, electrical components, films, and textiles that require outstanding thermal and UV stability (white powder form)	SAYTEX BT-93 flame retardant is a unique additive that combines stable, aromatic bromine with an imide structure. SAYTEX BT-93W flame retardant is a unique, white-colored additive that combines stable, aromatic bromine with an imide structure	32588-76-4	C ₁₈ H ₄ Br ₈ N ₂ O ₄	PBT evaluation list	Additive
Decabromodiphenyl ethane	Firemaster® 2100R		84852-53-9	C ₁₄ H ₄ Br ₁₀	PBT evaluation list	Additive
	SAYTEX® 8010 Bromine-based flame retardants for electronic enclosures, electronic and electrical components, insulation foams and textiles (powder form)	SAYTEX 8010 flame retardant is a non-diphenyl oxide-based product containing a high level of aromatic bromine				
	FR-1410	Decabromodiphenyl Ethane FR-1410 is an additive flame retardant containing 82% aromatic bromine. Its high bromine content coupled with its exceptional thermal stability makes it the material of choice for a large variety of applications. Major application areas include HIPS, Low and High Density Polyethylene, Polypropylene (Homopolymers and Copolymers), Elastomers, PBT, Polyamides, UPE and Epoxy...				
1,3-dibromo-5-(2-[3,5-dibromo-4-(2,3-dibromopropoxy)phenyl]propan-2-yl)-2-(2,3-dibromopropoxy) benzene	FR-720	FR-720 is an additive flame retardant containing both aromatic and aliphatic bromine. FR-720 is suitable for polyolefin and styrenic resins and it is especially recommended for UL-94 class V-2. It is also applicable in class V-0 polypropylene. FR-720 is cost efficient and maintains good physical properties of the compound...	21850-44-2	C ₂₁ H ₂₀ Br ₈ O ₂	PBT evaluation list, ED evaluation list	Additive
2,4,6-tribromophenol	PH-73FF™	PH-73FF™ is a reactive intermediate containing over 70% bromine recommended for phenol-based reactions in a free-flowing briquette form. PH-73FF™ by Lanxess is a free flowing, non-caking, low dusting, halogenated, flame retardant. It is a reactive intermediate containing over 70% bromine recommended for phenol-based reactions in a free-flowing briquette form. PH-73FF™ possesses uniform size & shape and high bulk density. It is also used as an antifungal agent (with FIFRA approval) or chemical intermediate.	118-79-6	C ₆ H ₃ Br ₃ O	PBT evaluation list	Reactive
	FR-613	FR-613 is a reactive flame retardant with a high content of aromatic bromine, used mainly as an intermediate for high molecular weight flame retardants. It is also an effective fungicide and wood preservative. ...				

PBT evaluation list: Under assessment as Persistent, Bioaccumulative and Toxic; ED evaluation list: Under assessment as Endocrine Disrupting

- EU 2014. Commission Decision 2014/955/EU of 18 December 2014 amending Decision 2000/532/EC on the list of waste pursuant to Directive 2008/98/EC of the European Parliament and of the Council.
- EU 2017. Council Regulation (EU) 2017/997 of 8 June 2017 amending Annex III to Directive 2008/98/EC of the European Parliament and of the Council as regards the hazardous property HP 14 'Ecotoxic'. Official Journal of the European Union. 14.6.2017. L 150/1.
- Fantke P, Weber R, Scheringer M (2015) From incremental to fundamental substitution in chemical alternatives assessment. *Sustainable Chemistry and Pharmacy* 1, 1-8. DOI: 10.1016/j.scp.2015.08.001
- Haarman A, Magalini F, Courtois J. 2020. SOFIES. Study on the Impacts of Brominated Flame Retardants on the Recycling of WEEE plastics in Europe. SOFIES for BSEF. 44 p.
- Hennebert P, Beggio G. 2021. Sampling and sub-sampling of granular waste: Part 1 - Size of a representative sample in terms of number of particles and application to waste containing rare particles in concentration. Submitted to *Detritus*.
- Hennebert P. 2019. Sorting of waste for circular economy: sampling when (very) few particles have (very) high concentrations of contaminant or valuable element (with bi- or multi-modal distribution). 17th International Waste Management and Landfill Symposium (Sardinia 2019), 30/09 – 04/10/2019, Cagliari, Italy.
- Hennebert P. 2020. Concentrations of brominated flame retardants in plastics of electrical and electronic equipment, vehicles, construction, textiles and non-food packaging: a review of occurrence and management. *Detritus*. DOI 10.31025/2611-4135/2020.13997 <http://eurlex.europa.eu/legalcontent/EN/TXT/PDF/?uri=CELEX:32014D0955&rid=1>
- ICL Industrial products. 2012. Fire protection for automotive and transportation. 6 p. <http://icl-ip.com/wp-content/uploads/2012/10/FR-Transportation-2012.pdf> ; http://icl-ip.com/segment_category/automotive/ . Product information sheets consulted December 2020.
- Lucas D, Petty SM, Keen O, Luedeka B, Schlummer M, Weber R, Barlaz M, Yazdani R, Riise B, Rhodes J, Nightingale D, Diamond ML, Vijgen J, Lindeman A, Blum A, Koshland CP (2018) Methods of Responsibly Managing End-of-Life Foams and Plastics Containing Flame Retardants: Part I *Environmental Engineering Science* 35 (6), 573-587 <https://doi.org/10.1089/ees.2017.0147>
- Wagner S, Schlummer M (2020) Legacy additives in a circular economy of plastics: Current dilemma, policy analysis, and emerging countermeasures. *Resources, Conservation & Recycling* 158 (2020) 104800. <https://doi.org/10.1016/j.resconrec.2020.104800>

IMPLEMENTATION STAGE FOR CIRCULAR ECONOMY IN THE DANISH BUILDING AND CONSTRUCTION SECTOR

Lisbeth M. Ottosen ^{1,*}, Lotte B. Jensen ¹, Thomas F. Astrup ², Tim C. McAlloone ³, Morten Ryberg ⁴, Christian Thuesen ⁴, Søren Lütken ⁴, Solbritt Christiansen ⁵, Anne J. Damø ⁶ and Mads H. Odgaard ⁷

¹ Department of Civil Engineering, Technical University of Denmark, Building 118, Lyngby 2800, Denmark

² Department of Environmental Engineering, Technical University of Denmark, Building 115, 2800 Lyngby, Denmark

³ Department of Mechanical Engineering, Technical University of Denmark, Building 404, 2800 Lyngby, Denmark

⁴ Department of Technology, Management and Economics, Technical University of Denmark, Building 424, 2800 Lyngby, Denmark

⁵ Department of Engineering Technology, Technical University of Denmark, Laurrupvang 15, 2750 Ballerup, Denmark

⁶ Department of Chemical Technology, Technical University of Denmark, Building 229, 2800 Lyngby, Denmark

⁷ Office for Research, Advice and Innovation, Technical University of Denmark, Building 101, 2800 Lyngby, Denmark

Article Info:

Received:

2 March 2021

Revised:

7 June 2021

Accepted:

14 June 2021

Available online:

11 September 2021

Keywords:

Circular economy

Construction and building sector

Scaling of solutions

ABSTRACT

The building and construction sector is selected by the European Commission as a key product value chain in the transition towards circular economy (CE) due to the major resource consumption, waste generation and GHG emissions from this sector. This paper reports the result from qualitative and semi-structured interviews with 30 Danish stakeholders from the sector on the current stage of implementation of CE and the research/innovation needs to scale circular construction from niche to the new normal. The interviews showed a large variety in the stakeholder's stage of transition from hardly knowing the term to having CE as a major driver in their business. Some meant that scaling of CE is close to impossible and that material reuse will never develop to more than a niche, whereas others already offer full-scale circular solutions to clients. The interviews pointed at a need for a common definition and terminology for CE, methods for documenting the gains from the circular solutions (economic and environmental), methods for technical documentation of the quality of reused materials, processes which enables scaling, methods to implement CE in various systems such as digitalization and building passports, new value chains and framework conditions in support of circularity. Regardless these needs, few demonstration projects of major importance to gain general knowledge have been finalized or are planned in Denmark. These demonstrations have different approaches: using today's waste from different industries as construction materials; reusing construction materials (the basic building, elements or processed materials); and designing new buildings for disassembly to enable future reuse.

1. INTRODUCTION

The World's population in 2020 stands at 7.8 billion (Worldometer, 2021) people and it is projected to increase to 8.5 billion in 2030 (United Nations, 2015). With rising income and living standards, global consumption of resources such as minerals, metals and food crops increases, generating pressures on natural resources and the environment (OECD 2012). The situation is alarming and politicians at all levels point at circular economy (CE) as the only viable solution. At European level, "The circular economy package" adopted by the Commission (European Commission, 2015), created an important momentum to support the transition towards CE, and the recent "Circular

Economy Action Plan for a Cleaner and More Competitive Europe" (European Commission, 2020)" continues and strengthen the strategy. The CE is a concept of reducing the ecological footprint by finding new concepts of the flow of matter in manufacturing processes, assuming its closed loop. The transition towards a sustainable CE model is by many seen as a solution to keep the consumption of the Earth's resources within planetary boundaries.

Building and construction is pointed out as a key product value chain in the transition towards CE in the EU (European Commission, 2015, 2020) (Hertwich, 2021). The sector requires vast amounts of resources - it accounts for about 50% of all extracted material. At the same time, the



* Corresponding author:
Lisbeth M. Ottosen
email: lo@byg.dtu.dk



sector is responsible for over 35% of the EU's total waste generation. Greenhouse gas emissions (GHG) from material extraction, manufacturing of construction products, construction and renovation of buildings are estimated at 11% of total national GHG emissions (UNEP 2019). Greater material efficiency could save about 80% of those emissions according to (European Commission, 2020). The major importance of the construction and building sector for the consumption of natural resources, the GHG emissions and waste generation are strong incitements for transforming the sector towards a CE.

At company level, moving towards CE (and other sustainability-driven business models) requires a fundamental change that runs through its entire organization and it also involves its stakeholders (Ritzén & Sandström, 2017). CE in the building sector may be considered at different stages: (1) parts that can be reused as a whole without any extra processing, (2) reused parts of the construction that need to be remanufactured, and (3) parts that require a process of recycling, e.g. after a demolition of buildings, building materials are shredded and reprocessed into new elements (Gorecki, 2018).

The major interest and awareness within research in transforming the construction and building sector to a CE can be seen from the large number of comprehensive literature surveys on the topic, e.g. (Benachio et al. 2020), (López Ruiz et al. 2020), and (Mhatre et al 2021). Mhatre et al. (2021) describes how the number of research papers within CE in the built environment have been increasing. Since the first research article on this topic was published in 2007, there has been an incremental rise in the number of publications and especially after 2016 (there were 105 papers in the first half of 2020). Thus, the research community around the topic is growing. To establish a vision it is important to both understand the current situation - e.g. what is already being done towards CE, or what capabilities provide a basis for this, as well as to identify what opportunities are present and desirable (Blosma et al 2019). In the acknowledgement of this, the work reported in this paper sets off in interviewing the construction and building sector itself, and on the description of the transformation seen from the inside towards the larger perspectives. Major findings from a sector development project "Circular construction and building sector" are reported – a project, which takes off in the Danish construction sector's own understanding of challenges, barriers and opportunities in the transition towards CE. A major aim is to identify the challenges faced by the sector itself and to evaluate the research and innovation that can aid meeting these challenges.

2. METHOD

At the Technical University of Denmark (DTU), the board of directors decided (2019) to conduct the sector development project "Circular construction and building sector" presented in this paper. The DTU procedure for such projects is to frame and focus the topic on collaboration with the major relevant Danish associations, which are also project owners. A local, interdisciplinary university team is set. This team is responsible for the execution of the project.

The core of the project is a series of interviews with different stakeholders. The university team compiles the findings from the interviews. The outcome of the interviews is presented at a workshop where the associations, the interviewed persons and the university team meet and discuss the compiled result. The common conclusions are drawn on basis of the inputs from the workshop. The outcome is published in a report (in Danish), which for the present sector development project is planned for the spring 2021.

The Danish associations in the present project were the Danish Association of Architectural Firms (www.danskeark.dk), the Danish Construction Association (www.danskyggeri.dk), the Federation of Danish Building Industries (www.danskindustri.dk/brancher/di-byg), the Danish Association of Consulting Engineers (www.frinet.dk) and SEGES (www.seges.dk). The associations suggested different, specific stakeholders for interviews based on their relative importance in the industry and maturity on circular practices. Altogether 30 interviews were conducted among Danish construction clients, architectural companies, consulting engineering companies, construction material producers, contracting companies, public institutions (waste management and recycling, authorities e.g. municipalities responsible of building facility management) and trade associations. Few selected public institutions and organizations in the Netherlands and Belgium were interviewed as well to set the Danish findings in perspective with other countries driving the circularity agenda. The stakeholders were interviewed one by one by 1-4 members of the research team. The interviews were qualitative and semi-structured (Brinkmann & Kvale 2018) each lasting 1-2 hours and based on a common question guide with 17 questions organized in 2 sections and 4 themes.

The first section of questions, three in number, were clarifying questions about the company/institution (value creation from products/services, customers/users and national/international market).

The second section of questions were focused around CE and had a sequence of themes to be covered:

- Burning platform. Is there a burning platform in Denmark and internationally? What is it? Which part of the build environment constitutes the major needs/possibilities?
- Tendencies related to CE. Questions on which tendencies were seen within major topics of CE from the key words: recirculation, building design, building passes, economy and environmental assessments, value chains, digitalization, city and regional perspectives, scaling of solutions, standardization, incitement, procurement rules, risk and responsibility, and the role of technology.
- Transformation towards CE: This group of questions had the key words: visions, necessary leadership, requests to society, challenges and possibilities, export options
- Research and innovation needs: The major challenges and also specifically the major research needs. The companies were also asked about their experiences on collaboration with researchers.

Due to the semi structured nature of the interviews, there was openness to change the sequence and questioning form. The interviews had periods with dialog on the answers and stories told by the interviewees until the themes from the interview guide were covered. After each interview, the core findings were documented and summarized. The analysis was undertaken by the research team enabling triangulation of data and theoretical perspectives given the interdisciplinary organization of the team. The findings were subsequently validated through an online workshop with participation of the interviewed persons, the five associations and the university researchers. The results from the interviews were outlined and discussed.

The university departments involved in the project were DTU Civil Engineering, DTU Environment, DTU Mechanical Engineering, DTU Management, DTU Engineering Technology, and DTU Chemical Engineering. The project is led by the DTU Office for Research, Advice and Innovation. The core of the interdisciplinary university team were the authors of this paper.

3. RESULTS

3.1 General status on CE in the Danish construction and building sector

Through the 30 interviews, it was evident that there is a lack of common understanding of the term CE in the Danish construction and building sector. This even though the EU has pointed at the sector as a key value chain in the transition. The lack is in line with what has been reported in literature on a broader term, e.g. (Kirchherr et al 2017) states from a review of more than hundred papers and reports that CE means different things to different people. A basic explanation for a CE economy is 'where the value of products, materials and resources is maintained in the economy for as long as possible, and the generation of waste minimised' (European Commission, 2015). In (Kirchherr et al 2017) CE is defined as "an economic system that replaces the 'end-of-life' concept with reducing, alternatively reusing, recycling and recovering materials in production/distribution and consumption processes". Thus the core of CE is based on material and resource use. However, in the interviews, the companies often equaled CE to GHG emissions or UNs 17 SDGs in general terms.

3.2 The sector about the burning platform

The burning platform identified by the companies was related to the major trends threatening the state of the globe, mainly GHG emissions but also increasing population and following resource scarcity and waste generation was often mentioned. However, these megatrends were not translated into a direct burning platform for the companies themselves necessitating their transition towards CE, i.e. the companies did not mention at all that they felt a push towards taking any action themselves. For the interviewed companies already active in implementing CE (partly or a more thorough reorganization) the basis for doing so was established on an idealistic standpoint or because adapting CE was seen as a way to specialize and thus as a business opportunity.

When describing challenges close to the stakeholders, the loss of common craftsmanship during the past 50 years of industrialization of the construction sector was mentioned from a few of them as a coming need to cope with in relation to a transition to CE. From some of the large engineering companies it was also mentioned that attracting young people depends increasingly on having a green profile and that the change in mindset will grow from the young generation. Throughout the interviews there was no specific part of the built environment which was pointed out to constitute the major needs/possibilities in relation to CE, however it was mentioned, that the transformation must include both renovation and new buildings.

3.3 The sector on the transformation towards CE

The possibility for scaling CE from being a niche to common practice was often brought up during the interviews. Some believed that scaling of CE in construction is close to impossible in practice and thus that material reuse will never develop to more than a niche, whereas others believed that it was definitely possible to scale the construction with reused materials and that it will be the new normal. Many pointed and responsibility when reusing or using recycled materials was pointed out as a major obstacle. As materials and components directly reused are not certified, the accompanied risk needs to be assumed by the construction client or the consulting engineering company. Standardization was suggested as the way forward. Many of the interviewed persons expressed that as long as the circular solutions are more expensive than today's linear solutions, a general transformation to CE will not happen.

At the final common workshop, which gathered the interviewed persons, strong emphasis was laid on a national road map as a tool to move the sector forward. A vision of transforming Denmark to a living lab for CE in the construction industry was brought forward and supported by many of the participants.

3.4 The sector on major challenges and research needs

A major objective of the present sector development project was to identify the technological challenges and research/innovation needs that sector is facing in relation to a transition to CE, and hereby to foster concrete ideas for collaboration between universities and companies. Those of the companies, who were experienced in working with university researchers pointed at common MSc and PhD students as a good way of collaboration. The conducted interviews pointed at the need for:

- Common definition and terminology for circular economy;
- Methods for documenting the value (economic and environmental) of circular materials and building processes;
- Technical knowledge on minimizing the risk when choosing to reuse or recycle construction materials;
- Implementation of circular solutions in digital tools (such as BIM) as well as in material- and building passports;

- Circular processes which can enable scaling;
- Methods to ensure full circularity of materials and building elements;
- Systems for connecting value chains in the building and construction industry with other adjacent value chains.
- Framework and conditions for tendering, services, building regulations etc. for support to circularity

4. DISCUSSION

The fast-growing awareness of CE to be the strategy to follow to simultaneously combat resource depletion and lower the GHG emissions as well as waste generation, and the major role of the building and construction sector both as part of the problem and thus also a part of the solution, necessitate revisiting the current practice in the sector, which is built on a linear use of materials. The interviews in the current investigation showed that the Danish construction and building sector was aware of the sectors responsibility in relation to a more sustainable society. All the interviewed persons showed interest (and most also enthusiasm) in the developments combating the global threats, but many expressed reservations whether the sector in general and not at least the building owners will value environmental concerns before economy. This was seen as a major obstacle. Lopéz Ruiz et al. (2020) reviewed the transformation of the construction and demolition sector to a CE, and concluded that research in this sector has mainly focused on aspects regarding reuse and recycling from an environmental performance perspective and that the integration of economic criteria is still limited. Thus the attention to the limited focus on economic issues in the transition, raised from the interviewed persons, is an issue beyond the Danish sector.

The CE agenda does not apply only to closing the loop and use “waste as resource”. The transition to a CE can be achieved through an agenda integrating three strategies a) closing resource loops via recycling along the material value chain b) narrowing loops i.e. increasing resource efficiency by using less material input for production and producing less waste for final disposal, and c) slowing loops i.e. lengthening the use phase via development of long-life goods and materials and product-life extension measures (Baldassarre et al 2019). These three strategies are in line with the waste hierarchy, i.e. reduce, reuse, recycle and recover (European Parliament and the Council, 2008). Academia as well as practitioners use the waste hierarchy as basis for development of a CE framework (Prieto-Sandoval et al. 2018). Those of the interviewed persons, who did not automatically equate CE to lowering CO₂ emissions or SDGs, were focused around closing the loops. Neither of the interviewed included narrowing or slowing loops in their reflections.

One of the needs pointed out by many of the interviewed, was the need for a common definition and understanding of CE as well as standardization. Recently, the Danish Standards was appointed (December 2020) by CEN to lead and run a new European technical committee on CE related to the building sector - CEN/TC 350/SC1 circular economy in the construction sector. As a first step, a framework for

the CE terminology will be developed so that there is common international agreement on what is meant by CE in the sector. Thus work is in progress on developing a common international terminology, and this must be considered very important step in order for the sector to unite in the transition, which is already a political strategy nationally and in the EU. Pointing at standardization as major important, the Danish sector was in line with the general viewpoint, as e.g. Benachio et al (2020) reported from a systematic literature review that the consensus is that there is good level of awareness of the need of change from the linear to the CE in the construction industry, however practitioners argue about the lack standardized methods and practices to help them implement in their construction projects.

5. CONCLUSIONS

The state of the transformation to CE of the Danish construction and building sector was the focus in the current project initiated by the Technical University of Denmark. Five trade associations were involved in framing the project, and 30 interviews were carried out with different stakeholders in the sector. The interviews showed lack of common definition for CE in the sector, that the companies were at different stages in the transition (some had no actual plans whereas others had CE as the main driver for business), and that clarification of risk/responsibility issues is necessary at many levels in order to implement CE in the sector. This point to a second conclusion regarding the sectors own viewpoint of having incomplete or insufficient measures to determine pathways for the changes required by the sector. Important demonstration projects have been build or are planned, however, to scale and to common practice the interviews pointed at needs for: methods for documenting the economic and environmental gains, technical methods for documenting the quality of reused materials, processes which enables scaling and development of new value chains. The interviews also indicated that it may be necessary to update the framework conditions so they support the transformation to CE, and some pointed at a need for an external push to move the sector towards a CE.

ACKNOWLEDGEMENTS

The board of directors at DTU for choosing “Circular construction and building” as theme. Danish Association of Architectural Firms, the Danish Construction Association, the Federation of Danish Building Industries, the Danish Association of Consulting Engineers and SEGES for the collaboration on framing the project. We are grateful to all interviewed persons for open and inspiring sharing of knowledge and viewpoints.

REFERENCES

- Baldassarre, B., Schepers, M., Bocken, N., Cuppen, Korevaar, G., Calabretta, G. (2019) Industrial Symbiosis: towards a design process for eco-industrial clusters by integrating Circular Economy and Industrial Ecology perspectives, *J. Clean. Prod.* 216, 446–460
- Benachio, G.L.F., Freitas, M.C.D., Tavares, S.F. (2020) Circular economy in the construction industry: A systematic literature review. *Journal of Cleaner Production* 260, 121046

- Blomsma, F., Pieroni, M., Kravchenko, M., Pigosso, D.C.A., Hildenbrand, J., Kristinsdottir, A.R., Kristoffersen, E. Shahbazi, S., Nielsen, K.D., Jönbrink, A.-K., Li, J., Wiik, C., McAloone, T.C. (2019) Developing a circular strategies framework for manufacturing companies to support circular economy-oriented innovation. *J. Clean. Prod.* 241, 118271
- European Commission (2015). Closing the Loop - an EU Action Plan for the Circular Economy. Communication from the Commission to the European Parliament, the Council, the European Economic and Social Committee and the Committee of the Regions. COM(2015) 614 final.
- European Commission (2020). Circular Economy Action Plan for a Cleaner and More Competitive Europe. Communication from the Commission to the European Parliament, the Council, the European Economic and Social Committee and the Committee of the Regions.
- European Parliament and the Council (2008) Directive 2008/98/EC of the European Parliament and of the Council of 19 november 2008 on waste and repealing certain directives. *Off. J. Eur. Communities*, L312/3 (2008), pp. 3-30.
- Gorecki, J. (2019) Circular Economy Maturity in Construction Companies. Conference Series: Materials Science and Engineering 471(11), 112090
- Hertwich, E. G. (2021). Increased carbon footprint of materials production driven by rise in investments. *Nature Geoscience*, 1-5.
- Kirchherr, J.; Reike, D.; Hekkert, M. Conceptualizing the circular economy: An analysis of 114 definitions. *Resources, Conservation & Recycling* 127 (2017) 221–232
- Brinkmann, S., & Kvale, S. (2018). *Doing interviews* (Second ed.). SAGE Publications Ltd
- Lejrbo (2020) <https://www.lejrbo.dk/om-lejrbo/byggeri/circle-house> (In Danish, visited Sept. 2020))
- Lendager (2013) <https://lendager.com/en/architecture/upcycle-house-en/> (Visited Sept, 2020)
- Lendager (2018) <https://lendager.com/arkitektur/upcycle-studios/> (In Danish, visited Sept, 2020)
- López Ruiz, L.A.L., Ramón, X.R., Domingo, S.G. (2020) The circular economy in the construction and demolition waste sector – A review and an integrative model approach. *Journal of Cleaner Production* 248, pp. 119238
- Mhatre, P., Gedam, V., Unnikrishnan, S., Verma, S. (2021) Circular economy in built environment – Literature review and theory development. *Journal of Building Engineering* 35, 101995
- Musicon (2020) <https://musicon.dk/> (In Danish, visited Sept. 2020)
- Næste Skur (2019) <https://www.naeste.dk/> (In Danish, visited February 2021)
- OECD(2012) Sustainable materials management, making better use of resources
- Prieto-Sandoval, V., Jaca, C., Ormazabal, M. (2018) Towards a consensus on the circular economy. *Journal of Cleaner Production* 179, 605-615
- Ritzén, S., Sandström, G.Ö. (2017) Barriers to the Circular Economy – integration of perspectives and domains. *Procedia CIRP* 64, 7 – 12
- United Nations, Department of Economic and Social Affairs, Population Division (2015). *Population 2030: Demographic challenges and opportunities for sustainable development planning* (ST/ESA/SER.A/389)
- UNEP, 2019. 2019 global status report for buildings and construction: Towards a zero-emission, efficient and resilient buildings and construction sector. Global Alliance for Buildings and Construction, International Energy Agency and the United Nations Environment Programme.
- Worldometer (2021) <https://www.worldometers.info/world-population/> (visited February 2021)

EFFICIENT AND SAFE SUBSTRATES FOR BLACK SOLDIER FLY BIOWASTE TREATMENT ALONG CIRCULAR ECONOMY PRINCIPLES

Moritz Gold ^{1,2,*}, Davis Ileri ³, Christian Zurbrügg ², Trevor Fowles ⁴ and Alexander Mathys ¹

¹ ETH Zurich, Sustainable Food Processing, Department of Health Science & Technology, Institute of Food, Nutrition & Health, Zurich, Switzerland

² Eawag: Swiss Federal Institute of Aquatic Science and Technology, Department of Sanitation, Water and Solid Waste for Development (Sandec), Dübendorf, Switzerland

³ Sanergy, New Technology Commercialization, Nairobi, Kenya

⁴ University of California, Department of Entomology and Nematology, Davis CA, USA

Article Info:

Received:

1 February 2021

Revised:

23 April 2021

Accepted:

31 May 2021

Available online:

30 September 2021

Keywords:

Hermetia illucens

Sustainability

Organic waste

Animal feed

Assessment

Waste recovery hierarchy

ABSTRACT

Black soldier fly larvae (BSFL) treatment is an emerging technology for the valorisation of nutrients from biowaste. Selecting suitable substrates for BSFL treatment is a frequent challenge for researchers and practitioners. We conducted a systematic assessment of BSFL treatment substrates in Nairobi, Kenya to source more substrate for upscaling an existing BSFL treatment facility. The applied approach is universal and considers four criteria: 1) substrate availability and costs, 2) BSFL process performance, 3) product safety, and 4) waste recovery hierarchy. Data were collected from previous waste assessments or semi-structured key informant interviews and sight tours of waste producers. Waste nutritional composition and BSFL process performance metrics were summarised in the “BSFL Substrate Explorer”, an open-access web application that should facilitate the replication of such assessments. We show that most biowaste in Nairobi is currently not available for facility upscaling due to contamination with inorganics and a lack of affordable waste collection services. A mixture of human faeces, animal manure, fruit/vegetable waste, and food waste (with inorganics) should be pursued for upscaling. These wastes tend to have a lower treatment performance, but in contrast to cereal-based byproducts, food industry byproducts, and segregated food waste, there is no conflict with animal feed utilization. The traceability of substrates, source control, and post-harvest processing of larvae are required to ensure feed safety. The criteria presented here ensures the design of BSFL treatment facilities based on realistic performance estimates, the production of safe insect-based products, and environmental benefits of products compared to the status quo.

1. INTRODUCTION

Biowastes significantly contribute to the global waste problem (Gustavsson et al., 2011; Wilson et al., 2015). Currently, biowaste is frequently not safely managed, leading to the wastage of nutrients, energy, and water (Chen et al., 2020; Diener et al., 2014; Hoornweg & Bhada-Tata, 2012). Biowaste management also contributes to global challenges, such as poor urban health, degradation of the natural environment, and climate change.

Black soldier fly larvae (BSFL) treatment is an emerging technology for biowaste treatment (Gold et al., 2018; Zurbrügg et al., 2018). The technology uses the immature life stage of the black soldier fly (*Hermetia illucens*, Diptera:

Stratiomyidae) that feeds on a large variety of biowastes and turns them into a compost-like residue (Gold et al., 2018). Insect biomass can be separated from the residue and processed into raw materials for various applications such as lubricants, biodiesel and pharmaceuticals, and currently most promising, for animal feed markets (Barragán-Fonseca et al., 2017; Bosch et al., 2014; Makkar et al., 2014), for example, dried larvae or protein meal as a feed ingredient for poultry, fish, pigs, and pets.

Throughout the past decades, research and implementation has indicated that the technology has the potential to produce higher treatment product revenues, result in reduced greenhouse gas emissions compared to other biowaste treatment technologies, such as composting, and



produce insect-based feeds with a lower environmental impact than the status quo (Ermolaev et al., 2019; Gold et al., 2018; Mertenat et al., 2019; Smetana et al., 2019). In addition, the technology can operate at various scales, modularity, and levels of automation (Diener et al., 2011; Ites et al., 2020). These advantages have been demonstrated by the global industrial-scale implementation of BSFL technology in recent years, for example, the Netherlands, China, Chile, the USA, Germany, Kenya, South Africa, and Malaysia. However, to have a significant global impact on waste management and the sustainability of the food system, more insect-based biowaste treatment facilities are needed (Gold et al., 2018).

One main challenge faced by utilities, municipalities, insect companies, and entrepreneurs is the selection of suitable biowastes for BSFL treatment. Process performance as measured by bioconversion rate, and larval mass, and larval biomass composition, such as protein and lipid content, vary among substrates (Gold et al., 2018; Gold et al., 2020a; Lalander et al., 2019). In addition, chemical and microbial contaminants in different biowastes require careful consideration to ensure product safety (Van der Fels-Klerx et al., 2018). Moreover, substrates may already have a value when used in, for instance, animal feed and biogas production. Alternatively, the provision of the waste has high costs due to decentralised collection, long distances from the treatment facilities, or high amounts of inorganic materials (plastic, glass, and paper) that need to be removed prior to BSFL treatment (Dortmans et al., 2017).

Here, we present a systematic approach to identify suitable substrates for BSFL treatment by considering waste availability and costs, the BSFL process performance of the biowaste, the waste recovery hierarchy, and product safety. The applied approach is universal and enables the design of BSFL treatment facilities based on realistic performance estimates, the production of safe insect-based products, and environmental benefits of products in comparison to the status quo. This study also developed the “BSFL Substrate Explorer”, an open-access web application (moritzgold.shinyapps.io/BSF_app/) with tools to explore waste compositional data and BSFL process performance and formulate efficient biowaste mixtures.

2. MATERIALS AND METHODS

This case study was conducted in Nairobi, Kenya, using a combination of primary and secondary research. At the beginning of the assessment, approximately 20 tonnes/day of human faeces and fruit and vegetable waste were treated at an existing BSFL treatment facility. The BSFL were processed into dry larvae and sold to feed millers, and the residue was composted and sold as a soil conditioner. The assessment was completed with the aim of sourcing more biowaste for the upscaling of the facility (> 100 tonnes of waste per day).

2.1 Selection criteria

The biowaste assessment approach considered four criteria (Figure 1): waste availability and costs, the BSFL process performance of the biowaste, the waste recovery

hierarchy, and product safety. These criteria can be processed step by step, either in parallel, or iteratively. The process performance of the biowaste is important because it influences the treatment time and larval and residue amounts produced per unit of biowaste. Ultimately, process performance influences operational costs and revenues from treatment products. Considering the waste recovery hierarchy as well as waste availability and potential waste costs is important because wastes with high process performances may already have uses, for example, as animal feed, and therefore, conversion of the waste may not produce affordable treatment products, or wastes may already be part of meaningful resource recovery (Smetana et al., 2019). Product safety is critical for BSFL treatment because treatment products are used for human food production, and wastes can include contaminants relevant to animal and human health (Van der Fels-Klerx et al., 2018).

2.2 Availability and costs

Biowaste availability and the costs of wastes in Nairobi were assessed using criteria proposed by Lohri et al. (2015). These criteria include biowaste quantity, biowaste cost, waste characteristics (mixing of organics with inorganics), and the existing use of waste, for example, landfilling and composting. Biowaste quantities and costs were mainly assessed using previous waste assessments conducted in Nairobi (Baud et al., 2004; Njoroge et al., 2014; Kasozi & Von Blottnitz, 2010; Kirai et al., 2009). Data were validated by semi-structured key informant interviews and sight tours of waste producers. These included restaurants and hotels, slaughterhouses, animal farms, supermarkets, and food industries.

2.3 Process performance

2.3.1 Review of performance metrics

The process performance of biowastes with BSFL was estimated using values provided in the literature of typical BSFL performance metrics, for example, larval mass, bioconversion rate, and waste reduction (Banks et al., 2014; Bava et al., 2019; Diener et al., 2009; Gold et al., 2021; Gold et al., 2020a; Jucker et al., 2017; Lalander et

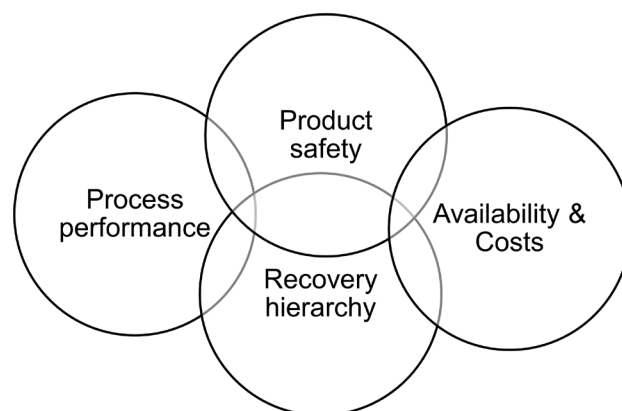


FIGURE 1: Criteria considered for selection of BSFL treatment substrate in Nairobi, Kenya.

al., 2019; Liu et al., 2018; Meneguz et al., 2018; Miranda et al., 2019; Nguyen et al., 2013; Nyakeri et al., 2019; Rehman et al., 2017; Somroo et al., 2019; Spranghers et al., 2017; Tschirner & Simon, 2015). The feeding rate and treatment time within these studies were 40–250 mg waste/larva/day and 6–27 days, respectively. Some wastes, including grass, wastewater sludge, or water hyacinths tended to be unsuitable for BSFL treatment because of very low growth (Dieu et al., 2015; Lalander et al., 2019; Liu et al., 2018) and were not included in the performance summary. Research to increase the growth of BSFL on these substrates by pre-treatments (Isibika et al., 2019) and co-conversion with beneficial bacteria (Mazza et al., 2020; Rehman et al., 2019) is ongoing.

2.3.2 Biowaste analyses for mixture formulation

A single biowaste stream cannot fulfil the entire treatment capacity (>100 tonnes/day); therefore, we analysed biowastes for gross nutrient composition. The formulation of biowaste mixtures based on similar nutrient content, especially protein and carbohydrates, has been tested as a promising approach for efficient and reliable BSFL treatment (Gold et al., 2020a; Barragán-Fonseca et al., 2018). Crude protein, lipids, neutral detergent fibre (NDF), acid detergent fibre (ADF), and ash were analysed using standard procedures used for animal feeds (Gold et al., 2020a). Protein was estimated by multiplying nitrogen with waste-specific factors (Chen et al., 2017; Mariotti et al., 2008; Sriperum et al., 2011). Hemicelluloses were determined as the difference between NDF and ADF. ADF was assumed to be a reliable estimate of the fibre (cellulose and lignin) content. Samples were pit latrine sludge (n = 3), human faeces with sawdust (n = 4), fruit and vegetable waste (n = 1), vegetable waste (n = 2), poultry feed (n = 1), food waste from hotels (n = 9), food waste from restaurants (n = 2), cereal-based by-products (n = 1), fruit waste (n = 4), and slaughterhouse waste (n = 2). To generalise our approach, values provided in the literature for the same parameters were summarised (Girromini et al., 2017; Gold et al., 2020a; Gold et al., 2020b; Gold et al., 2021; Liu et al., 2018; Meneguz et al., 2018; Shumo et al., 2019; Vrugink, 2020).

2.3.3 Open-access web application

Process performance and waste compositional data, as well as the formulation of biowaste mixtures, were included in an open-access web application called the “BSFL Substrate Explorer” (moritzgold.shinyapps.io/BSF_app/). Process performance (n = 60) and biowaste compositional data (n = 67) were analysed using R version 312 3.6.2 (R Core Team, 2020). Data were manipulated using tidyverse (Wickham et al., 2019) and were visualised by boxplots using ggplot2 (Wickham, 2016). In addition, compositional data were visualised in a two-dimensional plane following a principal component analysis (PCA) using the FactoMineR (Le et al., 2008) and factoextra package (Kassambara & Mundt, 2020). The calculation of the nutrient content of biowaste mixtures was also included in the Shiny-based web application (Barragán-Fonseca et al., 2018; Gold et al., 2020a). These analyses were translated into the web application using the Shiny (Chang et

al., 2020) and shinydashboard package (Chang & Ribeiro, 2018). Shiny-based applications are interactive and change outputs, for example, plots and descriptive statistics, based on user input.

2.4 Product safety

Biowaste contains various contaminants such as microbes, for example, pathogenic bacteria and viruses, (heavy) metals, and/or chemicals, for example, pharmaceutical and pesticide residues (Gold et al., 2018; Van der Fels Klerx et al., 2018). We used the available BSFL literature, as well as general animal feed safety considerations of the Food and Agriculture Organization of the United Nations (FAO) (FAO, 1997) to identify potential waste contaminants in the identified wastes, their fate in BSFL treatment, and BSFL post-harvest processing.

2.5 Waste recovery hierarchy

BSFL treatment frequently aims to provide biowaste treatment and products with lower environmental impact than the status quo. Biowastes or byproducts with use as food or feed do typically do not provide environmental benefits in comparison to the status quo (Bosch et al., 2019; Smetana et al., 2016; Smetana et al., 2019). Using the waste recovery hierarchy concept (UNEP, 2013) and published life cycle assessments (LCAs) results (Bosch et al., 2019; Smetana et al., 2019), we discuss whether environmental benefits are likely to be associated with diverting the identified wastes to BSFL treatment. Even though results are very case specific (e.g. depending on substrate, energy type and production, post-processing of frass and larvae), typical environmental benefits over production of conventional protein-rich feed ingredients and composting are lower greenhouse gas emissions and land use (Bosch et al., 2019; Mertenat et al., 2019).

3. RESULTS AND DISCUSSION

3.1 Availability and costs

In Nairobi, domestic and non-domestic biowaste is generated to upscale the BSFL treatment facility. Most biowaste in Nairobi is domestic, i.e., household waste. When considering the population (4.4 million, KEBS (2019)), the average city-wide waste generation estimate (0.65 kg/capita/day) and average waste composition (59% of domestic waste is estimated to be organic), approximately 1,690 tons of household biowaste is generated per day (Kasozi & Von Blottnitz, 2010). Determining the quantities of non-domestic biowaste, for example, from schools, restaurants, hotels, and markets, is more challenging because of an unknown number of sources (>3,000) (Kirai et al., 2009) and variable waste generation rates per source (Table 1). Approximately 20-30% of all biowaste generated in the city has previously been estimated to be non-domestic using the estimate of total domestic waste generation (Kasozi & Von Blottnitz, 2010; Kirai et al., 2009). Consequently, using the estimate for domestic waste generation and average waste composition (74% of waste is organic) (Kirai et al., 2009), approximately 529-906 tonnes of non-domestic biowaste is generated per day. Based on previous work by

TABLE 1: Non-domestic waste generation (in kg) per day and facility from different sources.

Source	Waste examples	Waste generation (kg/day)
Hotels	Food scraps	200-2,000 ^{1,2}
Restaurants	Food scraps	2,100 ²
Markets	Food scraps, discarded food (e.g., fruit and vegetable peels)	> 19,000 ²
Shopping malls	Food scraps	1,100 ²
Commercial animal farms	Pig and cow manure	25,000 ²
Slaughterhouses	Blood, rumen content	45,000 ¹ 16,000 ²
Supermarkets	Discarded fruits and vegetables	2,500 ²
Food industry	Discarded fruits and vegetables, byproducts from juice production, canneries and bread baking	0.5-100 ¹

¹ own data, ² Kirai et al (2009)

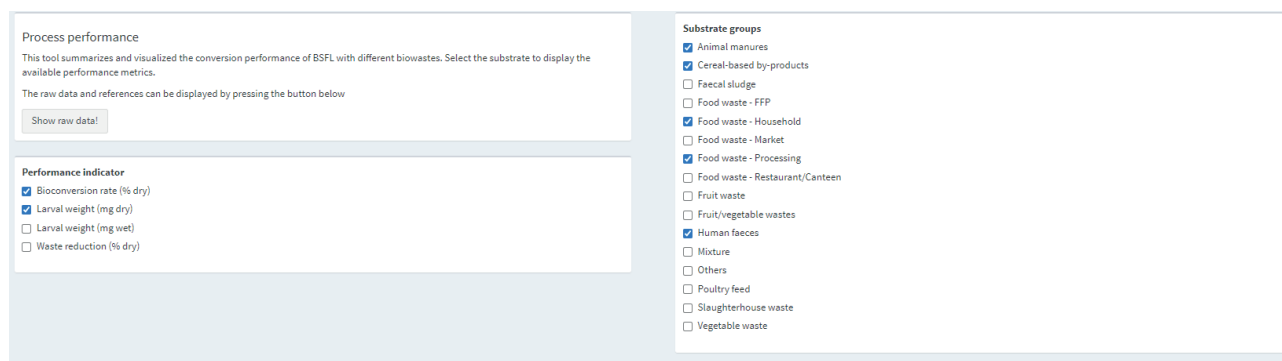
Kirai et al. (2009) and the interviews and field visits conducted in the present study, non-domestic biowaste in Nairobi consists of: fruit and vegetable wastes, for example, from canneries, juice producers, and retailers; animal manure, for example, dairy and pig farms; food waste, for example, retailers, markets, hotels, restaurants, and shopping malls; cereal-based byproducts, for example, spent grain from breweries, press cakes from oil production, byproducts from flour and animal feed mills, and slaughterhouse waste, for example, rumen content and blood. Solids in wastewater and faecal sludge are additional poorly managed and valorised wastes in Nairobi that could be poten-

tially utilized as BSFL substrates.

3.2 Process performance

Figure 2 demonstrates the “Conversion performance” tab of the web application. It summarises the performance metrics of the BSFL treatment based on the substrate group and the performance metrics selected by the user. The summary can support the selection of efficient substrates and provides realistic performance estimates for treatment design (e.g., waste reduction) and estimations of treatment product quantities (e.g., bioconversion rate). Use of the web application shows that animal manure, faecal sludge, fruit and vegetable waste, and slaughterhouse waste, which are suitable for up-scaling based on availability and cost in Nairobi, typically result in lower larval weight and bioconversion rate than food waste, cereal-based byproducts, or human faeces.

The process performance of individual wastes is of limited value in Nairobi because a single waste stream cannot meet the entire treatment capacity (>100 tonnes/day). In this case, knowledge of an efficient biowaste mixture and the associated process performance is required. Typically, biowaste mixtures have been identified in trial and error feeding experiments with different biowaste mixtures (Nyakeri et al., 2019; Rehman et al., 2017). The formulation of biowaste mixtures based on nutritional composition, for example, overall nutrient content, protein, and carbohydrates, has recently emerged as a more systematic approach (Barragán-Fonseca et al., 2018; Gold, et al., 2020a). This approach considers that protein, digestible carbohydrates (a fraction of hemicelluloses), lipids, and the overall nutrient generally correlated with rearing performance. However, such an approach requires accurate waste com-



Performance indicator (boxplot)

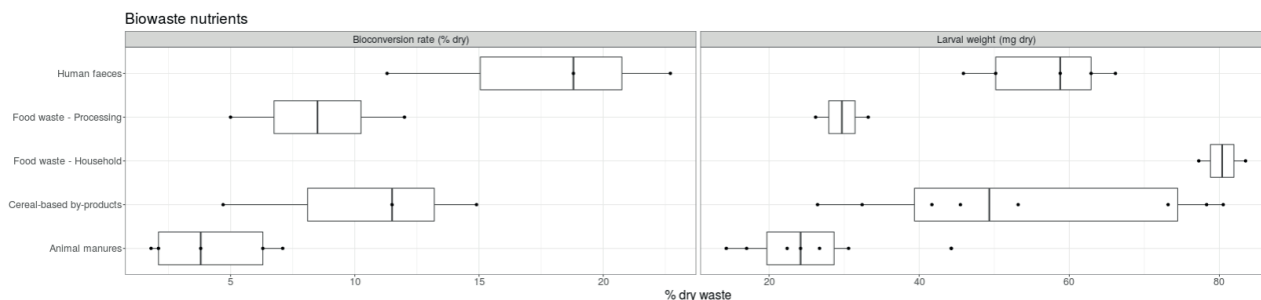


FIGURE 2: The “Conversion performance” tab of the web application summarises process performance results based on the substrate group and performance metric selected by the user. Descriptive statistics are included in a table below the boxplot (not shown in this Figure).

positional data that are not always available.

Before the formulation of biowaste, it is helpful to gain a general understanding of the contents of important nutrients in the available wastes, such as protein, lipids, digestible carbohydrates (e.g. glucose and starch), hemicelluloses, fibres, and ash. Protein, lipids and digestible carbohydrates and potentially some fraction of hemicelluloses are thought to have a positive influence on process performance (Barragán-Fonseca et al., 2018; Gold et al., 2020a; Gold et al., 2018b). Fibres are important for substrate texture, but above yet unknown contents can decrease process performance (Liu et al., 2018). The substrate organic content (100% - ash) has also been shown to positively correlate with process performance (Lalander et al., 2019). The “Nutrient composition” tab of the web application (Figure 3) dynamically summarises and visualises the waste nutrient composition based on the BSFL substrate group (see Gold et al. (2018a)) and the nutrient parameters selected by the user. It shows a PCA biplot and summarises descriptive statistics in a table, for example, mean, standard deviation (sd), minimum (min), and maximum (max). The boxplots and PCA biplot demonstrated a large variability in nutrient composition among samples of the same substrate group. This is to be expected, because waste comes from different sources (e.g., different fruits or vegetables) and different waste management systems (e.g., waste storage durations). Food wastes were the most variable because this substrate group includes former food stuffs (FFS), and waste from households, markets, canteens, and restaurants, which can differ greatly in nutrient composition. Despite this variability, the vector directions of the PCA biplot allow broad categories of waste based on nutrient composition. For example, considering the wastes available in Nairobi, animal manure and faecal sludge are high in fibres and low in lipids, and fruit and vegetable wastes are low in proteins and lipids. Despite its importance for BSFL performance, no conclusions can be drawn on digestible carbohydrate contents in these substrates due to few or lacking results. Food waste is the substrate group with the highest nutrient content, and is typically high in proteins, lipids, digestible carbohydrates, and hemicelluloses, and low in ash and fibres. Consequently, to increase process performance, it could be beneficial to mix animal manure and faecal sludge with food waste. Information from compositional databases for food (ndb.nal.usda.gov), feed (feedipedia.org), and food wastes (foodwasteexplorer.eu) should also be considered beyond our web application.

Barragán-Fonseca et al. (2018) and Gold et al. (2020a) formulated biowaste mixtures using Microsoft Excel, without sharing the actual Excel tool. The “Substrate mixture formulation” tab (Figure 4) provides this calculation in a

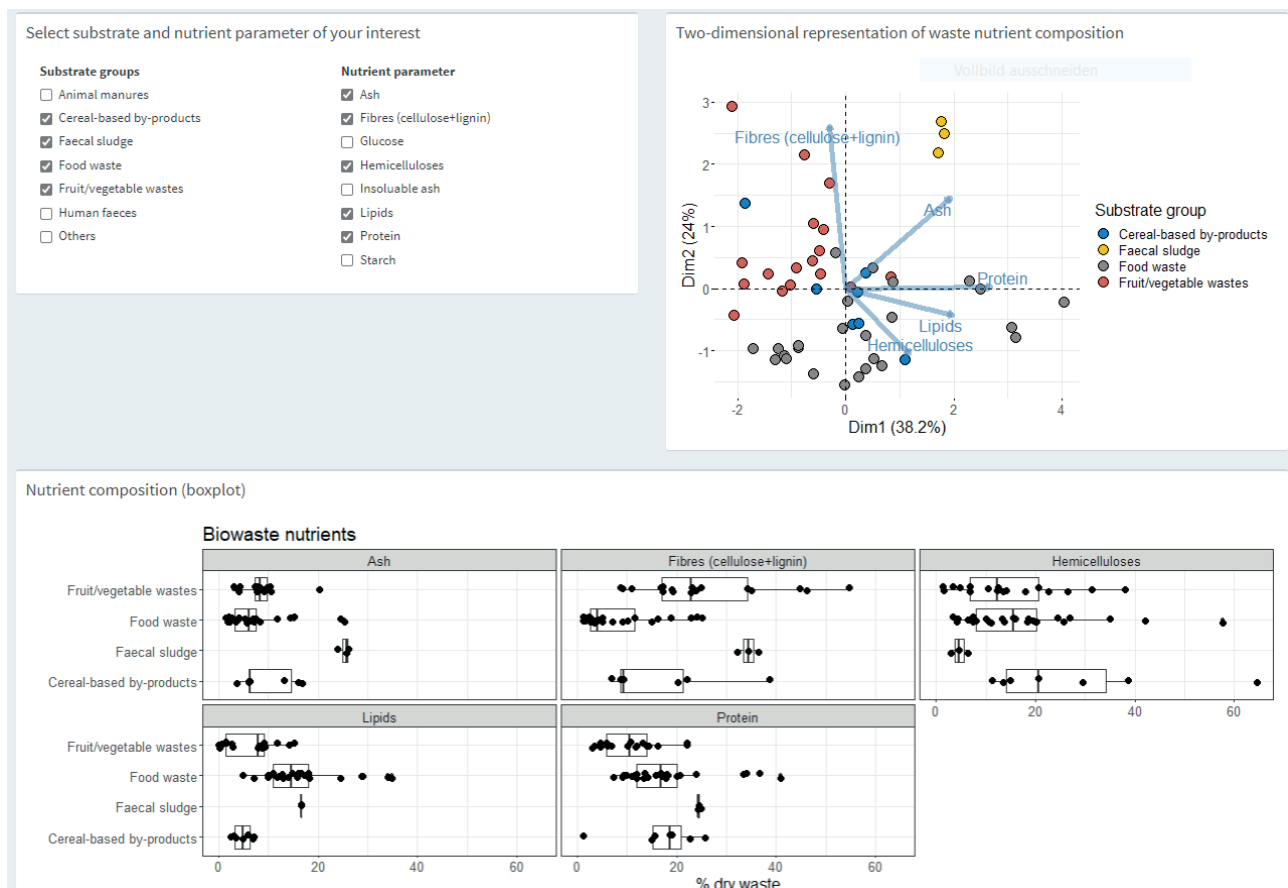


FIGURE 3: The “Nutrient composition” tab of the web application summarises the waste nutrient composition based on the substrate group and nutrient parameter selected by the user. Descriptive statistics are included in a table below the plots (not shown in this Figure).

web application. It dynamically calculates the nutrient composition of biowaste mixtures (in wet and dry mass) based on the nutrient content of the individual wastes (Figure 3) with information on the quantity and moisture content of the wastes provided by the user. The web application considers the nutritional variability by displaying the range of the nutritional composition of the biowaste mixture, calculated with the minimum and maximum nutrient content for each ingredient. For the wastes ultimately selected for facility upscaling, this tool can be used to calculate the proportion of each waste that needs to be added to have similar nutrient content among batches. Balancing content among batches in these nutrients by mixing wastes can make the process performance more reliable. However, some variability will remain because the formulation relies on intrinsically variable waste compositional data (Figure 3). In addition, maintaining all macronutrients within fixed limits among batches is difficult in practice because wastes typically have variable amounts of each macronutrient.

3.3 Product safety

Table 2 summarises the potential hazards in the BSFL substrates identified in Nairobi. As BSFL live in their feeding substrate and the substrate passes through their digestive tract during feeding, substrate contaminants have a potential to accumulate on surfaces or be taken up with other

digestion products into larval tissue (Gold et al., 2018a; Van der Fels Klerx et al., 2018). In addition, animal pathogens in substrates can populate the larval digestive tract. When considering the current knowledge on the fate of contaminants in BSFL treatment, heavy metals especially cadmium and arsenic in biowastes are a significant hazard for animal feed safety. In contrast to most microbes, for example, bacterial and viral pathogens that can be present in unprocessed BSFL but can be inactivated by heat treatment, some heavy metals have been shown to bioaccumulate in the larval tissue (Van der Fels Klerx et al., 2018; Diener et al., 2015; Schmitt et al., 2019). Spore-forming pathogens in substrates that are potentially transferred to the surface or digestive tracts of BSFL, such as *Bacillus cereus* and *Clostridium botulinum*, are also of special concern because they can survive heat treatment. Aflatoxin B1 (a common mycotoxin) and human/veterinary drugs and chemosporeicals have so far not been detected in BSFL grown on contaminated substrates (Bosch et al., 2017; Charlton et al., 2015; Lalander et al., 2016; Purschke et al., 2017). Hydrocarbons, for example, mineral oil hydrocarbons, dioxins, polychlorinated biphenyls (PCBs), and traces of plastic in substrates can accumulate following processing by BSFL in the larval tissue. However, concentrations of these contaminants were below legal limits at moderate substrate contaminant levels, for example, 3–6% plastic fragments (van der Fels-Klerx et al., 2020).

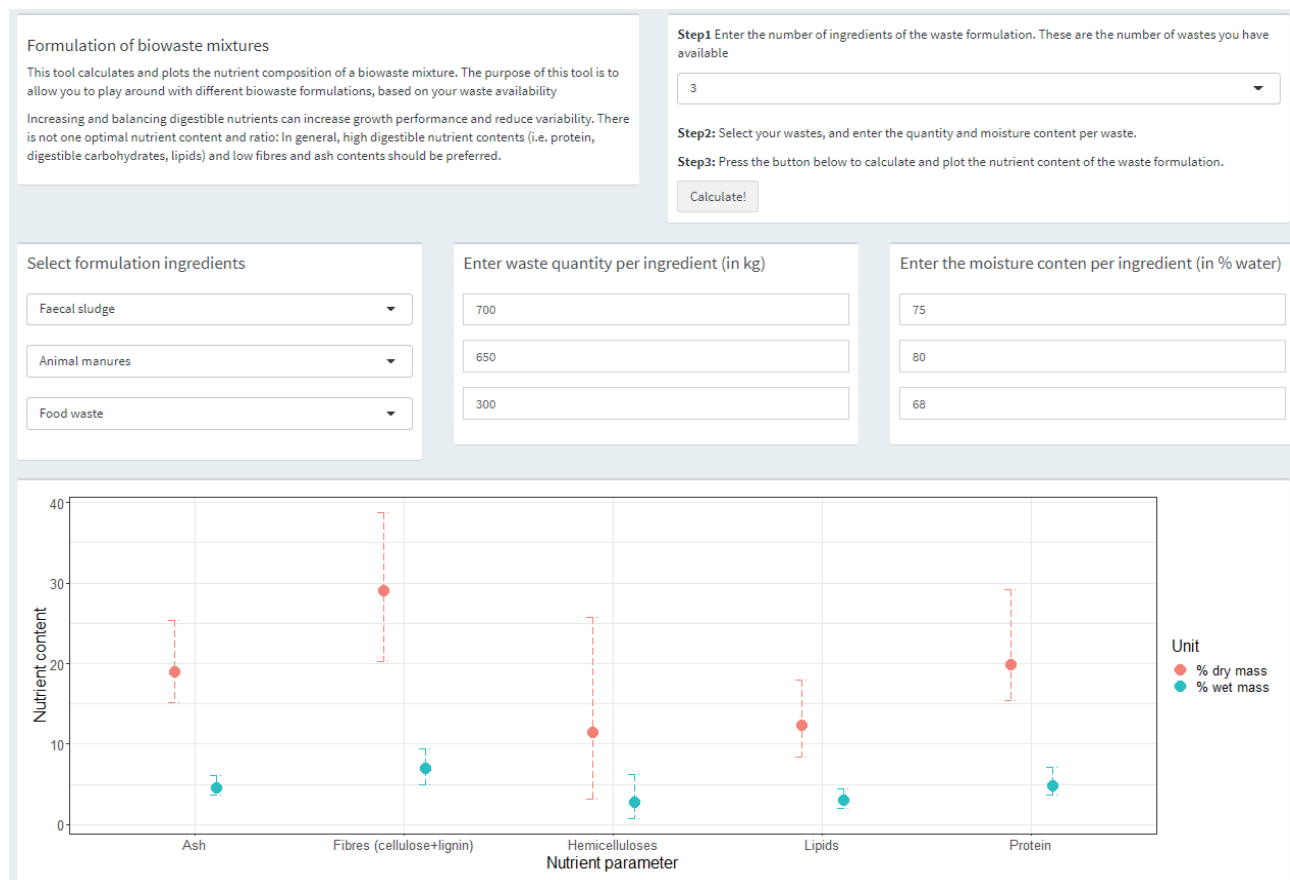


FIGURE 4: The “Substrate mixture formulation” tab of the web application calculates the nutrient composition of a biowaste mixture based on the substrate, quantity, and moisture content provided by the user.

TABLE 2: Potential hazards in BSFL substrates. A = mycotoxins, B = human/veterinary drugs, C = agricultural chemicals, D = microbial pathogens and their toxins (e.g. Botulinum toxin), E = metals, and F = misfolded prion proteins (Bosch et al., 2017; FAO 1997; Gold et al. 2018; Lalander et al., 2016; Purschke et al., 2017).

Waste	Hazard
Human faeces and excreta	B, D
Wastewater and faecal sludge	B, D, E
Animal manure	B, C, D, E
Slaughterhouse waste	D, F
Household waste	D, E
Cereal-based byproducts	A, D
Food & restaurant waste	A, D
Food processing waste	A, D

Strategies aimed at these hazards to meet legal feed limits include the selection of traceable substrates with low contaminant concentrations, mixing of substrates with low and higher contaminant concentrations, a series of post-processing steps to reduce contamination levels, for example, pasteurization (EC, 2011) including good hygiene practices (IPIFF 2019). At the BSFL treatment facility in Nairobi, only human faeces collected from standardised and well operated source-separating toilets are used. Separation of faeces from urine means that an estimated two-thirds of the excreted drug residues are disposed of elsewhere (Lienert et al., 2007). Furthermore, mixing faeces with sawdust in the toilet, and co-processing this mixture with discarded fruits and vegetables, that is, FFS, further reduces drug residue concentrations. Although not yet shown in the few completed studies, in cases where drug residues are carried over to BSFL, heat treatment contributes to their inactivation (Tian et al., 2017). All substrates identified in Nairobi may include microbial pathogens; therefore, live BSFL should not be fed to animals. Further research is needed to determine how the hazards in wastewater sludge, for example, heavy metals, and slaughterhouse waste, for example, misfolded prion proteins, can be managed.

3.4 Waste recovery hierarchy

BSFL treatment is frequently selected with the aim of providing biowaste treatment and products with lower environmental impact than the status quo (Mertenat et al., 2019; Smetana et al., 2019). To deliver this goal, the waste recovery hierarchy is a useful and established concept. It indicates the order of preferences of waste reduction and management measures. The order of most preferred to least preferred measures includes prevention, reduction, recycling, recovery, and disposal (UNEP, 2013). We propose to extend this concept to encompass the treatment of biowaste with BSFL (Figure 5). BSFL treatment should be the most preferred measure following waste prevention, for example, by strategies to avoid food waste, and waste reduction (including reuse), for example, by using animal feed. For this Nairobi case study, it means although cereal-based byproducts and some food and fruit/vegetable wastes have favorable nutrient content and process performance with BSFL they should not be diverted to BSFL treatment

because of their potential use as animal feed and part in meaningful resource recovery. In addition, BSFL treatment should be considered before other waste treatment technologies, such as anaerobic digestion or composting, to recycle nutrients back into the food chain. Biowaste, for example from the food processing industry, can therefore, enter a circular value chain (Cappelozza et al., 2019).

3.5 Trade-offs between selection criteria

The present Nairobi case study has demonstrated that selecting substrates for BSFL treatment is a trade-off between larval biomass production efficiency and substrate costs, with overarching considerations for the safety and sustainability of the larval-based products. Substrates that have the highest performance typically have high costs and are already used as animal feed, and this concurs with the waste hierarchy concept and circular economy principles. The remaining substrates that are available at reasonable costs have lower performances and require careful consideration to ensure product safety.

Based on the four-criteria assessment here, a mixture of human faeces, animal manure, fruit/vegetable waste, and food waste should be targeted for upscaling the BSFL treatment facility in Nairobi. Biowaste mixtures with similar nutrient contents can be calculated with the “Substrate mixture formulation” tab (Figure 4) of the web application. Multiplication or further expansion of the facility requires changes in Nairobi’s waste management system, such as increased separation of biowaste from inorganic wastes and financially viable collection services. Seventy to eighty percent of Nairobi’s biowaste is household waste mixed with inorganics, which makes it unsuitable for BSFL treatment (Kirai et al., 2009). Furthermore, only 30–50% of waste in Nairobi is collected (Aryampa et al., 2019; Kasozi & Von Blottnitz, 2010). Achieving universal waste management services in Nairobi is challenging, particularly when considering that more than 50% of the population lives in informal areas.

All original data presented in this study is publicly available. The “BSFL Substrate Explorer” at the time of writing this paper can be downloaded at Eric/open (<https://open-data.eawag.ch>), the Eawag Research Data Institutional Repository (DOI: 10.25678/00051D). The current version can be found at https://github.com/MoritzGold/BSF_app.

ACKNOWLEDGEMENTS

This research was funded by the Sawiris Foundation for Social Development (Engineering for Development (E4D) Scholarship Program), Eawag, and supported by the ETH Zurich Foundation, ETH Global, and Bühler AG. The development of the web application would not have been possible without the encouragement and technical support of Lars Schöbitz (Lars Schöbitz GmbH).

REFERENCES

Aryampa, S., Maheshwari, B., Sabiiti, E., Bateganya, N. L., & Bukenya, B. (2019). Status of waste management in the East African cities: Understanding the drivers of waste generation, collection and disposal and their impacts on Kampala City’s sustainability. *Sustainability*, 11(19), 1–16.

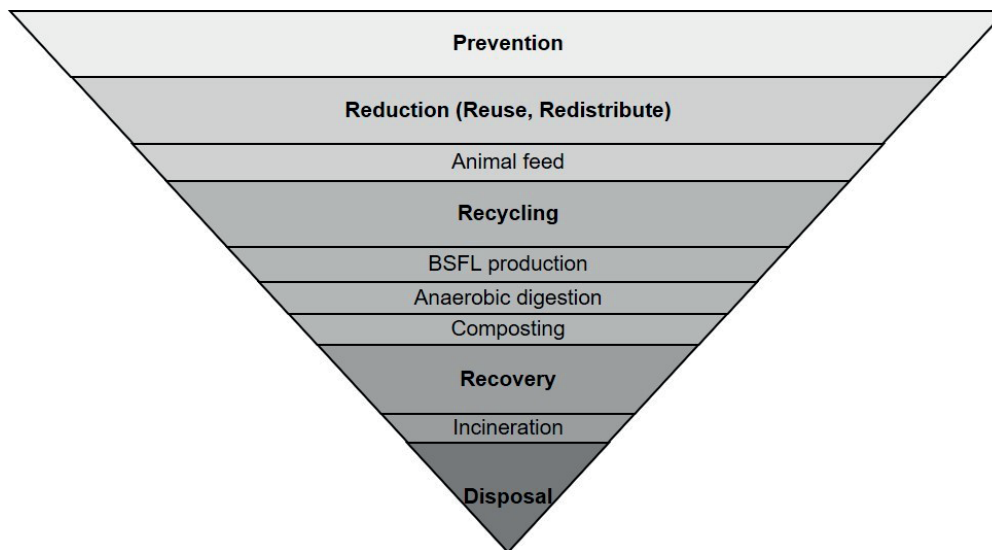


FIGURE 5: Biowaste recovery hierarchy including BSFL treatment. Adapted from Papargyropoulou et al. (2014) and UNEP (2013).

- Banks, I. J., Gibson, W. T., & Cameron, M. M. (2014). Growth rates of black soldier fly larvae fed on fresh human faeces and their implication for improving sanitation. *Tropical Medicine and International Health*, 19(1), 14–22.
- Barragán-Fonseca, K. B., Dicke, M., & van Loon, J. J. A. (2017). Nutritional value of the black soldier fly (*Hermetia illucens* L.) and its suitability as animal feed – a review. *Journal of Insects as Food and Feed*, 3(2), 105–120.
- Barragán-Fonseca, K., Pineda-Mejia, J., Dicke, M., & Van Loon, J. J. A. (2018). Performance of the Black Soldier Fly (Diptera: Stratiomyidae) on Vegetable Residue-Based Diets Formulated Based on Protein and Carbohydrate Contents. *Journal of Economic Entomology*, 111(6), 2676–2683.
- Baud, I. S. A., Post, J., & Furedy, C. (2004). *Solid waste management and recycling: actors, partnerships and policies in Hyderabad, India and Nairobi, Kenya*. Kluwer Academic Publishers.
- Bava, L., Jucker, C., Gislou, G., Lupi, D., Savoldelli, S., Zucali, M., & Colombini, S. (2019). Rearing of *hermetia illucens* on different organic by-products: Influence on growth, waste reduction, and environmental impact. *Animals*, 9(6), 289.
- Bosch, G., Fels-Klerx, H., Rijk, T., & Oonincx, D. G. A. B. (2017). Aflatoxin B1 Tolerance and Accumulation in Black Soldier Fly Larvae (*Hermetia illucens*) and Yellow Mealworms (*Tenebrio molitor*). *Toxins*, 9(6), 185.
- Bosch, G., van Zanten, H. H. E., Zamprogna, A., Veenenbos, M., Meijer, N. P., van der Fels-Klerx, H. J., & van Loon, J. J. A. (2019). Conversion of organic resources by black soldier fly larvae: Legislation, efficiency and environmental impact. *Journal of Cleaner Production*, 222, 355–363.
- Bosch, Guido, Zhang, S., G.A.B., D., & Hendriks, W. H. (2014). Protein quality of insects as potential ingredients for dog and cat foods. *Journal of Nutritional Science*, 3(29), 1–4.
- Chen, C., Chaudhary, A., & Mathys, A. (2020). Nutritional and environmental losses embedded in global food waste. *Resources, Conservation and Recycling*, 160, 104912.
- Chang, W., Cheng, J., Allaire, J., Xie, Y., & McPherson, J. (2020). shiny: Web Application Framework for R. R package version 1.4.0.2. <https://cran.r-project.org/package=shiny>
- Chang, W., & Ribeiro, B. B. (2018). shinydashboard: Create Dashboards with "Shiny". R package version 0.7.1. <https://cran.r-project.org/package=shinydashboard>
- Charlton, A. J. J., Dickinson, M., Wakefield, M. E., Fitches, E., Kenis, M., Han, R., Zhu, F., Kone, N., Grant, M., Koko, G., Devic, D., Bruggeman, G., Devic, E., Bruggeman, G., Prior, R., & Smith, R. (2015). Exploring the chemical safety of fly larvae as a source of protein for animal feed *Journal of Insects as Food and Feed*, 1(1), 7–16.
- Chen, X., Zhao, G., Zhang, Y., Han, L., & Xiao, W. (2017). Nitrogen-to-protein conversion factors for crop residues and animal manure common in China. *Journal of Agricultural and Food Chemistry*, 65(42), 9186–9190.
- Diener, S., Semiyaga, S., Niwagaba, C. B., Muspratt, A. M., Gning, J. B., Mbéguéré, M., Ennin, J. E., Zurbrügg, C., & Strande, L. (2014). A value proposition: Resource recovery from faecal sludge - Can it be the driver for improved sanitation? *Resources, Conservation and Recycling* 88, 32–38.
- Diener, S., Zurbrügg, C., Gutiérrez, F. R., Nguyen, D. H., Morel, A., Kootatatep, T., & Tockner, K. (2011). Black soldier fly larvae for organic waste treatment - prospects and constraints. 2nd International Conference on Solid Waste Management in Developing Countries, Khulna, Bangladesh, 52(February), 1–8.
- Diener, S., Zurbrügg, C., Tockner, K. (2015). Bioaccumulation of heavy metals in the BSF, *Hermetia illucens*, and effects on its life cycle. *Journal of Insects as Food and Feed*, 1(4), 261–270.
- Diener, Stefan, Zurbrügg, C., Tockner, K. (2009). Conversion of organic material by BSF larvae: establishing optimal feeding rates. *Waste Management & Research* 27(6), 603–610.
- Dieu, T. T. M., Thien, N. N., Hang, N. T. T., & Chung, P. N. (2015). Possibility of degrading water hyacinth by black soldier larvae *International Journal of Innovative Science, Engineering & Technology*, 2(2), 174–180.
- Dortmans, B., Diener, S., Verstappen, B. M. & Zurbrügg, C. (2017). *Black soldier fly biowaste processing: A step-by-step guide*. Swiss Federal Institute of Aquatic Science and Technology (Eawag).
- Ermolaev, E., Lalander, C., Vinnerås, B. (2019). Greenhouse gas emissions from small-scale fly larvae composting with *Hermetia illucens* *Waste Management*, 96, 65–74.
- European Commission (EC) (2011). Commission Regulation (EU) No 142/2011: Health rules regarding animal by-products and derived products not intended for human consumption. *Official Journal of the European Union*
- Food and Agricultural Organization (FAO) (1997). *Animal feeding and the safety of food* (FAO Expert Consultation Report).
- Giromini, C., Ottoboni, M., Tretola, M., Marchis, D., Gottardo, D., Caprarulo, V., Pinotti, L., Ottoboni, M., Tretola, M., Marchis, D., & Gottardo, D. (2017). Food Additives & Contaminants : Part A Nutritional evaluation of former food products (ex-food) intended for pig nutrition. *Food additives & contaminants: Part A*, 34(8), 1436–1445.
- Gold, M., Tomberlin, J. J. K., Diener, S., Zurbrügg, C., & Mathys, A. (2018a). Decomposition of biowaste macronutrients, microbes, and chemicals in black soldier fly larval treatment: A review. *Waste Management*, 82, 302–318.
- Gold, M., Spiess, R., Zurbrügg, C., Kreuzer, M., Mathys, A., 2018b. Digestibility of different dietary fibres by black soldier fly larvae. *Bornimer Agrartech. Berichte* 100.

- Gold, M., Cassar, C. M., Zurbrügg, C., Kreuzer, M., Boulos, S., Diener, S., & Mathys, A. (2020a). Biowaste treatment with black soldier fly larvae: Increasing performance through the formulation of biowastes based on protein and carbohydrates. *Waste Management*, 102, 319–329.
- Gold, M., von Allmen, F., Zurbrügg, C., Zhang, J., and Mathys, A. (2020b). Identification of bacteria in two food waste black soldier fly larvae rearing residues *Frontiers in Microbiology*, 11, 2897.
- Gold, M., Fowles, T., Fernandez-Bayo, J. D., Palma Miner, L., Zurbrügg, C., Nansen, C., Bischel, H. N., Mathys, A. (2021). Effects of rearing system and microbial inoculation on black soldier fly larvae growth and microbiota when reared on agri-food by-products *Journal of Insects as Food and Feed*.
- Gower & Schröder, P. (2018). Cost-benefit assessment of community-based recycling and waste management in Pakistan
- Gustavsson, J., Cederberg, C., Sonesson, U., van Otterdijk, R. & Meybeck, A. (2011). *Global Food Losses and Food Waste Extent, Causes, and Prevention*.
- Hoorweg D, Bhada-Tata P (2012). What a Waste. A global review of solid waste management. In *Urban Development Series Knowledge Papers No. 15*.
- Isibika, A., Vinnerås, B., Kibazohi, O., Zurbrügg, C., Lalander, C. (2019). Pre-treatment of banana peel to improve composting by the BSF (*Hermetia illucens* (L.)), Diptera : Stratiomyidae) larvae. *Waste Management*, 100, 151–160.
- Ites S, Smetana S, Toepfl S, Heinz V (2020). Modularity of insect production and processing as a path to efficient and sustainable food waste treatment. *Journal of Cleaner Production*, 248. <https://doi.org/10.1016/j.jclepro.2019.119248>
- Jucker, C., Erba, D., Leonardi, M. G., Lupi, D., Savoldelli, S. (2017). Assessment of vegetable and fruit substrates as potential rearing media for *Hermetia illucens* (Diptera: Stratiomyidae) larvae. *Environmental Entomology*, 46(6), 1415–1423.
- Njoroge K, Kimani M, Ndunge D (2014). Review of Solid Waste Management: A Case Study of Nairobi. *Research Inventy: International Journal of Engineering and Science*, 4(2), 2319–6483.
- Kasozi, A. & Von Blottnitz, H. 2010. *Solid Waste Management in Nairobi: A Situation Analysis*
- Kassambara, A. & Mundt, F. (2020). factoextra: Extract and Visualise the Results of Multivariate Data Analyses. R package version 1.0.7. <https://cran.r-project.org/package=factoextra>
- Kenyan Bureau of Standards (KEBS) (2019). 2019 Kenya Population and Housing Census.
- Kirai, P., Gachugi, J. & Scheinberg, A. (2009). *Converting City Waste Into Compost: Pilot Nairobi: Phase one - Inventory and Assessment*.
- Lalander, C., Diener, S., Zurbrügg, C., Vinnerås, B. (2019). Effects of feedstock on larval development and process efficiency in waste treatment with BSF (*Hermetia illucens*). *Journal of Cleaner Production*, 208, 211–219.
- Lalander, C., Senecal, J., Gros Calvo, M., Ahrens, L., Josefsson, S., Wiberg, K., Vinnerås, B., 2016. Fate of pharmaceuticals and pesticides in fly larvae composting *Science of the Total Environment*, 565, 279–286.
- Le, S., Josse, J., Husson, F. (2008). FactoMineR: An R package for multivariate analysis. *J Statistical Software*, 25(1), 1–8.
- Liu, Z., Minor, M., Morel, P. C. H., & Najar-rodriguez, A. J. (2018). Bioconversion of three organic wastes by black soldier fly (Diptera: Stratiomyidae) larvae. *Environmental Entomology*, 47(6), 1609–1617.
- Lohri, C. R., Faraji, A., Ephata, E., Rajabu, H. M., & Zurbrügg, C. (2015). Urban biowaste for solid fuel production : Waste suitability assessment and experimental carbonisation in Dar es. *Waste Management & Research*, 33(2), 175–182.
- Makkar, H. P. S., Tran, G., Heuzé, V., & Ankers, P. (2014). State-of-the-art on use of insects as animal feed *Animal Feed Science and Technology*, 197, 1–33.
- Mariotti, F., Tomé, D., Mirand, P. P. (2008). Converting nitrogen into protein Beyond 6.25 and Jones' factors. *Critical Reviews in Food Science and Nutrition*, 48(2), 177–184.
- Mazza, L., Xiao, X., ur Rehman, K., Cai, M., Zhang, D., Fasulo, S., Tomberlin, J. K., Zheng, L., Soomro, A. A., Yu, Z., & Zhang, J. (2020). Management of chicken manure using black soldier fly (Diptera: Stratiomyidae) larvae assisted by companion bacteria. *Waste Management*, 102, 312–318.
- Meneguz, M., Schiavone, A., Gai, F., Dama, A., Lussiana, C., Gasco, L. (2018). Effect of rearing substrate on growth performance , waste reduction efficiency, and chemical composition of black soldier fly (*Hermetia illucens*) larvae. *Journal of the Science of Food and Agriculture*, 98, 5776–5784.
- Mertenat, A., Diener, S., & Zurbrügg, C. (2019). Black Soldier Fly bio-waste treatment: Assessment of global warming potential. *Waste Management*, 84, 173–181.
- Miranda, C. D., Cammack, J. A., & Tomberlin, J. K. (2019). Life-history traits of the BSF, *Hermetia illucens* (L.) (Diptera: Stratiomyidae) reared on three manure types. *Animals*, 9(5).
- Nguyen, T. T. X., Tomberlin, J. K., and Vanlaerhoven, S. 2013. Influence of Resources on *Hermetia illucens* (Diptera: Stratiomyidae) Larval Development. *J. Med. Entomol*, 50(4), 898–906.
- Nyakeri, E. M., Ayieko, M.A., Amimo, F. A., Salum, H., & Ogola, H. J. O. (2019). An optimal feeding strategy for black soldier fly larvae biomass production and faecal sludge reduction. *Journal of Insects as Food and Feed*, 1(1), 1–14.
- Purschke, B., Scheibelberger, R., Axmann, S., Adler, A., and Jäger, H. 2017. Impact of substrate contamination with mycotoxins, heavy metals, and pesticides on growth performance and composition of black soldier fly larvae (*Hermetia illucens*) for use in the feed and food value chain. *Food additives & contaminants: Part A*, 34(8), 1410–1420.
- R Core Team. (2020). R: A language and environment for statistical computing. <https://www.r-project.org/>
- Rehman, K. ur, Rehman, A., Cai, M., Zheng, L., Xiao, X., Somroo, A. A., Wang, H., Li, W., Yu, Z., & Zhang, J. (2017). Conversion of mixtures of dairy manure and soybean curd residue by BSF larvae (*Hermetia illucens* L.). *Journal of Cleaner Production*, 154, 366–373.
- Rehman, K. ur, Rehman, R., Somroo, A. A., Cai, M., Zheng, L., Xiao, X., Rehman, A., Rehman, A., Tomberlin, J. K., Yu, Z., & Zhang, J. (2019). Enhanced bioconversion of dairy and chicken manure by the interaction of exogenous bacteria and BSF larvae. *Journal of Environmental Management*, 237(February), 75–83.
- Schmitt, E., Belghit, I., Johansen, J., Leushuis, R., Lock, E. J., Melsen, D., Ramasamy Shanmugam, R. K., Loon, J. Van, & Paul, A. (2019). Growth and safety assessment of feed streams for BSF larvae: A case study with aquaculture sludge. *Animals*, 9(4), 189.
- Shumo, M., Osga, I. M., Khamis, F. M., Tanga, C. M., Fiaboe, K. K. M., Subramanian, S., Ekesi, S., van Huis, A., & Borgemeister, C. (2019). The nutritive value of BSF larvae reared on common organic waste streams in Kenya. *Scientific Reports*, 9(1), 1–13.
- Smetana, S., Palanisamy, M., Mathys, A., Heinz, V., 2016. Sustainability of insect use for feed and food: Life Cycle Assessment perspective. *J. Clean. Prod.*, 137, 741–751.
- Smetana, S., Schmitt, E. & Mathys, A. (2019). Sustainable use of *Hermetia illucens* insect biomass for feed and food: Attributional and consequential life cycle assessment. *Resources, Conservation and Recycling*, 144, 285–296.
- Somroo, A. A., ur Rehman, K., Zheng, L., Cai, M., Xiao, X., Hu, S., Mathys, A., Gold, M., Yu, Z., & Zhang, J. (2019). Influence of *Lactobacillus buchneri* on soybean curd residue co-conversion by black soldier fly larvae (*Hermetia illucens*) for food and feedstock production. *Waste Management*, 86, 114–122.
- Spranghers, T., Ottoboni, M., Klootwijk, C., Ovyen, A., Deboosere, S., De Meulenaer, B., Michiels, J., Eeckhout, M., De Clercq, P. & De Smet, S. (2017). Nutritional composition of black soldier fly (*Hermetia illucens*) prepupae reared on different organic waste substrates *Journal of the Science of Food and Agriculture*, 97(8), 2594–2600.
- Sriperm, N., Pesti, G. M., & Tillman, P. B. (2011). Evaluation of the fixed nitrogen-to-protein (N:P) conversion factor (6.25) versus ingredient specific N:P conversion factors in feedstuffs. *Journal of the Science of Food and Agriculture*, 91(7), 1182–1186.
- Tschirner, M. & Simon, A. 2015. Influence of different growing substrates and processing on the nutrient composition of black soldier fly larvae destined for animal feed *Journal of Insects as Food and Feed*, 1(4), 249–259.
- United Nations Development Program (UNEP). (2013). *Guidelines for National Waste Management Strategies: Moving from Challenges to Opportunities*.
- Van der Fels-Klerx, H. J., Camenzuli, L., Belluco, S., Meijer, N., & Ricci, A. (2018). Food Safety Issues Related to the Uses of Insects for Feeds and Foods *Comprehensive Reviews in Food Science and Food Safety*, 17, 1172–1183.
- van der Fels-Klerx, H. J., Meijer, N., Nijkamp, M. M., Schmitt, E., & van Loon, J. J. A. (2020). Chemical food safety of using former foodstuffs for rearing black soldier fly larvae (*Hermetia illucens*) for feed and food use. *Journal of Insects as Food and Feed*, 6(5), 475–488.

- Vruggink, M. (2020). Protein-rich animal feed: Development of an Assessment Framework for Black Soldier Fly Larvae Substrate Suitability Master thesis École Polytechnique Fédérale de Lausanne (EPFL).
- Wickham et al. (2019) Welcome to the tidyverse. *Journal of Open Source Software*, 4(43).
- Wickham, H. (2016). *ggplot2: Elegant Graphics for Data Analysis*. Springer-Verlag.
- Wilson, D. C., Rodic, L., Modak, P., Soos, R., Carpintero, A., Velis, K., Iyer, M., & Simonett, O. 2015. Global waste management outlook
- Zurbrügg, C., Dortmans, B., Fadhila, A., Verstappen, B., Diener, S., 2018. From Pilot to Full-Scale Operation of a Waste-To-Protein Treatment Facility. *Detritus*, 1, 18–22.

INNOVATIVE RECYCLING OF END OF LIFE SILICON PV PANELS: RESIELP

Pietrogianni Cerchier ^{1,*}, Katya Brunelli ¹, Luca Pezzato ¹, Claire Audoin ², Jean Patrice Rakotoniaina ², Teresa Sessa ³, Marco Tammaro ⁴, Gianpaolo Sabia ⁵, Agnese Attanasio ⁶, Chiara Forte ⁷, Alessio Nisi ⁷, Harald Suitner ⁸ and Manuele Dabalà ¹

¹ Department of Industrial Engineering, University of Padova, via Marzolo 9, 35131, Italy

² University Grenoble Alpes, CEA, Liten, Campus Ines, 73375 Le Bourget du Lac, France

³ Relight, via Lainate 98/100, 20017 Rho, Italy

⁴ ENEA, Energy and Sustainable Economic Development, Division Resource Efficiency, Piazzale E. Fermi 1, 80055, Naples, Italy

⁵ ENEA, Energy and Sustainable Economic Development, Division Resource Efficiency, via M.M. Sole 4, 40129 Bologna, Italy

⁶ CETMA, Diagnostic and Civil Engineering Area, Advanced Materials & Processes Consulting Division, s.s. 7 Appia, 72100 Brindisi, Italy

⁷ I.T.O. S.r.l., via Achille Costa 60, 73044 Galatone, Italy

⁸ PROJEKTKompetenz.eu GmbH, Franz-Josef-Str. 19/7, 5020 Salzburg, Austria

Article Info:

Received:

30 September 2020

Revised:

16 April 2021

Accepted:

23 June 2021

Available online:

30 September 2021

Keywords:

PV panels recycling

Silicon

Glass

End of Life PV panels

Recycling

ABSTRACT

In Europe, an increasing amount of End of Life (EoL) photovoltaic silicon (PV) panels is expected to be collected in the next 20 years. The silicon PV modules represent a new type of electronic waste that shows challenges and opportunities. ReSiELP was a European project that aimed at recovery of valuable materials (aluminum, glass, copper, silicon, and silver) from EoL silicon PV modules. During the project a pilot plant, constituted by a furnace, a gas abatement system, an apparatus for the mechanical separation and a hydrometallurgical plant was designed and built. The pilot plan was realized to upscale recycling technology to TRL 7, with a 1500 panels/year capacity. The feasibility of industrial-scale recovery and the reintegration of all recovered materials in their appropriate value chain was investigated. The results obtained showed that 2N purity silicon and 2N purity silver can be recovered with high efficiency. In order to realize a zero-waste plant, a hydrometallurgical process was developed for the wastewater treatment. Moreover, the use of recovered glass for building materials was investigated and the obtained performance seemed comparable with commercial products.

1. INTRODUCTION

Millions of photovoltaic (PV) panels have been installed worldwide over the past three decades, and, considering an estimated lifetime between 20 to 30 years, more than 2M tons of End-of-Life (EoL) PV panels are expected to be collected in next 15 years. Once the modules reach their end-of lifetime, they are considered waste and in Figure 1 is shown the estimate amount of this waste in Europe for the next years, considering 20 years as average time gap from installation to disposal (Jager-Waldau, 2017). A report published by the International Energy Agency Photovoltaic Power Systems Programme (IEA PVPS) and the International Renewable Energy Agency (IRENA) in 2016 has forecast that PV modules waste globally will amount to 1.7–8.0 million tons cumulatively by 2030 and to 60-78 million tons cumulatively by 2050 (IRENA and IEA-PVPS, 2016).

This enormous amount of EoL Silicon (PV) modules would require the implementation of a circular value chain to ensure a secure supply of raw materials and to limit disposal in landfill (Choi & Fthenakis, 2010). Silicon metal has been considering a critical raw material by European Commission since 2014 (European Commission, 2015), and, therefore, it would be crucial to recover it from EoL PV panels. Moreover, silicon production needs intensive energy consumption whereas its recovery reduce the energy consumption (Müller, Wambach, & Alsema, 2006), thus making its recycling advantageous to the environment.

According to European Commission, 85% of the solar panels currently manufactured are based on crystalline silicon (c-Si) technologies (Dias, Benevit, & Veit, 2016; Paiano, 2015). A typical c-Si PV panel today is approximately composed by : 76 wt% glass, 10 wt% polymer, 8 wt% aluminum, 5 wt% silicon, 1 wt% copper, less than 0.1



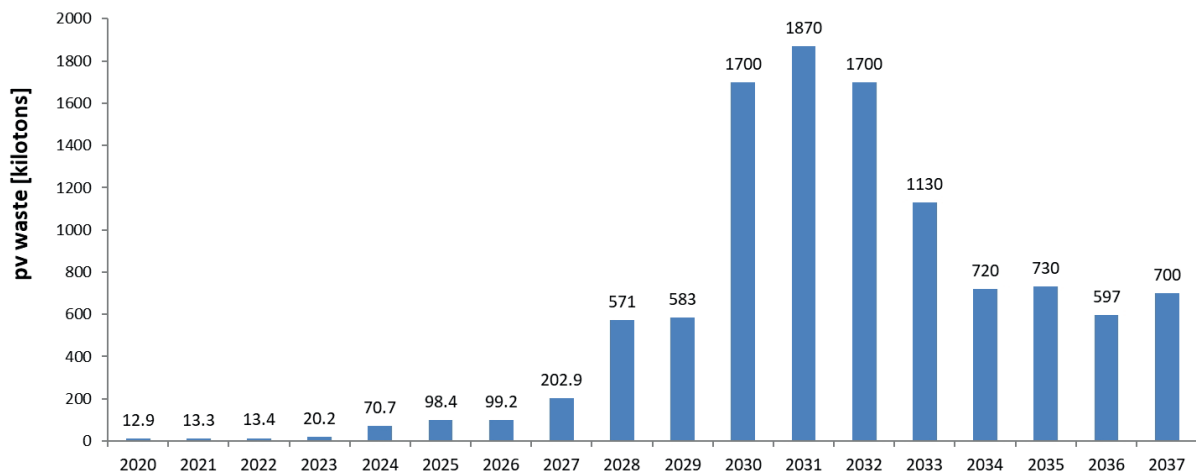


FIGURE 1: Estimated annual waste volumes (ktons) of end-of-life PV panels in Europe.

wt% silver, and tin and lead (Weckend, Wade, & Heath, 2017). End-of-life solar PV panel management is a newly emerging field that needs further research and development (Xu, Li, Tan, Peters, & Yang, 2018). As a matter of fact, despite the richness of EoL panels in valuable materials, only one industrial plant currently exists in Europe for dismantling and recycling of EoL PV panels and it is based on mechanical treatments.

ReSiELP (www.resielp.eu), a European project supported by EIT RawMaterials from 2017 to 2020, involved several partners (universities, research institutes and SME's) from different European countries. ReSiELP aimed at recovering from EoL PV panels, other than aluminum, glass and copper, also the others valuable materials such as silicon and silver using a thermo-mechanical-hydrometallurgical process, and at implementing a zero-waste innovative recycling loop (Sgarloto, et al., 2018). ReSiELP proposed a circular economy with a product centric zero-waste approach, as shown in Figure 2. The project was mainly focused on the development of a recovery and purification process to obtain Si with such purity as to be reused as raw material in the PV production. The process included also the recovery of glass, copper and silver to allow their reintegration in their value chain. Moreover, the use of recovered glass as building material was investigated. In order to minimize the environmental impact of the recycling plant and to realize

a zero-waste process, a treatment for the wastewater coming from the process was studied

2. RESIELP PROJECT OVERVIEW

2.1 The recovery process

The thermo-mechanical-hydrometallurgical process for the recycling of EoL PV panels, developed at TRL5 by the group of metallurgy of Padova University, was upscaled at pilot plant (technology readiness level TRL7). The group of metallurgy of Padova University designed and built the new plant, that was installed at Relight company located in Rho (Milan). In detail, were designed and built the furnace, the gas abatement system, the apparatus for the mechanical separation and the hydrometallurgical plant (Figure 3).

The recycling process is shown in Figure 4 and was composed of four parts:

1. Dismantling and cutting;
2. Heating treatment;
3. Material separation;
4. Chemical treatments;
5. Silver recovery.

In the plant, the aluminum frames and the power optimizers were first manually removed from the collected panels. The panels were then cut in half and one half-panel per batch was put in the furnace and treated at $450^{\circ}\pm 550^{\circ}\text{C}$ for 20÷30 minutes to burn the polymeric part of encapsulant and backsheets.

The heating treatment was followed by the separation of the materials to divide Si cells from glass and copper ribbons. This step was performed with an apparatus built by the University of Padova and exploiting a patented process. The Si PV cells were chemically treated in the hydrometallurgical plant to remove aluminum paste, using a basic solution of sodium hydroxide, and silver contacts using a nitric acid solution. To verify the efficiency of the hydrometallurgical treatments, silicon cells were investigated by SEM (Cambridge Stereoscan 440) equipped with EDS.

The silver was recovered from the acid solution by a hydro-pyro metallurgical process.

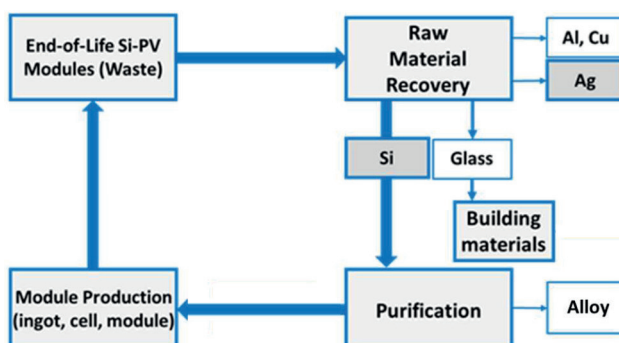


FIGURE 2: ReSiELP concept.

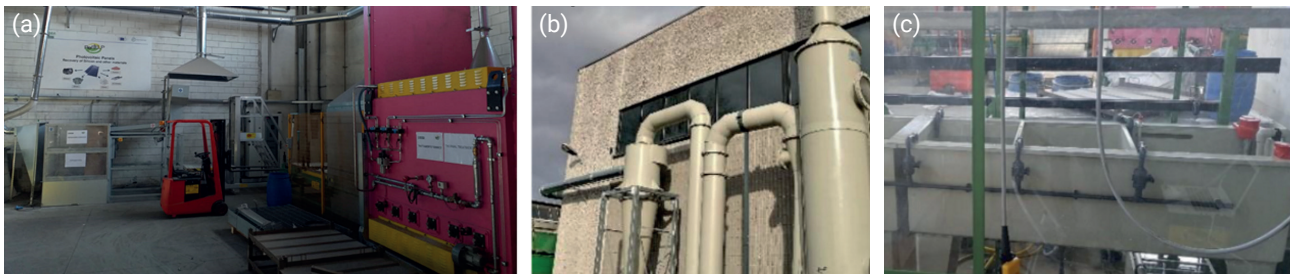


FIGURE 3: Images of pilot plant for the recycling process: a) furnace and separation system; b) gas abatement system; c) hydrometallurgical plant.

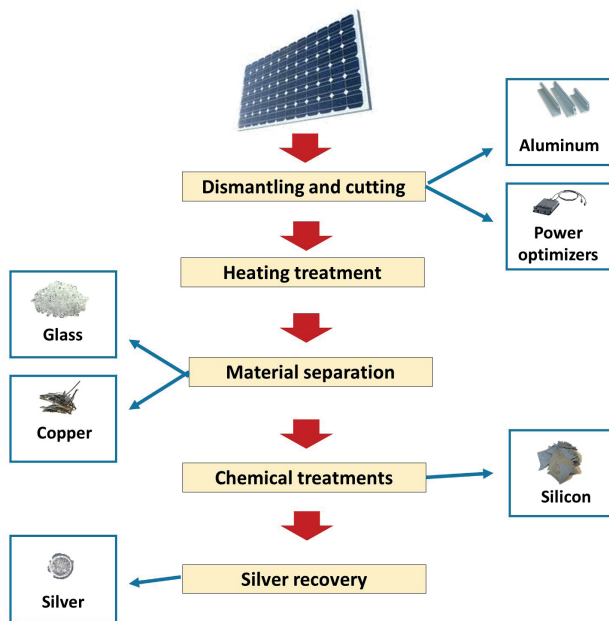


FIGURE 4: Estimated annual waste volumes (ktons) of end-of-life PV panels in Europe.

The recovered silicon and silver were finally analyzed with by a Spectro GENESIS inductively coupled plasma (ICP) mass spectrometer to determine the purity.

2.2 The wastewater treatment

ENEA studied a process to treat the wastewater coming from the hydrometallurgical plant to reduce the environmental impact of the process and to obtain a zero-waste approach.

The hydrometallurgical treatment for the recovery of metals from PV cells produced three main types of wastewater:

1. Acid wastewater;
2. Basic wastewater;
3. Washing wastewater.

Laboratory tests to identify the optimal conditions for the pollutants removal were carried out. For these experiments the more polluted basic and acid liquid streams were considered. The scope was to test conventional treatment technique in order to recover the water. The idea was making basic and acid wastewater react together in order

to precipitate the metals contained in the solutions.

The first tests were carried out on alkaline hydrometallurgical wastewater by precipitation obtained varying the pH. In the preliminary set of tests, reported hereafter, the analysis was performed on the alkaline solution. Such stream was sampled and settled and total solid concentrations were determined for the mixed solution and the supernatant after settling. For such analytical determination the supernatant was filtered with a Whatman glass microfiber filter GFC (1,2 µm).

The supernatant was then treated dosing acid solutions in order to change the pH and promote precipitation process. Both H₂SO₄ (1.8 M) and HCl (1.16 M) acid solutions were separately tested: these laboratory-made solutions were slow dropwise added to 100 mL sample of basic wastewater.

These tests made it possible to identify the optimal pH corresponding the best metal removal efficiency. The removal rates achieved at the different reached pH were determined taking some amounts of the supernatant and using an ICP-MS instrument (Perkin-Elmer Sciex Elan 6000 ICP-MS).

According to lab tests, equipment dedicated to the recycling of wastewater was installed in the pilot plant.

2.3 Innovative glass application

The construction sector is constantly required to become more sustainable, for instance in terms of raw materials consumption. The valorisation of recycled materials, as partial replacement of conventional materials commonly used in construction materials, is a promising way to reduce consumption of natural materials and depletion of resources. The use of glass fractions, recovered from EoL PV-panels, is a sustainable option that can be implemented into building materials and the development of precast building components. Some works up to TRL 5 were carried out using recycled glass of different origin for building materials development (Tamanna, Mohamed Sutan, Lee, & Yakub, 2013; Korjakins, Shakhmenko, Bajare, & Bumanis, 2012). However, to the best of our knowledge, building materials incorporating recycled glass from PV-panels have not been produced on industrial scale so far. In ReSiELP project, CETMA and ITO worked together for the valorization of glass from PV-panels recycling which was re-used for the development of sustainable building materials (e.g. mortars, concretes) and precast components. This recy-

bled material, after a mechanical treatment to be available in different sizes, was investigated as partial replacement of conventional aggregates, fillers and/or cements used for mortars/concretes/precast components production. Materials formulations were designed with the aim to maximize reused glass fractions taking into consideration the requirements of specific building applications (e.g. masonry mortars, concretes for prefabrication). The most promising concrete formulations were implemented at industrial scale with the production of precast components, thus demonstrating the potential of the developed solutions in operational environment (TRL7). Some prototypes of prefabricated slabs were produced in ITO industrial plants as demonstrators of the Project. The process as well as the equipment used for the production of these innovative building materials are conventional: this represents an important advantage of the investigated solutions.

3. RESULTS AND DISCUSSION

3.1 The recovery process

EoL PV panels were collected by Relight and treated according to the process developed by University of Padova.

After collection of EoL PV panels, the aluminum frame and the power optimizer were manually removed and each panel was cut in half. The half-panels without the aluminum the power optimizer are showed in Figure 5.

Several tests were performed to optimize the heating treatment parameters at industrial scale and were found the optimal temperature and time to induce the complete burning of the polymeric fraction (Figure 6). In comparison with mechanical and chemical treatments, this heating treatment prevented damages to the fragile Si cells, thus allowing an efficient recovery of materials. In fact, the Si cells, even if they got broken during the dismantling of PV panels and collection, were recovered in pieces with a me-

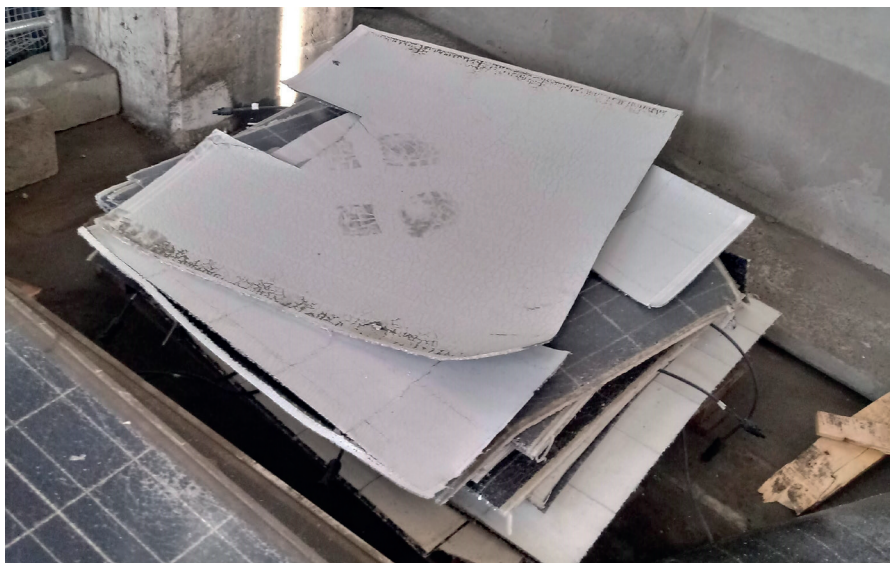


FIGURE 5: Example of PV halve panels prepared for heating treatment.



FIGURE 6: EoL PV panel after heat treatment in ReSiELP furnace.

dium size of 5 cm², whereas mechanical treatments used in the other plants reduce them in very thin powder. This size facilitated the separation and hydrometallurgical treatment.

All recovered materials are shown in Figure 7. With manual disassembly was possible to recover the 100% of aluminum frames (Figure 7b), whereas the separation system allowed the recovery of 98% of copper ribbons and glass (Figure 7c,f). 60% of silicon cells were suitable for hydrometallurgical treatment whereas a fraction was represented by glass and silicon powder that was not possible to separate.

The hydrometallurgical treatment of the Si PV cells, after the optimization of the process parameters, allowed the recovery of demetallized Si-cells using basic and acid solutions to remove aluminum paste and silver contacts, respectively (Figure 8). The process allowed recovering silicon cells with 2N purity (Figure 7d). The silver was subsequently recovered from the acid solution of treatment with a hydro-pyrometallurgical process (Figure 7e).

In conclusion, the reliability of recovery plant processes

has reached a high operating level (TRL7, as planned) with a capacity of 1500 panels/year. During the project 10 tons of EoL PV panels was treated to produce: 140 kg of silicon (Si-cells based) with 2N purity, 2 kg of silver with 2N purity, 6980 kg of glass with high purity, 1790 kg of aluminum frames and 88 kg of copper ribbons. Copper ribbon, aluminum frame and silver have been sold during the project. Silicon needed a purification in order to be reused in PV value chain.

3.2 The wastewater treatment

The basic wastewater contains mainly Al derived from the backsheet of silicon cells. In the laboratory test on the basic wastewater, the initial pH was ≈ 13.8 and was lowered below 3. Independently on the acid solution used (HCl or H₂SO₄), the formation of a suspension was observed for a pH value of about 13, while at pH around 3 a complete solubilization of the precipitated materials took place probably due to amphoteric characteristics. The analysis of the wastewater before and after the treatment is reported in Table 1.

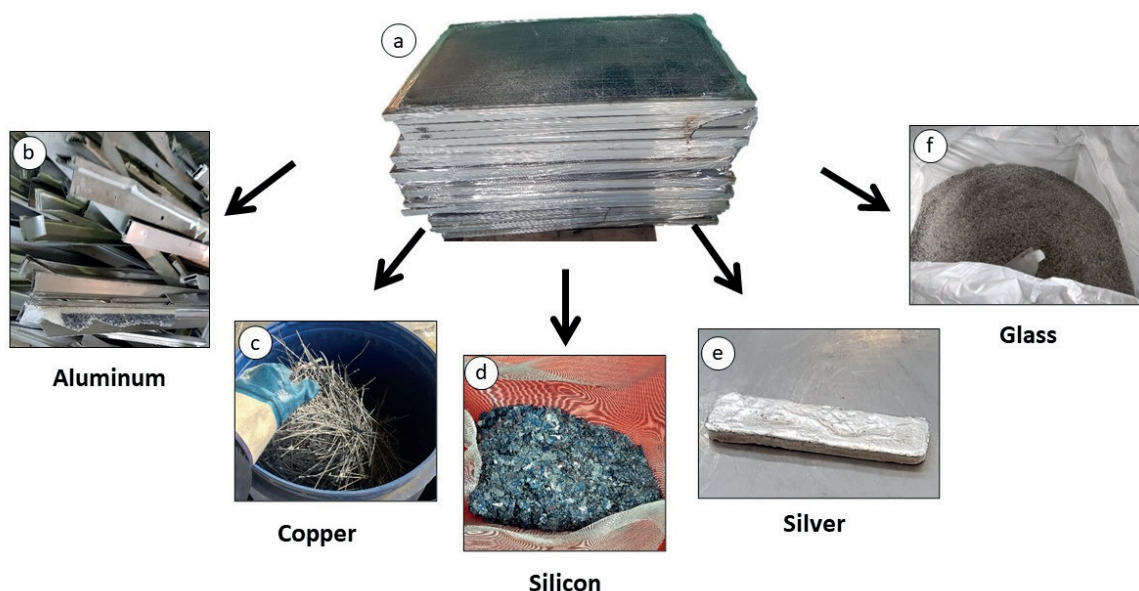


FIGURE 7: PV waste (a) and materials recovered by ReSiELP pilot plant (b, c, d, e, f).

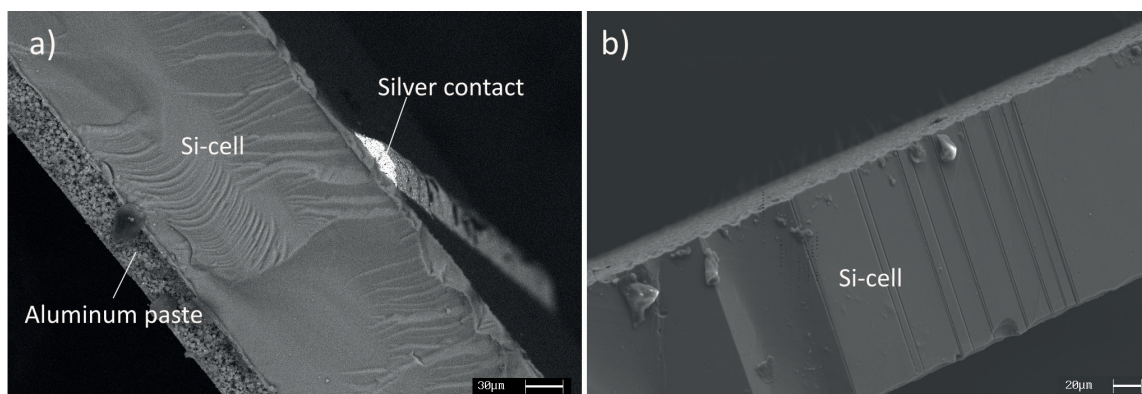


FIGURE 8: SEM images of silicon cell before (a) and after (b) the hydrometallurgical treatment.

TABLE 1: Concentration of contaminants in basic wastewater before and after neutralization with H₂SO₄ at pH 7.

Contaminant	Concentration [ppm] before neutralization (pH 13.1)	Concentration [ppm] after neutralization (pH 7.0)	Removal yield of neutralization [%]
Al	1941.00	0.90	99.95
Pb	6.98	0.07	98.94
Cu	4.92	0.17	96.57
Zn	2.07	0.17	91.74
Fe	0.45	0.07	85.49

The best results were reached at pH value around the neutrality. The concentration of pollutants before and after neutralization with H₂SO₄ solution are reported in Table 1.

As it can be seen, the removal rate was very high for the main contaminants in the wastewater: 99.95% for Al and 98.94% for Pb.

3.3 Innovative glass application

For the purpose of glass reuse for sustainable building materials production, different glass fractions were characterized in terms of physical properties (e.g. particle size distribution, density, water absorption, fineness). Based on the measured properties several sustainable mortars and concretes formulations, incorporating reused glass for partial replacement of aggregates or cements, were designed and produced. The use of recycled glass as partial replacement of aggregates seemed promising for these materials. Mortars and concretes were tested evaluating technical performance such as density, consistency on fresh state as well as mechanical properties development at different curing stages (Figure 9). In an industrial perspective, the performance of these building materials have been assessed, referring to technical standards prescriptions, for specific construction products (e.g. masonry mortars, concretes for prefabrication). A bedding mortar of class M₅ has been produced, having similar physical-mechanical performance of mortars available on the market. Concretes with consistency up to class S5 and compressive strength 61 MPa have been produced and implemented in the industrial plant. In total four pre-dalles slabs, with dimensions 1.2 m x 2.4 m and 1.2 x 6.0 m, were manufactured and the structural check confirmed

performance similar to other conventional slabs produced for the market.

4. CONCLUSIONS

During the ReSiEILP project a pilot plant was designed and built by the group of metallurgy of Padova University. The tests showed that the materials contained in PV waste can be recovered with high efficiency and purity. Moreover, a hydrometallurgical process was developed by ENEA for the wastewater treatment in order to make the new plant zero waste. Concerning the PV glass reuse for building materials production, sustainable mortar and concrete formulations incorporating reused glass fractions were studied and produced by CETMA and ITO. The performance of these formulations was assessed for specific construction applications (prefabricated components) and seemed comparable with commercial products.

ACKNOWLEDGEMENTS

This activity has received funding from the European Institute of Innovation and Technology (EIT), a body of the European Union, under the Horizon 2020, the EU Framework Programme for Research and Innovation.

REFERENCES

- Choi, J., & Fthenakis, V. (2010). Design and optimization of photovoltaics recycling infrastructure. *Environ. Sci. Technol.*, 44, 8678–8683. <https://doi.org/10.1021/es101710g>
- Dias, P. R., Benevit, M. G., & Veit, H. M. (2016). Photovoltaic solar panels of crystalline silicon: Characterization and separation. *Waste Manag. Res.*, 34(3), 235-245. <https://doi.org/10.1177/0734242X15622812>

**FIGURE 9:** Building materials with glass from PV-panels: mechanical test on mortar (a) and industrial production of concrete (b).

- European Commission, (2015). Report on critical raw materials for EU.
- Jäger-Waldau, A. (2017). PV Status Report 2017.
- Korjakins, A., Shakhmenko, G., Bajare, D., & Bumanis, G. (2012). Effect of ground glass fineness on physical and mechanical properties of concrete. Proceedings of the 10th International Congress for Applied Mineralogy (ICAM) (pp. 395-402). Berlin: Springer. https://doi.org/10.1007/978-3-642-27682-8_47
- Müller, A., Wambach, K., & Alsema, E. (2006). Life Cycle Analysis of Solar Module Recycling Process. Mater. Res. Soc. Symp. Proc. (p. 895). Materials Research Society.
- Paiano, A. (2015). Photovoltaic waste assessment in Italy. Renew. Sust. Energ. Rev., 41, 99-112. <https://doi.org/10.1016/j.rser.2014.07.208>
- Sgarioto, S., Cerchier, P., Brunelli, K., Pezzato, L., Dabala, M., Tammaro, M., . . . Rakotoniaina, J. (2018). ReSiELP: Recovery of Silicon and other materials from End-of-Life Photovoltaic Panels. Proceedings of SUM2018. Bergamo.
- Tamanna, N., Mohamed Sutan, N., Lee, D., & Yakub, I. (2013). Utilization of waste glass in concrete. chez 6th International Engineering conference, Energy and Environment (ENCON) (pp. 323-329). At Kuching: Research Publishing. https://doi.org/10.3850/978-981-07-6059-5_090
- IRENA and IEA-PVPS (2016), End-of-Life Management: Solar Photovoltaic Panels. International Renewable Energy Agency and International Energy Agency Photovoltaic Power Systems.
- Xu, Y., Li, J., Tan, Q., Peters, A. L., & Yang, C. (2018). Global status of recycling waste solar panels: A review. J. Waste Manag., 75, 450-458. <https://doi.org/10.1016/j.wasman.2018.01.036>

PHOTOVOLTAIC MODULE RECYCLING: THERMAL TREATMENT TO DEGRADE POLYMERS AND CONCENTRATE VALUABLE METALS

Priscila Silva Silveira Camargo ^{1,*}, Andrey da Silva Domingues ¹, João Pedro Guê Palomero ¹, Angela Cristina Kasper ¹, Pablo Ribeiro Dias ² and Hugo Marcelo Veit ¹

¹ Department of Materials Engineering, Federal University of Rio Grande do Sul (UFRGS), Av. Bento Gonçalves, 9500, 91509-900, Porto Alegre, RS, Brazil

² School of Photovoltaics and Renewable Energy Engineering, University of New South Wales, UNSW, Sydney, NSW 2052, Australia

Article Info:

Received:
1 March 2021
Revised:
1 July 2021
Accepted:
26 July 2021
Available online:
xxxxxxxxxxxxxx

Keywords:

WEEE Recycling
Crystalline silicon photovoltaic module
Thermal Treatment
Valuable Metals
Silver
Polymers

ABSTRACT

This work investigated the thermal treatment to separate and concentrate economically valuable materials from laminates of crystalline silicon photovoltaic modules (i.e., photovoltaic modules without the aluminum frame and the junction box). Chemical characterization of the metal content was performed by X-Ray Fluorescence (XRF). The polymers of the backsheet were also characterized by Fourier Transform Infrared Spectroscopy (FTIR). The influence of the atmosphere (oxidizing and inert) on the decomposition of the backsheet was investigated by Thermogravimetric Analysis (TGA). Moreover, non-comminuted samples were tested for 4 thermal time lengths (30, 60, 90, and 120 min) in the furnace under ambient air. The degradation of the polymers was measured and 3 material fractions were obtained: silicon with silver and residual polymers (SS), glass and copper ribbons. Furthermore, there was no statistical difference between the mass losses of the samples submitted for 90 (13.62 ± 0.02 wt.%) and 120 min at 500°C (p-value = 0.062). In the SS fraction, silver was 20 times more concentrated than in the ground photovoltaic laminate and 30 times more concentrated than high silver concentration ores. The SS fraction (about 6 wt.%) also presented low copper concentration and a high concentration of lead (hazardous metal). About 79 wt.% glass was obtained, as well as 1% copper ribbons ($55.69 \pm 6.39\%$ copper, $23.17 \pm 7.51\%$ lead, $16.06 \pm 2.12\%$ tin). The limitations of the treatment and its environmental impact are discussed, and suggestions for industrial-scale application are given.

1. INTRODUCTION

1.1 Solar Photovoltaic Energy

In 2019, solar photovoltaic (PV) energy accounted for 22.9% of the global renewable energy market, staying behind hydro (44.7%) and wind (23.4%) energy, in terms of installed capacity (IRENA, 2021a). PV installed capacity has grown at unprecedented rates since the early 2000s in worldwide (Weckend et al., 2016) as it went from 22,817 MW in 2009 to 578,553 MW in 2019 (IRENA, 2021b). The energy from PV sources is a competitive technological alternative to other traditional energy sources since it is inexhaustible on the human time scale and is also more sustainable (Pinho & Galdino, 2014; Tao & Yu, 2015). In Germany, for example, the consumption of 47.5 TWh of PV energy avoided about 29 million tons of carbon dioxide emissions in 2019 (ISE, 2020).

1.2 c-Si Photovoltaic Module Components

Crystalline silicon (c-Si) is the oldest technology (first generation) used in modules from PV panels. Currently, this technology represents 95.4% of the solar panel market (ISE, 2020). Crystalline silicon PV modules are composed of several materials, such as high-transparency tempered glass, layers from ethyl vinyl acetate (EVA), crystalline silicon PV cells, copper and silver metal contacts, antireflection and passivation layers, a polymer backsheet and an aluminum frame. The backsheet is composed of a combination of polymers, that can contain polyvinyl fluoride (PVF or Tedlar®), polyethylene terephthalate (PET), among others (Dias et al., 2017; Huang et al., 2017; Weckend et al., 2016).

Ultra-pure silicon (doped with boron, phosphorus, and aluminum) is used in c-Si PV cells. This material absorbs solar radiation and converts it into electrical current (De-

* Corresponding author:
Priscila Silva Silveira Camargo
email: engamb.pricamargo@gmail.com

Bergalis, 2004; Pinho & Galdino, 2014; Strachala et al., 2017). A silver-aluminum paste is printed, in a grid pattern, on the front and back of the cell in order to form an electric field. The conductive copper ribbons are soldered (with lead and tin solder) along surfaces from PV cells (Huang et al., 2017).

1.3 Photovoltaic Waste

PV modules have a useful life estimated of about 25 - 30 years (Paiano, 2015). However, an increasing number of modules will reach the end of their lifespan before that time due to the damage during installation or storms, component failures, or economic incentives to replace older modules by new modules with higher efficiency (Tao et al., 2020).

Projections from International Renewable Energy Agency (IRENA) indicated that the global generation of PV waste could reach 8 million tons in 2030 and approach 80 million tons in 2050, considering an early loss scenario (Weckend et al., 2016). Considering a regular loss scenario, where only End-of-Life (EoL) panels are replaced, the projections are 1.7 million tons for 2030 and 60 million tons for 2050.

In Europe, EoL PV panels started to be considered as "Waste of Electrical and Electronic Equipment" (WEEE) by the European WEEE Directive 2012/19/EU. Moreover, a reverse logistics system has been imposed on suppliers, manufacturers, importers and resellers of PV modules that are obliged to collect and recycle EoL PV modules (Padoan et al., 2019; Weckend et al., 2016).

1.4 Environmental Risk

Typically, more than 90% of PV modules mass is composed by glass, polymers and aluminum, which can be classified as non-hazardous waste. However, there are components in smaller proportion that require more attention such as silver, tin, lead and others metals in crystalline silicon panels. Furthermore, cadmium and arsenic - hazardous metals - are present in some thin film technologies (Weckend et al., 2016). These hazardous elements can cause environmental and public health problems in case of incorrect disposal (Aryan et al., 2018; Fthenakis, 2000).

According to BioIS report (2011), a particular concern is the large amount of lead in c-Si, approximately 12.67 g in a panel with about 22 kg. BioIS report (2011) informed that a c-Si module at its End-of-Life, disposed of in the environment, when leached by the rain, can release between 13% and 90% of the amount of lead found. Tamaro et al. (2016) performed leaching tests on crushed and broken samples of different PV technologies, with sizes between 0.5 and 3 cm. Moreover, they investigated 18 releasable metals by chemical and ecotoxicological analysis. Some hazardous metals such as lead, chromium, nickel, tin and cadmium exceeded the legal limits of European and Italian laws for drinking water, soil discharge and inert disposal in landfills. By ecotoxicological evaluation, adverse effects were indicated mainly due to the occurrence of lead, tin and cadmium. In the same work, high amounts of lead (30 t) and cadmium (2.9 t) releasable from c-Si and thin film panels, respectively, were also predicted for 2050.

Nain & Kumar (2020) analyzed the release of metals from broken and unbroken solar panels that were exposed

to three synthetic solutions of pH 4, 7, 10 and one real municipal solid waste (MSW) landfill leachate for one year. The results suggested that encapsulant degradation plays a critical role and has a positive correlation with metal dissolution. They also indicated that the mass of exposed modules per volume of water increases the probability of leached metals exceeding standard limits. Nain & Kumar (2020) reported that the increase in leaching contamination after one year of disposal of polycrystalline silicon modules was 54.19%.

Furthermore, Nain & Kumar (2020) observed that the leaching of metals in stormwater solutions was minimal, except for a few metals. For the initial months after disposal, the PV cells and films maintain their integrity because of encapsulation. So, disposal of EoL solar PVs in MSW landfills could result in less leaching from semiconductor layers. Therefore, they concluded that aggressive short-term standard waste characterization tests, such as Whole Effluent Toxicity Methods (WET/EPA) and Toxicity Characterization Leaching Procedure (TCLP/EPA), could poorly represent the release of metals from encapsulated materials in landfill leachate. They reported that the results obtained do not indicate that the disposal of PV in landfills is environmentally safe, but that there is a need for further investigations on different aspects, such as the effect of microbial activity, temperature variations, and composition of MSW waste on metal solubilization from PVs.

There is also concern about the release of poly/brominated flame retardants (Padoan et al., 2019), ozone-depleting chemicals such as Chlorofluorocarbons (CFCs). PV modules composition also contain fluoropolymers, such as Polyvinyl Fluoride (PVF) or Polyvinylidene Fluoride (PVDF), especially in the backsheets. These components can be harmful to both human health and the environment (Mulvaney, 2014; Yi et al., 2014). The burning of these fluoropolymers is a source of persistent compounds such as carbon fluorides, fluoroacids, dioxins, and furans (Aryan et al., 2018). Burning PVF generates HF at 350°C and benzene at 450°C (Huber et al., 2009).

1.5 Economic Potential

On the other hand, the disposal of PV modules in landfills is a wastage of valuable raw materials (such as silver, silicon, copper, gallium, indium, germanium, and tellurium) and conventional materials, such as aluminum and glass (Aryan et al., 2018; BioIS, 2011; Strachala et al., 2017).

In addition, this waste can represent opportunities in developing or transition economies, where waste collection and recycling services are often dominated by informal sectors (Weckend et al., 2016). Some of the materials recovered from Si modules can be sold directly on the commodities market. The largest amount of recovered materials are glass fragments (which must be free of Si cells) and Cu ribbons for reuse in the solar industry (Tao et al., 2020).

Preliminary estimates suggest that technically recoverable raw materials from PV panels could cumulatively yield a value of up to USD 450 million (in 2016 terms) by 2030. This is equivalent to the amount of raw material currently required to produce approximately 60 million new panels or 18 GW of power generation capacity. By 2050, the re-

coverable value could cumulatively exceed USD 15 billion, equivalent to 2 billion panels or 630 GW (Kadro & Hagfeldt, 2017; Weckend et al., 2016).

According to Tao et al. (2020), silver represented 35.2% of the economic value obtained from recovering materials from a module, considering the price of USD 574.23/kg (Silver Price, 2019). In addition, copper represented 5.2% of the total economic value, considering the price of USD 5.0/kg (Rockaway Recycling, 2019). On February 26th 2021, the silver price was USD 857.73/kg (Silver Price, 2021) and the copper price was USD 9.17/kg (Insider, 2021).

Huang et al. (2017) estimated the costs of a recycling process for the valuable materials derived from silicon PV modules. The authors affirm that revenue earned is enough to cover the recycling cost and maintain a profitable recycling business without any government support. However, Deng et al. (2019) concluded that glass recycling is economically viable only in countries where landfill rates are high or module landfilling is prohibited. In addition, mechanical processing and thermal recycling need to have their costs reduced by at least 30% to become economically viable. According to the authors, the application of large-scale recycling requires governments to act in reduction costs and regulation, manufacturers include recycling in design, and that recyclers search methods for silver and Si wafer recovery at lower processing costs. The study recommends that governments, manufacturers and recyclers work collaboratively to build a recycling network. In another paper, authors concluded that the circular use of high-purity silicon and intact silicon wafers from EoL PV modules can be economically feasible with a reduction of 20% in manufacturing cost in the second-life modules, despite some efficiency reductions (Deng et al., 2020).

1.6 PV Modules Recycling Methods

Currently, silver is the metal of greatest interest in the recycling process c-Si panel (Dias et al., 2016; Tao & Yu, 2015) because it is a precious metal and its recovery adds economic value to the recycling of PV modules (Chancerel et al., 2009; Padoan et al., 2019). In the hydrometallurgical process, nitric acid is often applied to separate silver from PV cells. In this case, the purified crystalline silicon (solid phase) can be filtered, whereas the soluble silver in the leachate can be recovered from the residual acid by electrolysis or precipitation (Dias et al., 2016; Klugmann-Radziemska et al., 2010; Klugmann-Radziemska & Ostrowski, 2010; Kuczyńska-Łażewska et al., 2018; Latunussa et al., 2016; Shin et al., 2017).

Dias et al. (2018) separated waste of silicon-based PV modules using an electrostatic separator after mechanical milling. Granata et al. (2014) investigated the recycling of polycrystalline silicon, amorphous silicon and CdTe PV panels by two alternative sequences of physical operations: two-blade crusher rotors followed by thermal treatment and two blade crusher rotors followed by hammer crushing. The best option was the treatment route that involved (1) crushing by two-blade rotor crusher; (2) hammer crushing; (3) thermal treatment at 650°C of fractions larger than 1 mm; and (4) screening through a 0.08 mm sieve. By these operations, around 85% of the total weight of the

panels was recovered as glass from the fractions larger than 0.08 mm. Concerning the thermal treatment, they obtained about 10% weight loss for silicon panels, referring to degradation of the EVA.

Physical methods can be used to concentrate silver and silicon, and to reduce the consumption of chemical reagents. It is known that the major components of c-Si panels, including glass, aluminum, and copper, can be recovered with cumulative yields greater than 85%, relative to panel mass, through purely mechanical separation. It is understood that physical treatments such as crushing and grinding have the advantage of being inexpensive and allowing direct glass recovery. However, they cannot achieve the recovery of high-value materials such as silver, which requires more elaborate treatments. However, without a combination of thermal, chemical, or metallurgical steps, the impurity levels of the recovered materials could be high enough to reduce resale prices (Latunussa et al., 2016; Sander et al., 2007). Another concern is that crushing and grinding produce a large amount of dust and noise pollution (Xu et al., 2018).

Thermal decomposition is commonly used to separate material layers and remove polymers, as well as to recover materials such as glass, silicon, silver and copper (Dias et al., 2017; Fiandra et al., 2019; Gustavsson et al., 2006; Wang et al., 2012). Polymers thermal degradation should be performed in conjunction with an industrial-scale air pollution treatment system due to emissions (Huber et al., 2009).

Danz et al. (2019) studied the pyrolysis of PVF from the backsheet. The authors observed that the main pyrolysis reactions occurred between 400°C and 500°C and that temperature increases beyond the upper bound did not produce a significant mass loss. Farrell et al. (2019) looked at the effect of pyrolysis on EVA backsheet and two-stage decomposition was observed. In the first stage in which a temperature range was from 310 to 390°C, there was the removal of acetic acid from the vinyl acetate monomer within the EVA structure, with a mass loss of approximately 22.6 wt.%. In the secondary stage, at a temperature range of 410-510°C, there was a mass loss of 75.7 wt.%. Prado (2019) reported that 80% of the backsheet from the PV module was decomposed between 400 and 500°C in a nitrogen atmosphere. Dias et al. (2017) also evaluated the pyrolysis of the polymers from PV modules and reported that 75 wt.% was degraded when it reached 500°C in a nitrogen atmosphere.

Fiandra et al. (2018) compared the mass loss of thermal degradation under inert atmosphere (nitrogen) and oxidizing atmosphere (air). The authors reported that the oxygen present in an atmosphere can accelerate the process of EVA and backsheet degradation. Thus, because of this and the lower costs, it was decided to work with an oxidizing atmosphere (ambient air). Under oxidizing conditions, it was observed that heat treatment at 450°C was significantly less efficient than at 500 and 600°C. However, there was no significant difference between 500 and 600°C. The optimal operating conditions were 500°C and oxidizing atmosphere with a dwell time of 1 h.

Right after thermal treatment of non-comminuted PV samples, Fiandra et al. (2018) and Fiandra et al. (2019)

used sieves with different size apertures to separate the material obtained into three fractions: copper ribbons, glass and silicon. However, these papers do not detail how many or which sieves were used. In order to recycle polycrystalline silicon, amorphous silicon and CdTe PV panels, Granata et al. (2014) used 5 different sieves (8 mm, 5 mm, 1 mm, 0.4 mm, 0.08 mm) after crushing operations and thermal treatment.

Pagnanelli et al. (2017) utilized sieving after mechanical treatment, i.e., a triple crushing, obtaining three fractions: an intermediate fraction (0.4–1 mm) of directly recoverable glass (17 wt.%); a coarse fraction (>1 mm) requiring further thermal treatment in order to separate EVA-glued layers in glass fragments; a fine fraction (<0.4 mm) requiring chemical treatment to dissolve metals and obtain another recoverable glass fraction.

Dias et al. (2016) studied two methods to concentrate silver from waste modules. In the first method, the modules were milled, sieved, and leached in nitric acid solution with sodium chloride. In the second method, PV modules were milled, sieved, subjected to pyrolysis at 500°C, and leached in nitric acid solution with sodium chloride.

Weckend et al. (2016) explained that sieves are one of the typical pieces of equipment used in panel recycling to separate impurities and other materials such as glass. Magnets, crushers, eddy-current devices, optical sorters, inductive sorters, and exhaust systems are also used. Nevertheless, sieving systems are often used to separate materials from other waste electrical and electronic equipment, such as LEDs (Cenci et al., 2021), Li-ion batteries (Granata et al., 2012), portable batteries (Bernardes et al., 2004) and cell phones (Kasper, 2011).

The removal of the polymers results in cleaner silicon without the presence of organic matter. Thus, it is important to define better thermal parameters that result in more concentrated materials. The objective of this study was to define parameters such as atmosphere type, temperature and time to be used in thermal treatment, aiming at the degradation of polymers and the concentration of materials, especially silver, because the recovery of this precious metal is important to add economic value to make recycling feasible. This work studied how the thermal treatment time influences the mass loss (degraded polymers) and the chemical composition of the obtained material fractions.

2. MATERIALS AND METHODS

In Figure 1, the methodology applied in this work is outlined. Preliminary results of this work were presented at the Fifth Symposium on Urban Mining and Circular Economy Virtual Event held on November 18 - 20, 2020. The full paper was published in the proceedings of SUM 2020 (ISBN: 9788862650236). In this study, a donated cracked polycrystalline silicon PV module was used. The unit was manufactured in 2018. It had a mass of 22 kg and dimensions of 1956 mm x 992 mm x 40 mm.

2.1 Characterization

The object of this work was the c-Si PV laminate, that is, module without frame and junction box. Thus, the first step

was manual dismantling to remove the aluminum frame and the junction box.

2.1.1 Chemical Analysis

Subsequently, the c-Si PV laminate was fragmented into smaller pieces so that it would fit in the mill. The fragments from the laminate were comminuted in a knife mill, using a screen with 1 mm opening. The knife mill used was the SM300 model of the Retsch brand (Figure 2a). For characterization, 500 g of sample was ground, at 1500 rpm, until it reached a particle size less than 1.0 mm (verified in bench sieves). To ensure homogeneity and representativeness, the ground PV laminate was quartered (Figure 2b), and subsequently, three samples were analyzed (twice each sample) by X-ray fluorescence analysis (XRF). The portable analyzer used was a Thermo Nilton XL3t model of the Thermo Scientific brand (Figure 2c).

In the XRF analysis performed in this work, it was not possible to identify elements with atomic mass less than 12, such as hydrogen, oxygen and carbon. Thus, in this paper, we will identify this category as "Unidentified Elements" (UE). Polymers are mostly composed of these elements. Thus, the mass of the polymers present is included in this category when analyzed by XRF. Glass is composed mainly of SiO₂ and, consequently, part of its mass is also unidentified by the equipment. "X-ray diffraction analysis" (XRD) is required to differentiate the silicon from the glass and the crystalline silicon from the PV cell by chemical analysis. However, it is possible to visually differentiate these materials in the samples.

Furthermore, the white backsheet composed of polymers was also removed manually and separately characterized. The white backsheet composed of polymers was chemically identified using Fourier Transform Infrared Spectroscopy Analysis (FTIR). The FTIR Spectrophotometer used was a Spectrum 1000 model of the Perkin Elmer brand. The identification of these polymers is important to indicate the possible gaseous emissions of the studied processing route, based on the scientific literature.

2.1.2 Thermogravimetric Analysis

Three Thermogravimetric Analysis (TGA) were carried out to determine what is the ideal temperature for thermal treatment and what is the best atmosphere (inert or oxidizing) to be used. The thermogravimetric equipment used was the model Q50 of TA Instruments brand.

Thus, in the first stage, the backsheet material samples were subjected to TGA under two different atmospheres in order to verify which atmosphere would provide the greatest thermal decomposition. Inert atmosphere (gaseous nitrogen) was used in one sample. In another sample oxidizing atmosphere (synthetic air) was used.

After this preliminary analysis, a third sample of the ground PV laminate was also analyzed by TGA. In this stage, sample comminuted (particle size 1 mm) was then quartered to guarantee homogeneity, and a 10 mg sample was analyzed. This analysis allowed to determine the temperature of the highest thermal degradation, which was chosen as the operating temperature for the thermal treatment.

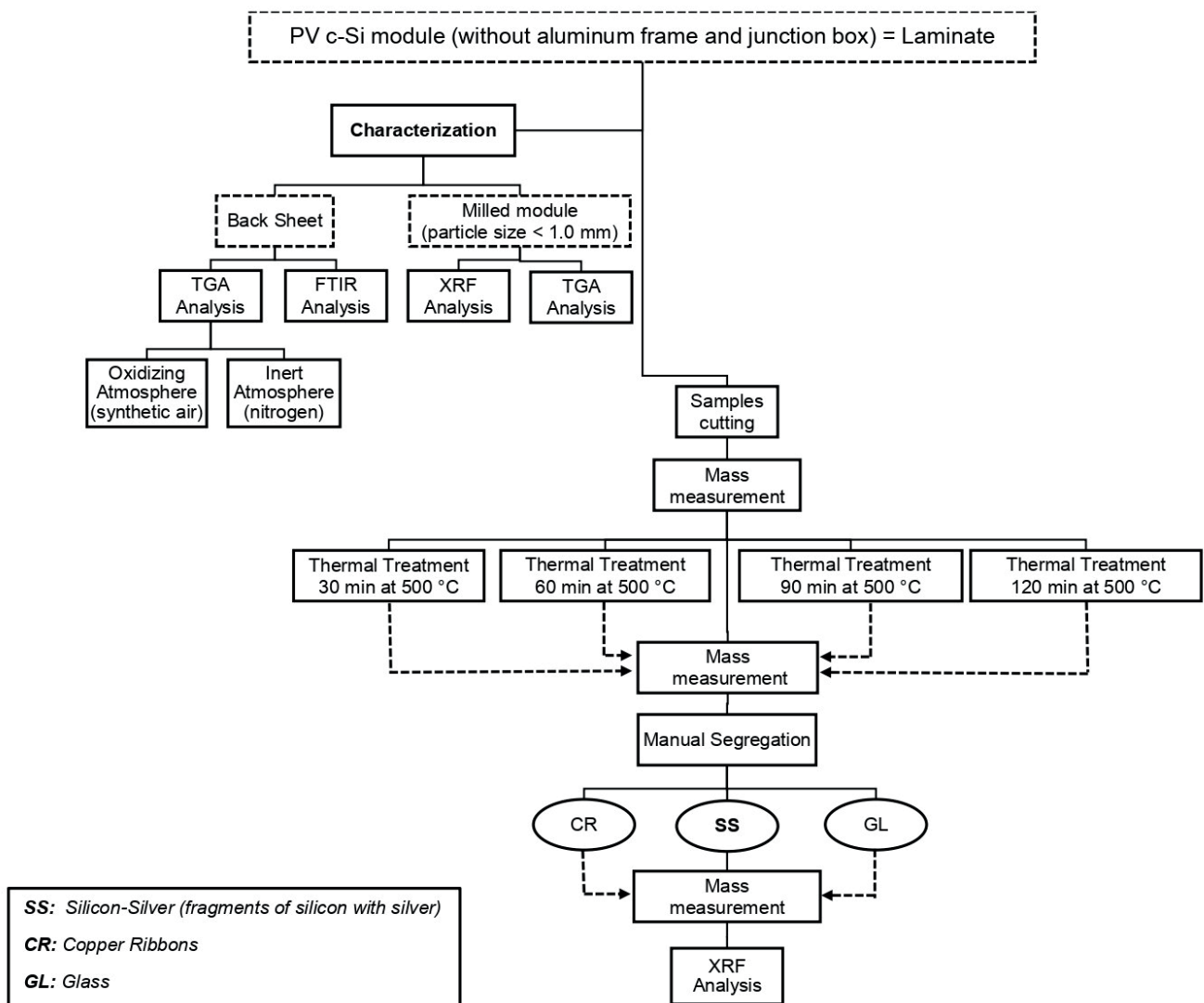


FIGURE 1: Flowchart of the general methodology applied in the work.

The three analyses were performed with a heating rate of 20°C/min, and the peak temperature was 940°C.

2.2 Thermal Degradation and Silver Concentration

The objective to work with thermal treatment on samples without comminution was to degrade the polymers present and separate the layers from PV cells. In this study, the samples used were 8 cm x 8 cm (Figure 3a), with an average mass of 57.33 g and a standard deviation of 2.27 g. Each sample was deposited in a ceramic crucible with the polymeric back layer facing upwards (Figure 3b), under an oxidizing atmosphere (ambient air), and heating rate of 9° C/min from an initial temperature of 50°C. The thermal treatment was carried out in a Sanchis N1100H furnace (Figure 3c), installed inside an extractor with a gas suction system.

At the operating constant temperature (500°C), determined by TGA analysis, different times of residence in the furnace were tested (30, 60, 90 and 120 min.). All tests were performed in triplicate. After 24 h inside the turned-off furnace, the samples reached room temperature. The

mass of the sample was then measured. Thus, the mass reduction relative to the original sample was calculated to understand the relationship between time and the degradation of polymeric matter, in mass percentage.

Subsequently, the glass (GL) and copper ribbon (CR) fractions, visually identified by color difference, were manually separated from the fraction composed of silicon fragments (with a printed matrix of silver paste) and residual polymers (SS). All fractions had their masses measured to calculate the percentage mass relation. The SS samples (totaling 12 samples) were macerated and analyzed by XRF (three measurements for each sample). The silver concentrations of the ground PV laminate were compared with the SS samples from the furnace times applied (30, 60, 90 and 120 min at 500°C).

In addition, statistical tests were applied to analyze and compare the percentage values of thermal degradation of the 4 residence times studied. The procedure used is described in detail in the works of Callegari-Jacques (2003), Scheff (2016) and Hoffman (2019). The parameters submitted to the statistical analysis were the "Percentages of

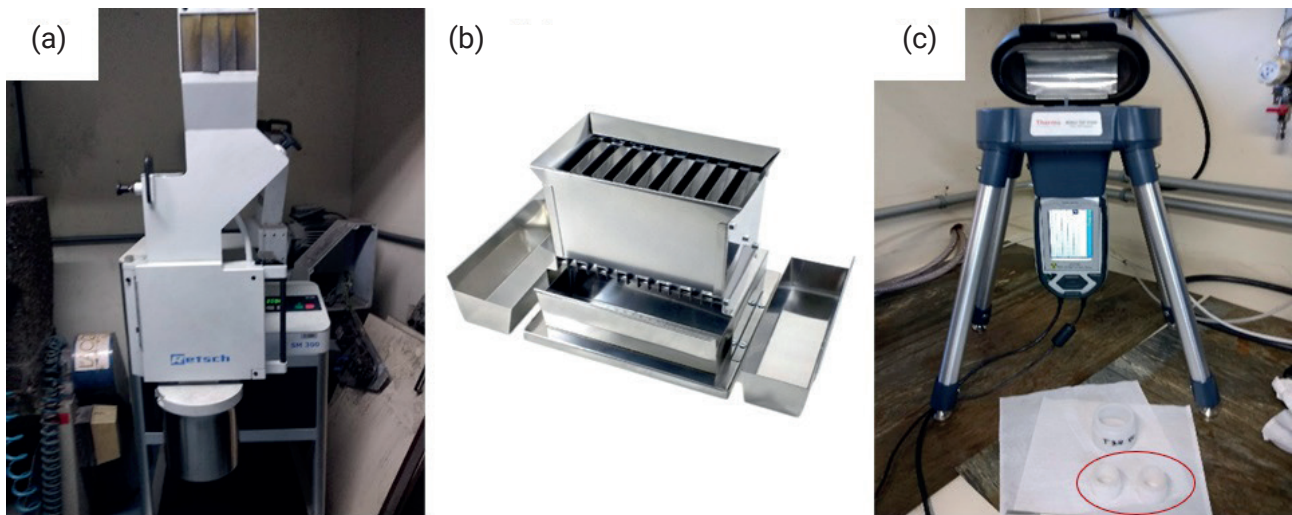


FIGURE 2: Metal content characterization (a) knife mill (b) stainless steel sample quarters (c) portable XRF analyzer and sample storage capsules for analysis, highlighted in red.

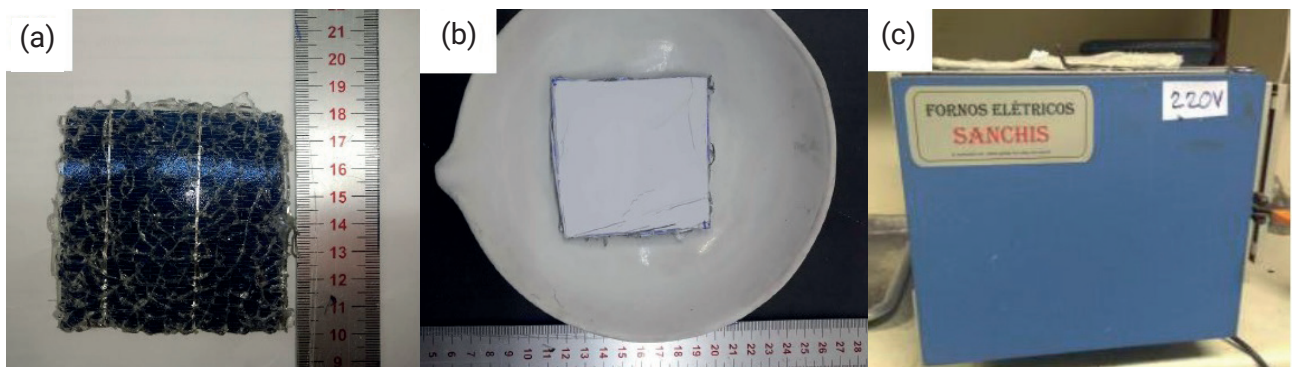


FIGURE 3: (a) Sample with dimensions 8 x 8 cm (b) Sample before heat treatment in a ceramic crucible (c) Sanchis N1100H furnace.

Thermal Degradation” for each of “Thermal Time Lengths (minutes)”, i.e., 30, 60, 90, and 120 minutes. The ANOVA test (parametric condition) and the Kruskal-Wallis test (non-parametric condition) are indicated for comparison between sample groups. The special conditions for performing the ANOVA test are homogeneity between the variances of the sample groups and the normal distribution of the data. If these conditions are satisfied by the Shapiro-Wilk (normality check) and Levene (homogeneity of variances check) tests, the ANOVA test can be performed. Otherwise, the comparison between sample groups should be performed by the non-parametric Kruskal-Wallis method.

Once the ANOVA and Kruskal-Wallis tests result in non-similarity between the sample groups analyzed, multiple comparison tests should be performed to define which sample group is significantly different from the others and whether it is considered larger or smaller. Calligari-Jacques (2003), Scheff (2016) and Hoffman (2019) indicated Tukey’s multiple comparison test for the parametric data condition and Dunn’s multiple comparison test for the non-parametric condition. The tests were performed at a 95% confidence level, where p-value conditions greater or less than 0.05 indicate acceptance of the null hypothesis

or rejection, respectively. Minitab 17 software was used to perform the tests.

3. RESULTS AND DISCUSSION

3.1 Characterization

3.1.1 Chemical Analysis

As shown in Table 1, the average silver concentration detected in this study was 151.1 ± 9.1 ppm, which can be considered low even compared to others works. The amount of silver found was closer to the values of Pagnanelli et al. (2017), 77.8 ppm, and Tao et al. (2020), 60 ppm. These studies reported lower silver concentrations. Jung et al. (2016) reported an intermediate silver amount, while Latunussa et al. (2016) and Dias et al. (2016) found higher concentrations. The cited studies report a range of silver concentrations from 60 to 632 ppm, i.e., a 10-fold variation.

Factors such as the PV panel brand, country of origin, year of manufacture, among others, can contribute for explain this wide variation in the reported silver concentrations. This fact is corroborated by some studies. According to Peeters et al. (2017), there is a tendency for the concentration to decrease over time. For example, modules manufactured in 2000 had 2,182 ppm silver, while in 2015, it had

TABLE 1: Elemental concentrations of the ground PV laminate, obtained by XRF analysis, compared with data from other studies.

Ground PV Laminate	Dias et al. (2016)	Latunussa et al. (2016)	Jung et al. (2016)	Pagnanelli et al. (2017)	Tao et al. (2020)	
Valuable Metals (ppm)						
Ag	151.1 ± 9.1	632	530	378.9	77.8	60
Cu	1530.8 ± 27.6	2984	NI	6660.0	18.8	6.000
Majority Elements (wt.%)						
UE	58.1 ± 2.7	NI	NI	NI	NI	NI
Si	31.7 ± 1.7	NI	NI	NI	NI	NI
Ca	6.9 ± 0.5	NI	NI	NI	NI	NI
Mg	0.8 ± 0.2	NI	NI	NI	NI	NI
Minority Elements (ppm)						
Fe	3626.1 ± 53.1	NI	NI	NI	870.2	NI
Ti	1482.7 ± 16.6	NI	NI	NI	26.2	NI
Sb	1194.5 ± 161.0	NI	NI	NI	NI	NI
Sn	552.9 ± 77.1	558	NI	NI	NI	1.200
Pb	353.4 ± 39.1	418	NI	211.6	NI	< 1.000
Ni	183.7 ± 19.0	NI	NI	NI	NI	NI
Zn	43.9 ± 8.1	NI	NI	NI	450.3	NI

NI: Not Informed

UE: Unidentified Elements by XRF Analysis. They are elements with atomic mass less than 12, such as hydrogen, oxygen, and carbon.

1239 ppm (Soltech, 2016). Weckend et al. (2016) also emphasized that the trend is to reduce the application of these metals in PV, stating that less than 0.1% of the module is composed of silver and other metals (mainly tin and lead).

Furthermore, 1530.8 ± 27.6 ppm of copper was detected in the ground PV laminate of this study. Comparing the studies of various authors, it is observed that there is a high variation between the concentrations, from 18.8 to 10,000 ppm. However, most of the already cited studies showed values above 5,700 ppm. Peeters et al. (2017) explained that copper is expected to gradually replace silver in c-Si panels, so it can be assumed that the copper content of PV panels will increase over time. The copper content comes mainly from the ribbons arranged on the PV cell to collect the generated power. These copper ribbons could be sent directly for recycling if they are separated from the rest.

Another important point was the detection of lead, a hazardous metal. The PV laminate studied showed 353.4 ± 39.1 ppm of lead, and other cited works indicate values between 200 and 1000 ppm. The origin of the lead could be from lead-tin solders, used to join the copper ribbons to the PV cell. The tin concentration was 552.9 ± 77.1 ppm, i.e., 1.6 times higher than the amount of lead. Iron, titanium, antimony, nickel, and zinc also were detected. Concerning these metals, further studies and more precise analyses are needed for better chemical characterization. However, the purpose of this work is to have an easily measured comparison parameter, especially for silver, to evaluate the concentration capacity of the developed route.

The components detected in more proportion in the samples were the silicon (31.7 ± 1.7 wt.%) and unidentified elements (UE = 65.81 ± 2.7 wt.%). The silicon is used both as a component of the PV cell, as much as a component of glass, and can be differentiated by XRD. About 58 wt.% (a

high amount) is composed of unidentified elements. These elements can be from the polymeric fraction and the oxygen present in the silicon dioxide (the main component of glass). The removal of glass and polymer layers, and consequent reducing the UE, can contribute to concentrating silver by physical methods. Besides, considerable quantities (%) of calcium and magnesium also were detected in the ground samples, which are derived from glass.

Ethylene-vinyl acetate (EVA), polyvinyl fluoride (PVF or Tedlar®) and polyethylene terephthalate (PET) were identified in backsheet composition by analysis of the FTIR spectrum (Figure 4).

Concerning EVA, the literature reports that ethylene absorption bands occur in 2920 cm⁻¹, 2850 cm⁻¹, 1470 cm⁻¹, 720 cm⁻¹ while vinyl acetate bands occur in 1740 cm⁻¹, 1240 cm⁻¹, 1020 cm⁻¹ and 610 cm⁻¹ (Meszlényi & Körtvélyessy, 1999). In Figure 4, it can be observed EVA bands in 2927 and 2856 cm⁻¹ resulting from symmetrical and asymmetric C—H stretching, in 1733,15 cm⁻¹ caused by C=O stretching of the ester group, and in 1236,36 cm⁻¹ due to COO stretching.

Regarding PVF, three characteristic peaks appear in 850 cm⁻¹, 1400 cm⁻¹ e 1200 cm⁻¹. The first two peaks happen due to the C—F stretching vibration, whereas the third peak results from the C—C bonding (Koenig & Mannion, 1966; Zerbi & Cortili, 1970). An absorption band from strong intensity was observed in 1000 at 1110 cm⁻¹ (peak in 1116, 47 cm⁻¹) due to C—F stretching vibration, typical from PVF.

With respect to PET, typical deformations exist in the regions of 2900 cm⁻¹ referent to the CH₃ group; 1715 cm⁻¹ and another in 730 cm⁻¹ relating to the C=O group. Also, there are peaks in 1460 cm⁻¹ and 977 cm⁻¹ which are corresponding to EG, as well as in 1250 cm⁻¹ referent to the (C=O)-O group. The band at 725 cm⁻¹ appears at lower frequencies than is usual for a benzene ring because of

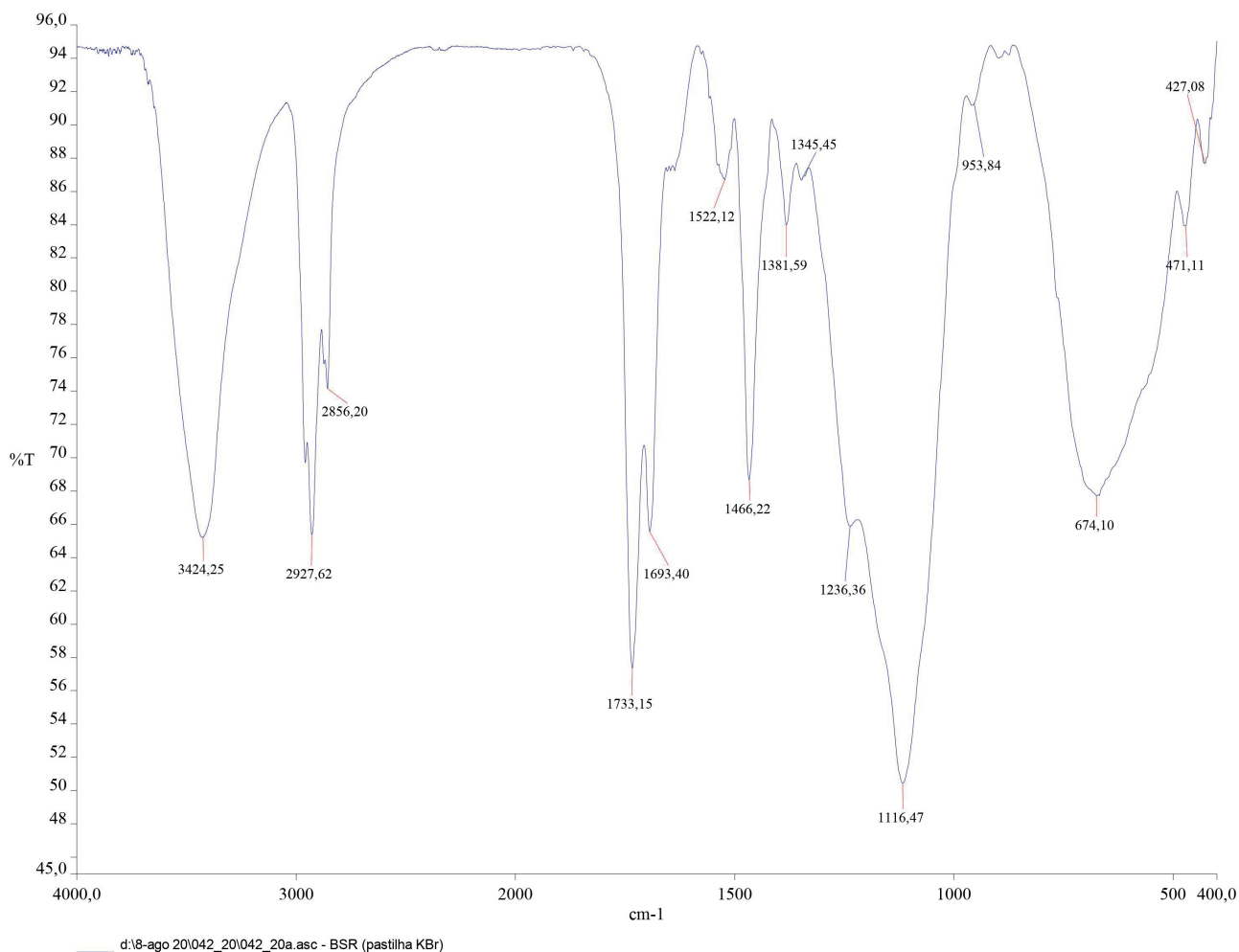


FIGURE 4: FTIR of the backsheet.

the extensive delocalization of the system of π -electron in the molecule, characterizing a para-substituted ring. When the ester group is attached to an aromatic ring, the C=O stretching vibration absorbs at lower frequencies, 1720 cm^{-1} . The aromatic part is easily identifiable by the C=C stretching of the ring at $1150, 1600\text{-}1500, 1235\text{ cm}^{-1}$ and one or more deformation modes at $850\text{-}700\text{ cm}^{-1}$. Two peaks are characteristic of the terephthalate in the region of the C—O stretching vibration at 1110 and 1263 cm^{-1} (Santos, 2009). In Figure 4, the characteristic band of C—H stretching from the aromatic ring may be visualized in approximately 3400 cm^{-1} . The band at 2921 cm^{-1} is relative to the CH₂ bonds, when the ester group is attached to an aromatic ring, and the C=O axial strain absorbs at lower frequencies (in this case at 1717 cm^{-1}). The aromatic part is easily identifiable by the C=C deformation of the ring at $1600\text{-}1450\text{ cm}^{-1}$, and two characteristic peaks of the terephthalate in the region of the C—O deformation at 1100 and 1300 cm^{-1} .

This analysis was hindered because the backsheet is a multilayer material. In this case, some characteristic bands of materials may be overlapped and/or extended. However, this identification is corroborated by studies reported by other authors (Adothu et al., 2020; Aryan et al., 2018; Danz et al., 2019; Dias et al., 2017; Farrell et al., 2019; Huang et

al., 2017; Peeters et al., 2017; Pinho & Galdino, 2014; Sander et al., 2007).

3.1.2 Thermogravimetric Analysis

The backsheet samples used in the TGA were not comminuted. Instead, pieces were taken from the module and, therefore, well represented a PV laminate. Therefore, the TGA closely represents what would occur in the backsheet when kept intact in a thermal degradation.

Figure 5 shows that the backsheet lost 92.5 wt.% of its mass at 500°C in a nitrogen atmosphere. The sample reached 95 wt.% of reduction at 900°C , i.e., from 500°C onwards there was a slow decomposition. The module used in our study showed higher percentage values of thermal degradation than the other mentioned studies. However, it presented stages similar to those reported by other authors, that is, significant decomposition up to 500°C and slow degradation from that temperature onwards. The temperature of 500°C allows for the highest decomposition under nitrogen atmosphere for the polymers from the PV module (Dias et al., 2017), for backsheet (Prado, 2019), for PVF (Danz et al., 2019) and EVA (Farrell et al., 2019), as well as for the samples seen in our study (Figure 5).

In an oxidizing atmosphere (synthetic air), it can be

seen in Figure 6 that there was an approximate reduction of 90 wt.% of the mass at 500°C. When reaching 600°C, the sample reached 97.5 wt.% of reduction. From 600°C to 900°C the curve stabilized. Therefore, in an oxidizing atmosphere, 97.5 wt.% of the mass was reduced at 600°C, while in an inert atmosphere, 95 wt.% of degradation was reached only at 900°C. In both atmospheric conditions, there were two stages of decomposition.

The main thermal degradation products of PVF are HF (at 350°C) and benzene (at 450°C). PVF decomposes in the

air at temperatures above 350°C by dehydrofluorination. Benzene is formed by chain scission and subsequent cyclization of PVF films at high temperatures but maintains considerable strength after thermal aging at 217°C (Drobny, 2001; Huber et al., 2009; Scheirs, 1997). The first stage of the curve can be attributed to these reactions.

Figure 7 shows the TGA analysis of the PV laminate under oxidizing conditions. As seen in Figure 7, the thermal degradation curve stabilized at 500°C, with 20% of mass loss, referent to the polymeric fraction. Other authors have

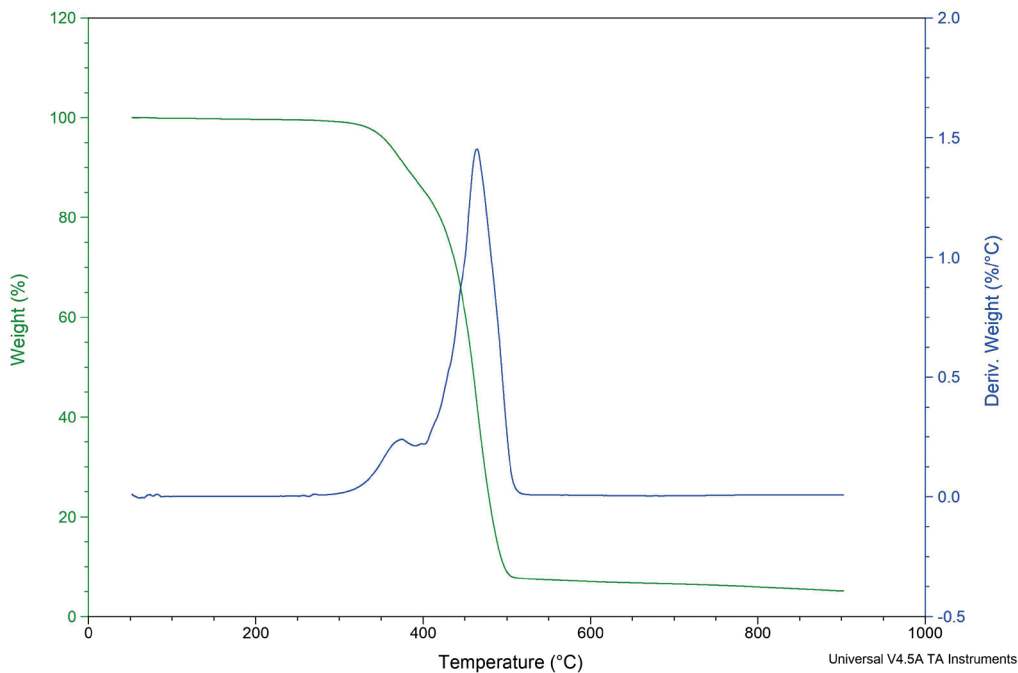


FIGURE 5: TGA of the backsheet under inert atmosphere (nitrogen gas).

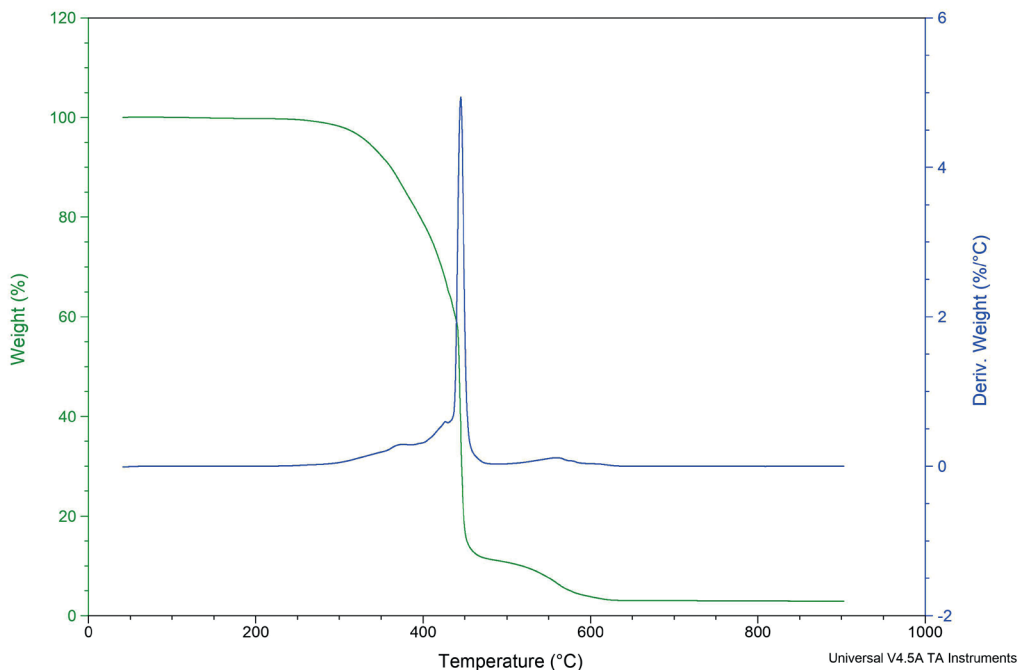


FIGURE 6: TGA of the backsheet under oxidizing atmosphere (synthetic air).

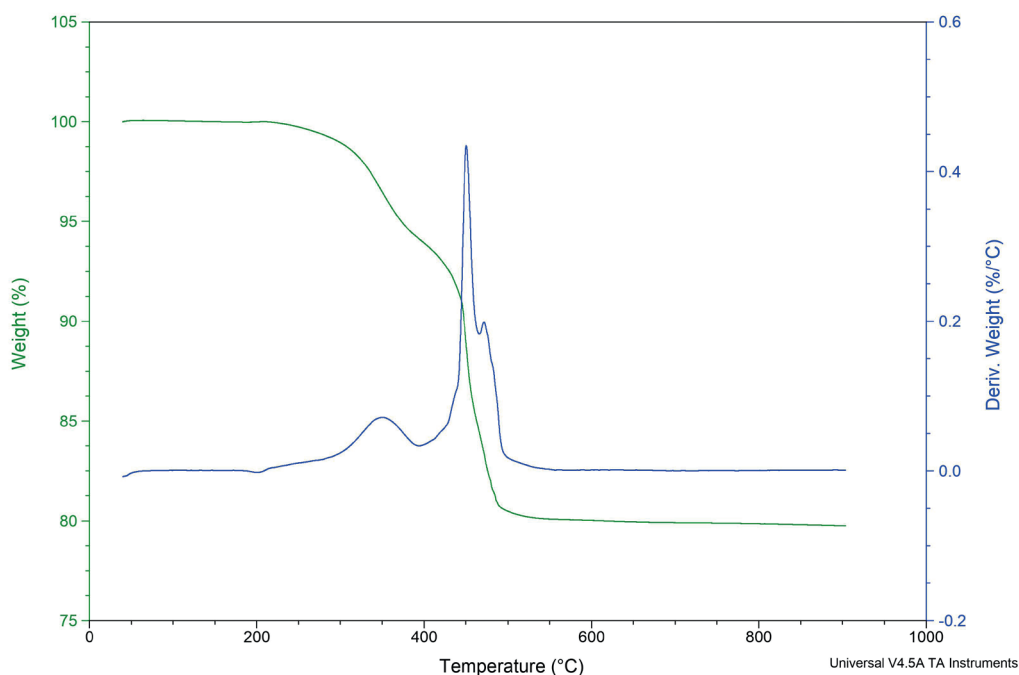


FIGURE 7: TGA of the ground PV laminate under oxidizing atmosphere (synthetic air).

also indicated 500°C, in an oxidizing atmosphere (Fiandra et al., 2018) and a nitrogen atmosphere (Dias et al., 2017), as the ideal temperature for thermal degradation.

3.2 Thermal Degradation and Silver Concentration

In samples submitted to the 30 min of thermal treatment (at 500°C constant temperature), it was possible to observe the presence of dark-colored polymeric residues (Figure 8a). In samples submitted at heat treatment by 60 min (Figure 8b) or more, it was possible to observe that these residues have become white and have gradually decreased (Figure 8d). Thus, with the increase in the treatment time, the polymeric fraction was reduced and the sample stayed with a visually cleaner appearance. The removal of polymeric residues is necessary to purify the SS fraction. In a later stage of leaching silver with nitric acid, where the silicon fragments would be retained in the filtrate, the presence of polymers could reduce the quality of this recovered silicon. Considering that the TGA analysis identified that 20% of mass can be thermally degraded, values of mass loss must stay close to this level.

Table 2 shows the average percentage of thermally degraded mass as well as the percentages of the glass (GL), silicon-silver (SS), and copper ribbon (CR) fractions for each furnace dwelling time.

The thermal degradation followed by manual segregation increased the silver concentration concerning the ground PV laminate (Table 2), due to the removal of polymers, the glass fraction and copper ribbons. In SS samples, the average concentration was 3074.7 ± 440.6 ppm, i.e., its concentration was approximately 20 times greater than the ground PV laminate (152.4 ± 9.1 ppm). According to Sverdrup et al. (2014), high concentration silver ore has 60 to 100 ppm silver. Through the route presented, a con-

centration 30 times higher than that present in the ore was obtained. Thus, with recycling PV modules, the demand for mining and its consequent impacts is reduced.

According to Table 2, the percentage values of lost mass ranged from 12.82 ± 0.15 wt.% to 13.62 ± 0.02 wt.%. Initially, increasing the oven time increased the percentage of the mass degraded (Table 2). By visual analysis, it was also possible to see that the amount of polymeric residue decreases as the thermal treatment time increases (Figure 8). According to the ANOVA test, there is a statistical difference in at least one of the sample groups (p -value = 0.001, accepting the alternative hypothesis of difference between sample groups). The Tukey test reports that the values for 90 and 120 min are similar to each other and higher than the others (p -value = 0.062, greater than 0.05, accepting the null hypothesis of similarity between the sample groups). Thus, the statistical tests showed that the degradation stabilized at two longer times. The means of degraded mass for 90 and 120 min were the largest, although the 120-min samples visually showed less polymeric residue (Figure 8d). Possibly, the mass of these polymers present in the 90-min samples is so small that it does not result in significant differences. The 90-min application was indicated and justified to avoid unnecessary energy consumption. The sequence of tests and the respective results are presented in "APPENDIX - STATISTICAL ANALYSIS OF THERMAL DEGRADATION".

The TGA/DSC analysis of the ground module with the backsheet (Figure 7) shows that it is possible to thermally remove 20 wt.% of the total mass. Despite the high energy consumption, maximum removal of about 13.62 ± 0.02 wt.% was achieved, i.e., about 68% effectiveness. The presence of the backsheet may hinder the transport of heat and oxygen, reducing decomposition. As already mentioned,

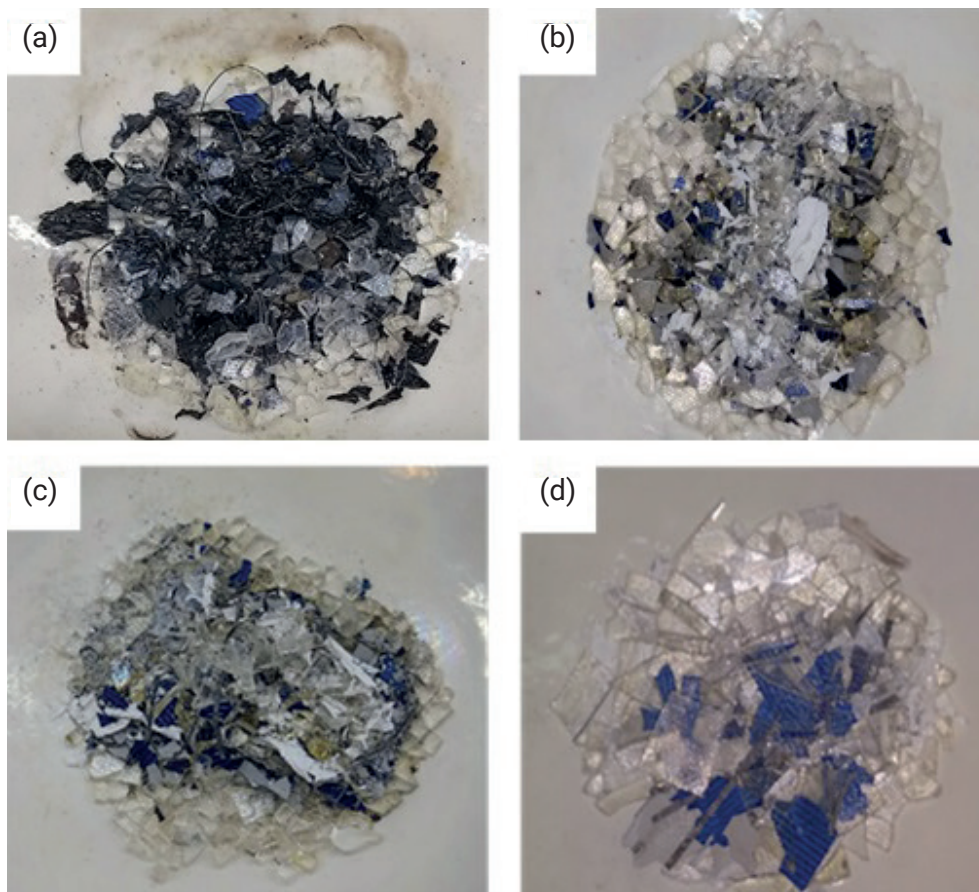


FIGURE 8: Different samples after furnace, which were kept at constant 500°C temperature for (a) 30 min (b) 60 min (c) 90 min (d) 120 min.

the backsheet is composed of PVF and its burning generates HF (350°C) and benzene (450°C) (Huber et al., 2009), in addition to dioxins and furans. Therefore, removing the backsheet before burning could result in benefits such as more silicon purification, reduced furnace time and lower toxic emissions.

The fractions obtained after heat treatment showed similar percentage amounts, as shown in Table 2. The

samples showed average percentage values of 6.23 ± 0.19 wt.% for SS. Fiandra et al. (2019) recovered 6.37 wt.% of the equivalent fraction. This value not only reflects the amount of silicon but also a load of undecomposed polymers. Therefore, a higher decomposition will result in a lower percentage.

An average value of 79.37 ± 0.43 wt.% of glass was obtained GL fraction. Other studies have indicated 70 wt.%

TABLE 2: Silver concentrations (ppm) for the ground PV laminate and SS samples for the furnace times applied at 500°C. Percentage mass removed after thermal degradation related to the decomposition of the polymers present. Percentage Mass of Fractions SS, CR and GL obtained in the samples after the furnace.

	Silver (ppm) ^{a,d}	% Lost Mass ^e	wt.% SS ^f	wt.% CR ^f	wt.% GL ^f
Ground PV Laminate ^a	152.4 ± 9.1	Not applicable	Not applicable	Not applicable	Not applicable
30 min at 500°C ^b	2990.6 ± 288.5	12.82 ± 0.15	6.21 ± 0.29	1.07 ± 0.20	79.90 ± 0.33
60 min at 500°C ^b	3135.2 ± 469.2	13.18 ± 0.16	6.12 ± 0.17	1.38 ± 0.21	79.32 ± 0.29
90 min at 500°C ^b	2934.9 ± 509.1	13.62 ± 0.02	6.38 ± 0.16	1.04 ± 0.11	78.96 ± 0.04
120 min at 500°C ^b	3280.7 ± 422.8	13.28 ± 0.17	6.24 ± 0.06	1.22 ± 0.22	79.27 ± 0.42

SS: Silicon fragments with a printed matrix of silver paste and residual polymers

CR: Copper ribbon

GL: Glass

^a Polycrystalline silicon module without aluminum frame and junction box that was ground in a knife mill - particle size smaller than 1 mm.

^b Silver concentration for the SS (Silicon-Silver) sample, after maceration.

^c X-ray Fluorescence Analysis.

^d Ore with a high concentration of silver has 60-100 ppm of this element, according to (Sverdrup et al., 2014).

^e Regarding the decomposition of the polymeric fraction, after furnace treatment.

^f Mass percentages of the manually segregated fraction.

(Latunussa et al., 2016), 71.20 wt.% (Fiandra et al., 2019), 74.16 wt.% (Fiandra et al., 2018), and 74 wt.% (Tao et al., 2020), of glass present in the PV modules. An average value of 1.19 ± 0.22 wt.% of copper ribbons was obtained in the CR fraction, while Fiandra et al. (2019) recovered 0.51 wt.% to ribbons.

In this work, the segregation of the fractions was performed manually on a laboratory bench. However, it is necessary to study methods applicable on an industrial scale. The glass fragments could be segregated by suction cups and sieving systems, while copper ribbons could be separated by electrostatic separation (Dias et al., 2018). Silicon fragments break easily, which reduces their size, so they could be separated by sieving as well.

Table 3 presents the concentrations of silver, copper, unidentifiable elements (UE), silicon, lead and tin of the SS fractions according to furnace times, compared to the composition of the ground PV laminate. UE are the elements with atomic mass less than 12, such as hydrogen, oxygen, and carbon, which were not identified by the XRF equipment that was being used.

Besides the silver increment, a reduction of about 5.6 to 16.4 times in the amount of copper present in the SS fraction was observed because this material stayed in the CR

fraction after the manual separation. It was also possible to observe an increase in the amount of silicon (1.7 to 1.8 fold) and a reduction in the mass of unidentified elements (1.8 to 2.1 fold). The increase in the degraded percentage was consistent with the reduction in unidentified elements. The UE ratios by percent decomposition were 2.4 for 30 min, 2.2 for 60 min, 2.0 for 90 min, and 2.2 for 120 minutes. Other elements that were also more concentrated in the SS fraction were lead and tin. Despite the removal of the copper ribbons, the lead amount increased 3.0 to 4.6 times, and tin increased 3.0 to 3.6 times. In a study about the composition of Si cells extracted from modules (in weight percent), Tao et al. (2020) reported that 2.9% of composition was tin and 2.4% was lead. So, it is important to develop methods for these metals to be removed from the SS fraction, since this fraction, subsequently, will undergo an acidic leaching process to recover the silver.

The GL fraction is composed of fragments of tempered glass from the PV laminate. As seen in Table 4, the concentrations of the GL fraction were not altered by the variation from 30 to 120 min in thermal treatment. Visually, the glass fragments were similar regardless of the thermal treatment time. The average composition was 67.03 ± 1.02 wt.% of the unidentified elements, 25.41 ± 0.83 wt.% of

TABLE 3: Composition of SS fractions, obtained by XRF analysis, compared to the ground PV laminate.

Ground PV Laminate		SS _{30m}	SS _{60m}	SS _{90m}	SS _{120m}
Valuable Metals (ppm)					
Ag	151.1 ± 9.1	2990.6 ± 288.5	3135.2 ± 469.2	2934.9 ± 509.1	3280.7 ± 422.8
Cu	1530.8 ± 27.6	93.5 ± 6.9	94.3 ± 16.5	119.7 ± 28.3	274.0 ± 45.5
Majority Elements (wt.%)					
UE	58.1 ± 2.7	31.3 ± 2.9	29.4 ± 3.6	27.4 ± 2.2	28.9 ± 2.3
Si	31.7 ± 1.7	52.7 ± 1.4	56.1 ± 3.0	56.8 ± 3.1	55.1 ± 1.1
Hazardous Metals (ppm)					
Pb	353.4 ± 39.1	1233.8 ± 221.6	1051.9 ± 54.0	1394.6 ± 160.2	1628.4 ± 400.5
Sn	552.9 ± 77.1	2003.7 ± 628.4	1963.3 ± 590.3	1764.9 ± 615.8	1664.1 ± 628.7

UE: Unidentified Elements by XRF Analysis. They are elements with atomic mass less than 12, such as hydrogen, oxygen, and carbon.

TABLE 4: Composition of GL fractions, obtained by XRF analysis, compared to the ground PV laminate.

Ground PV Laminate		GL _{30m}	GL _{60m}	GL _{90m}	GL _{120m}
Valuable Metals (ppm)					
Ag	151.1 ± 9.1	9.5 ± 1.9	8.0 ± 1.9	8.1 ± 1.6	9.8 ± 2.8
Cu	1530.8 ± 27.6	25.6 ± 3.8	21.1 ± 3.6	23.5 ± 4.3	20.5 ± 4.1
Majority Elements (wt.%)					
UE	58.1 ± 2.7	66.8 ± 0.7	68.0 ± 1.2	66.7 ± 0.6	66.3 ± 0.3
Si	31.7 ± 1.7	25.6 ± 0.4	24.5 ± 1.0	25.7 ± 0.4	25.9 ± 0.2
Ca	6.9 ± 0.5	6.3 ± 0.1	6.1 ± 0.1	6.3 ± 0.03	6.3 ± 0.03
Mg	0.8 ± 0.2	0.6 ± 0.2	0.7 ± 0.2	0.7 ± 0.2	0.8 ± 0.1
Hazardous Metals (ppm)					
Pb	353.4 ± 39.1	6.8 ± 0.3	8.2 ± 2.2	7.1 ± 1.7	7.6 ± 0.5
Sn	552.9 ± 77.1	57.1 ± 10.8	71.8 ± 5.0	64.0 ± 12.9	56.5 ± 19.7

UE: Unidentified Elements by XRF Analysis. They are elements with atomic mass less than 12, such as hydrogen, oxygen, and carbon.

TABLE 5: Composition of CR fractions, obtained by XRF analysis, compared to the ground PV laminate.

Ground PV Laminate	CR _{30m}	CR _{60m}	CR _{90m}	CR _{120m}	
Majority Elements (wt.%)					
Cu	0.153 ± 0.003	53.0 ± 6.2	51.8 ± 7.7	60.9 ± 3.3	56.6 ± 1.9
Pb	0.035 ± 0.004	25.1 ± 7.7	28.0 ± 9.5	19.8 ± 3.7	19.3 ± 3.6
Sn	0.055 ± 0.008	16.0 ± 0.8	15.2 ± 3.1	15.3 ± 1.2	18.1 ± 0.6
Other Elements (wt.%)					
Ag	0.015 ± 0.001	2.4 ± 0.3	2.6 ± 0.4	2.1 ± 0.4	2.6 ± 0.2
Si	31.73 ± 1.66	1.5 ± 1.2	1.0 ± 0.6	0.7 ± 0.3	1.0 ± 0.6

silicon, 6.24 ± 0.10 wt.% of calcium, and 0.73 ± 0.20 wt.% of magnesium. These data show us how much the composition of the glass interferes in the general composition of the module because 79% of the PV laminate resulted in glass fragments (Table 2).

The amounts of copper and silver in the GL fraction found were proportionally small, 21.35 ± 6.78 ppm and 8.69 ± 2.13 ppm, respectively. The small silver amount found in the glass fragments may be from the fine dust of the SS fraction, which cannot be removed manually.

The composition of the CR fraction remained similar for all thermal treatment times (Table 5). The average composition was $55.69 \pm 6.39\%$ copper, $23.17 \pm 7.51\%$ lead, and $16.06 \pm 2.12\%$ tin. As previously commented, lead and tin are used by solder copper ribbons on the PV cell, thus, its presence in this fraction is justified. Moreover, there was $2.41 \pm 0.39\%$ silver and $0.47 \pm 0.06\%$ silicon in this fraction. Considering that the CR fraction represents only 1 wt.% of the PV laminate, any amount of SS adhered to the surface of the ribbon will represent a considerable percentage in the total composition, higher than the concentration in the ground PV laminate.

4. CONCLUSIONS

When comparing the XRF analysis of the ground PV laminate with values from other authors, it was observed that the metal content of crystalline silicon PV modules varies. By FTIR analysis, the backsheet composition was identified as PVF, PET and EVA, which is consistent with studies by other authors. The TGA analysis revealed that the backsheet from PV reached higher percentages of thermal degradation in a lower temperature range, when under an oxidizing atmosphere. In an inert atmosphere, 92.5 wt.% of the backsheet was decomposed at 500°C, and 95 wt.% at 900°C. In an oxidizing atmosphere, 90 wt.% of the mass was reduced at 500°C, but 97.5 wt.% at 600°C. It was also observed that 20 wt.% of PV laminate was degraded at 500°C, and from this temperature up to 900°C, there was no mass loss.

The thermal treatment used in this study resulted in 3 fractions: silicon-silver (6.23 ± 0.19 wt.%), glass (79.37 ± 0.43 wt.%) and copper ribbons (1.19 ± 0.22 wt.%). It was also found that 13.62 ± 0.02 wt.% of the polymer mass is degraded in 90 min of thermal treatment. The application of 120 min is not justified because it requires additional time and energy to obtain a statistically similar result (p-value = 0.062, greater than 0.05, accepting the null hypothesis

of similarity between the sample groups). Also, the adopted procedure concentrated silver from 152.4 ± 9.1 ppm to 3074.7 ± 440.6 ppm on average, an approximately 20 times increase in relation to the ground PV laminate.

The TGA/DSC analysis of the ground backsheet shows that, theoretically, it is possible to thermally remove 20 wt.% of the total mass. However, in this study, maximum removal of about 13.62 ± 0.02 wt.% was achieved, i.e., about 68% effectiveness. Although the treatment was effective in concentrating silver, other alternatives can be studied to reduce the thermal treatment time and reducing the environmental impact of burning PVF. The glass and copper ribbons fractions maintained similar compositions regardless of the thermal treatment time. The silicon-silver fraction also showed high concentrations of lead, which is a hazardous metal. Further studies are needed to separate and recover these metals.

ACKNOWLEDGEMENTS

This research is supported by the CNPQ - Conselho Nacional de Desenvolvimento Científico e Tecnológico and the other Brazilian government agencies CAPES, Finep and Fapergs.

REFERENCES

- Adothu, B., Bhatt, P., Zele, S., Oderkerk, J., Costa, F. R., & Mallick, S. (2020). Investigation of newly developed thermoplastic polyolefin encapsulant principle properties for the c-Si PV module application. *Materials Chemistry and Physics*, 243(January), 122660. <https://doi.org/10.1016/j.matchemphys.2020.122660>
- Aryan, V., Font-Brucart, M., & Maga, D. (2018). A comparative life cycle assessment of end-of-life treatment pathways for photovoltaic backsheets. *Progress in Photovoltaics: Research and Applications*, 26(7), 443–459. <https://doi.org/10.1002/pip.3003>
- Bernardes, A. M., Espinosa, D. C. R., & Tenório, J. A. S. (2004). Recycling of batteries: A review of current processes and technologies. *Journal of Power Sources*, 130(1–2), 291–298. <https://doi.org/10.1016/j.jpowsour.2003.12.026>
- BioIS. (2011). Study on photovoltaic panels supplementing the impact assessment for a recast of the WEEE directive – Final report. (Issue April). http://ec.europa.eu/environment/waste/weee/pdf/Study_on_PVs_Bio_final.pdf
- Callegari-Jacques, S. M. (2003). *Bioestatística: Princípios e aplicações*. Artmed.
- Cenci, M. P., Christ, F., Berto, D., Silva, P., Camargo, S., & Veit, H. M. (2021). Separation and concentration of valuable and critical materials from wasted LEDs by physical processes. *Waste Management*, 120, 136–145. <https://doi.org/10.1016/j.wasman.2020.11.023>
- Chancerel, P., Meskers, C. E. M., Hagelüken, C., & Rotter, V. S. (2009). Assessment of Precious Metal Flows During Preprocessing of Waste Electrical and Electronic Equipment. *Journal of Industrial Ecology*, 13(5), 791–810. <https://doi.org/10.1111/j.1530-9290.2009.00171.x>

- Danz, P., Aryan, V., Möhle, E., & Nowara, N. (2019). Experimental Study on Fluorine Release from Photovoltaic Backsheet Materials Containing PVF and PVDF during Pyrolysis and Incineration in a Technical Lab-Scale Reactor at Various Temperatures. *Toxics*, 7(3), 47. <https://doi.org/10.3390/toxics7030047>
- DeBergalis, M. (2004). Fluoropolymer films in the photovoltaic industry. *Journal of Fluorine Chemistry*, 125(8), 1255–1257. <https://doi.org/10.1016/j.jfluchem.2004.05.013>
- Deng, R., Chang, N. L., Ouyang, Z., & Chong, C. M. (2019). A techno-economic review of silicon photovoltaic module recycling. *Renewable and Sustainable Energy Reviews*, 109(March), 532–550. <https://doi.org/10.1016/j.rser.2019.04.020>
- Deng, R., Chang, N., Lunardi, M. M., Dias, P., Bilbao, J., Ji, J., & Chong, C. M. (2020). Remanufacturing end-of-life silicon photovoltaics: Feasibility and viability analysis. *Progress in Photovoltaics: Research and Applications*, pip.3376. <https://doi.org/10.1002/pip.3376>
- Dias, P., Javimczik, S., Benevit, M., Veit, H., & Bernardes, A. M. (2016). Recycling WEEE: Extraction and concentration of silver from waste crystalline silicon photovoltaic modules. *Waste Management*, 57, 220–225. <https://doi.org/10.1016/j.wasman.2016.03.016>
- Dias, P. R., Javimczik, S., Benevit, M., & Veit, H. (2017). Recycling WEEE: Polymer characterization and pyrolysis study for waste of crystalline silicon photovoltaic modules. *Waste Management*, 60, 716–722. <https://doi.org/10.1016/j.wasman.2016.08.036>
- Dias, P., Schmidt, L., Gomes, L. B., Bettanin, A., Veit, H., & Bernardes, A. M. (2018). Recycling Waste Crystalline Silicon Photovoltaic Modules by Electrostatic Separation. *Journal of Sustainable Metallurgy*, 4(2), 176–186. <https://doi.org/10.1007/s40831-018-0173-5>
- Drobny, J. G. (2001). *Technology of fluoropolymers*. CRC Press.
- Farrell, C., Osman, A. I., Zhang, X., Murphy, A., Doherty, R., Morgan, K., Rooney, D. W., Harrison, J., Coulter, R., & Shen, D. (2019). Assessment of the energy recovery potential of waste Photovoltaic (PV) modules. *Scientific Reports*, 9(March), 1–13. <https://doi.org/10.1038/s41598-019-41762-5>
- Fiandra, V., Sannino, L., Andreozzi, C., Corcelli, F., & Graditi, G. (2019). Silicon photovoltaic modules at end-of-life: Removal of polymeric layers and separation of materials. *Waste Management*, 87, 97–107. <https://doi.org/10.1016/j.wasman.2019.02.004>
- Fiandra, V., Sannino, L., Andreozzi, C., & Graditi, G. (2018). End-of-life of silicon PV panels: A sustainable materials recovery process. *Waste Management*, 84, 91–101. <https://doi.org/10.1016/j.wasman.2018.11.035>
- Fthenakis, V. M. (2000). End-of-life management and recycling of PV modules. *Energy Policy*, 28(14), 1051–1058. [https://doi.org/10.1016/S0301-4215\(00\)00091-4](https://doi.org/10.1016/S0301-4215(00)00091-4)
- Granata, G., Pagnanelli, F., Moscardini, E., Havlik, T., & Toro, L. (2014). Recycling of photovoltaic panels by physical operations. *Solar Energy Materials and Solar Cells*, 123(2014), 239–248. <https://doi.org/10.1016/j.solmat.2014.01.012>
- Granata, Giuseppe, Moscardini, E., Pagnanelli, F., Trabucco, F., & Toro, L. (2012). Product recovery from Li-ion battery wastes coming from an industrial pre-treatment plant: Lab scale tests and process simulations. *Journal of Power Sources*, 206, 393–401. <https://doi.org/10.1016/j.jpowsour.2012.01.115>
- Gustavsson, J. P. R., Segal, C., Dolbier, W. R., Ameduri, B., & Kostov, G. (2006). Combustion and thermal decomposition of fluorinated polymers. *Combustion Science and Technology*, 178(12), 2097–2114. <https://doi.org/10.1080/00102200600860681>
- Hoffman, J. I. E. (2019). Analysis of Variance. I. One-Way. In *Basic Biostatistics for Medical and Biomedical Practitioners* (pp. 391–417). Elsevier. <https://doi.org/10.1016/B978-0-12-817084-7.00025-5>
- Huang, W.-H. H., Shin, W. J., Wang, L., Sun, W.-C. C., & Tao, M. (2017). Strategy and technology to recycle wafer-silicon solar modules. *Solar Energy*, 144, 22–31. <https://doi.org/10.1016/j.solener.2017.01.001>
- Huber, S., Moe, M., Schmidbauer, N., Hansen, G., & Herzke, D. (2009). Emissions from the incineration of fluoropolymer materials. *Nilu Insider*. (2021). Copper price on Feb 26, 2021. <https://markets.businessinsider.com/commodities/copper-price>
- IRENA. (2021a). Distribution of renewable energy technologies within a country, area or region of choice in relation to renewable energy power capacity and electricity generation figures. <https://www.irena.org/Statistics/View-Data-by-Topic/Capacity-and-Generation/Technologies>
- IRENA. (2021b). International Renewable Energy Agency - Statistics Time Series:Trends in Capacity and Generation of Renewable Energy:Trends in Capacity and Generation of Renewable Energy. <https://www.irena.org/Statistics/View-Data-by-Topic/Capacity-and-Generation/Statistics-Time-Series>
- ISE. (2020). *Photovoltaics Report - Prepared by Fraunhofer Institute for Solar Energy Systems, ISE with support of PSE Projects GmbH (Issue September)*. www.ise.fraunhofer.de
- Jung, B., Park, J., Seo, D., & Park, N. (2016). Sustainable System for Raw-Metal Recovery from Crystalline Silicon Solar Panels: From Noble-Metal Extraction to Lead Removal. *ACS Sustainable Chemistry and Engineering*, 4(8), 4079–4083. <https://doi.org/10.1021/acssuschemeng.6b00894>
- Kadro, J. M., & Hagfeldt, A. (2017). The End-of-Life of Perovskite PV. *Joule*, 1(1), 29–46. <https://doi.org/10.1016/j.joule.2017.07.013>
- Kasper, A. C. (2011). Characterization and recycling of materials present in cell phone scraps. *Caracterização e reciclagem de materiais presentes em sucatas de telefones celulares*. UFRGS.
- Klugmann-Radziemska, E., & Ostrowski, P. (2010). Chemical treatment of crystalline silicon solar cells as a method of recovering pure silicon from photovoltaic modules. *Renewable Energy*, 35(8), 1751–1759. <https://doi.org/10.1016/j.renene.2009.11.031>
- Klugmann-Radziemska, E., Ostrowski, P., Drabczyk, K., Panek, P., & Szkodo, M. (2010). Experimental validation of crystalline silicon solar cells recycling by thermal and chemical methods. *Solar Energy Materials and Solar Cells*, 94(12), 2275–2282. <https://doi.org/10.1016/j.solmat.2010.07.025>
- Koenig, J. L., & Mannion, J. J. (1966). Infrared study of poly(vinyl fluoride). *Journal of Polymer Science Part A-2: Polymer Physics*, 4(3), 401–414. <https://doi.org/10.1002/pol.1966.160040310>
- Kuczyńska-Łażewska, A., Klugmann-Radziemska, E., Sobczak, Z., & Klimczuk, T. (2018). Recovery of silver metallization from damaged silicon cells. *Solar Energy Materials and Solar Cells*, 176(December 2017), 190–195. <https://doi.org/10.1016/j.solmat.2017.12.004>
- Latunussa, C. E. L., Ardente, F., Blengini, G. A., & Mancini, L. (2016). Life Cycle Assessment of an innovative recycling process for crystalline silicon photovoltaic panels. *Solar Energy Materials and Solar Cells*, 156, 101–111. <https://doi.org/10.1016/j.solmat.2016.03.020>
- Latunussa, C., Mancini, L., Blengini, G., Ardente, F., & Pennington, D. (2016). Analysis of Material Recovery from Silicon Photovoltaic Panels. In *EUR 27797 Luxembourg (Luxembourg) Publications Office of the European Union (Issue March)*. <https://doi.org/10.2788/786252>
- Meszlényi, G., & Körtvélyessy, G. (1999). Direct determination of vinyl acetate content of ethylene-vinyl acetate copolymers in thick films by infrared spectroscopy. *Polymer Testing*, 18(7), 551–557. [https://doi.org/10.1016/S0142-9418\(98\)00053-1](https://doi.org/10.1016/S0142-9418(98)00053-1)
- Mulvaney, D. (2014). Are green jobs just jobs? Cadmium narratives in the life cycle of Photovoltaics. *Geoforum*, 54, 178–186. <https://doi.org/10.1016/j.geoforum.2014.01.014>
- Nain, P., & Kumar, A. (2020). Metal dissolution from end-of-life solar photovoltaics in real landfill leachate versus synthetic solutions: One-year study. *Waste Management*, 114, 351–361. <https://doi.org/10.1016/j.wasman.2020.07.004>
- Padoan, F. C. S. M., Altimari, P., & Pagnanelli, F. (2019). Recycling of end of life photovoltaic panels: A chemical prospective on process development. *Solar Energy*, 177(July 2018), 746–761. <https://doi.org/10.1016/j.solener.2018.12.003>
- Pagnanelli, F., Moscardini, E., Granata, G., Abo Atia, T., Altimari, P., Havlik, T., & Toro, L. (2017). Physical and chemical treatment of end of life panels: An integrated automatic approach viable for different photovoltaic technologies. *Waste Management*, 59, 422–431. <https://doi.org/10.1016/j.wasman.2016.11.011>
- Paiano, A. (2015). Photovoltaic waste assessment in Italy. *Renewable and Sustainable Energy Reviews*, 41, 99–112. <https://doi.org/10.1016/j.rser.2014.07.208>
- Peeters, J. R., Altamirano, D., Dewulf, W., & Dufloy, J. R. (2017). Forecasting the composition of emerging waste streams with sensitivity analysis: A case study for photovoltaic (PV) panels in Flanders. *Resources, Conservation and Recycling*, 120, 14–26. <https://doi.org/10.1016/j.resconrec.2017.01.001>
- Pinho, J. T., & Galdino, M. A. (2014). *Engineering Manual for Photovoltaic Systems* (J. T. (UFPA) Pinho & M. A. (Cepel) Galdino (eds.); March 2014). Centro de Pesquisas de Energia Elétrica (Cetel) - Centro de Referência para Energia Solar e Eólica Sergio de Salvo Brito (Cresesb) - Grupo de trabalho de Energia Solar (GTES). <http://www.cresesb.cepel.br>

- Prado, P. F. de A. (2019). Reciclagem de painéis fotovoltaicos e recuperação de metais. [Universidade de São Paulo]. <https://doi.org/10.11606/D.3.2019.tde-30012019-141410>
- Rockaway Recycling. (2019). Metal Prices. <https://Rockawayrecycling.Com/Scrap-Metal-Prices>.
- Sander, K., Schilling, S., Reinschmidt, J., Wambach, K., Schlenker, S., Müller, A., Jelitte, Springer, J., Fouquet, D., Jelitte, A., Stryi-Hipp, G., & Chrometzka, T. (2007). Study on the Development of a Take Back and Recovery System for Photovoltaic Products. In Components (Issue 03). Oekopol GmbH, BMU Project Report (co-financed by EPIA and BSW solar) 03MAP092:
- Santos, L. (2009). Avaliação da Eficiência da Separação de Plásticos de Resíduos Sólidos Urbanos por Métodos de Dissolução Seletiva. 1–150.
- Scheff, S. W. (2016). One-Way Analysis of Variance. In *Fundamental Statistical Principles for the Neurobiologist* (pp. 97–133). Elsevier. <https://doi.org/10.1016/B978-0-12-804753-8.00006-3>
- Scheirs, J. (1997). *Modern Fluoropolymers: High Performance Polymers for Diverse Applications*. Chichester, John Wiley & Sons.
- Shin, J., Park, J., & Park, N. (2017). A method to recycle silicon wafer from end-of-life photovoltaic module and solar panels by using recycled silicon wafers. *Solar Energy Materials and Solar Cells*, 162(September 2016), 1–6. <https://doi.org/10.1016/j.solmat.2016.12.038>
- Silver Price. (2019). Silver Price. <https://silverprice.org>
- Silver Price. (2021). Silver price on Feb 26, 2021. <https://silverprice.org>
- Soltech. (2016). Personal Communication, ed.
- Strachala, D., Hylský, J., Vaněk, J., Fafílek, G., & Jandová, K. (2017). Methods for recycling photovoltaic modules and their impact on environment and raw material extraction. *Acta Montanistica Slovaca*, 22(3), 257–269.
- Sverdrup, H., Koca, D., & Ragnarsdottir, K. V. (2014). Investigating the sustainability of the global silver supply, reserves, stocks in society and market price using different approaches. *Resources, Conservation and Recycling*, 83, 121–140. <https://doi.org/10.1016/j.resconrec.2013.12.008>
- Tammaro, M., Salluzzo, A., Rimauro, J., Schiavo, S., & Manzo, S. (2016). Experimental investigation to evaluate the potential environmental hazards of photovoltaic panels. *Journal of Hazardous Materials*, 306, 395–405. <https://doi.org/10.1016/j.jhazmat.2015.12.018>
- Tao, J., & Yu, S. (2015). Review on feasible recycling pathways and technologies of solar photovoltaic modules. *Solar Energy Materials and Solar Cells*, 141, 108–124. <https://doi.org/10.1016/j.solmat.2015.05.005>
- Tao, M., Fthenakis, V., Ebin, B., Steenari, B. M., Butler, E., Sinha, P., Corkish, R., Wambach, K., & Simon, E. S. (2020). Major challenges and opportunities in silicon solar module recycling. *Progress in Photovoltaics: Research and Applications*, 28(10), 1077–1088. <https://doi.org/10.1002/pip.3316>
- Wang, T.-Y. Y., Hsiao, J.-C. C., & Du, C.-H. H. (2012). Recycling of materials from silicon base solar cell module. 2012 38th IEEE Photovoltaic Specialists Conference, 002355–002358. <https://doi.org/10.1109/PVSC.2012.6318071>
- Weckend, S. (IRENA), Wade, A., & Heath, G. (IEA-P. (2016). End of Life Management Solar PV Panels. www.irena.org
- Xu, Y., Li, J., Tan, Q., Peters, A. L., & Yang, C. (2018). Global status of recycling waste solar panels: A review. *Waste Management*, 75, 450–458. <https://doi.org/10.1016/j.wasman.2018.01.036>
- Yi, Y. K., Kim, H. S., Tran, T., Hong, S. K., & Kim, M. J. (2014). Recovering valuable metals from recycled photovoltaic modules. *Journal of the Air and Waste Management Association*, 64(7), 797–807. <https://doi.org/10.1080/10962247.2014.891540>
- Zerbi, G., & Cortili, G. (1970). Structure of poly-(vinyl fluoride) from its infrared spectrum. *Spectrochimica Acta Part A: Molecular Spectroscopy*, 26(3), 733–739. [https://doi.org/10.1016/0584-8539\(70\)80117-9](https://doi.org/10.1016/0584-8539(70)80117-9)

WOOD GASIFICATION. INFLUENCE OF PROCESS PARAMETERS ON THE TAR FORMATION AND GAS CLEANING

Marek Dudyński *

Modern Technologies and Filtration Sp. z o. o., ul. Przybyszewskiego 73/77 lok. 8, 01-824 Warszawa, Poland

Article Info:

Received:
25 February 2021
Revised:
14 June 2021
Accepted:
21 June 2021
Available online:
30 September 2021

Keywords:

Biomass gasification
Oxygen reforming
Gas engine

ABSTRACT

The article presents an analysis of influence of biomass pre-treatment and change of gasifying agent on the performance of an oxygen-steam-air updraft gasification plant and a technological process capable of delivering high quality producer gas. The paper shows that high temperature gasification process is stable for wood pellets, torrefied pellets and dry wood chips leading to syngas with calorific value of 5-5.5 MJ/m³ and moderate tar content below 10g/m³. After collection of liquids removed from syngas during the cleaning process it has been observed that the hydrocarbon composition in the torrefied wood fuel sample differs significantly from samples derived from wood chips or wood pellets. The paper also covers the influence of oxygen-steam-air combination on the quality of producer gas showing it can produce gas with LHV greater than 8 MJ/m³. The effects of process parameters change on composition of tars collected with an absorption type gas purification unit, designed for dust and tar removal are also reported.

1. INTRODUCTION

The technology of biomass gasification for energy and fuel production is now a firmly established alternative to incineration (Farzad, 2016; Sikarwar et al. 2017; Kirsanovs, 2017) in small to large scale installations (Kurkela, 2016; Dudyński, 2018). In cases of more specialized applications such as liquid fuels production or successful energy generation with piston engines the tar present in producer gas must be removed with cheap and efficient processes if the technology were to achieve commercial viability and compete with wind and solar installation (Broer, 2015). The amount of tar and other contaminants in the gas depends on several factors such as: the pre-treatment of biomass – e.g., drying and compactification for wood pellets, torrefaction or partial pyrolysis for torrefied pellets, the specifics of the gasification process and apparatus, the choice of the gasification agent, temperatures of the process and details of the gasification chamber construction (Dudyński et. al, 2015; Dudyński, 2019). We compare the composition and volume of tars and hydrocarbons collected from producer gas coolers during air gasification of wood chips, wood pellets and torrefied wood pellets. We then chose wood chips as the fuel for tests using three different gasification agent compositions – air, air and steam, and air, steam and oxygen – and compare the resulting composition of producer gas and various hydrocarbons collected in various stages of the gas purification process. The system used

for the experiment is an updraft gasifier equipped with a steam generator and oxygen enrichment unit presented on Figure 1 equipped with an absorptive gas cleaning system described in (Dudyński, 2019).

The gasification systems can be used for effective energy production in a variety of ways (Arena et al. 2010; Bang-Møller et al., 2010) The conventional solution of generating energy from locally produced biomass waste, wood pellets or wood chips by utilizing producer gas burning for steam generation process, which is then used for integrated heat or/and electricity production is now a firmly established method (Dudyński et al. 2012; Dudyński 2018). This solution has found widespread use in cogeneration installations (Kirsanovs et al., 2017), but the electric energy effectiveness is usually far below 20% for small systems. Improvements are possible with application of a gas engine with effectiveness up to 30%, but such solutions are still under development. Gas for piston engines should contain less than 50mg/m³ of solid particles and up to 100 mg/m³ of tar. Attaining such gas parameters for updraft gasifiers, requires intensive gas cleaning making such systems expensive and difficult to operate in small plants (Koido at al., 2017). The more innovative solid oxide fuel cells (SOFC) systems with much higher effectiveness of electric energy production are also under active development (Brunashi et al., 2017). SOFC systems operating on producer gas are a promising technology improving both the electrical and heat efficiency of the systems however they also require

* Corresponding author:
Marek Dudyński
email: marek.dudynski@mtf.pl

comprehensive gas cleaning and operate at high temperature exceeding 900K thus requiring dry, high temperatures resistant, filter systems (Poncratz et al., 2021) which creates new problems for designs and operations (Marcantonio et al., 2020). An excellent review of biofuel production from biomass gasification including recent hydrogen production facilities can be found in (Molino et al., 2018). Supercritical water gasification for hydrogen production is described in (Correa et al., 2018). It can be an important route for bio hydrogen production from biomass. These new technologies which include steam gasification and supercritical water gasification, show a high potential in field-scale applications, but the selectivity and efficiency of hydrogen production must be improved in effective industrial applications to compare with other sources of hydrogen (Cao et al., 2020) and insight in the tar content and composition in the producer gas is of importance for all such research.

The fixed bed, updraft gasification systems are robust, reliable, and can scale up to higher capacities although they do require effective gas cleaning units and improvements of syngas quality to achieve successful coupling with piston engines. Air gasification is a notably simple and inexpensive form of the process, however due to nitrogen dilution of the producer gas it results in syngas LHV below 5.5 MJ/m_N^3 for dry biomass and even lower for wet materials like sawdust or feathers (Dudyński, 2015; Chmielniak, 2019). Typical tar levels for updraft air gasification range from 10 to 150 g/m_N^3 . The tar levels are inversely related with syngas temperature, with a notable, sharp drop for temperatures over 1050K (Bassu, 2018). Steam is a very promising choice of gasification agent as it leads to high H_2 content but requires temperatures over 1000K for the water gas and water shift reaction to be effective. In industrial installations a mixture of steam and air is applied to improve gas quality. A steam generator requires additional energy but in can be obtained from heat recuperated from the piston engines used for electricity generation which in turn leads to the improvement of overall efficiency of the system. One of the most promising methods of improving gas quality is to replace air as the gasification agent with oxygen enriched air, mixed with steam to enhance the calorific value of the gas and limit the tar levels (Liu et al., 2018; Dudyński, 2019). We developed such a system, the details of its design and the results of its operation on dry wood chips, pellets or torrefied material and various gasification gases are presented below.

The oxygen generator is a large energy consumer and in the presented system up to 20% of the electric energy which can be produced with clean gas is internally used, however this can be improved in larger systems. Therefore, the electricity and energy consumed in the fuel feed, oxygen and steam production, syngas transport and cleaning systems are not included in the efficiency calculations for the process.

2. THE GASIFICATION UNIT

The paper presents a new, oxygen-steam-air driven biomass gasification system and process capable of producing syngas with calorific value up to 8 MJ/m_N^3 on a tar

free basis. This device is an improvement on the biomass gasification units successfully used in many industrial localisations in Poland, intended for energy production using waste from technological processes as fuel (Kwiatkowski et al., 2013; Dudyński, 2018). The operating scheme of the system is presented on Figure 1. In respect to the installation presented in (Dudyński, 2019) the feed system was changed by adding a hydraulic press for wet or bulky materials and technical details of equipment mixing oxygen rich air with steam and hot air making the system more flexible. Moreover, all coolers have been grouped into a single system and scrubber order in the gas purification system have been rearranged leading to improved performance.

The thermocouple T1 is located at the bottom of the gasification chamber, T2 above the cones delivering the air+steam mixture, T3 at the center of the gasification zone, two meters from the bottom and T4 at the top of the chamber close to the syngas outlets. The gasification chamber is 6000 mm high with an inside diameter of 2000 mm. This installation allows for gasification of different biomass materials including bulky and wet ones as the residence time can be as long as 8 hrs. Various tests for different materials and conditions can thus be performed.

The presented system is a gasification fixed bed 2MW unit which can use hot air, hot air – steam mixture and up to 40% oxygen air – steam – hot air combination as gasification agents. It uses heat from producer gas cooling to heat up the primary and secondary air to temperatures above 520K. The primary air can be mixed with 450K steam to form controllable gasifying gases which are injected into the chamber at the bottom of the installation. Combination of these two streams allows the system to operate in two distinct modes suitable for different feeds.

Low bed height – low steam content in primary air which can be applied for wet low calorific fuels. The producer gas has a temperature above 1000K at the outlet, LHV below 3.5 MJ/m^3 and less than 10 g/m^3 of tars.

High bed height - high steam content in primary air, effective for dry, high calorific fuels. The gas temperature in the gas chamber is 650K, the LHV above 5 MJ/m^3 and tar content can be well above 10 g/m^3 .

We presented the extended discussion of the gasifying process in the low bed mode for wet feather fuel in (Dudyński et al., 2012; Kwiatkowski et al., 2013) and in the present work the high bed mode is analysed.

The oxygen rich air, containing up to 40% of oxygen and flow speed standing up to at $100 \text{ m}^3\text{h}^{-1}$ is produced in a separate unit utilising molecular sieves. This air stream is mixed with steam prior to its application in the gasification process. The role of steam is twofold. First it performs as an oxygen dispersive medium preventing occurrences of high temperature spots at the bottom of the gasifier, where the char and gas burning processes are the most intense. Application of oxygen rich air can cause the temperatures to locally exceed 2000K posing a serious threat to the gasifier and equipment. Steam and additional air lower the oxygen content to a maximum of 25% causing the temperatures in the bottom part of the gasifying chamber to stay well below 1500K thus ensuring the operations are smooth and safe. These temperatures are still very high and in or-

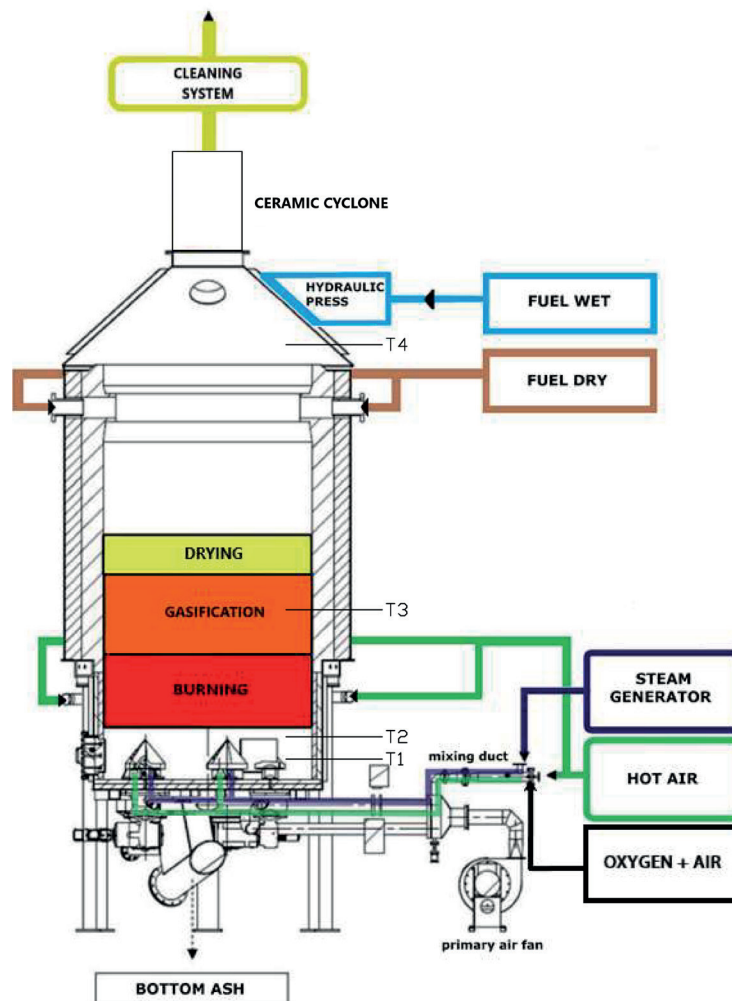


FIGURE 1: Operating scheme of the biomass gasifying unit.

der to prevent ash sintering we must take care to eliminate sand from biomass fuels and keep the temperature in the lower part of the gasifier where ash is predominantly present below 900K to prevent ash and silica agglomeration and melting. The hot gases move up in the chamber and in the upper part of the gasification unit the overheated steam and CO_2 can react with fixed carbon and tars to produce CO and H_2 in a water-gas and water shift reaction, efficient in high temperatures thus significantly improving the producer gas quality and generally lowering temperatures in the carbon burning zone. We constructed a unit allowing for various combinations of gasification gases delivered via a multilayer and multipoint injection system. At the bottom of the gasifier four rotating cones equipped with multiple inlets are located. The oxygen rich air mixed with steam is injected into the bottom part of the unit through these cones. Approximately 50% of the oxygen necessary for the gasification process is provided through these four injection ports and most of the hot CO_2 and H_2O , necessary for the process, is produced in the bottom area of the reactor. The remaining air necessary for the process is injected with 32 nozzles located above the cones, close to the bottom of the pyrolysis zone. The delivered air reacts with the hot pyrolytic carbon producing a CO rich gas and extending

the high temperature zone in the gasifier thus intensifying the process of wood drying and carbonising occasionally, in cases of very dry materials, even extending the drying process with flash pyrolysis of smallest particles. Such a solution guarantees a more uniform distribution of the gases and solid material in the chamber, and therefore improves the mixing of the carbonised material with gasifying agents. This enhances the effectiveness of the gas production and unification of the temperature's distribution in the gasification process. The control unit allows us to continuously change the parameters and the composition of the gasifying gases leading to better control of the producer gas parameters.

The system maintains 0.2 kPa of negative pressure below the atmospheric pressure (1013.25 hPa) in the upper part of the gasification chamber. The air flow at the bottom of the gasifier can be adjusted to maintain control and conditions of the process as well as the stability of syngas generation. The test begins with wood chips being fed to the gasifier. After achieving stable conditions for bed height and temperature distribution inside the gasification chamber the fuel feed is adjusted to the required capacity and the test runs commence. It means that all test start with gasifier containing approximately 2000kg of charcoal

from wood chips with a layer of ash at the bottom. We commence all tests with the same initial conditions keeping a constant level of material in the gasifier.

Dry fuels are fed with two screw conveyors, one on each side of the gasifier, to maintain the level of the bed. Liquid fuels can be introduced with a pump system. Both dry and liquid fuels are fed in a continuous fashion. Wet bulky materials on the other hand are introduced with a hydraulic loading drawer in a discontinuous fashion.

Gas leaving the gasification unit still contains high amounts of carbon dust and heavy hydrocarbons which must be removed before gas is fed into the engine. With high levels of tars and carbon dust the produced gas requires a very efficient purification system. There are various methods of gas cleaning and virtually every wood gasification unit developed their own unique technology (Boerrgter et al., 2004; Bocci et al., 2010; Dudyński, 2019). Our system consists of a high temperature ceramic cyclone, integrated with the gasifier for particle removal, one air cooler, two water coolers capable of lowering the gas temperature below 60°C, water scrubber, oil scrubber for elimination of tars and hydrocarbons and an active carbon filter for final gas conditioning. The operating scheme for this unit presents on Figure 2 indicating the material flow and temperatures during the process.

Syngas cleaning takes place by precipitation and removal of tars and heavy hydrocarbons contained therein by

adequate cooling of the gas in several stages and absorption of other impurities in the syngas by gas flow through two absorption devices (scrubbers). The first scrubber uses water and the other fuel oil as absorbent. Both scrubbers are equipped with demisters placed immediately before the outlet, which keeps the scrubbing liquids inside the apparatus.

The gas from the gasification of wood is transported to the first exchanger (cooler I) in a counter-current system, the gas will be cooled to temperatures in the range of 100-110°C then the gas moves to the fan and is pumped to a two-stage heat exchanger system. On the second and third levels of cooling, the temperature of the gas drops below the precipitation point of tar and the hydrocarbons flow down the walls of the exchangers into the lower parts, where a discharge spigot enables liquefied contaminants to be collected. An important factor determining the possibility of precipitation of tars and preventing the formation of carbon deposits and clogging of exchangers is to maintain appropriate temperatures at the inlet and outlet of each cooler.

The gas then flows to the water scrubber, where it is cleaned of remaining impurities: dust, tars, and water-soluble hydrocarbons. After passing through the water scrubber, the gas will then be fed to the absorption column (oil scrubber), where the residual hydrocarbons will be washed away by the oil. After cleaning, the gas will be transported

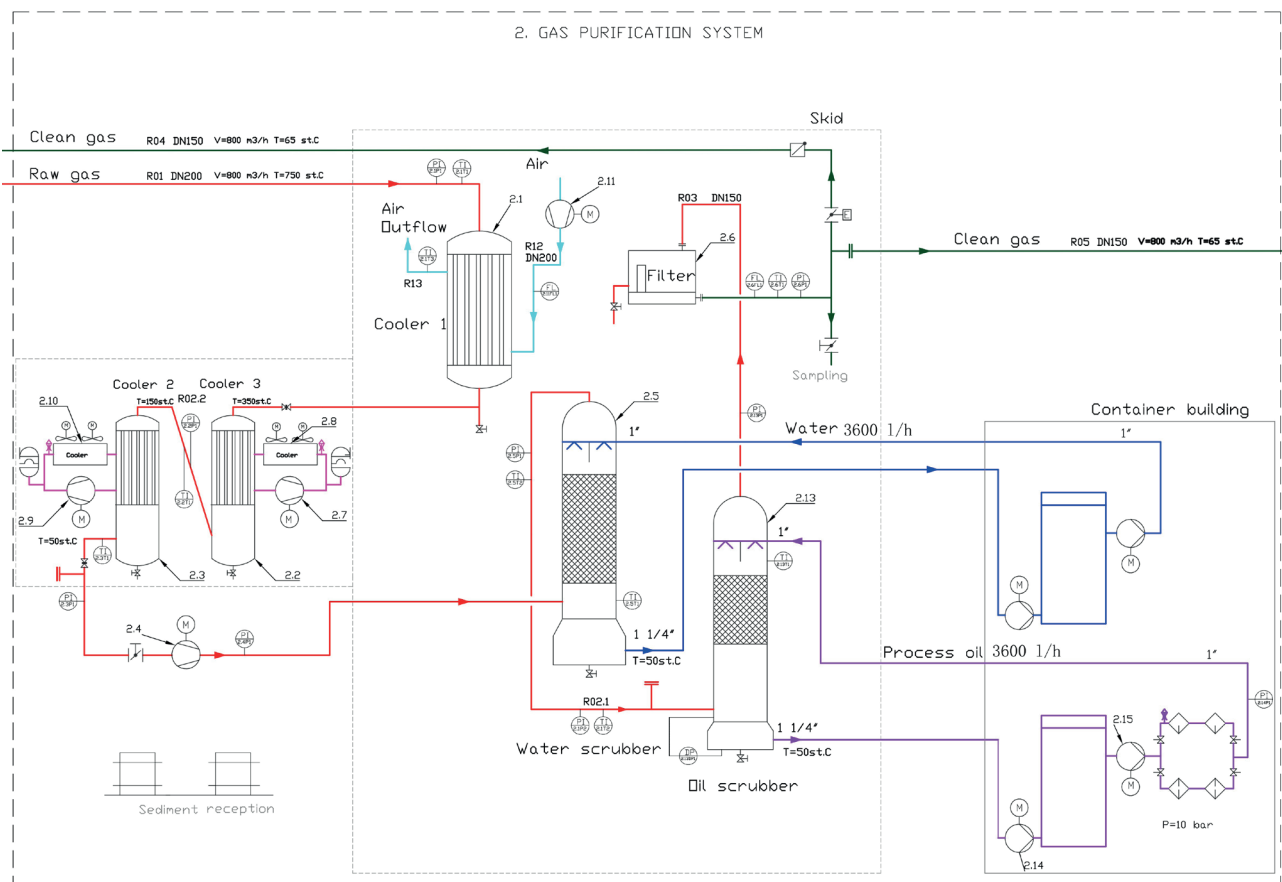


FIGURE 2: Operating scheme of a gas purification unit.

to the engine or returned to the combustion chamber.

The oil flowing through the scrubber is pumped to the clarifier and then to a candle filter unit. The purified and cooled oil is then returned to the absorption column (oil scrubber). The water flowing through the scrubber is pumped to the clarifier and then recycled to the installation. In the future it will be used as a source for steam for the gasification process.

Fuel inflow is up to 500 kg/h, air flow in the gasifier is 600 m_N³/h the raw syngas flow up to 800-900 m_N³/h. In the first heat exchanger up to 1000 m_N³/h of air is used. The oil flow is 3.6m³/h and in the water scrubber utilises 3.6m³/h of water. The oil/syngas ratio is 2.5/1 and water/syngas is 3.6/1.

3. MATERIALS AND METHODS

The industrial tests have been divided into two stages. First, the analysis of influence of the biomass pre-treatments such as drying, pelletisation and torrefaction on the composition of the tars and liquids collected in the coolers of our cleaning system with methodology like that used in our previous tests (Dudyński et al., 2015). Three types of fuel have been used - dry wood chips, wood pellets obtained with flash drying of sawdust at 550K, and pellets from sawdust torrefied at 560-580K. The liquid condensate was cooled and then separated into water containing liquid carbohydrates and solid heavy tar. The tars were dissolved in solvents and like liquid parts analysed with gas chromatography where components were measured. The heavy tars were additionally analysed with a simulated distillation method to define boiling points of components.

3.1 Gas chromatography

All water and tar samples were analysed using gas chromatography (GC) techniques: Flame Ionisation Detector (GC-FID) (for quantification) and a Mass Spectrometer (MS) (for peak identification) fitted with a High Polarity HP-FFAP column. The HP-FFAP column (50 m x 0.2 mm x 0.33 μm) is a high polarity column suited for analyses of organic acids, free fatty acids, and phenols. Approximately one μL of sample was injected into the FC column with a split of 200 (if samples were too diluted a split of a 100 was used). The GC oven was programmed as follows: Initial temperature of 60°C, ramp up of 6°C per minute to 240°C and then hold the temperature for 30 minutes (until all compounds have eluted). Gas flow through the column was 1.2 per minute (helium in GC-MS and hydrogen in GC-FID).

3.2 Simulated distillation

Simulated distillations (SimDis) were conducted for prepared tar samples to determine the boiling point distribution of extracts from biomass gasification tars. Simulated distillation was conducted on a high temperature GC-FD fitted with an ARX 2887 Restek column (10 m x 0.53 mm x 0.53 μm). Approximately 0,2 μL sample was injected into the GC column per analysis. The GC oven program was as follows: initial temperature of 40°C, ramp up of 15°C per minute to 540°C and then hold the temperature for 10 minutes.

The second stage of our experiment consists of gasifying the dry wood chips (max 25% of water) as an example of the most popular biomass feedstock with three different gasifying agents. During the test gas samples have been collected at the inlet and outlet of the purification systems, and we measured the effect of application of the complete purification scheme on the resulting producer gas quality. Additionally, water samples were collected at the outlet of each cooler separately and each sample was analysed with gas chromatography to determine the hydrocarbon composition. Table 1 presents the proximate and elementary analysis of the feedstock used for tests in our industrial experiment.

The gradual carbonisation and decomposition of hemicellulose begins in 450K which can be easily reached during drying and pelletisation of sawdust, this process is exacerbated at higher temperatures (Partridge et al., 2020) leading to a gradual rise of carbon content in biomass feed from wood chips to pellets to torrefied pellets.

4. RESULTS

4.1 Collection of hydrocarbons

A test has been conducted for three fuel types - wood chips, wood pellets and torrefied pellets. The test for each material took six hours and involved the usage of 1800-2400 kg of fuel. The process was conducted as air gasification with the gas leaving the gasifier in ranges 900-1100 K. The equivalence rate ER in the experimental runs was ER=0.38-0.4 in case of woodchip, ER=0.34 for torrefied pellets and 0,36 for wood pellets. Ash analysis shows that the carbon conversion rate was greater than 99% and the dry syngas/dry fuel ratio was 2.45 m_N³/kg. Figure 3 presents the temperatures measured in various spots inside the gasifier - at the bottom T1, at the lower part of the gasification chamber T2, at the center of the gasification zone T3, as well as the temperature of gas leaving the gasifier. It can be observed that for dry fuel the air gasification becomes a high temperature process leading to moderate tar loads in producer gases.

It can be seen from the temperatures distribution that the process is remarkably stable in all three cases. For dry fuels, the syngas and gasification zone temperatures are very close indicating that the drying zone is very narrow.

TABLE 1: Properties of gasified biomass feeds.

	Unit	Wood pellets	Torrefied pellets	Wood Chips
Water content	[%]	10	4.5	20-25
Volatiles	[%]	79.1	70.6	81.36
Fixed-Carbon	[%]	19.2	39.5	18.3
Ash	[%]	0.5	0.9	0.7
Ultimate analysis (dry basis)				
C	[%]	50.6	56.0	48.8
H	[%]	5.9	5.0	5.7
O	[%]	43.3	38.6	45.5
N	[%]	0.2	0.4	0.1
LHV	[MJ/kg]	17.7	20	14.4-15.5

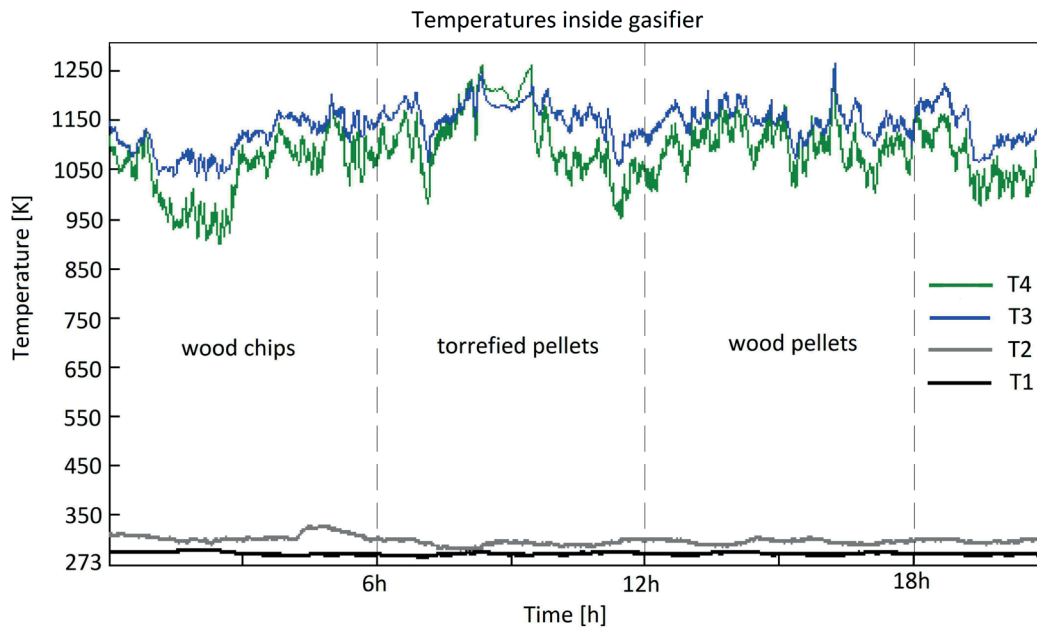


FIGURE 3: Operating scheme of the biomass gasifying unit.

The summary of the gasification process can be found in Table 2.

The syngas leaving entering and leaving the purification system was analysed with a gas chromatograph (Varian CP-4900) calibrated to determine the levels of following compounds H_2 , CO , CO_2 , CH_4 , C_2H_2 , C_2H_6 , C_3H_8 , N_2 and O_2 . The levels of CO , CO_2 , CH_4 and O_2 were also independently measured by an online gas analyser Ultramat 23 while Colomet 6 was used for secondary hydrogen measurements. The gravimetric determination of liquid hydrocarbons was conducted with samples taken every two hours. The averaged results were presented in Table 3.

Tar samples from all three coolers were collected into a single barrel per fuel type - thus producing three barrels in total which were then analysed in a laboratory. The bulk results are presented in Table 4.

4.2 The heavy tar analysis

The collected water was black in colour and at the bottom contained solid (gummy like) substance being a composition of heavy tar. These substances constituted less than 1% of mass of collected liquids. The elementary analysis of these materials is presented in Table 5, these samples were collected separately for each of three woody biomass materials. As the test requires more time to collect the liquid condensates in amounts allowing for solid tars to be easily separated the process was conducted as air gasification with the gas leaving the gasifier in ranges of 900-1000K.

We dissolved the tar in three solvents (ethanol, tetrahydrofuran (THF), and 1-methyl-2-pyrrolidone (NMP)) and the chromatographic results averaged (as different solvents present different molecular composition of the same tar).

TABLE 2: Process parameters of air gasification during tar collection.

Fuel	Syngas temperature [K]	Fuel stream [kg/h]	Air stream [m ³]	$m_a/m_{fuel(dry)}$	Dry gas stream [m ³ /kg of dry fuel]	LHV [MJ/m ³]	Process efficiency% [Egas/Efuel]
Wood chips	1020	400	500	2.05	3.06	5.0-5.1	65.4
Torrefied pellets	1120	300	500	2.15	3.06	5.5	68.6
Wood pellets	1080	310	500	2.12	3.0	5.2	65.8

TABLE 3: Average parameters of syngas during tar collection.

Fuel	Syngas components % of vol (Dry gas)							Calorific value of cold syngas [MJ/m ³]	Tars [mg/m ³]
	H ₂	N ₂	CO	CO ₂	CH ₄	C ₂ H ₄	Others hydrocarbons		
Wood chips	6.2	60.9	16.7	12	2.8	1	0.4	5.06	6500
Torrefied pellets	7.4	59.3	18	8.8	4.4	1.1	0.3	5.5	3200
Wood pellets	6.8	59.1	17.3	11.8	3.7	0.9	0.4	5.2	5100

TABLE 4: Summary of tar collection in cooler system.

	Unit	Wood chips	Torrefied pellets	Wood pellets
Liquid collected	[kg]	115	41	60
Hydrocarbons collected	[kg]	10.8	2.5	8.5
Hydrocarbons to fuel	[kg/kg]	0.0045	0.0016	0.0047

TABLE 5: Elementary analysis of the biomass raw tars.

		Wood pellets	Torrefied pellets	Wood Chips
Dry mass				
C	[%]	62.2	38.6	55.1
H	[%]	7.4	8.1	7.2
N	[%]	4.5	0.8	1.7
S	[%]	0.0	0.0	0.0
O (by difference)	[%]	26.1	52.6	36.1
Calorific values	[MJ/Kg]	26.4	17.7	22.2
H/C (atomic)		1.4	2.5	1.6
H/O (atomic)		4.5	2.5	3.2

The results of analysis are presented in Table 6.

The tar from wood chips contains mainly alkylphenols, organic acid and small amounts of polyfunctional aromatic oxygenates. Wood pellets tar contained linear and cyclic aliphatic oxygenates, polyfunctional aromatic oxygenates and alkylphenols. Torrefied pellets tar contained acids, aliphatic alcohols, alkylphenols, aliphatic oxygenates and alcohols. The tars were strongly different with shorter molecules length often observed in more pre-treated material. The biomass tar contained a range of molecular sized chains including large polymeric molecules which are larger and spatially more complicated than these observed in coals or charcoal feedstocks (Vrengenhil et al., 2009). The process of torrefaction changes lengths and structures of

hydrocarbons in collected tars as can be clearly seen from simulated distillation analysis presented below.

4.3 Simulated distillation

The simulated distillation was conducted for all samples to determine the boiling point distribution of extracts from three feedstocks. The results clearly indicate that intensive drying and torrefaction lower the complicated structure of wood thus the tar derived from more pre-treated material have simpler structures (lower boiling point). We present on Figure 4. the result of distillation of tars.

We can see clearly from Figure 4 that the process of wood torrefaction lower significantly the maximal boiling point of heaviest tars derived from the material confirming our observation that the structure and lengths of hydrocarbons obtained in the gasification process simplify in comparison with tar extracted from fresh wood or wood pellets. In future work more careful analysis with more carbonized material like charcoal and annealed charcoal should be conducted for more conclusive results.

4.4 The analysis of water condensates

The water condensates derived from each of three feedstocks were analysed with help of gas chromatography and are presented in Table 7.

The main organic species determined by GC-MS in water condensates were acids, aliphatic alcohols, alkylphenols, and linear and cyclic oxygenates but in slightly different proportions than in appropriate tars from these materials. As the hydrocarbons in tars were oxygenated and highly reactive further work should consider characterisation on site during test or rapid quenching to stop fast degradation or polymerisation with other molecules which change the results of measurements.

These results are not conclusive. The variations of the hydrocarbon composition in differently prepared feedstocks can be partially attributed for the effects of the intensive drying as in case of wood pellets or torrefaction at

TABLE 6: GC-MS composition of the tars from three feedstocks.

		Wood pellets	Torrefied pellets	Wood Chips
Molecular component				
Aliphatic	[%]	0.1	0.8	0.4
Acids	[%]	11.1	50.15	22.1
Aliphatic esters	[%]	0.2	0.05	0.1
Aliphatic aldehydes and ketones	[%]	1.6	0.8	5.7
Aliphatic alcohol	[%]	1.8	7.7	0.7
Alkylbenzenes	[%]	0.8	0.4	5.2
Alkylphenols	[%]	21.9	11.8	34.1
Furan	[%]	0.1	1.2	7.9
Furan (polyfunctional oxygen)	[%]	5.2	0.0	1.1
Linear and cyclic aliphatic oxygenates (polyfunctional oxygen)	[%]	27.0	10.7	6.2
Aromatic oxygenates	[%]	25.0	12.2	15.2
Nitrogen and sulfur heteroatoms	[%]	4.2	4.0	1.2
Total	[%]	100	100	100

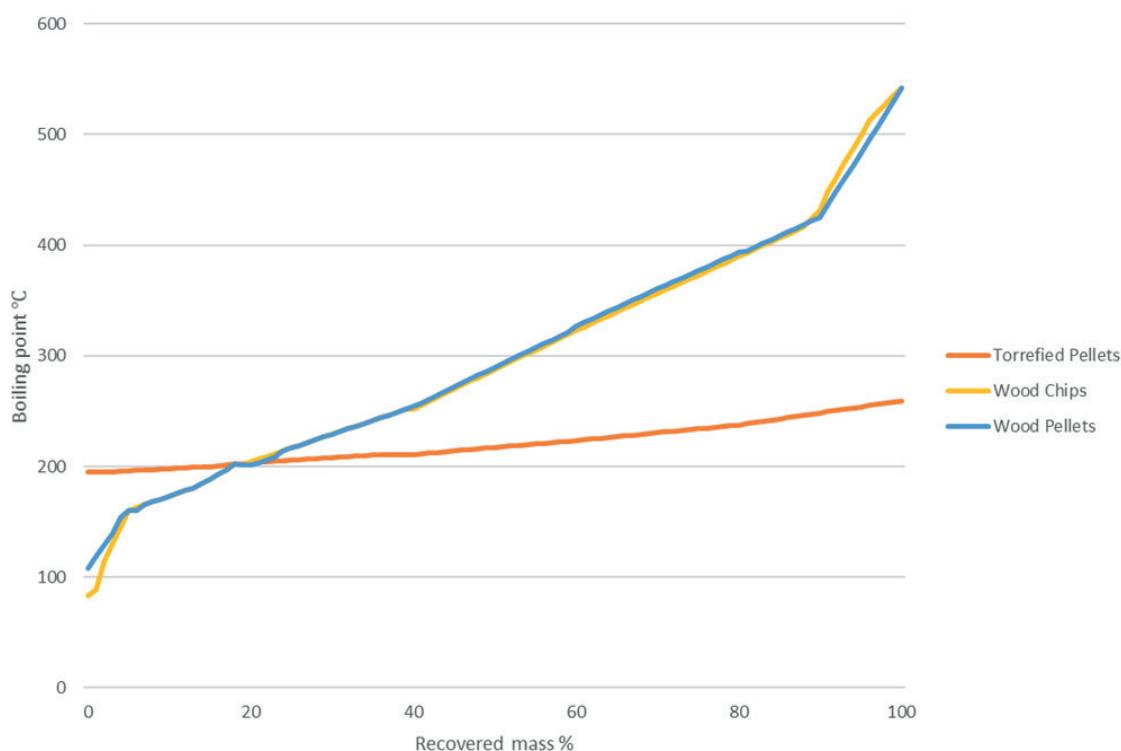


FIGURE 4: Simulated distillation of tar derived from wood pellets and torrefied pellets.

elevated temperatures which simplified the original wood chemical structure and lowered the maximal lengths of molecular chains of derived tars. On the other hand, gasification and pyrolysis as processes in an industrial scale gasifier depend on the humidity, compactification, and oxygen content of the material as these determine speed, layer profiles in the bed and temperatures of the gasification process resulting in different distribution of hydrocarbons lengths in tars collected in the process and the temperatures and speed can seriously change the molecular distribution of derived hydrocarbons. These relations shall be

investigated more closely in future but clearly suggest the advantage of using torrefied material as preferred feed for gasification to reduce tar content in gas. Such approach was used in entrained flow gasification process for liquid fuel production developed in (Eberhard et al., 2020).

4.5 The gasification runs with different gasification gases

The system can operate on wood chips or pellets, with both air-steam mixtures and oxygen enriched gasification gases. We tested the process with dry wood chips at 20-

TABLE 7: GC-SM composition of water condensates.

		Wood pellets	Torrefied pellets	Wood Chips
Molecular component				
Aliphatic	[%]	0.1	0.3	0.9
Acids	[%]	66.9	59.3	63.9
Aliphatic esters	[%]	0.7	2.0	1.6
Aliphatic aldehydes and ketones	[%]	4.9	3.7	5.2
Aliphatic alcohol	[%]	9.3	7.3	3.9
Alkylbenzenes	[%]	0.1	0.3	1.2
Alkylphenols	[%]	6.7	13.5	10.6
Furan (polyfunctional oxygen)	[%]	3.4	1.8	1.8
Linear and cyclic aliphatic oxygenates (polyfunctional oxygen)	[%]	7.4	11.4	10.45
Aromatic oxygenates (polyfunctional oxygen)	[%]	0.1	0.1	0.05
Nitrogen and sulfur heteroatoms	[%]	0.4	0.2	0.2
Total	[%]	100	100	100
Total organic content in water	[%]	14.1	6.1	9.4

25% humidity and average diameter of 5-20 mm. We have compared the producer gas quality during simple air gasification (Run 1) with mixture of air and steam (Run 2) and finally with steam-oxygen-air composition (Run 3); these are presented below in Table 9. These runs were conducted under high bed condition with temperatures of the gas leaving gasifier kept at 800-850K. Temperature distribution in the gasifier is presented on Figure 5 for air and air-steam gasification and on Figure 6 for oxygen-steam-air gasification runs.

We observe that in contrast to air and stem-air gasification the introduction of oxygen into the gasification process changes the dynamics of the process leading to elevation of temperatures in gasification and pyrolysis zones and as a result the process requires more effort to stabilize.

The gas parameters measured during these runs are presented in Table 8.

The amount of wood used in each test was dependent on the effectiveness of the gasification process as the level of material in the gasifying chamber was kept constant. In all tests the amount of oxygen in gasification gases was also kept constant and approximately equal to 150 kg/h not counting water in the biomass feeds in different com-

binations of air, steam and oxygen enriched air making the results directly comparable. We observed the difference in thermal output of each run showing the dynamics of the process measured in the effective amount of wood gasified during each test was different due to the different temperatures inside the bed and different reactiveness of the gasification gases. In this experiment ER=0.4 for air gasification, ER=0.42 for air-steam and ER=0.36 for oxygen-steam-air mixture. The contamination of the producer gas leaving the gasifier after the cyclone were analysed and are presented in Table 9 below for each run.

The following table presents the energy balance of the gasification process calculated by estimating the energy added to the system with fuel and hot gasification gasses and removed due to production, transport, and cooling of syngas.

It can be observed that the LHV of the clean producer gas for each run is in good agreement with experimental values from gas composition measurements as can be seen in Table 9.

The tar contents of the gas leaving the gasifier and the composition of tars in water collected in various stages of the purification process during each run has been

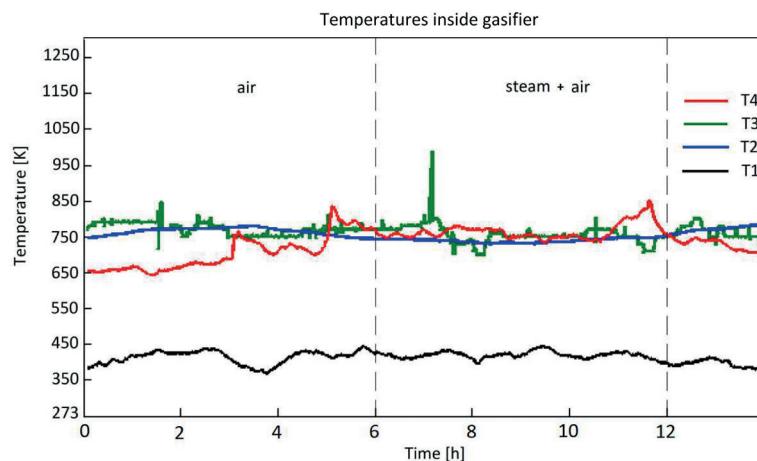


FIGURE 5: Distribution of temperatures in gasifier during air and air-steam gasification.

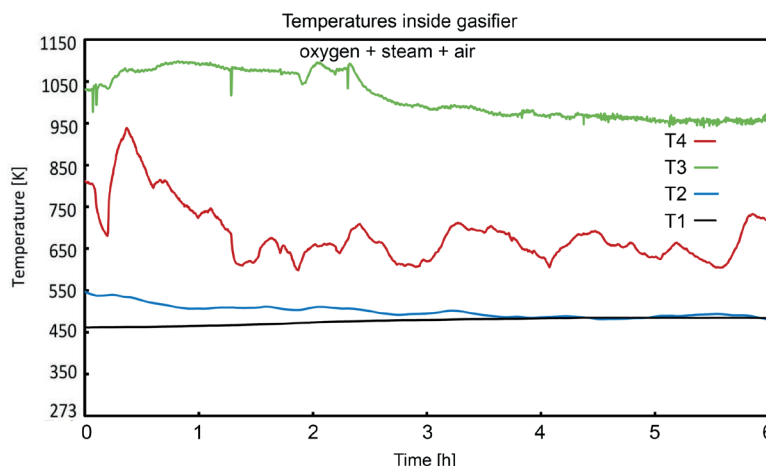


FIGURE 6: Distribution of temperatures in gasifier during oxygen-steam-air gasification.

TABLE 8: The parameters of the process and properties of the producer gas after purification.

		Run 1	Run 2	Run 3
Parameter				
Thermal output	[MW]	1.35	1.0	1.8
Fuel	[kg ^h]	410	310	480
Air flow	[m ³ h ⁻¹]	600	500	400
Oxygen content	[%]	21	21	25.8
Steam flow	[kg ^h]	0	20	25
Syngas Parameters After Purification				
CO	[%]	30,10	26.47	34.01
H ₂	[%]	9.0	8.35	22.40
CH ₄	[%]	2.67	1.80	4.14
CO ₂	[%]	8.42	7.60	16.40
Syngas LHV	[MJm ⁻³]	5.0-5.5	4.0- 4.6	7.2-7.8

measured. Table 11 presents the composition of the cyclic hydrocarbons in water condensates obtained in various stages of the purification unit for oxygen-steam-air gasification as a general characterization of cooler water condensates has been done in the first test. The levels of cyclic hydrocarbons dissolved in water has been chosen as good indicators of changes of tars characteristics in the gasification process due to different gasifying gasses combination.

From the analysis of the effluents from each cooler it has been found that the selectivity of the system is low. Mostly water was collected in each cooler with only slightly different combinations of hydrocarbons. To prevent clogging the implemented pipe system is wide enough (40-60 mm) to allow gas in the central part of the cooler to remain hot, while water could condensate on the pipe surfaces. It has been decided to treat all the effluents from the three coolers and water scrubber as if from a single unit. The problem of improving selectivity of the coolers system will be addressed in a future work. The system was intended for lowering the syngas temperatures and only a fraction of liquids contained in the gases condensate in the coolers. It shall operate in much lower temperatures to act effectively as liquids reductors in syngas which requires specific technical solutions. Afterwards the contamination levels of the producer gas leaving the oil scrubber have been measured and as it contains less than 100 mg/Nm³ of heavier tar and less the of 600 mg/Nm³ of light hydrocarbons mainly benzene, toluene and xylene it was suitable for use in gas engine unit.

TABLE 10: Energy balance of the process.

	Unit	Run 1	Run 2	Run 3
Enthalpy in fuel	[MJ/h]	5945	4495	6960
Net enthalpy loss in the system (including syngas cooling)	[MJ/h]	-1299	-1035	-1261
Ethalpy loss in removed tar	[MJ/h]	-340	-684	-615
Enthalpy in cold syngas	[MJ/m _N ³]	5.10	4.08	7.28
Process efficiency	%	73	64.5	73

TABLE 9: The producer gas contaminations.

	Run 1	Run 2	Run 3
Substance	$\left[\frac{mg}{Nm^3}\right]$	$\left[\frac{mg}{Nm^3}\right]$	$\left[\frac{mg}{Nm^3}\right]$
Dust	673.6	847.3	817.3
Benzene	6050	12700	12810
Toluene	2120	4890	2980
Xylene	210	450	440
Sum of BTX	8380	18000	16230
Heavy organic compounds	1700	2120	1860
Naphthalene	1.83	0.20	0.21
Acenaphthylene	0.20	0.86	0.77
Acenaphthene	0.05	0.18	0.17
Fluorene	0.42	1.26	1.15
Phenanthrene	2.63	7.24	6.43
Anthracene	0.69	1.93	1.76
Fluoranthene	1.22	4.09	4.86
Pyrene	1.19	4.27	5.35
Benzo [a] anthracene	0.33	0.92	1.24
Chrysene	0.28	0.83	1.10
Benzo [b] fluoranthene	<0.01	0.80	1.66
Benzo [j] fluoranthene	0.31	0.80	1.61
Benzo [k] fluoranthene	0.11	0.31	0.48
Benzo [a] pyrene	0.26	0.75	1.21
Indeno [1.2.3-cd] pyrene	0.13	0.32	0.51
Benzo [ghi] perylene	0.18	0.50	0.77
Sum of polycyclic aromatic hydrocarbon compounds	9.82	25.25	29.27

* including polycyclic aromatic hydrocarbon compounds

The results clearly indicate that the application of the various combinations of oxygen, steam and air composition significantly influences the properties of the producer gas leading to significant growth of calorific value but not necessarily lowering the amount of tar and light hydrocarbons in the raw gases as is clearly seen at Table 6. We observe that the high selectivity of the tar removing system is more consistent with the application of gas engines as only the heavy hydrocarbons need to be removed but light hydrocarbons like benzene, xylene, toluene can be safely burned in the gas engine. In such cases use of dry torrefied or carbonised material as a feedstock can be a much simpler route for reducing the levels of contamination of producer gas. For a producer gas to be a source of fuel

TABLE 11: The hydrocarbon concentration in coolers condensate water (%).

Water condensate	Cooler 1	Cooler 2	Cooler 3
Acetaldehyde	0.015	0.027	0.021
Acetone	0.016	0.027	0.024
Methacrolein	0.002	0.003	0.003
2,3-butanedione	0.010	0.019	0.018
Butanal	0.001	0.003	0.002
2-butanone	0.005	0.011	0.009
2-butenal	-	0.003	-
2-butanone, 3-methyl-	-	0.002	0.001
Benzene	0.042	0.032	0.035
3-buten-2-one, 3-methyl-	0.03	0.006	0.005
2-pentatone	-	0.002	0.002
2,3-pentanedione	-	0.003	0.002
Toluene	0.013	0.008	0.006
Cyclopentanone	-	0.002	0.002
1,3,5,7-cyclooctatetraene	0.004	0.002	0.002
2-cyclopenten-1-one, 2-methyl	-	0.001	0.002
Phenyl, 2-methyl	0.003	0.002	0.004
Indene	0.004	0.005	0.004
Phenol, 2-methoxy-	0.001	0.002	0.003
Phenol, 2, 6-dimethyl	0.001	0.001	0.003
Creosol	0.002	0.003	0.005
Azulene	0.003	0.007	0.006

for SOFC or hydrogen conversion the further work on the oxygen-air-steam gasification process and more promising catalytic tar reducing technology shall be tested and compared with the unit analysed here (Xue-Yu Ren et al., 2020).

5. CONCLUSIONS

We have conducted a series of tests for the steam-oxygen-air gasification installation and procedures with three different materials and three different gasification schemes with particular attention on the amount and characterisation of the tars and hydrocarbons produced in the process and present in the producer gas. We analysed the influence of pretreatment of biomass on the syngas quality indicating the influence of torrefaction on lowering the tar content of the gas. The oxygen enriched air combined with steam can lead to gas with LHV higher than 8 MJ/m_N^3 sufficient for use in gas engine or fuel cell for efficient electric energy generation. Our goal was to analyse the technical and thus economic aspects connected with the gas cleaning process required when the gas is to be applied for a more efficient and sophisticated way of application than burning and use of steam turbine cycle. There are many steam-oxygen gasification schemes recently tested (Broer et al., 2015; Kurkela et al., 2016; Dudyński, 2019) on laboratory or small-scale units with comparable results indicating the potential of this method to improve the technology of biomass gasification (Baláš et al., 2016). Application of

the oxygen-steam-air combination improves significantly the LHV of the producer gas to the levels comparable with downdraft gasifiers (Kirsanovs et al., 2017) showing that such technology can be technically viable for effective heat and electricity generation. The main problem for this method of syngas improvement to be commercially applicable in small scale installations is the issue of reducing the cost of oxygen generation and disposal of wastewater and oil. Many improvements are under way: excess heat can be used for chip drying, waste oil, water and tars are to be used internally in the process for steam generation while the use of torrefied material or charcoal as a fuel is an interesting possibility for future long-time tests.

ACKNOWLEDGEMENTS

The financial support by the Polish National Centre for Research and Development (grant number BIOENERGY-11/BIO-CCHP/2018) for the BIO-CCHP project within the framework of the 11th Joint Call of ERA-NET Bioenergy is gratefully acknowledged.

REFERENCES

- Arena, Umberto & Di Gregorio, Fabrizio & Santonastasi, M.. (2010). A techno-economic comparison between two design configurations for a small scale, biomass-to-energy gasification based system. *Chemical Engineering Journal*. 162. 580-590. <https://doi.org/10.1016/j.cej.2010.05.067>.
- Baláš, M., Lisý, M., Moskalík, J., & Skála, Z. (2016). Steam Influence on Biomass Gasification Process. The holistic approach to environment, 6(3), 127-132. [orcid.org/0000-0002-4968-1535](https://doi.org/10.1016/j.cej.2016.03.015)
- Bang-Møller, C., & Rokni, M. (2010). Thermodynamic performance study of biomass gasification, solid oxide fuel cell and micro gas turbine hybrid systems. *Energy Conversion and Management*, 51(11), 2330-2339. <https://doi.org/10.1016/j.enconman.2010.04.006>
- Basu P. (2018) Chapter 6 - Tar Production and Destruction. *Biomass Gasification, Pyrolysis and Torrefaction (Third Edition)*, 189-210. Academic Press <https://doi.org/10.1016/B978-0-12-812992-0.00006-6>
- Bocci E., Sisinni M., Moneti M., Vecchione L., DiCarlo A., Villarini M. (2014). State of the art of small scale biomass gasification power systems: a review of the different typologies. *Energy Procedia* 45,247-256. <https://doi.org/10.1016/j.egypro.2014.01.027>
- Boerrigter, H., Calis H.P., D.J. Slort D.J., Bodenstaff H., Kaandorp A.J., den Uil H., Rab L.M. (2004) Gas Cleaning for Integrated Biomass Gasification (BG) and Fischer-Tropsch (FT) Systems. ECN-C-04-056 <https://publicaties.ecn.nl/PdfFetch.aspx?nr=ECN-C-04-056>
- Broer, K. M., Woolcock, P. J., Johnston, P. A., & Brown, R. C. (2015). Steam/oxygen gasification system to produce clean syngas from switchgrass. *Fuel*, 140, 282-292. <https://doi.org/10.1016/j.fuel.2014.09.078>
- Brunaccini G., Sergi F., Aloisio D., Ferraro M., Blesznowski M., Kupecki J., Motylinski K., Antonucci V., Modeling of a SOFC-HT Battery hybrid system for optimal design of off-grid base transceiver station, *International Journal of Hydrogen Energy* 2017;42(46):27962-27978, <https://doi.org/10.1016/j.ijhydene.2017.09.062>
- Cao, L., Yu, I., Xiong, X., Tsang, D., Zhang, S., Clark, J. H., Hu, C., Ng, Y. H., Shang, J., & Ok, Y. S. (2020). Biorenewable hydrogen production through biomass gasification: A review and future prospects. *Environmental research*, 186, 109547. doi.org/10.1016/j.envres.2020.109547
- Chmielniak T, Sobolewski A, Bigda J, Iluk T. (2019) Biomass-Based Low Capacity Gas Generator as a Fuel Source. In Szubiel M, Filipowicz M. (Eds) *Biomass in Small Scale Energy Applications: Theory and Practice*. (Chapter 12) CRC Press
- Correa C, Kruse A, (2018). Supercritical water gasification of biomass for hydrogen production – Review. *The Journal of Supercritical Fluids*, Volume 133, Part 2, 573-590. <https://doi.org/10.1016/j.supflu.2017.09.019>

- Dudyński M., Kwiatkowski K., Bajer K. (2012). From feathers to syngas – technologies and devices. *Waste Management* 32, 685-691. <https://doi.org/10.1016/j.wasman.2011.11.017>
- Dudyński, M. C. van Dyk J., Kwiatkowski K., Sosnowska M. (2015). Biomass gasification: Influence of torrefaction on syngas production and tar formation. *Fuel Processing Technology*. Volume 131, , Pages 203-212. doi.org/10.1016/j.fuproc.2014.11.018
- Dudyński, M. (2018). Gasification of Selected Biomass Waste for Energy Production and Chemical Recovery. *Chemical Engineering Transactions* 65, 391-396. <https://doi.org/10.3303/CET1865066>
- Dudyński, M. (2019). Novel oxygen-steam gasification process for high quality gas from biomass. *Detritus*. Vol.06. pp.68-76. <https://doi.org/10.31025/2611-4135/2019.13814>
- Eberhard M., Santo U .Michelfelder B., Gunther A., Weigand P, Matthes J, Waiber P, Hagenmeyer V., Kolb T., (2020). The Bioliq Entrained-Flow Gasifier – A Model for the German Energiewende. *ChemBioEng Reviews* 7(5). doi.org/10.1002/cben.202000006
- Kirsanovs, V., Blumberga, D., Karklina, K., Veidenbergs, I., Rochas, C., Vigants, E., & Vigants, G. (2017). Biomass gasification for district heating. *Energy Procedia*, 113, 217-223. <https://doi.org/10.1016/j.egypro.2017.04.057>
- Kurkela, E., Kurkela, M., & Hiltunen, I. (2016). Steam–oxygen gasification of forest residues and bark followed by hot gas filtration and catalytic reforming of tars: Results of an extended time test. *Fuel Processing Technology*, 141, 148-158. <https://doi.org/10.1016/j.fuproc.2015.06.005>
- Kwiatkowski, K., Krzysztoforski, J., Bajer, K., & Dudyński, M. (2013). Bioenergy from feathers gasification–Efficiency and performance analysis. *Biomass and bioenergy*, 59, 402-411. DOI: 10.1016/j.biombioe.2013.07.013
- Liu, L., Huang, Y., Cao, J., Liu, C., Dong, L., Xu, L., & Zha, J. (2018). Experimental study of biomass gasification with oxygen-enriched air in fluidized bed gasifier. *Science of The Total Environment*, 626, 423-433. <https://doi.org/10.1016/j.scitotenv.2018.01.016>
- Marcantonio, V.; Monarca, D.; Villarini, M.; Di Carlo, A.; Del Zotto, L.; Bocci, E (2020). Biomass Steam Gasification, High-Temperature Gas Cleaning, and SOFC Model: A Parametric Analysis. *Energies* , 13, 5936 doi.org/10.3390/en13225936
- Molino A, Larocca V, Chianese S, Musmarra D. Biofuels Production by Biomass Gasification: A Review. *Energies*. 2018; 11(4):811. <https://doi.org/10.3390/en11040811>
- Pongratz, G., Subotić, V., Schroettner, H. et al. (2021) Investigation of solid oxide fuel cell operation with synthetic biomass gasification product gases as a basis for enhancing its performance. *Biomass Conv. Bioref.* 11, 121–139 doi.org/10.1007/s13399-020-00726-w
- Sikarwar V.S., Zhao M., Paul S. Fennell P.S., Anthony E., (2017). Progress in biofuel production from gasification. *Progress in Energy and Combustion Science* 61, 189-248. <https://doi.org/10.1016/j.pecs.2017.04.001>
- Vreugdenhil B.J., Zwart R.W.R. (2009). Tar formation in pyrolysis and gasification. ECN-E-08-087 <https://publicaties.ecn.nl/PdfFetch.aspx?nr=ECN-E-08-087>
- Xue-Yu Ren, Xiao-Bo Feng, Jing-Pei Cao, Wen Tang, Zhi-Hao Wang, Zhen Yang, Jing-Ping Zhao, Li-Yun Zhang, Yan-Jun Wang, and Xiao-Yan Zhao. (2020) Catalytic Conversion of Coal and Biomass Volatiles: A Review. *Energy & Fuels* 34 (9), 10307-10363. <https://doi.org/10.1021/acs.energyfuels.0c01432>

ANTIMONY AND VANADIUM IN INCINERATION BOTTOM ASH – LEACHING BEHAVIOR AND CONCLUSIONS FOR TREATMENT PROCESSES

Franz-Georg Simon *, Christian Vogel and Ute Kalbe

Division 4.3 Contaminant Transfer and Environmental Technologies, Bundesanstalt für Materialforschung und -prüfung (BAM), 12200 Berlin, Germany

Article Info:

Received:
18 February 2021
Revised:
1 June 2021
Accepted:
16 June 2021
Available online:
11 September 2021

Keywords:

Incineration bottom ash
Leaching behavior
Lysimeter
Secondary building material

ABSTRACT

Due to its large mineral fraction, incineration bottom ash (IBA) from municipal solid waste incineration is an interesting raw material that can be used for road construction or to produce secondary building materials. However, leaching chloride, sulfate, and potentially harmful heavy metals may cause problems in using IBA in civil engineering. Investigating leaching behavior is crucial for the assessment of the environmental compatibility of IBA applications. Various test procedures are available for that purpose. In the present study, a long-term leaching test of a wet-mechanically treated IBA was performed in a lysimeter for almost six years. While concentrations of chloride, sulfate and the majority of the heavy metals started to decrease rapidly with progressive liquid-to-solid ratio (L/S), antimony (Sb) and vanadium (V) behaved differently. At the beginning of the lysimeter test, the Sb and V concentrations were low, but after approximately one year of operation at an L/S ratio of around 0.8 L/kg, a steady increase was observed. It was shown that this increase is the result of low Ca concentrations due to the formation of CaCO_3 . With the data, the solubility products from Ca-antimonate and Ca-vanadate were calculated. The unusual leaching behavior of Sb and V should be kept in mind when considering field scenarios and evaluating the impact on the environment.

1. INTRODUCTION

Around 26 million metric tons of combustible waste were incinerated per year in Germany in 100 thermal waste treatment plants (66 of which are municipal solid waste incineration plants) (BDE et al., 2018). According to information from the German Association of Thermal Waste Treatment (Interessengemeinschaft Thermische Abfallbehandlung, ITAD) (ITAD, 2019), around 5.7 million tons of incineration bottom ash (IBA) from municipal solid waste incinerators were generated in Germany in 2017. In the course of processing bottom ash, 382,000 tons of iron (Fe) and 95,000 tons of non-ferrous metals (NFe) were separated annually in accordance with state of the art techniques (Verein Deutscher Ingenieure, 2014). Due to the mostly applied wet extraction out of the furnace chamber, these metals are often integrated in a heterogeneous and unstable matrix (Šyc et al., 2020). In general, the recovery of elemental metals is still a challenge in terms of recovery rate and purity.

The vast majority of IBA is made up of the mineral fraction (90%), in which the metals with a high affinity for

oxygen (calcium, aluminum, magnesium, etc.) are bound in oxidic form in the bottom ash and cannot be recovered economically in elemental form. In terms of their composition, however, these oxides are similar to raw materials that can be used to produce secondary building materials (Bayuseno & Schmahl, 2010; Bunge, 2018). Large quantities of the mineral fraction are reused for sub-base material in road construction (Di Gianfilippo et al., 2018; Hyks & Šyc, 2019). A three-month ageing period has been established as the common practice for further treatment of bottom ash before reuse applications. In the course of this ageing, the pH value of bottom ash decreases, and contaminants are immobilized by processes like carbonation, hydration, and oxidation. In particular, the leaching of heavy metals is reduced to environmentally acceptable levels as required for disposal of IBA on landfills (Simon et al., 1995). However, leaching chloride, sulfate, and potentially harmful heavy metals may cause problems in using IBA in civil engineering. The legal requirements for using IBA in Europe are described in detail elsewhere (Blasenbauer et al., 2020). Some countries have set limit values for the total content measured after acidic digestion and/or limit values for elu-



ate concentrations. To assess leaching behavior, a number of test methods are statutory, so that for a comparison, the limit values for concentrations in mg/L have to be converted to leached content E in mg/kg by multiplying by the respective liquid-to-solid ratio (L/S in L/kg), commonly 2 L/kg or 10 L/kg.

Leaching tests can be performed as batch tests (e.g. according DIN EN 12457-2 (EN 12457-2, 2002-09) with an L/S of 10 L/kg) or as column tests (e.g. according to DIN 19528 (DIN 19528, 2009-01) up to an L/S ratio of 4 L/kg for basic characterization or an L/S ratio of 2 L/kg for the column test in the compliance test option in Germany). In batch tests, the concentrations in the eluate are analyzed after a fixed agitation period (usually 24 h), whereas in column tests the eluate is generated continuously over the complete test duration. Concentrations can be determined for individual L/S ratios. DIN 19528 prescribes the L/S ratios 0.3, 1.0, 2.0, and 4.0 L/kg. Rather than in batch tests, the dynamic behavior of leaching can be assessed by column tests (Grathwohl & Susset, 2009). However, column tests are more time-consuming. Information on long-term leaching behavior can be gained from lysimeter experiments, which take even more time (Krüger et al., 2012). However, lysimeter tests are better for simulating field scenarios and long-term leaching behavior than laboratory column tests, particularly due to the unsaturated conditions and realistic contact time with the leachant (Krüger et al., 2012; López Meza et al., 2010).

Previously, it has been shown that the elements antimony (Sb) and vanadium (V) exhibit unusual leaching behavior in leaching tests (Cornelis et al., 2006, 2012). Total contents of IBA are reported with an average of 73 mg/kg (range from 18-250 mg/kg) for Sb and 41 mg/kg (19-248 mg/kg) for V, respectively (Hjelmar et al., 2013). The source for Sb is very likely plastic in municipal solid waste, in which it is used as a flame-retardant agent or catalyst (Okkenhaug et al., 2015). In addition, Sb is a critical element, because released toxic Sb(V) from secondary construction materials can sorb onto inorganic oxides and organic matter in soils (Diquattro et al., 2021) which may affect environmental health by ecotoxic effects and bioaccessibility (Bagherifam et al., 2021). Therefore, to analyze the long-term leaching behavior of Sb and V we performed a lysimeter experiment with treated IBA which was performed for almost 6 years up to an L/S ratio of 4.1 L/kg.

2. MATERIALS AND METHODS

The IBA material for the experiments was sampled on November 5, 2013 at a municipal solid waste incineration (MSWI) bottom ash treatment plant in Germany. Fe and NFe metals had already been removed by standard methods (magnetic and eddy current separation). A wet-mechanical process step was implemented in the plant to remove the finest fraction below 0.25 mm, amounting to approximately 10% (Holm & Simon, 2017). This finest fraction contained around 60% of the initial sulfate (Kalbe & Simon, 2020) and is usually landfilled. Two mineral fractions (0.25-4 mm and 4-60 mm) were generated by different sieving steps. The mineral fractions from 0.25-4 mm and from 4-60 mm were

sampled, air-dried, and homogenized separately. Material larger than 45 mm was removed from the 4-60 mm fraction by sieving. Representative subsamples of both fractions were generated by partitioning the sample and then a mixed sample at a ratio of 40:60 (0.25-4 mm:4-45 mm) was assembled to the final 0.25/45 mm test material employed for the leaching experiments reported here. This condition was expected as the status on an intermittent storage site before reuse of such material.

Two laboratory scale lysimeters (30 cm in diameter) were operated with approximately 60 kg IBA each from March 2014 until February 2020 to investigate the long-term leaching behavior of a 0.25/45-mm mineral material obtained by using a wet processing technology to treating IBA directly after incineration. The resulting bulk density of the sample in the lysimeters was 1.46 g/cm³; the corresponding porosity was 45%; and one pore volume amounted to 18.4 L. Artificial rainwater was used as leachant (pH ≈ 6, constituents NO₃⁻, Cl⁻, SO₄²⁻, Na⁺, K⁺, Ca²⁺, Mg²⁺) (Sanusi et al., 1996). The lysimeters were irrigated in proportion to an average annual precipitation rate of 600 mm/a, leading to a liquid to solid ratio (L/S) of about 0.7 L/kg per year of operation. The L/S ratios of the two lysimeter experiments finally reached after almost six years were 4.17 (lysimeter 1) and 4.09 (lysimeter 2) L/kg, respectively. The lysimeters were then dismantled and the remaining material analyzed for their main constituents.

Eluates were aliquoted after sampling. For chemical analysis, one aliquot was preserved using concentrated nitric acid (DIN EN ISO 5667-3, 2013-03) to measure cations, and one aliquot remained untreated for anion analysis. The eluates were stored at 4° C until measurement. pH values were measured with a Schott CG 841 pH-meter equipped with a WTW SenTix 41 pH electrode (DIN ISO 10390, 2005-12), the electric conductivity with a WTW LF 437 microprocessor conductivity meter (DIN ISO 11265, 1997-06), and turbidity with a HACH 2100N turbidity meter (DIN EN ISO 7027, 2016-11).

Cations (Al, As, Ba, Ca, Cd, Co, Cr, Cu, Fe, Hg, K, Mg, Mn, Mo, Na, Ni, Pb, Sb, Sn, Sr, V, Zn, Se) were quantified using an iCAP 7000 ICP-OES equipped with an ASX-260 Autosampler (Thermo Scientific, Dreieich, Germany) in accordance with (DIN EN ISO 11885, 2009-09). ICP-MS measurements were performed on 10-fold dilutions with an iCAP Q (Thermo Scientific, Dreieich) in accordance with (DIN EN ISO 17294-2, 2017-01) for elements below the detection limit of the ICP-OES. Results for the elements not reported in this work can be found elsewhere (Kalbe & Simon, 2020).

Anions (Cl⁻, SO₄²⁻) were determined with the Dionex IC320 ion chromatograph with the AS 40 Autosampler, ASRS 300 suppressor, AS-9-HC separation column with column oven, and a conductivity detector in accordance with DIN EN ISO 10304 (DIN EN ISO 10304-1, 2009-07). The separation was isocratic with a mixture of carbonate/bicarbonate in aqueous solution (8 mmol/L / 1 mmol/L) as eluent.

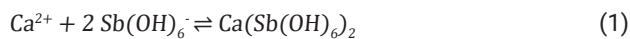
3. RESULTS

It is known that the leaching behavior of IBA strongly depends on the pH (Chandler et al., 1997). Leaching tests

with unaged IBA result in pH values above 12, due to the $\text{Ca}(\text{OH})_2$ content. At high pH values, various heavy metals exist in a soluble form, e.g. $\text{Pb}(\text{OH})_4^{2-}$, so that leaching limits even for landfilling may be exceeded (Simon et al., 1995). During the required ageing period of three months, $\text{Ca}(\text{OH})_2$ reacts with CO_2 from the air and rain to form CaCO_3 , leading to lower pH values and usually lower heavy metal release (Schnabel et al., 2021), e.g. Pb forms sparingly soluble PbCO_3 or $\text{Pb}(\text{OH})_2$. This is in agreement with our study. The observed pH values did not change significantly during the lysimeter tests and were 9.9 ± 0.5 . Furthermore, for the applied wet processed IBA material tested in this study, the chloride and sulfate leaching in the lysimeters was reduced (see Fig. 1a). The sulfate release kept almost constant up to an L/S of about 0.7 L/kg, limited by CaSO_4 solubility, then dropped to around 500 mg/L (L/S 1.25 to 3.25 L/kg), and finally decreased to approximately 250 mg/L. The chloride concentration dropped quickly, starting at 7300 mg/L, and later (from L/S = 1.5 L/kg) remained at an almost constant level of 50 mg/L, which was significantly higher than the chloride concentration in the artificial rainwater used as leachant. Overall, 2×140 single concentrations c_i measured (with i the individual volume of the collected eluates) for chloride are displayed in Figure 1a. Multiplication by the respective L/S ratio gives the leached content E_i in mg/kg, from which the cumulative release U (with $U = \sum E_i$, also in mg/kg) can be calculated. The cumulative release of chloride is displayed in Figure 1b.

A similar behavior is observed for calcium (Ca, see Figure 1c) and most of the heavy metals. In contrast, the behavior of Sb and V differ from the usual decrease of concentrations c_i as a function of L/S ratio. At the beginning of the lysimeter tests, the Sb concentrations were low, but at an L/S of around 0.8 L/kg, a steady increase was observed up to concentrations above $25 \mu\text{g/L}$ (see Figure 1d). Similarly, V started with values of c_i below $10 \mu\text{g/L}$ and reached values above $90 \mu\text{g/L}$ at higher L/S ratios (data not illustrated).

This phenomenon has already been observed by other researchers (Cornelis et al., 2006, 2012; Johnson et al., 1999). Antimony forms sparingly soluble calcium antimonate see equation (1).



The solubility product K_L of Sb-antimonate is a constant defined as

$$K_L = [\text{Ca}^{2+}]^m [\text{Sb}(\text{OH})_6^-]^2 \quad (2)$$

with m as an exponent for the Ca / Sb ratio.

The solubility product K_L is a constant that describes the solubility behavior of a sparingly soluble compound: if the concentration of one component drops, the concentration of the other component increases accordingly. This means that decreasing Ca concentrations as a result of the ageing process (formation of limestone, CaCO_3) lead to increasing Sb concentrations. The fact that there is a connection between the concentrations of Ca and Sb becomes apparent when the concentrations are plotted against each other (Figure 2 left). The same applies for vanadium (see Figure 2 right).

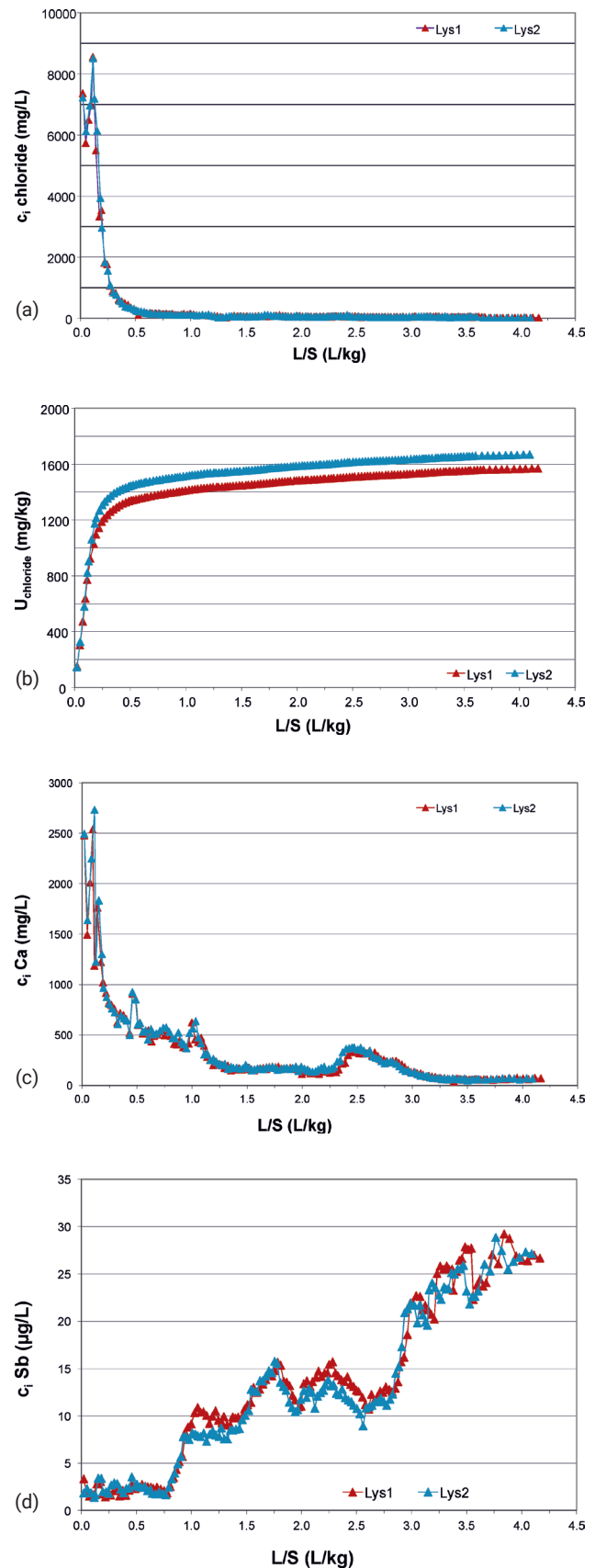


FIGURE 1: Results from the long-term lysimeter experiment as a function of L/S. a: Concentrations c_i of chloride. b: Cumulative release U of chloride. c: Concentrations c_i of calcium. d: Concentrations c_i of antimony.



$$K_L = [\text{Ca}^{2+}][\text{V}_2\text{O}_6^{2-}] \quad (4)$$

The experimental data (circles in Figure 2) were fitted with the solver module in MS Excel (EA, evolutionary algorithm). The best match was achieved in the case of Sb with $K_L = 8.9 \times 10^{-19} \text{ mol}^{3.7} \text{ L}^{-3.7}$ and $m = 1.7$. This leads to $\text{Ca}(\text{Sb}(\text{OH})_6)_2 \times \text{Ca}_{0.7}(\text{OH})_{1.4}$ as a chemical formula for Ca antimonate in IBA. Fitting the results for V gave $K_L = 1.9 \times 10^{-9} \text{ mol}^2 \text{ L}^{-2}$.

The standard leaching tests mobilize usually only small amounts of the complete reservoir of certain substances in IBA. Exceptions are substances with high solubility, such as alkaline metal compounds and chloride. Even the solubility of CaSO_4 at 2 g/L is high enough that a substantial amount is leached. During the whole duration of the experiment, 1600 mg/kg of chloride and 3000 mg/kg of sulfate were cumulatively released from the IBA in the lysimeters. However, it has to be considered that sulfate and chloride were constituents of the artificial rain (Sanusi et al., 1996) that was used as leachant. Nevertheless, after dismantling the lysimeters, the total content of sulfate and chloride found in the remaining material dropped from 13,400 to 10,400 and from 2,840 to 390 mg/kg, respectively.

4. DISCUSSION

As stated above, IBA is an inhomogeneous mixture of mineral phases and metals not suitable for recycling without processing. The concentrations especially of trace metals can vary by one order of magnitude. However, the described leaching mechanisms, e.g. pH dependence of Pb leaching or Sb mobilization as function of Ca concentration, are largely independent of waste composition, type of furnace or location of the incinerator (Hjelmar et al., 2013). The findings here are therefore relevant not only for the IBA from the sampled plant in Germany but also in general for IBA.

The separation of elemental metals is simple and can be carried out using magnets (Fe metals) and eddy current separators (NFe metals). In Germany, an average of 6.6% Fe and 2.0% non-ferrous metals are extracted from IBA (Gleis & Simon, 2016). The potential would be even greater (Kuchta & Enzner, 2015) if the separation of NFe metals

was extended to small grain sizes. Recovering the mineral fraction, which accounts for about 90%, is much more difficult. Applications exist primarily as an unbound base layer in road construction, see for example (Hyks & Hjelmar, 2018).

Numerous contaminants could be minimized with improved processing technologies. Wet treatment means that easily soluble substances such as chlorides are transferred to the washing water. The simultaneous separation of a fine fraction <0.25 mm reduces the sulfate content, mainly calcium sulfate, by more than 60% (Holm & Simon, 2017; Kalbe & Simon, 2020). Broken glass can be separated using sensor-based methods (Šyc et al., 2018). Heavy metal compounds have a higher specific density than other minerals in the bottom ash, so that a reduction of the content of heavy metal compounds is possible by density sorting (Holm et al., 2018).

According to the final draft of the German Ordinance on Secondary Building Materials (Bundesrat, 2020), new regulations are planned for reusing IBA. Accordingly, two quality classes are going to be introduced for IBA (abbreviated HMVA-1 and HMVA-2). To use the mineral fractions of IBA e.g. in road construction, at least class HMVA-2 must be achieved with maximum concentrations in the eluate of $L/S = 2 \text{ L/kg}$, as displayed in Table 1.

To compare the results of the experiment (Exp. Data, Table 1) with the limit values (HMVA-1 and HMVA-2, Table 1), the data for cumulative release U must be divided by the respective L/S ratio. The calculated concentrations (see Table 1, right column) comply with the limit values for HMVA-2; however, the concentration of Mo is close to the limit. It is known that Mo is leached as oxyanion MoO_4^{2-} already at low L/S ratios and preferably at pH values above 8 (Dijkstra et al., 2006; van der Sloot et al., 2001). Mobilization of Mo in standard leaching tests is between 1 and 5%, which is much higher than for other heavy metals (e.g. $\text{Cu} < 0.01\%$) (Kalbe & Simon, 2020).

5. CONCLUSIONS

Unlike most leached substances, which decrease as a function of the L/S ratio, the leaching values for Sb and

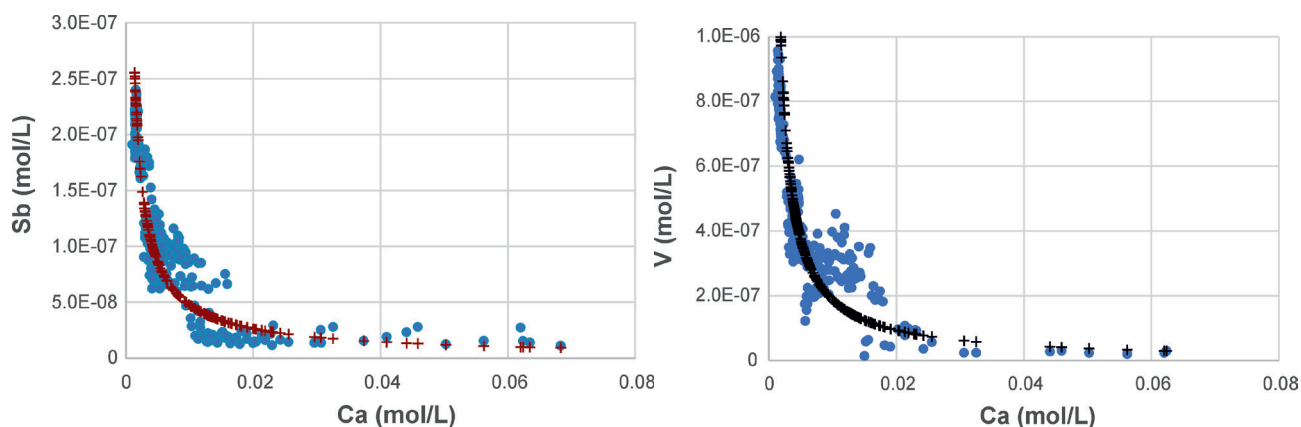


FIGURE 2: Concentration of Sb (left) and V (right) in the lysimeter experiment as a function of Ca concentration (circles). The crosses are the result of a fit with MS Excel.

TABLE 1: Requirements for IBA according to the German Ordinance on Secondary Building Materials (leaching test DIN 19528, L/S = 2 L/kg; classes HMVA-1 and HMVA-2) compared with the calculated concentration from the lysimeter experiment (Exp. Data - average of lysimeter 1 and 2).

Parameter	Dimension	HMVA-1	HMVA-2	Exp. data
pH value		7 - 13	7 - 13	
Electrical conductivity	µS/cm	2,000	12,500	
Chloride	mg/L	160	5,000	768
Sulfate	mg/L	820	3,000	1,110
Antimony	µg/L	10	60	7.1
Chromium (total)	µg/L	150	460 *	25.0
Copper	µg/L	110	1,000 *	152.1
Molybdenum	µg/L	55	400	388.0
Vanadium	µg/L	55	150	31.1

* for certain applications Cu ≤ 230 µg/L, Cr (total) ≤ 110 µg/L

V increased over time in the long-term lysimeter experiment. These different behaviors are shown exemplarily in Figure 3 for Ca, Cu, Sb, and V. The concentrations of Ca and Cu drop considerably during the lysimeter experiment, i.e., with the advancing ageing process with increasing L/S in the lysimeter experiment. At an early sampling time (t1) directly after combustion or after processing without ageing, heavy metal concentrations in the leachate may be still too high. However, Sb and V should initially not exceed any limit values for processed IBA. At a later point in time (t2), heavy metals like Cu are still present in the material but are immobilized. At this point, Sb and V may already be released and are approaching the limit values (see Table 1). Our experiment shows that the release of Sb and V from the IBA is not minimized over the time of almost six years. Thus, the long-term use of IBA in e.g. secondary building materials can pose a potential risk for the environment.

The release of Sb and V is dependent on the availability of Ca, which is increasingly precipitated during the ageing process as sparingly soluble CaCO₃. On one hand, this

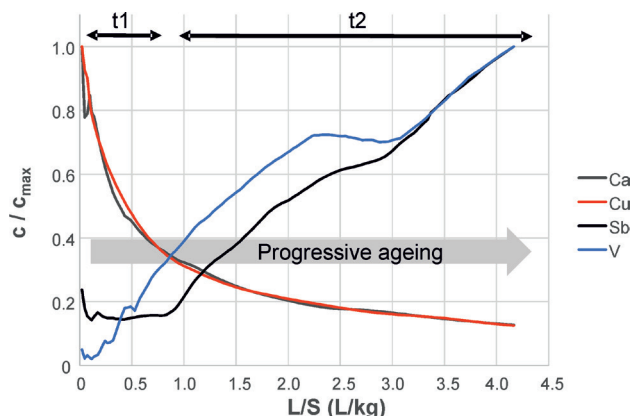


FIGURE 3: Concentrations of Ca, Cu, Sb, and V as a function of L/S. Assessment at the end of period t1 would allow use of the treated IBA, whereas in period t2 the concentration of Sb and V might exceed the limit values.

effect is desired, because pH values decrease to values below 11, leading to immobilization of most heavy metal compounds. On the other hand, decreasing Ca concentrations lead to the dissolution of Ca-antimonates and Ca-vanadates. Here, the availability of Ca²⁺ is decisive. Mobilized Sb and V can possibly be sorbed on ferrous minerals or form sparingly soluble Fe-antimonates or Fe-vanadates (Van Caneghem et al., 2016). Economically viable technical measures for the targeted depletion of Sb and V have not been reported yet. The limit values for class HMVA-1 are not reachable even for wet-treated IBA as used as test material in the investigation presented here. Chloride concentrations as low as 160 mg/L (see Table 1) might be achievable for separated fractions from IBA, e.g. after dry extraction of bottom ash in the waste incineration plant (Bürgin et al., 1995). Here, a more inert coarse fraction above 2 or 4 mm can be easily separated by sieving (Simon & Andersson, 1995; Šyc et al., 2020). However, wet treatment alone already provides a significant improvement of quality regarding the environmental compatibility in the use scenario.

ACKNOWLEDGEMENTS

Part of the work was funded with the Central Innovation Programme for SMEs (ZIM) of the German Federal Ministry for Economic Affairs and Energy (HORECA, KF 2201051MF2).

REFERENCES

- Bagherifam, S., Brown, T. C., Wijayawardena, A., & Naidu, R. (2021). The influence of different antimony (Sb) compounds and ageing on bioavailability and fractionation of antimony in two dissimilar soils. *Environmental Pollution*, 270, 116270. doi: <https://doi.org/10.1016/j.envpol.2020.116270>
- Bayuseno, A. P., & Schmahl, W. W. (2010). Understanding the chemical and mineralogical properties of the inorganic portion of MSWI bottom ash. *Waste Manage.*, 30(8–9), 1509-1520. doi: 10.1016/j.wasman.2010.03.010
- BDE, BDSV, bvse, ITAD, PlasticsEurope, VDM, VDMA, VCI, & VKU. (2018). Statusbericht der deutschen Kreislaufwirtschaft, Einblicke und Aussichten (Status report of the German circular economy, insights and prospects).
- Blasenbauer, D., Huber, F., Lederer, J., Quina, M. J., Blanc-Biscarat, D., Bogush, A., Bontempi, E., Blondeau, J., Chimenos, J. M., Dahlbo, H., Fagerqvist, J., Giro-Paloma, J., Hjelm, O., Hyks, J., Keane, J., Lupsea-Toader, M., O'Caollai, C. J., Orupöld, K., Paják, T., Simon, F.-G., Svecova, L., Šyc, M., Ulvang, R., Vaajasaari, K., van Caneghem, J., van Zomeren, A., Vasarevičius, S., Wégner, K., & Fellner, J. (2020). Legal situation and current practice of waste incineration bottom ash utilisation in Europe. *Waste Manage.*, 102, 868-883. doi: 10.1016/j.wasman.2019.11.031
- Bundesrat. (2020). Verordnung zur Einführung einer Ersatzbaustoffverordnung (Ordinance on secondary building materials). Decision of the Federal Council 587/20
- Bunge, R. (2018). Recovery of Metals from Waste Incineration Bottom Ash. In: O. Holm & E. Thome-Kozmiensky (eds.), *Removal, Treatment and Utilisation of Waste Incineration Bottom Ash* (pp. 63-143). Neuruppin: TK Verlag.
- Bürgin, M., Schmidt, V., & Simon, F. G. (1995). Method for recovering valuable materials from refuse incineration slag. Patent application EP 0 691 160 A1, Den Haag: European Patent Office
- Chandler, A. J., Eighmy, T. T., Hartlen, J., Hjelm, O., Kosson, D. S., Sawell, S. E., van der Sloot, H. A., & Vehlou, J. (eds.). (1997). *Municipal solid waste incineration residues: An international perspective on characterisation and management of residues from municipal solid waste incineration* (Vol. 67). Amsterdam: Elsevier.

- Cornelis, G., Van Gerven, T., & Vandecasteele, C. (2006). Antimony leaching from uncarbonated and carbonated MSWI bottom ash. *J. Haz. Mat.*, 137(3), 1284-1292. doi: <https://doi.org/10.1016/j.jhazmat.2006.04.048>
- Cornelis, G., Van Gerven, T., & Vandecasteele, C. (2012). Antimony leaching from MSWI bottom ash: Modelling of the effect of pH and carbonation. *Waste Manage.*, 32(2), 278-286. doi: <https://doi.org/10.1016/j.wasman.2011.09.018>
- Di Gianfilippo, M., Hyks, J., Verginelli, I., Costa, G., Hjelmar, O., & Lombardi, F. (2018). Leaching behaviour of incineration bottom ash in a reuse scenario: 12years-field data vs. lab test results. *Waste Manage.*, 73, 367-380. doi: <https://doi.org/10.1016/j.wasman.2017.08.013>
- Dijkstra, J. J., van der Sloot, H. A., & Comans, R. N. J. (2006). The leaching of major and trace elements from MSWI bottom ash as a function of pH and time. *Appl. Geochem.*, 21, 335-351. doi: <https://doi.org/10.1016/j.apgeochem.2005.11.003>
- DIN 19528: 2009-01. Elution von Feststoffen - Perkulationsverfahren zur gemeinsamen Untersuchung des Elutionsverhaltens von organischen und anorganischen Stoffen für Materialien mit einer Korngröße bis 32 mm - Grundlegende Charakterisierung mit einem ausführlichen Säulenversuch und Übereinstimmungsuntersuchung mit einem Säulenschnelltest (Leaching of solid materials - Percolation method for the joint examination of the leaching behaviour of organic and inorganic substances for materials with a particle size upto 32 mm - Basic characterization using a comprehensive column test and compliance test using a quick column test). Berlin: German Institute for Standardization.
- DIN EN ISO 5667-3: 2013-03. Wasserbeschaffenheit - Probenahme - Teil 3: Anleitung zur Konservierung und Handhabung von Wasserproben. (Water quality - Sampling - Part 3: Guidance on the preservation and handling of water samples). Berlin: German Institute for Standardization.
- DIN EN ISO 7027. (2016-11). Wasserbeschaffenheit - Bestimmung der Trübung. In: *Water quality - Determination of turbidity (ISO 7027:1999)*. Berlin: German Institute for Standardization.
- DIN EN ISO 10304-1: 2009-07. Wasserbeschaffenheit - Bestimmung von gelösten Anionen mittels Flüssigkeits-Ionenchromatographie - Teil 1: Bestimmung von Bromid, Chlorid, Fluorid, Nitrat, Nitrit, Phosphat und Sulfat. (Water quality - Determination of dissolved anions by liquid chromatography of ions - Part 1: Determination of bromide, chloride, fluoride, nitrate, nitrite, phosphate and sulfate). Berlin: German Institute for Standardization.
- DIN EN ISO 11885. (2009-09). Wasserbeschaffenheit - Bestimmung von ausgewählten Elementen durch induktiv gekoppelte Plasma-Atom-Emissionsspektrometrie (ICP-OES). In: *Water quality - Determination of selected elements by inductively coupled plasma optical emission spectroscopy (ICP-OES)*. Berlin: German Institute for Standardization.
- DIN EN ISO 17294-2: 2017-01. Wasserbeschaffenheit - Anwendung der induktiv gekoppelten Plasma-Massenspektrometrie (ICP-MS) - Teil 2: Bestimmung von ausgewählten Elementen einschließlich Uranisotope (Water quality - Application of inductively coupled plasma mass spectrometry (ICP-MS) - Part 2: Determination of selected elements including uranium isotopes). Berlin: German Institute for Standardization.
- DIN ISO 10390: 2005-12. Bodenbeschaffenheit - Bestimmung des pH-Wertes. (Soil quality - Determination of pH (ISO 10390:2005)). Berlin: German Institute for Standardization.
- DIN ISO 11265. (1997-06). Bodenbeschaffenheit - Bestimmung der spezifischen elektrischen Leitfähigkeit In: *Soil quality - Determination of the specific electrical conductivity* Berlin: German Institute for Standardization.
- Diquattro, S., Castaldi, P., Ritch, S., Juhasz, A. L., Brunetti, G., Scheckel, K. G., Garau, G., & Lombi, E. (2021). Insights into the fate of antimony (Sb) in contaminated soils: ageing influence on Sb mobility, bioavailability, bioaccessibility and speciation. *Science of The Total Environment*, 145354. doi: <https://doi.org/10.1016/j.scitotenv.2021.145354>
- EN 12457-2: 2002-09. Characterization of waste - Leaching; Compliance test for leaching of granular and sludges - Part 2: One stage batch test at a liquid to solid ratio of 10 l/kg with particle size below 4 mm (without or with size reduction). Brussels: CEN European Committee for Standardisation.
- Gleis, M., & Simon, F. G. (2016). Novellierung des BVT-Merkblattes Abfallverbrennung – Sachstand, Entwicklungstendenzen und neue Verfahren zur Aufbereitung von Rostaschen und Filterstäuben. In: K. J. Thomé-Kozmiensky (ed.), *Mineralische Nebenprodukte und Abfälle 3 - Aschen, Schlacken, Stäube und Baurestmassen* (Vol. 3, pp. 163-172). Neuruppin: TK Verlag Karl Thomé-Kozmiensky.
- Grathwohl, P., & Susset, B. (2009). Comparison of percolation to batch and sequential leaching tests: Theory and data. *Waste Manage.*, 29(10), 2681-2688. doi: [10.1016/j.wasman.2009.05.016](https://doi.org/10.1016/j.wasman.2009.05.016)
- Hjelmar, O., van der Sloot, H. A., & van Zomeren, A. (2013). Hazard property classification of high temperature waste materials. Paper presented at the Fourteenth International Waste Management and Landfill Symposium, Sardinia, 2013, S. Margherita di Pula, Italy.
- Holm, O., & Simon, F. G. (2017). Innovative treatment trains of bottom ash (BA) from municipal solid waste incineration (MSWI) in Germany. *Waste Manage.*, 59, 229-236. doi: [10.1016/j.wasman.2016.09.004](https://doi.org/10.1016/j.wasman.2016.09.004)
- Holm, O., Wollik, E., & Bley, T. J. (2018). Recovery of copper from small grain size fractions of municipal solid waste incineration bottom ash by means of density separation. *Int. J. Sust. Eng.*, 11(4), 250-260. doi: [10.1080/19397038.2017.1355415](https://doi.org/10.1080/19397038.2017.1355415)
- Hyks, J., & Hjelmar, O. (2018). Utilisation of Incineration Bottom Ash (IBA) from Waste Incineration - Prospects and Limits. In: O. Holm & E. Thome-Kozmiensky (eds.), *Removal, Treatment and Utilisation of Waste Incineration Bottom Ash* (pp. 11-24). Neuruppin: TK Verlag.
- Hyks, J., & Šyc, M. (2019). Utilisation of Incineration Bottom Ash in Road Construction. In: S. Thiel, E. Thomé-Kozmiensky, F. Winter, & D. Juchelkova (eds.), *Waste Mangement, Vol. 9, Waste-to-Energy* (pp. 731- 741). Nietwerder: TK-Verlag.
- ITAD. (2019). Jahresbericht 2019 (Annual report 2019) <https://www.itad.de/service/downloads/itad-jahresbericht-2019-webformat.pdf>, Düsseldorf: ITAD – Interessengemeinschaft der Thermischen Abfallbehandlungsanlagen in Deutschland e.V
- Johnson, C. A., Kaeppeli, M., Brandenberger, S., Ulrich, A., & Baumann, W. (1999). Hydrological and geochemical factors affecting leachate composition in municipal solid waste incinerator bottom ash: Part II. The geochemistry of leachate from Landfill Lostorf, Switzerland. *J. Contam. Hydrol.*, 40(3), 239-259. doi: [https://doi.org/10.1016/S0169-7722\(99\)00052-2](https://doi.org/10.1016/S0169-7722(99)00052-2)
- Kalbe, U., & Simon, F.-G. (2020). Potential Use of Incineration Bottom Ash in Construction: Evaluation of the Environmental Impact. *Waste and Biomass Valorization*, 11(12), 7055–7065. doi: [10.1007/s12649-020-01086-2](https://doi.org/10.1007/s12649-020-01086-2)
- Krüger, O., Kalbe, U., Berger, W., Simon, F. G., & López Meza, S. (2012). Leaching Experiments on the Release of Heavy Metals and PAH from Soil and Waste Materials. *J. Hazard. Mater.*, 207-208, 51-55. doi: <https://doi.org/10.1016/j.jhazmat.2011.02.016>
- Kuchta, K., & Enzner, V. (2015). Ressourceneffizienz der Metallrückgewinnung vor und nach der Verbrennung. In: K. J. Thomé-Kozmiensky (ed.), *Mineralische Nebenprodukte und Abfälle 2* (pp. 105-116). Neuruppin: TK Verlag.
- López Meza, S., Kalbe, U., Berger, W., & Simon, F. G. (2010). Effect of contact time on the release of contaminants from granular waste materials during column leaching experiments. *Waste Manage.*, 30(4), 565-571. doi: <https://doi.org/10.1016/j.wasman.2009.11.022>
- Okkenhaug, G., Almås, Å. R., Morin, N., Halea, S. E., & Arp, H. P. H. (2015). The presence and leachability of antimony in different wastes and waste handling facilities in Norway. *Environ. Sci. Process Impacts*, 17(11), 1880-1891. doi: <https://doi.org/10.1039/C5EM00210A>
- Sanusi, A., Wortham, H., Millet, M., & Mirabel, P. (1996). Chemical composition of rainwater in Eastern France. *Atmos. Environ.*, 30(1), 59-71. doi: [https://doi.org/10.1016/1352-2310\(95\)00237-S](https://doi.org/10.1016/1352-2310(95)00237-S)
- Schnabel, K., Brück, F., Pohl, S., Mansfeldt, T., & Weigand, H. (2021). Technically exploitable mineral carbonation potential of four alkaline waste materials and effects on contaminant mobility. *Greenhouse Gases: Science and Technology*. doi: <https://doi.org/10.1002/ghg.2063>
- Simon, F. G., & Andersson, K. H. (1995). InRec™ process for recovering materials from solid waste incineration residues. *ABB Review*(9), 15-20
- Simon, F. G., Schmidt, V., & Carcer, B. (1995). Alterungsverhalten von MVA-Schlacken. *Müll und Abfall*, 27(11), 759-764

- Šyc, M., Simon, F. G., Biganzoli, L., Grosso, M., & Hyks, J. (2018). Resource Recovery from Incineration Bottom Ash: Basics, Concepts, Principles. In: O. Holm & E. Thome-Kozmiensky (eds.), *Removal, Treatment and Utilisation of Waste Incineration Bottom Ash* (pp. 1-10). Neuruppin: TK Verlag.
- Šyc, M., Simon, F. G., Hyks, J., Braga, R., Biganzoli, L., Costa, G., Funari, V., & Grosso, M. (2020). Metal recovery from incineration bottom ash: state-of-the-art and recent developments. *J. Haz. Mat.*, 393(122433), 1-17. doi: 10.1016/j.jhazmat.2020.122433
- Van Caneghem, J., Verbinnen, B., Cornelis, G., de Wijs, J., Mulder, R., Billen, P., & Vandecasteele, C. (2016). Immobilization of antimony in waste-to-energy bottom ash by addition of calcium and iron containing additives. *Waste Manage.*, 54, 162-168. doi: <https://doi.org/10.1016/j.wasman.2016.05.007>
- van der Sloot, H. A., Kosson, D. S., & Hjelmar, O. (2001). Characteristics, treatment and utilization of residues from municipal waste incineration. *Waste Manage.*, 21, 753-765. doi: 10.1016/S0956-053X(01)00009-5
- Verein Deutscher Ingenieure. (2014). *VDI 3460, Emission Control, Thermal waste treatment, Fundamentals (Part 1)*. Berlin: Beuth Verlag.

PHOSPHATE SLUDGE: OPPORTUNITIES FOR USE AS A FERTILIZER IN DEFICIENT SOILS

Ayoub Haouas ¹, Cherkaoui El Modafar ², Allal Douira ³, Saâd Ibnsouda-Koraichi ⁴, Abdelkarim Filali-Maltouf ⁵, Abdelmajid Moukhli ⁶ and Soumia Amir ^{1,*}

¹ Laboratoire Polyvalent en Recherche et Développement, Faculté Polydisciplinaire, Université Sultan Moulay Slimane, Beni Mellal, Morocco

² Laboratoire d'Agrobiotechnologie et Bioingénierie, Faculté des Sciences et Techniques, Université Cadi Ayyad, Marrakech, Morocco

³ Laboratoire de Botanique Biotechnologie et de Protection des Plantes, Faculté des Sciences, Université Ibn Tofail, Kenitra, Morocco

⁴ Laboratoire de Biotechnologie Microbienne et Molécules Bioactives, Faculté des Sciences et Techniques, Université Sidi Mohamed Ben Abdellah, Fès, Morocco

⁵ Laboratoire de Microbiologie et Biologie Moléculaire, Faculté des Sciences, Université Mohammed V, Rabat, Morocco

⁶ Unité de Recherche d'Amélioration génétique des plantes, Institut national de la Recherche Agronomique, Marrakech, Morocco

Article Info:

Received:
23 July 2020
Revised:
4 May 2021
Accepted:
14 June 2021
Available online:
11 September 2021

Keywords:

Sandy soil
Phosphate
Clay
Agriculture
Circular economy
Nutrients

ABSTRACT

Phosphate sludge (PS) is an industrial by-product produced in huge quantities by the phosphate beneficiation plants in Morocco. In order to valorize this by-product, it was examined for its potential use as a soil fertilizer. The physicochemical properties, elemental and mineral content, morphological structure, and component stability of raw PS were investigated. In addition, pathogenicity, phytotoxicity, and the capacity of PS to promote plant growth in deficient sandy soil have been studied. The obtained results showed that PS was characterized by low values of moisture (2.10%), electrical conductivity (EC) (0.77 mS/cm), and organic matter (OM) (0.61%), with a slightly alkaline pH (8.20). Nevertheless, this material carried interesting content of fertilizing elements such as phosphorus (P₂O₅) of 20.01%, calcium (CaO) of 39.72%, and magnesium (MgO) of 2.33%. Thus, PS did not present any pathogenic or phytotoxic risk with a high increase in tomato plant growth than the control of only soil. In conclusion, the results of this study could provide the primary practical guidance for the PS application in deficient soils characterized by sandy texture.

1. INTRODUCTION

In Africa, the agricultural sector faces environmental challenges that limit its development. Approximately 20% of arable land is currently not cultivable, and a further sharp decline is expected by 2080 (Fao, 2009). In addition, representative soils in Africa are sandy soils characterized by a deficient state of nutrients and low water-holding capacity resulting in low yields (Kihara et al., 2020). Fertilizing sandy soil is a promising solution that has been widely adopted to improve smallholder-farming systems, particularly in developing countries. However, due to the simultaneous increase in demand for phosphate fertilizers and the continuous depletion of phosphate reserves, the focus is today on the opportunities of recovering phosphate ores from secondary sources (i.e., low-grade ore and residues) (Karunanithi et al., 2015).

Morocco, represented by Office Chérifien du Phosphate (OCP), is a worldwide leader in the phosphate-based products industry. Moroccan phosphate ore is processed

through a combination of successive enrichment steps involving crushing, screening, washing and flotation (Khasawneh and Doll, 1979; Boujeljel et al., 2019). The washing and flotation steps generate large quantities of PS, reaching 28 million metric tons in 2010 (Haouas et al., 2021a). PS represents major economic and environmental problems, which by its accumulating induced a loss of recyclable materials, forms dikes, disfigures the landscape and reduces arable lands (Haouas et al., 2020). Until this time, few studies aimed to find appropriate ways for PS valorization, including the production of light aggregates (Loutou et al., 2013), geopolymers (Moukannaa et al., 2018) and composting (Haouas et al., 2021b).

PS as a phosphate rock by-product has the potential to be a sustainable, low cost and permanently available substrate for improving deficient soils, which will open up ways to its integration into the circular economy. Furthermore, the reuse of PS for land application can significantly reduce disposal costs and provide a source of mineral nutrients for many crops (Hakkou et al., 2018; Haouas et al.,

* Corresponding author:
Soumia Amir
email: samiarama@yahoo.fr

2021a). A standardized characterization of PS is required, as is the tracing of the guidelines for its possible use as an amendment (FAO, 2009). Until now, there are no guidelines for the safe use of PS in agriculture. For this reason, the present study had as objectives, (i) the characterization of physicochemical, mineralogical and structural properties of the PS, (ii) the evaluation of its safety in terms of phytotoxic and pathogenic factors, and (iii) the assessment of the fertilizing capacity using agronomic essay in sandy soil.

2. MATERIALS AND METHODS

2.1 Sampling

PS was collected from a deposit area around the phosphate laundry plant managed by OCP, SA in Khouribga City (center of Morocco) (32°44'16.2"N; 6°50'48.2"W), which was produced between 1990 and 2000 (Figure 1a). The total quantity of 10000 Kg of PS samples was taken from different points, and homogeneous subsamples (Figure 1b) were prepared using the quartering method (Atif et al., 2020).

As illustrated in Figure 2, the production chain of PS starts with the arrival of raw phosphate from the exploitation unit to the ore enrichment plants. The phosphate-rich fraction was separated from the gangue minerals by a series of enrichment treatment steps, started by screening through 3.15 mm sieves. The fraction greater than 3.15 mm is considered as sterile, while the particles less than 3.15 mm are divided into three parts of >160 µm, 160 µm-40 µm, and <40 µm during the washing process. The part of <40 µm constitutes the first part of the PS. The part between 3.15 mm and 160 µm is recovered as a concentrated phosphate, and the last part between 160 µm and 40 µm has been further treated by flotation. At this stage, the phosphate particles between 125 µm and 160 µm are separated from the other gangue minerals that make up the second part of the PS. The PS is then deposited on the surrounding lands of the enrichment factories (Haouas et al. 2021b).

2.2 Physicochemical and elemental analysis

The moisture content was determined immediately after sampling in an oven at 105°C for 48 hours. Measurement of pH and the EC was performed on PS fresh sample of 10 g stirred in 100 ml of distilled water using pH meter (PHSJ-3F) and conductivity meter (DDS-12DW) (AFNOR, 2000).

The ash content was calculated after calcination in a muffle furnace at 550°C for 6 hours using the following formula (Amir et al., 2005):

$$\text{Ash (\%)} = 100 - \left(100 \times \frac{W_d - W_c}{W_d}\right) \quad (1)$$

Wd: dry weight and Wc: calcined weight.

Total organic carbon (TOC) was determined by Anne's method (Tallou et al., 2020). This method combined the oxidation of OM with potassium dichromate ($K_2Cr_2O_7$) (0.4 N) in an acidic medium and the back-titration of excess potassium dichromate by Mohr salt ($Fe(NH_4)_2(SO_4)_2 \cdot 6H_2O$) (0.2 N). The OM content was determined by dividing the COT by 1.72 (Amir et al., 2005). The total Kjeldahl nitrogen (TKN) was measured by mineralization in the presence of sulfuric acid (98%) and the Kjeldahl catalyst. The steam distillation transformed the ammonium ions (NH_4^+) into ammonia (NH_3) through the alkaline medium of NaOH (40%). The NH_3 molecules are recovered in boric acid and then dosed by a volumetric acid/base assay (Chen et al., 2010).

Inductively coupled plasma - optical emission spectrometry (ICP-OES, THERMO ICAP 6500 DUO) was used to determine the total and water-soluble fraction of the elements. The anions were analyzed using ion chromatography with a liquid chromatograph (Metrohm, Switzerland). Analysis of the major elements of a finely ground dry sample was performed using an EPSILON 4 energy dispersive X-ray fluorescence spectrometer (EDXRF).

The phosphorus (P) fractionation procedure was performed based on sequential extraction, with a sample: solution ratio of 1:50. Indeed, for soluble P, the sample was treated with a solution of NH_4Cl (1M), NH_4F (5 M at pH 7) for the P bound to aluminum (Al), NaOH (0.1 M) for P

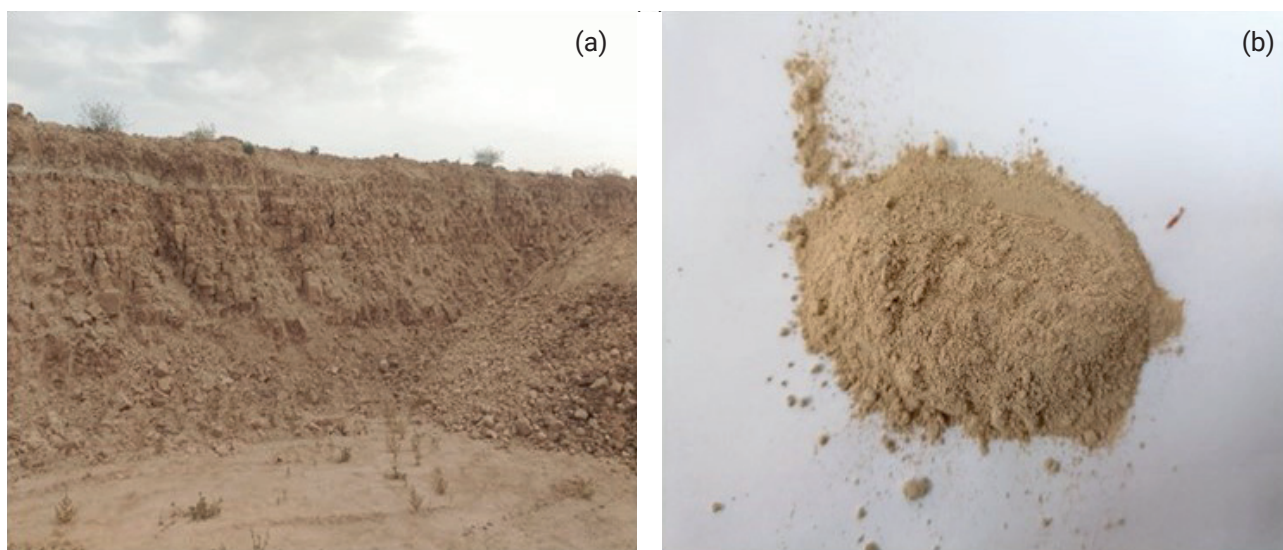


FIGURE 1: a) PS sampling site, b) PS subsample.

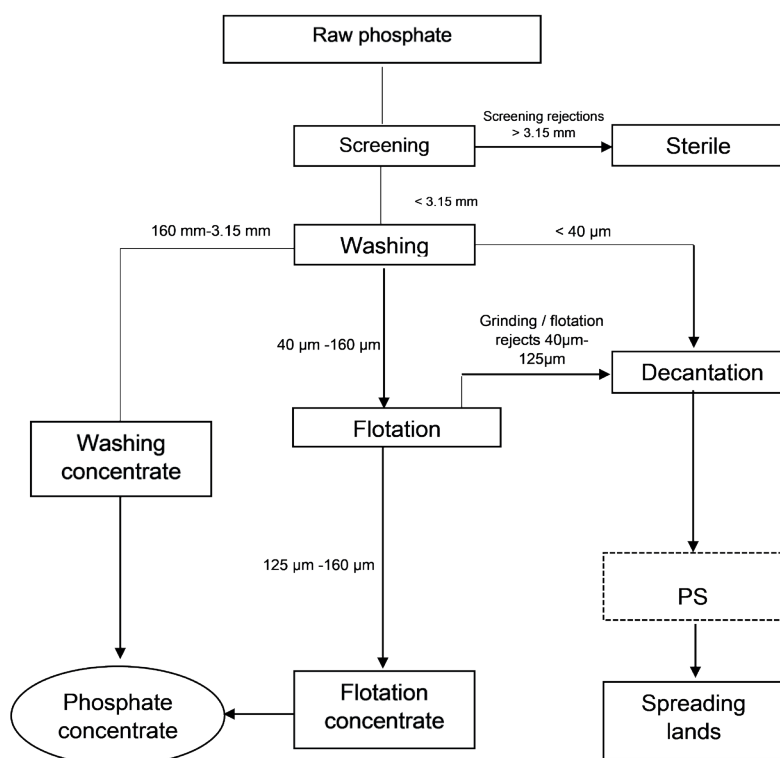


FIGURE 2: PS generation chain during phosphate treatment.

bound to iron (Fe), and finally by H_2SO_4 (0.5 M) for P bound to calcium (Ca), in this order. After each extraction, the supernatant was filtered through 0.2 μm filter paper, and the concentration of P extracted was determined using the molybdenum blue method (Chang and Jackson, 1957). In contrast, organic P was measured according to the Bray and Kurtz method (1945).

2.3 PS characterization

2.3.1 Thermal stability

Thermal stability is an important criterion to consider when studying the stability of organic substrates targeted for agricultural use. Thermogravimetric and differential thermal (TGA/DTA) analyses were performed to investigate the OM stability of PS using a TA instrument (SDT Q600) equipped with platinum crucibles and a heating rate of $10^\circ C/min$ from 25 to $1000^\circ C$ in an oxidizing atmosphere.

2.3.2 Fourier Transform Infrared- FTIR

FTIR spectroscopy (PerkinElmer 1600) was used to determine the functional groups of raw PS and monitor their relative changes during the heating process. For this purpose, a mixture of 1 mg (dry weight) of each sample and 400 mg of potassium bromide (KBr) was prepared as pellets by vacuum compression. Spectra of raw and heated PS samples were obtained after analysis over a range of $400-4000\text{ cm}^{-1}$ at 16 nm/sec .

2.3.3 Mineralogy and structure

Mineral phases of PS were characterized by X-ray diffraction (XRD, Philips X'Pert MPD diffractometer) equipped

with a copper anticathode ($K\alpha\ \frac{1}{4}\ 1.5418\ \text{\AA}$) operating at 40 kV and 40 mA. The analysis was carried out in the interval of angles 2θ between 5° and 70° . The processing of the diffractogram data obtained was carried out using the X'Pert High Score software. The phase indexing is based on comparing 2θ values with the ICSD database (Inorganic Crystal Structure Database). The surface morphology of the PS was observed by scanning electron microscopy (SEM) using Vega 3 Tescan microscope with an acceleration voltage of 20 kV.

2.4 Phytotoxicity evaluation

The germination test was conducted to monitor the phytotoxicity of PS. The PS extract at a concentration of 10% (w/v) was used to moisten 20 seeds of each species of tomato (*Solanum Lycopersicum*) and maize (*Zea mays*). Moistened seeds with PS extract and distilled water (control) have been germinated in Petri dishes in the dark at room temperature ($28^\circ C$) for 72 hours. The germination index (GI) was calculated using the following equation (Luo et al., 2018):

$$GI (\%) = \frac{NGS\ extract \times RL\ extract}{NGS\ water \times RL\ water} \times 100 \quad (2)$$

NGS: Number of Germinated Seeds.

RL: Root Length.

2.5 Enumeration of pathogens

PS sample of 10 g transported from the sampling site in sterile bags at $+4^\circ C$ was stirred in 90 ml of a buffer solution ($0.06\text{ M Na}_2\text{HPO}_4/\text{NaH}_2\text{PO}_4$) (1/9 v/v) at pH 7.6. A series of dilutions (10^{-1} to 10^{-10}) of the sample was made and

aseptically inoculated into the following selective growth media as described by Atif et al. (2020):

- Tergitol lactose agar for counting fecal coliforms.
- Bile-aesculin agar for fecal streptococci.
- Soybean Casein Digest agar for Escherichia coli.
- Baird Parker agar for Staphylococcus aureus.
- Macconkey agar + Crystal violet was used to count the colorless colonies of Salmonella.

All microbial counts have been calculated on the basis of fresh weight. The concentration of cells in the sample was determined by counting on a known dilution in Petri dishes using the following equation:

$$\text{CFU/g fresh weight} = \text{number of colonies} \times \text{dilution} \times 100 \quad (3)$$

CFU: Colony-forming unit.

2.6 Agronomic essay

The soil was taken from the Beni Mellal region of Morocco (32°23'58.8"N; 6°21'46.1"W). According to the FAO soil classification system, the soil has a sandy loam texture (FAO, 1999). The soil was slightly alkaline (pH 7.97 and EC =0.28 mS/cm) with a low P and OM content of 7.4 mg.kg⁻¹ and 0.2%, respectively. The experiment was conducted in pots containing 2 kg of soil that had been amended with PS concentrations of 0, 1, 5, 10, 20, 30, 40, 50, and 60%. One tomato seedling (Campbell 33 Techni) was placed in each pot; each treatment was replicated five times under greenhouse conditions (16 hours of the daily lighting period at temperatures ranged between 20°C and 30°C). During the experiment, the pots were regularly watered to maintain the moisture at 60% of the field capacity. Plants grown in amended soils (treatments) and control without

PS (0%) were harvested 80 days after sowing. After that, plant growth parameters were measured, including root lengths, shoot heights, fresh and dry weight of roots and shoots, and the number of lived leaves.

2.7 Statistical analysis

Each analysis was replicated three times, and the results were reported as means with standard deviations. ANOVA one-way with post-hoc Tukey HSD test were used to compare the means of plant growth parameters. Significant differences within (p <0.05) are represented by different lowercase letters (a–e) above the bars.

3. RESULTS AND DISCUSSION

3.1 Physicochemical and elemental properties

The results obtained from the physicochemical characterization of PS are shown in Table 1. The pH (8.20) was slightly alkaline, probably due to the high content of water-soluble Ca (Romanos et al., 2019). The EC was low in the range of 0.77 mS/cm, mainly due to the low concentrations of soluble salts such as K⁺, Na⁺, PO₄³⁻, and SO₄²⁻ (Table 1). This material was relatively dry with an average moisture content of 2.1%, 97.2% as ash and 0.61% as OM. The elemental composition of the PS sample was dominated by Ca (CaO =39.72%), P (P₂O₅ =20.01%), and silicon (SiO₂ =12.21%), with slight concentrations of TOC (0.38%) and TKN (0.07%). In addition, the total content of heavy metals in PS such as copper (Cu), cadmium (Cd), chromium (Cr), zinc (Zn), and lead (Pb), is below the limits accepted in European countries for biosolids used in agricultural soils (Collivignarelli et al. 2019). Therefore, many PS elements were present in the water-soluble form at low or undetect-

TABLE 1: The physicochemical characteristics and elemental composition of PS.

pH	EC (mS/cm)	Moisture	TOC	TKN	OM	Ash		
8.20 ±0.31	0.77 ±0.03	2.10 ±0.10	0.38 ±0.05	0.07 ±0.01	0.61 ±0.22	97.20 ±2.81		
Total major elements (wt%)								
SiO ₂	TiO ₂	Al ₂ O ₃	Fe ₂ O ₃	MgO	CaO	Na ₂ O	K ₂ O	P ₂ O ₅
12.21	0.23	2.98	1.18	2.33	39.72	0.66	0.41	20.01
Total trace elements (ppm)								
As	Cd	Co	Mn	Ni	Pb	Cr	Zn	Cu
10.34	1.01	1.50	29.59	7.06	0.21	15.95	30.78	4.54
Anions (mg/L)								
F ⁻	Cl ⁻	NO ₂ ⁻		NO ₃ ⁻	SO ₄ ²⁻	PO ₄ ³⁻		
2.61	4.09	<0.10		1.72	8.34	<0.10		
Water-soluble elements (mg/L)								
Mn	B	Ca	K	Mg	Na	Si	Fe	Zn
0.03	0.11	20.62	3.55	5.12	9.96	1.80	0.04	0.01
P fractions (mg/g)								
Al-P		Ca-P		Fe-P		Olsen P		Organic P
0.75 ±0.03		82.60 ±2.10		1.50 ±0.3		0.07 ±0.001		0.98 ±0.21

wt%: weight percent; ppm: parts per million

able concentrations (Table 1). Indeed, the most soluble elements of PS were Ca, sodium (Na), magnesium (Mg), chloride (Cl), and potassium (K), with concentrations of 20.62, 9.96, 5.12, 4.09, and 3.55 mg/L, respectively. The low dissolution of PS minerals in water can be attributed to the high cation exchange capacity (CEC) of sedimentary phosphate-derived materials (Zhang and Sun, 2017). PS contained a high amount of inorganic P in the form of Al-P, Fe-P, and Ca-P, with values of 0.75, 1.5, and 82.60 mg/g, respectively, when compared to soluble P (Olsen P =0.07 mg/g) and organic P (0.98 mg/g).

3.2 Mineralogical and structural characteristics

The SEM image (Figure 3) shows good porosity of the PS structure, which is 7.01% in the average pore area and $8.98 \pm 3.43 \mu\text{m}$ in the pore size. In addition, the SEM image reveals the presence of several mineral phases characterized by XRD as carbonate fluorapatite (50%), dolomite (24%), calcite (11%), quartz (8.5%), and smectite (6.5%) (Figure 4). A large part of these minerals is small particles (less than 2 μm), giving the PS a clayey appearance. The identified minerals in PS are inert microcrystals poorly wa-

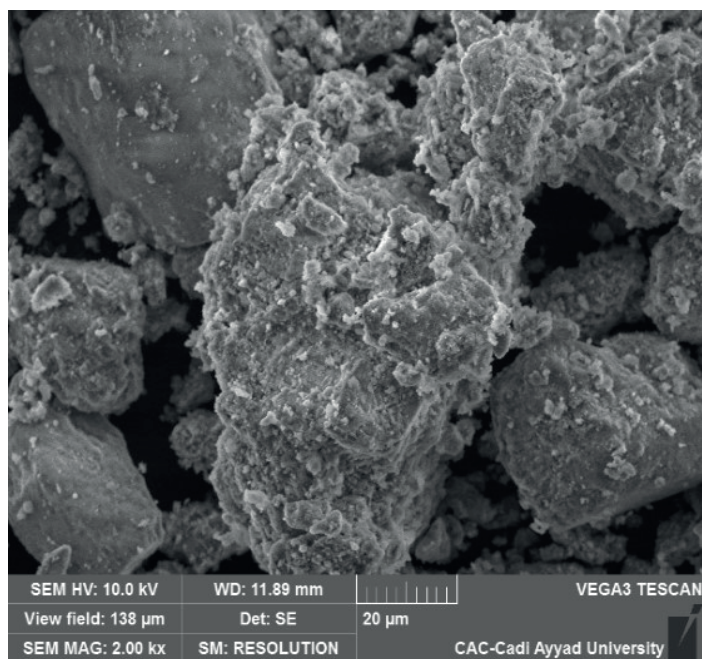


FIGURE 3: PS picture by SEM.

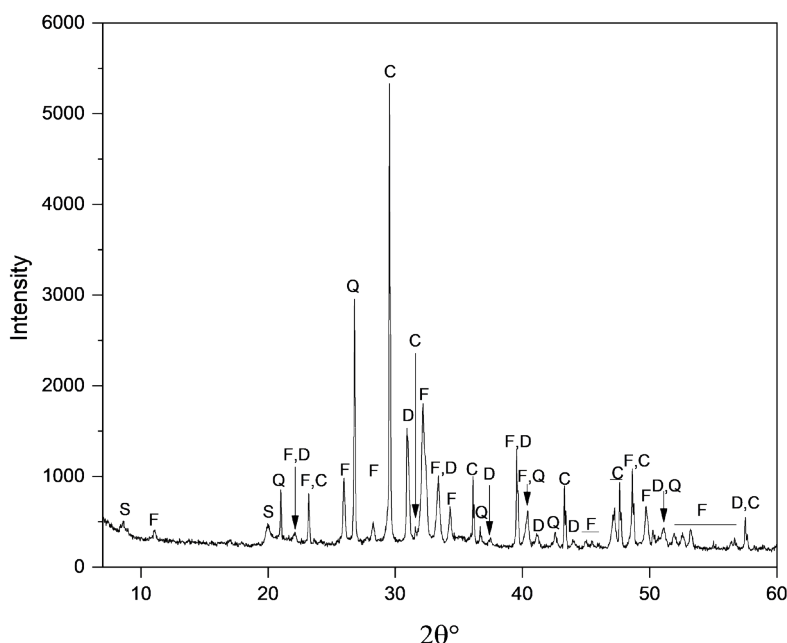


FIGURE 4: X-ray diffraction pattern of PS [F: Carbonate fluorapatite (PDF#01-073-9695); D: Dolomite (PDF # 01-073-2361); Q: Quartz (PDF # 01-074-3485); C: Calcite (PDF #0 1-085-1108); and S: Smectite (PDF # 29-1498)].

ter-soluble and could be sources of macro- and micronutrients (Dixon, 1992).

3.3 Thermal stability

The thermal stability of PS components is evaluated by DTA, TGA and FTIR analysis. The resultant thermal events of PS (Figure 5) were presented by the weight loss (WL) curve (TGA) and heat flow curve (DTA). FTIR spectra reveal the chemical composition of PS at the end of each thermal event, particularly at 412, 677, 832, 1000°C (Figure 6). Significant changes appeared in the intensity from the original positions of raw PS absorbance bands (Table 2).

The DTA and TGA curves show an endothermic peak ($T^{\circ}=105^{\circ}\text{C}$, $\text{WL}=3.95\%$) associated with the disappearance of absorbance at 3614 cm^{-1} and a relative decrease at 3248 , 3440 , and 3475 cm^{-1} in FTIR spectrum of raw PS. This could be attributed to the bending vibration of -OH groups in the water molecules, which indicates the loss of water (Loutou et al., 2013). In the temperature range between 171.5 and 413.6°C , the DTA and TGA curves represent a weak endothermic peak ($T^{\circ}=346^{\circ}\text{C}$, $\text{WL}=0.61\%$), which is associated with the OM degradation. Accordingly, the FTIR data of the PS sample at 412°C confirm the disappearance of the corresponding bands (2985 and 2862 cm^{-1}) of the symmetrical and asymmetrical vibration of the CH aliphatic groups (-CH₂ and -CH₃) (Amir et al., 2008). The large endothermic peak ($T^{\circ}=492^{\circ}\text{C}$, $\text{WL}=3.16\%$) refers to the dehydroxylation of smectite (Hajjaji et al., 2001). This event is linked to a decrease in the intensity of the band located between 3100 and 3700 cm^{-1} , which corresponds to hydroxyl stretching and deformation of Al-Al-OH of smectite. From 712°C to 1000°C , a strongly endothermic decomposition reaction of

carbonate compounds occurred at 836°C recorded in the DTA curve and accompanied by a significant WL of 13.14% due to the release of CO₂. This phenomenon was characterized by a decrease in the intensity of structures absorbing at 1416 , 1043 , and 877 cm^{-1} and the disappearance of absorbance bands at 2515 and 720 cm^{-1} in FTIR spectrum of PS treated at 832°C . These frequencies are assigned to the CO₃²⁻ groups of dolomite, calcite, and carbonate fluorapatite. After that, no significant changes occurred in the PS sample, and the same absorbance peaks were recorded in the FTIR spectrum at 1000°C .

These results confirm the XRD characterization of the mineralogical composition of PS (dolomite, calcite, quartz, smectite, and carbonate fluorapatite) and reveal the aliphatic structure of OM contained in PS. The aliphatic structure of OM is considered a readily available energy source for soil microorganisms (Amir et al., 2004).

3.4 Pathogenicity and phytotoxicity

In order to reduce the potential health risks associated with pathogens, potentially pathogenic organisms have been counted in PS, and the results were presented in Table 3. Fecal coliforms, Escherichia coli, fecal streptococci, Staphylococcus aureus, Salmonella have been classified as pathogenicity indicators of substrates intended for agricultural use. As there are no limit values or requirements for pathogens in phosphate materials for agricultural application, a comparison with organic fertilizers legislation is valid. The results confirm that the levels of pathogens in the PS are under the detection limit, or far below the limits set by most European countries for biosolids used for agriculture (Collivignarelli et al., 2019).

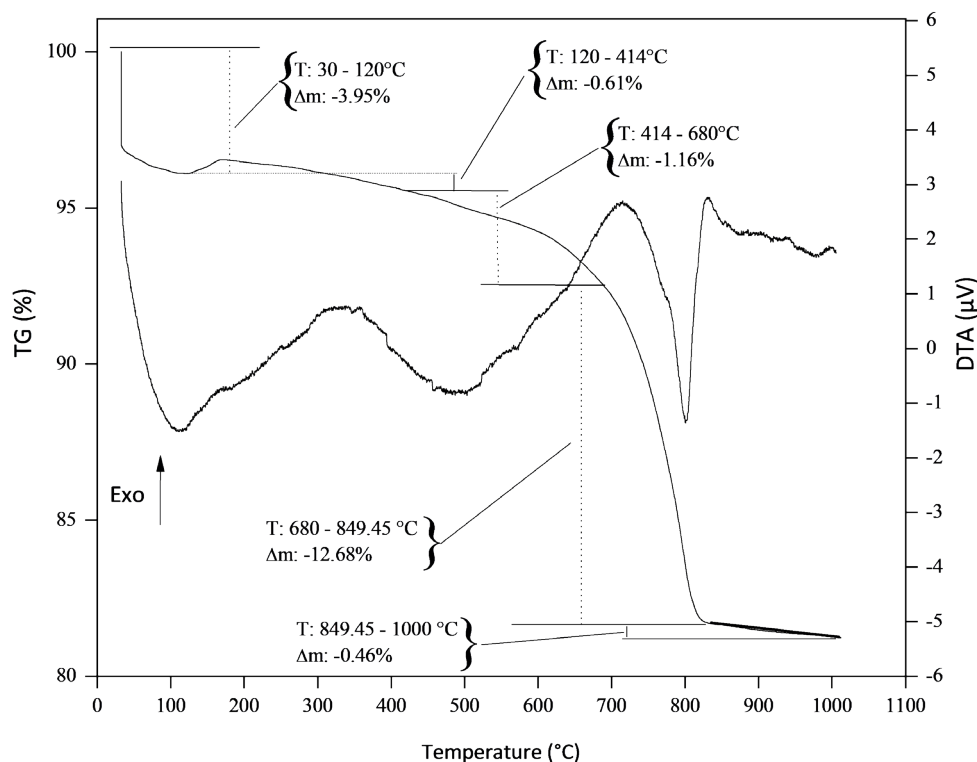


FIGURE 5: TGA and TDA curves.

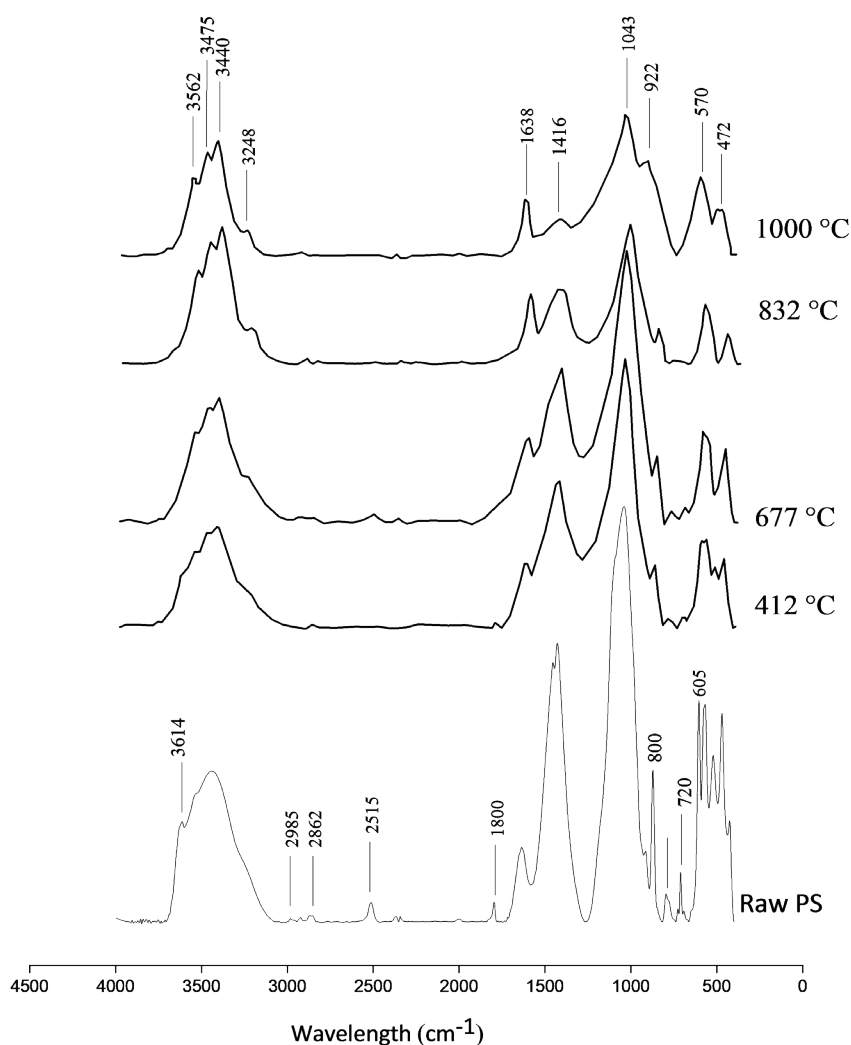


FIGURE 6: FTIR analysis of PS.

The results of the germination test carried out using tomato and maize seeds germinated in PS extract were presented in Figure 7. Several authors reported that a GI greater than 50% was a good indicator for non-phytotoxic samples (Levy and Taylor, 2003; Haouas et al., 2021b). The main factors leading to the inhibition of seed germination

are high concentrations of salts, certain heavy metals (e.g., arsenic (As), Pb, Cd, and Cr), and toxic organic compounds (e.g., polyphenols and organic acids) (Martínez-Ballesta et al., 2020). The PS extract exhibited no phytotoxic effect on maize and tomato seeds as their GI values exceeded 50% (Figure 7). This ability of PS to germinate maize and

TABLE 2: The main absorbance bands of PS in FTIR spectra and their assignments.

Bands and peaks (cm ⁻¹)	Assignments
922 and 570 cm ⁻¹	Symmetric stretching of PO ₄ ³⁻ of Carbonate fluorapatite
1416, 1043, 2515, 877 and 720 cm ⁻¹	CO ₂ ³⁻ groups of dolomite, calcite and carbonate fluorapatite
2985 and 2862 cm ⁻¹	-CH ₂ and -CH ₃ of aliphatic groups
3475, 3440, 3248, and 3614 cm ⁻¹	-OH groups in the water molecules and hydroxyl stretching and deformation of Al-Al-OH of smectite
800 cm ⁻¹	Si-O-Si symmetrical stretching vibration of quartz

The assignments are based on numerous studies (Regnier et al., 1994; Ojima et al., 2003; Amir et al., 2010; Loutou et al., 2013).

TABLE 3: Enumeration of pathogens in PS.

Types of Pathogens	Fecal Coliforms (×10 ²)	Escherichia Coli (×10 ³)	Fecal Streptococci (×10 ²)	Staphylococcus aureus	Salmonella
Average concentration (CFU /g fresh weight)	0.12 ±0.003	0.02 ±0.001	0.03 ±0.001	absent	absent

tomato seeds is due to the absence of phytotoxic factors and the presence of available nutrients (Martínez-Ballesta et al., 2020). It was reported that many nutrients found in PS improved seeds germination of many crops, including P and nitrogen (N) as macronutrients and molybdenum (Mo), boron (B), manganese (Mn), Zn as micronutrients (Imran et al., 2017; Rehman et al., 2018).

3.5 Plant growth promotion capacity

Plants grown in treatments and control have survived, and no plant death has been observed. Figure 8 indicates the appearance of randomly selected plants (one plant from each treatment and control). The effect of PS on plant growth was assessed by comparing the data obtained after the measurement of the growth parameters (root length, root dry and fresh weight, shoot height, shoot dry

and fresh weight and the number of lived leaves), and the results were presented in Figure 9 and 10.

The results related to the root part (Figure 9) show that the plants cultivated in the soil amended with 20% of PS had higher root length (29 cm) than other PS treatments and control. However, there was no significant difference in root length values (from 26.7 to 29 cm) between plants developed in 1, 10, 20, 40, and 50% of PS treatments. The concentration of 60% of PS in deficient soil recorded the lowest value of 15.7 cm. The application of PS to the soil could enhance the fresh weight of roots. In fact, Figure 9 shows a slight increase of root fresh weight ranged from 5.14 to 5.68 g in treatments prepared with 1, 5, 10, and 20% of PS, compared to control (0% of PS). For root dry weight, the control plants showed a maximum value of 1.54 g with a significant difference ($p < 0.05$) in PS treatments. While,

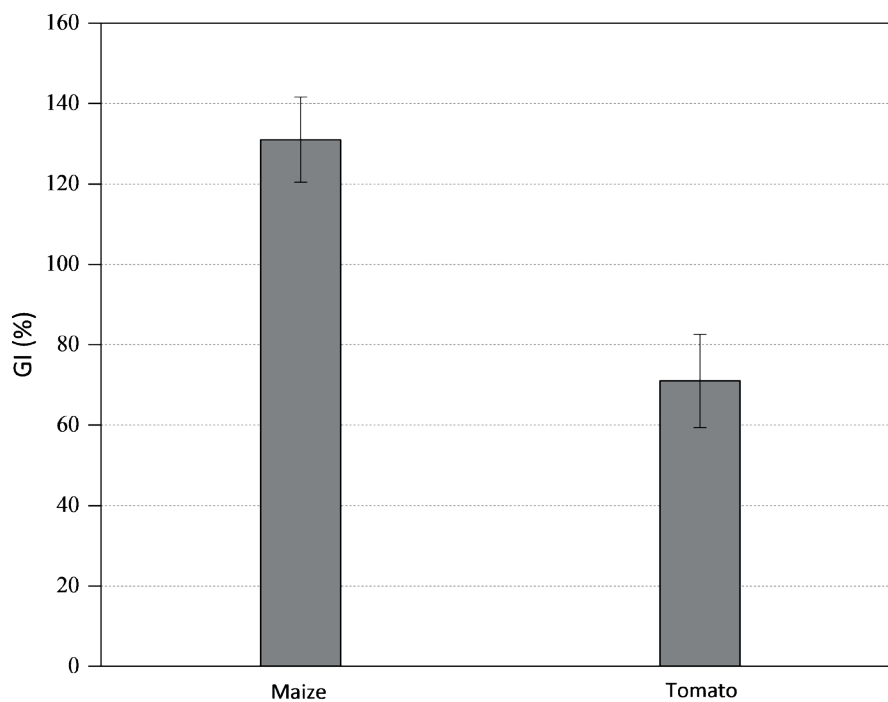


FIGURE 7: The GI of the tomato seeds in the PS extract.



FIGURE 8: Appearance of tomato plants after 80 days of growth in soil amended with different concentrations of PS.

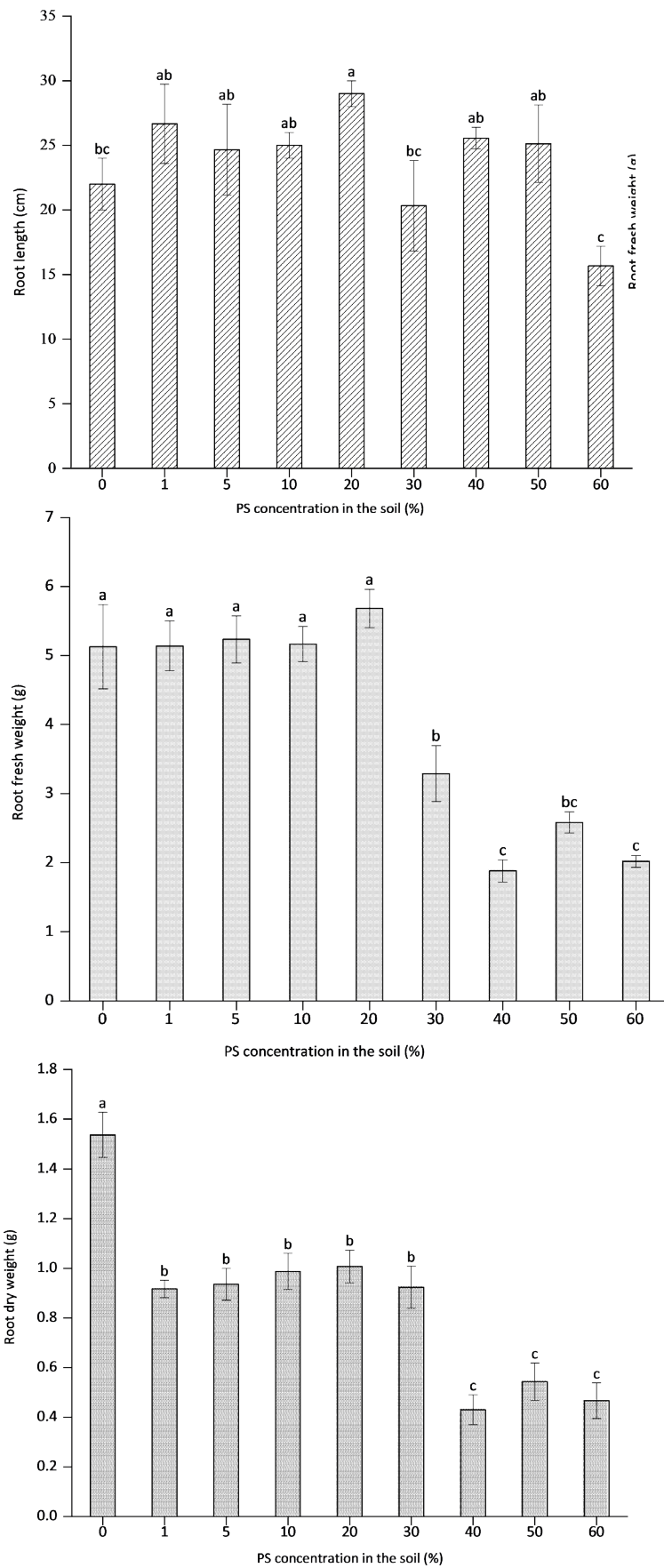


FIGURE 9: Length, fresh weight, and dry weight of the root part after 80 days of tomato plants grown in deficient soil amended with different concentrations of PS.

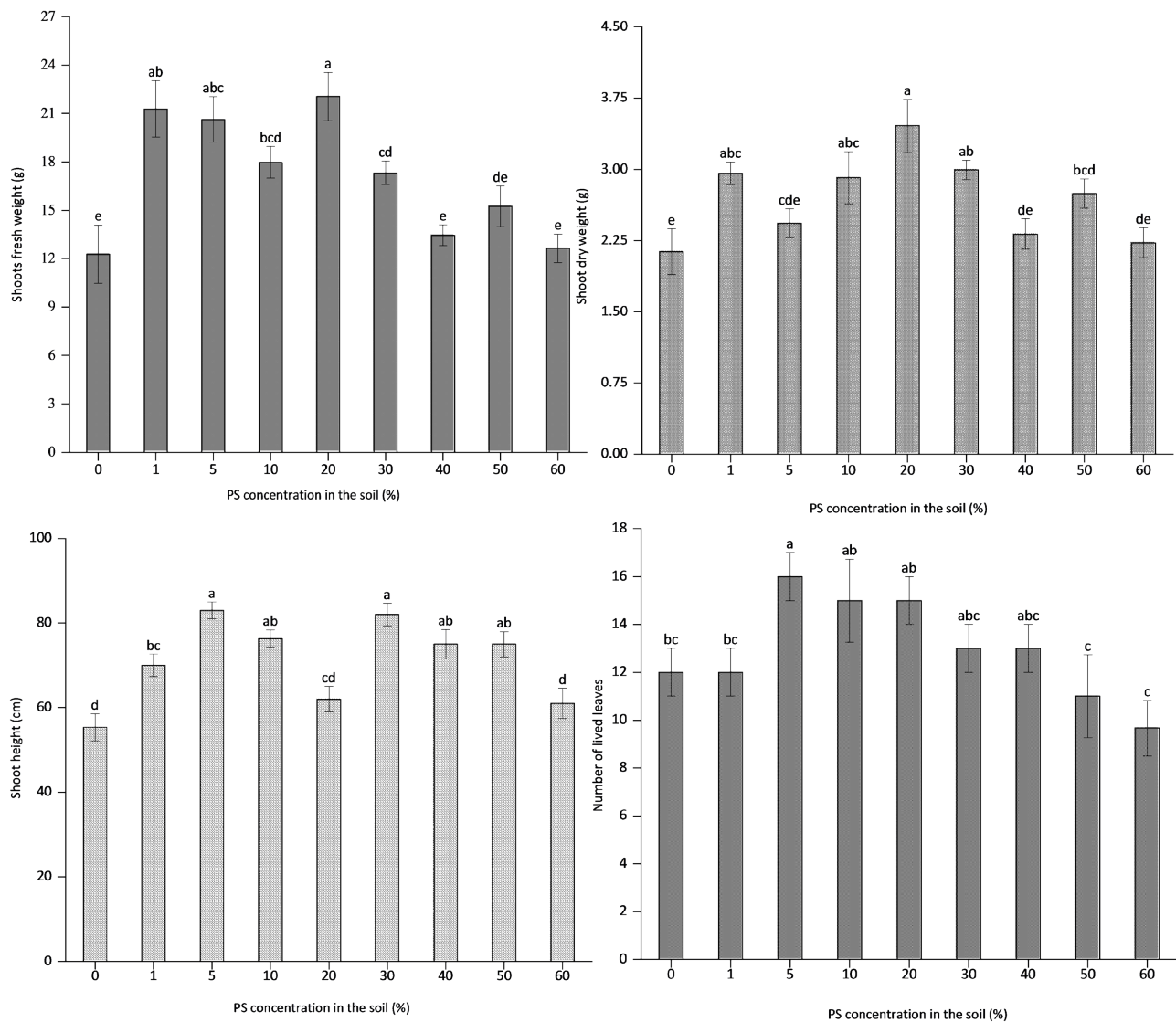


FIGURE 10: Height, fresh weight, dry weight, and the number of lived leaves of the shoot part after 80 days of tomato plants grown in deficient soil amended with different concentrations of PS.

high PS concentrations of 40, 50, and 60% recorded the lowest weight of root biomass (fresh and dry weight) of tomato plants.

The results related to the shoot part (Figure 10) show that the addition of PS to sandy soil increased the fresh weight, dry weight, and height of the plant shoots. Plants at concentrations of 1, 5, 10, 20, and 30% of PS had the highest shoot fresh weight of between 17.32 and 22.06 g. The application of PS at 20% significantly increased ($p < 0.05$) the shoot biomass compared to other concentrations of PS. While control plants showed the lowest values of 12.28 g and 2.13 g in fresh and dry weight, respectively. In addition, a significant effect of the PS amendment was observed on plant height and the number of lived leaves. In treatments of 1, 5, 10, 30, 40, and 50% of PS, recorded the highest values of shoot height fluctuated between 83 and 70 cm. In control with only soil, the value of shoot height was 55.3 cm. Concentrations from 5 to 40% of PS added

to the deficient soil increased the number of leaves of tomato plants (ranged from 13 to 16) compared to control (12 leaves). In contrast, the lowest number of leaves was registered in plants grown in the amended soil at 50 and 60% of PS.

PS at a concentration of 20% significantly improved root elongation, shoot fresh weight, and shoot dry weight and a concentration of 5% induced higher shoot height and number of lived leaves compared to control. In contrast, concentrations of up to 40% of PS (40, 50, and 60%) showed poor plant development and reduced root biomass compared to control. The enhancement of plant growth in the presence of PS amendments could be due to improved soil agronomic properties, leading to increased water and nutrient availability (Belay et al., 2020). The PS clay minerals may increase sandy soil's chemical and physical properties, making the water readily available for plant roots, leading to strong roots and tall and healthy shoots (Kay-

ama et al., 2016). It has been shown that clay addition to the sandy soil increased significantly 2.5 times the yield of maize (Gold dent KD 777) and cucumber (Shin toki wa) and also by 12.8% of squash (*Cucurbita Pepo*) compared to control (Ismail and Ozawa, 2007; Al-Omran et al., 2005).

The growth parameters (Figure 9, 10) reveal that the control plants were less developed than PS treatments, especially at 20% and 5%. This phenomenon could be attributed to the water shortage of the sandy soil used. The water deficit for plant uptake has been found to have a large impact on many cultivars, including tomato plants (Ximénez-Embún et al., 2018). In fact, it has been reported that clay-rich materials application in sandy soils increased the cropping yield due to improved water holding capacity (Ismail and Ozawa, 2007). However, incorporating a large quantity of clay-rich materials may negatively affect plant growth, as stated in this study, when the PS concentration exceeded 40% and mainly at 60%. Excess of clay fraction into the soil may cause several adverse effects when irrigated, such as waterlogging, which has led to roots asphyxiation and the reduction respiration activity of soil microorganisms (Gil et al., 2011). As reported in this study, smectite is the major fraction of PS clay minerals, which, due to its physical properties such as fine particle size, high surface area, and variable interlayer spacing, it could be the main responsible for clay effect on plant growth at 60% of PS (Dixon, 1991). On the other hand, the lack of nutrients and water states in the soil induces plants to develop deep and strong roots in search of water pockets and nutrients along with short and weak shoots, as stated in this study for plants cultivated in only sandy soil (control) (Hermans et al., 2006).

4. CONCLUSIONS

The characterization of PS is crucial to determine their benefit and potential risk criteria for farming soil. PS is a stable material with a high nutrient content such as P, Ca, and Mg. In addition, PS mineral clays had beneficial properties for improving the performance of deficient sandy soils, such as high water holding capacity and a slow release of nutrients compared to chemical fertilizers. PS was therefore shown to be free of pathogens and phytotoxic substances, indicating a low risk of contamination of the harvested products. Consequently, the use of a PS concentration of 20% is highly recommended. Thus, it should be combined with organic-rich material such as compost to replenish the low OM content in PS.

ACKNOWLEDGMENTS

The Authors would like to acknowledge the support through the R&D Initiative – Appel à projets autour des phosphates APPHOS – sponsored by OCP (OCP Foundation, R&D OCP, Mohammed VI Polytechnic University, National Center of Scientific and technical Research CNRST, Ministry of Higher Education, Scientific Research and Professional Training of Morocco MESRSFC) under the project entitled «Procédés biotechnologiques pour la valorisation des boues et des déchets miniers de phosphate:

Formulation d'un Phospho-compost bio-fertilisant pour application directe en agriculture productive et respectueuse de l'environnement» (Réf. BIO-MOD-01/2017).

COMPETING INTERESTS

Authors have declared that no competing interests exist.

REFERENCES

- AFNOR, 2000. Soil amendments and growing medium - Preparation of samples for physical and chemical testing, determination of dry matter content, moisture content and compacted density in the laboratory (in French). AFNOR France, NF EN 13040.
- Al-Omran, A.M., Sheta, A.S., Falatah, A.M. and Al-Harbi, A.R., 2005. Effect of drip irrigation on squash (*Cucurbita Pepo*) yield and water use efficiency in sandy calcareous soils amended with clay deposits. *Agric. Water Manag.* 73, 43-55.
- Amir, S., Hafidi, M., Merlina, G., Hamdi, H., Revel, J.C., 2004. Elemental analysis, FTIR and ¹³C-NMR of humic acids from sewage sludge composting. *Agronomie* 24, 13–18. <https://doi.org/10.1051/agro:2003054>
- Amir S., Hafidi M., Merlina G, Revel J.C., 2005. Sequential extraction of heavy metals during composting of sewage sludge. *Chemosphere* 59, 6, 801-810. <https://doi.org/10.1016/j.chemosphere.2004.11.016>.
- Amir, S., Benboukht, F., Cancian, N., Winterton, P., Hafidi, M., 2008. Physico-chemical analysis of tannery solid waste and structural characterization of its isolated humic acids after composting. *J. Hazard. Mater.*, 160, 2-3, 448-455. <https://doi.org/10.1016/j.jhazmat.2008.03.017>
- Anne, P., 1945. Sur le dosage du carbone organique des sols *Ann. Agron.*, 15, 161-172.
- Atif, K., Haouas, A., Aziz, F., Yasser Jamali, M., Tallou, A., & Amir, S., 2020. Pathogens Evolution During the Composting of the Household Waste Mixture Enriched with Phosphate Residues and Olive Oil Mill Wastewater. *Waste and Biomass Valorization*. 11, 1789–1797. <https://doi.org/10.1007/s12649-018-0495-3>
- Belay, S.A., Assefa, T.T., Prasad, P.V.V., Schmitter, P., Worqlul, A.W., Steenhuis, T.S., Reyes, M.R., Tilahun, S.A., 2020. The Response of Water and Nutrient Dynamics and of Crop Yield to Conservation Agriculture in the Ethiopian Highlands. *Sustainability* 12, 5989. <https://doi.org/10.3390/su12155989>
- Boujlel, H., Daldoul, G., Tlili, H., Souissi, R., Chebbi, N., Fattah, N., & Souissi, F., 2019. The Beneficiation Processes of Low-Grade Sedimentary Phosphates of Tozeur-Nefta Deposit (Gafsa-Metlaoui Basin: South of Tunisia). *Minerals*, 9(1), 2. <https://doi.org/10.3390/min9010002>
- Bray, R.H. and Kurtz, L.T., 1945. Determination of Total Organic and Available Forms of Phosphorus in Soils. *Soil Sci.*, 59, 39-45. <http://dx.doi.org/10.1097/00010694-194501000-00006>
- Chang, S. C., & Jackson, M. L., 1957. Fractionation of Soil Phosphorus. *Soil Sci.*, 84, 133–144. <https://doi.org/10.1097/00010694-195708000-00005>
- Chen, Y.X., Huang, X.D., Han, Z.Y., Huang, X., Hu, B., Shi, D.Z., & Wu, W.X., 2010. Effects of bamboo charcoal and bamboo vinegar on nitrogen conservation and heavy metals immobility during pig manure composting. *Chemosphere*, 78(9), 1177–1181. <https://doi.org/10.1016/j.chemosphere.2009.12.029>
- Collivignarelli, M. C., Abbà, A., Frattarola, A., Carnevale Miino, M., Padovani, S., Katsoyiannis, I., & Torretta, V., 2019. Legislation for the Reuse of Biosolids on Agricultural Land in Europe: Overview. *Sustainability*, 11(21), 6015. <https://doi.org/10.3390/su11216015>
- Dixon, J.B., 1991. Roles of clays in soils. *Appl. Clay Sci.* 5, 489–503. [https://doi.org/10.1016/0169-1317\(91\)90019-6](https://doi.org/10.1016/0169-1317(91)90019-6)
- FAO, 2009. Climate change in Africa: The threat to agriculture. <https://www.uncclearn.org/sites/default/files/inventory/fao34.pdf>. Accessed 26 December 2019
- FAO–UNESCO, 1999. World Soil Map, revised legend, Rome
- Gil, P.M., Ferreyra, R., Barrera, C., Zuniga, C., Gurovich, L.A., 2011. Improving soil oxygenation with hydrogen peroxide injection into heavy clay loam soil: effect on plant water status, CO₂ assimilation and biomass of avocado trees. *Acta Hort.*

- Hajjaji, M., Kacim, S., Alami, A., El Bouadili, A., El Mountassir, M., 2001. Chemical and mineralogical characterization of a clay taken from the Moroccan Meseta and a study of the interaction between its fine fraction and methylene blue. *Applied Clay Sci.* 20, 1e12.
- Hakkou, R., Benzaazoua, M., Bussi re, B., 2016. Valorization of Phosphate Waste Rocks and Sludge from the Moroccan Phosphate Mines: Challenges and Perspectives. *Procedia Engineering, SYMPHOS 2015 - 3rd International Symposium on Innovation and Technology in the Phosphate Industry* 138, 110–118. <https://doi.org/10.1016/j.proeng.2016.02.068>
- Haouas, A., El Modafar, C., Douira, A., Ibensouda-koraichi, S., Filali-maltouf, A., Moukhli, A., Amir, S., 2020. The effect of phosphate and organic additives on the stability of food waste in the full-scale composting. *PLANT CELL BIOTECHNOLOGY AND MOLECULAR BIOLOGY* 21 (39–40), 17–28. <https://ikprress.org/index.php/PCBMB/article/view/5428>.
- Haouas, A., El Modafar, C., Douira, A., Ibensouda-Koraichi, S., Filali-Maltouf, A., Moukhli, A., Amir, S., 2021a. *Alcaligenes aquatilis* GTE53: Phosphate solubilising and bioremediation bacterium isolated from new biotope "phosphate sludge enriched-compost." *Saudi J. Biol. Sci.* 28, 371–379. <https://doi.org/10.1016/j.sjbs.2020.10.015>
- Haouas, A., El Modafar, C., Douira, A., Ibensouda-Koraichi, S., Filali-Maltouf, A., Moukhli, A., Amir, S., 2021b. Evaluation of the nutrients cycle, humification process, and agronomic efficiency of organic wastes composting enriched with phosphate sludge. *J. Clean. Prod.* 302, 127051. <https://doi.org/10.1016/j.jclepro.2021.127051>
- Hermans, C., Hammond, J.P., White, P.J., Verbruggen, N., 2006. How do plants respond to nutrient shortage by biomass allocation?. *Trends Plant Sci.* 11, 610–617. <https://doi.org/10.1016/j.tplants.2006.10.007>
- Imran, M.; Volker, R.; Neumann, G., 2017. Accumulation and distribution of Zn and Mn in soybean seeds after nutrient seed priming and its contribution to plant growth under Zn and Mn deficient conditions. *J. Plant Nutr.* 40, 695–708.
- Ismail, S.M. and Ozawa, K., 2007. Improvement of crop yield, soil moisture distribution and water use efficiency in sandy soils by clay application. *Appl. Clay Sci.* 37, 81–89. <https://doi.org/10.1016/j.clay.2006.12.005>
- Karunanithi, R., Szogi, A. A., Bolan, N., Naidu, R., Loganathan, P., Hunt, P. G., et al., 2015. Chapter Three - Phosphorus Recovery and Reuse from Waste Streams. In D. L. Sparks (Ed.), *Advances in Agronomy* (Vol. 131, pp. 173–250). Academic Press. <https://doi.org/10.1016/bs.agron.2014.12.005>
- Kayama, M., Nimpila, S., Hongthong, S., Yoneda, R., Wichienopparat, W., Himmapan, W., Vacharangkura, T., Noda, I., 2016. Effects of Bentonite, Charcoal and Corncob for Soil Improvement and Growth Characteristics of Teak Seedling Planted on Acrisols in Northeast Thailand. *Forests* 7, 36. <https://doi.org/10.3390/f7020036>
- Khasawneh, F. E., & Doll, E. C., 1979. The Use of Phosphate Rock for Direct Application to Soils. In N. C. Brady (Ed.), *Adv. Agron.* (Vol. 30, pp. 159–206). Academic Press. [https://doi.org/10.1016/S0065-2113\(08\)60706-3](https://doi.org/10.1016/S0065-2113(08)60706-3)
- Kihara, J., Bolo, P., Kinyua, M., Rurinda, J., Piikki, K., 2020. Micronutrient deficiencies in African soils and the human nutritional nexus: opportunities with staple crops. *Environ Geochem Health* 42, 3015–3033. <https://doi.org/10.1007/s10653-019-00499-w>
- Levy, J.S., & Taylor, B.R., 2003. Effects of pulp mill solids and three composts on early growth of tomatoes. *Bioresour. Technol.* 89, 297–305. [https://doi.org/10.1016/S0960-8524\(03\)00065-8](https://doi.org/10.1016/S0960-8524(03)00065-8)
- Loutou, M., Hajjaji, M., Mansori, M., Favotto, C., & Hakkou, R., 2013. Phosphate sludge: thermal transformation and use as lightweight aggregate material. *J. Environ. Manage.* 130, 354–360. <https://doi.org/10.1016/j.jenvman.2013.09.004>
- Luo, Y., Liang, J., Zeng, G., Chen, M., Mo, D., Li, G., Zhang, D., 2018. Seed germination test for toxicity evaluation of compost: Its roles, problems and prospects. *Waste Manag* 71, 109–114. <https://doi.org/10.1016/j.wasman.2017.09.023>
- Mart nez-Ballesta, M. del C., Egea-Gilabert, C., Conesa, E., Ochoa, J., Vicente, M.J., Franco, J.A., Ba on, S., Mart nez, J.J., Fern andez, J.A., 2020. The Importance of Ion Homeostasis and Nutrient Status in Seed Development and Germination. *Agronomy* 10, 504. <https://doi.org/10.3390/agronomy10040504>
- Moukannaa, S., Loutou, M., Benzaazoua, M., Vitola, L., Alami, J., & Hakkou, R., 2018. Recycling of phosphate mine tailings for the production of geopolymers. *J. Clean. Prod.* 185, 891–903. <https://doi.org/10.1016/j.jclepro.2018.03.094>
- Ojima, J., 2003. Determining of Crystalline Silica in Respirable Dust Samples by Infrared Spectrophotometry in the Presence of Interferences. *J. Occup. Health* 45, 94–103. <https://doi.org/10.1539/joh.45.94>
- Regnier, P., Lasaga, A.c., Berner, R.A., Han, O.H., and Zilm, K.W., 1994. Mechanism of CO₂ substitution in carbonate-fluorapatite: Evidence from FTIR spectroscopy, ¹³C NMR, and quantum mechanical calculations. *Am. Mineral.* 79, 809–818.
- Rehman, A.; Farooq, M.; Naveed, M.; Nawaz, A.; Shahzad, B., 2018. Seed priming of Zn with endophytic bacteria improves the productivity and grain biofortification of bread wheat. *Eur. J. Agron.* 94, 98107.
- Romanos, D., Nemer, N., Khairallah, Y., & Abi Saab, M. T., 2019. Assessing the quality of sewage sludge as an agricultural soil amendment in Mediterranean habitats. *Int. j. recycl. org. waste agric.* 8(1), 377–383. <https://doi.org/10.1007/s40093-019-00310-x>
- Tallou, A., Salcedo, F.P., Haouas, A., Jamali, M.Y., Atif, K., Aziz, F., Amir, S., 2020. Assessment of biogas and biofertilizer produced from anaerobic co-digestion of olive mill wastewater with municipal wastewater and cow dung. *Environ Technol Inno* 20, 101152. <https://doi.org/10.1016/j.eti.2020.101152>
- Xim nez-Emb n, M.G., Gonz lez-Guzm n, M., Arbona, V., G mez-Cadenas, A., Ortego, F., Casta era, P., 2018. Plant-Mediated Effects of Water Deficit on the Performance of *Tetranychus evansi* on Tomato Drought-Adapted Accessions. *Front. Plant Sci.* 9. <https://doi.org/10.3389/fpls.2018.01490>
- Zhang, L., Sun, X., 2017. Addition of fish pond sediment and rock phosphate enhances the composting of green waste. *Biore-sour. Technol.* 233, 116–126. <https://doi.org/10.1016/j.biortech.2017.02.073>

LIFE CYCLE ASSESSMENT OF SEWAGE SLUDGE PYROLYSIS: ENVIRONMENTAL IMPACTS OF BIOCHAR AS CARBON SEQUESTRATOR AND NUTRIENT RECYCLER

Fabian Gievers^{1,2,*}, Achim Loewen¹ and Michael Nelles^{2,3}

¹ Faculty of Resource Management, HAWK-University of Applied Sciences and Arts, Rudolf-Diesel-Straße 12, 37075 Göttingen, Germany

² Chair of Waste and Resource Management, University of Rostock, Justus-v.-Liebig-Weg 6, 18059 Rostock, Germany

³ Deutsches Biomasseforschungszentrum gGmbH (DBFZ), The German Centre for Biomass Research, Torgauer Str. 116, 04347 Leipzig, Germany

Article Info:

Received:
13 December 2020
Revised:
26 May 2021
Accepted:
14 June 2021
Available online:
11 September 2021

Keywords:

Life cycle assessment
Pyrolysis
Sewage sludge
Biochar
Nutrient recovery
Carbon sequestration

ABSTRACT

The pyrolysis of sewage sludge is an alternative method to recycle the contained nutrients, such as phosphorus, by material use of the resulting biochar. However, the ecological effects of pyrolysis are not easy to evaluate. Therefore, a life cycle assessment (LCA) was carried out to determine the environmental impact of sewage sludge pyrolysis and to compare it with the common method of sewage sludge incineration. In order to identify the most sustainable applications of the resulting biochar, four different scenarios were analyzed. The modeled life cycles include dewatering, drying and pyrolysis of digested sewage sludge and utilization paths of the by-products as well as various applications of the produced biochar and associated transports. The life cycle impact assessment was carried out using the ReCiPe midpoint method. The best scenario in terms of global warming potential (GWP) was the use of biochar in horticulture with net emissions of 2 g CO₂ eq./kg sewage sludge. This scenario of biochar utilization can achieve savings of 78% of CO₂ eq. emissions compared to the benchmark process of sewage sludge mono-incineration. In addition, no ecological hotspots in critical categories such as eutrophication or ecotoxicity were identified for the material use of biochar compared to the benchmark. Pyrolysis of digested sewage sludge with appropriate biochar utilization can therefore be an environmentally friendly option for both sequestering carbon and closing the nutrient cycle.

1. INTRODUCTION

Pressure on limited natural nutrient resources, such as phosphorus (P), is increasing due to the growing world population and the resulting growing demand for fertilizers to ensure a sufficient food supply. Raw phosphates, which serve as the basis for the production of mineral fertilizers, come from mineral resources extracted mainly in Morocco and China (Cordell & White, 2011; Schoumans et al., 2015). Another source of P is municipal wastewater, which could theoretically replace up to 50% of the mineral P fertilizer applied annually in European agriculture (Egle et al., 2016). Therefore, a long-term strategy is needed to provide natural nutrients and enable waste-based nutrient recycling, especially for potentially critical raw materials like P. This paradigm shift from wastewater treatment as disposal to resource recovery requires new research approaches and treatment technologies and must be guided by the application of green engineering principles to ensure economic,

social and environmental sustainability (Peccia & Westerhoff, 2015). In recent years, most European legislation has agreed on the use of the nutrient and energy value of sewage sludge, but due to transition periods and the conflict between economic challenges and environmental safety, the implementation of new technologies will take decades (Christodoulou & Stamatelatos, 2016). Therefore, very little P is currently recovered, as the economics of recovery from waste streams are unfavorable compared to P extracted from mining. The economics could change in the near future as depletion of reserves leads to higher extraction costs and the peak of phosphorus mining could occur by 2030 (Elser & Bennett, 2011). The total value of P recycling should therefore be considered, including social and environmental aspects (Mayer et al., 2016). The data and the framework for modeling the environmental impact of these elusive aspects of recycling management can be provided by LCA (Haupt & Hellweg, 2019).

 * Corresponding author:
Fabian Gievers
email: fabian.gievers@hawk.de

Existing sewage sludge treatments such as co-combustion in the cement industry or in lignite-fired power plants reduce the P concentration in the ash and thus make P extraction more difficult and expensive. An ideal technology should offer maximum P recovery rates, good fertilization properties of the product, removal and destruction of potentially hazardous substances and low environmental and economic risks (Egle et al., 2016; Leinweber et al., 2018). Therefore, the pyrolysis of sewage sludge is a promising approach to implement a circular economy for nutrients and to eliminate pathogens and other organic pollutants (Bridle & Pritchard, 2004; Frišták et al., 2018; Glaser & Lehr, 2019; Méndez et al., 2013; Paz-Ferreiro et al., 2018) and carbon sequestration to fight the climate crisis (Alhashimi & Aktas, 2017; Ennis et al., 2012). Furthermore, pyrolysis fixes and immobilizes the heavy metals in the biochar matrix so that the risk of leaching is minimized compared to the direct agricultural application of the sludge (Agrafioti et al., 2013). In the past, several life cycle assessment (LCA) studies of fast pyrolysis, slow pyrolysis and intermediate pyrolysis of sewage sludge have been carried out to evaluate the sustainability of thermochemical conversion treatments of sewage sludge (Cao & Pawłowski, 2013; Li & Feng, 2018; Marazza et al., 2019; Salman et al., 2019; Samolada & Zabaniotou, 2014; Teoh & Li, 2020).

In this study, a LCA of the pyrolysis of digested sewage sludge with a special focus on different, biochar applications was carried out and the results were compared with the usual process chain of sewage sludge mono-incineration with subsequent ash landfilling excluding P-recovery. Besides an energetic and environmental evaluation of pyrolysis as a treatment process for sewage sludge, one goal was to determine the best utilization of sewage sludge bi-

ochar. Secondary aspects of this study focus on nutrient recycling ability, especially for P (Frišták et al., 2018), and the carbon sequestration potential of the biochar produced (Schmidt et al., 2018).

2. METHODS

2.1 Energy and material flows

In order to calculate all material and energy flows for the treatment process itself and the subsequent biochar application, a model for the process chains has been generated in the LCA software GaBi ts. It was assumed that the substrate originates from the anaerobic digestion of sewage sludge in an existing wastewater treatment plant (WWTP) with total solids (TS) content of 5% (volatile solids (VS): 48%). In the model the main parameters of the dewatering, the subsequent drying and the pyrolysis process were set to the following values (Table 1).

2.1.1 Material flows

Since all sewage sludge can contain heavy metals and potentially toxic inorganic and organic components, an untreated return of the sludge to the environment is no longer recommended. While organic compounds react during the pyrolysis process, heavy metals cannot be destroyed and accumulate in the biochar. The concentrations of heavy metals must be carefully monitored due to their potential toxic risk (Bauer et al., 2020; van Wesenbeeck et al., 2014), although they may be immobilized by the pyrolysis process (Agrafioti et al., 2013). The milder thermal reaction conditions during pyrolysis can destroy harmful organic substances while maintaining the bio-availability of nutrients such as nitrogen (N), potassium (K) and P, in contrast to the high temperatures during mono-incineration (Glaser &

TABLE 1: Parameters of digested sewage sludge pyrolysis in the LCA model.

Process Step	Unit	Value	Range	Reference
Dewatering of the sludge				
Input: digested sewage sludge	[kg]	1	-	Functional unit
Input: total solids	[%]	5	-	ecoinvent database
Flocculant	[g]	0,55	0,4–0,7	(Denkert et al., 2013)
Electricity	[kJ]	7,2	6,1-8,4	(Denkert et al., 2013)
Output: total solids	[%]	25	22-30	(Denkert et al., 2013)
Drying of the dewatered sludge				
Electricity	[kJ]	36	32-38	Calculated ^a
Thermal energy	[kJ]	612	590-650	Calculated ^a
Output: total solids	[%]	80	78-89	Calculated ^a
Pyrolysis				
Thermal energy	[kJ]	79	50-112	Calculated ^b
Electricity	[kJ]	21	15-36	Calculated ^b
Pyrolysis temperature	[°C]	550	450-700	Estimated ^b
Residence time	[h]	1	0,3-3	Estimated ^b
Output: biochar	[g]	23	21-30	(Tomasi Morgano et al., 2018)
Output: gas and liquid	[g]	30	23-32	(Tomasi Morgano et al., 2018)

^a Data from (ELIQUO, 2020) and (Jacobs et al., 2019) ^b Data from (PYREG, 2020) and (Tomasi Morgano et al., 2018)

Lehr, 2019; Paneque et al., 2019). To determine the best utilization of biochar, flows and accumulation of heavy metals, organic pollutants and valuable nutrients were modeled using the LCA software. It was assumed that the liquid phase and the gas produced as byproducts in pyrolysis processes will be incinerated on site to generate thermal energy for sludge drying and heating up the pyrolysis process. The press water from the dewatering of digested sewage sludge containing organic substances and nutrients is treated in the on-site WWTP, balanced according to their loads.

2.1.2 Energy flows

The energetic modeling of the pyrolysis process was carried out using literature and industrial data. Values for other energy flows, e.g. the electricity required for the dewatering process, were also taken from literature. The emissions of the aggregated background processes originate from the databases of GaBi and ecoinvent and the data for the benchmark process of sewage sludge mono-incineration were taken from the ecoinvent process, which was adapted to the geographical framework conditions.

2.2 Life Cycle Assessment

The LCA was carried out according to the requirements of the ISO 14040 and 14044 standards (Deutsches Institut für Normung, 2009).

2.2.1 Functional Unit

In order to compare the pyrolysis of sewage sludge with the given process of mono-incineration and possible other thermochemical treatment methods such as hydrothermal carbonization (Gievers et al., 2019), the functional unit (FU) was defined as "Treatment of 1 kg of sewage sludge after anaerobic digestion with a total solids content of 5%".

2.2.2 System Boundary

Because mono-incineration currently is mostly recommended as a treatment method for sewage sludge, this technology was used as a benchmark process with which pyrolysis was compared. The system boundary of the modeled system includes the dewatering, drying and pyrolysis

of sewage sludge, possible transportation and storage, power and heat generation and four different biochar applications. The energy for the pyrolysis was provided as electricity and thermal energy for the operation of the plant. In this study, the energy content of the pyrolysis gas and the pyrolysis liquid phase was too low to cover the demand for both sludge drying and pyrolysis, so additional energy from the combustion of biogas from sewage sludge digestion was used to provide the required process heat. This was particularly necessary for the start-up phase of the pyrolysis and the upstream drying process. For the utilization of the biochar the avoided burden approach was chosen to take into account the emissions of the processes replaced by the pyrolysis process chains. The use of biochar as a fuel replacing lignite or as a fertilizer replacing NPK fertilizers and peat was compared with the incineration and application of the fossil-based products. For a cascade use of biochar in the biogas process and in agriculture, the saving of maize silage due to the higher biogas yield with biochar was considered. The substitution of lignite was balanced by the energy content of biochar for co-incineration in lignite power plants using existing incineration capacities. The credits for peat in horticulture were calculated by weight, as well as the credits for the fertilizing properties of biochar, adjusted with equivalence factors. For the avoided NPK fertilization, the nutrient content of the biochar was counterbalanced. A total of four different utilization paths (S1-S4) were analyzed and compared with the benchmark process in terms of emissions (Figure 1).

2.2.3 Modeling Framework

As pyrolysis is not yet a market-penetrating technology for sewage sludge treatment, it is unlikely that the production and use of biochar as fuel or material will lead to structural changes in the fuel and fertilizer markets in the near future. Therefore, the current study is considered a microlevel decision support (type A) situation according to the ILCD guidelines where an attributional approach was applied in the assessment with generic data from the LCA databases of GaBi and ecoinvent for the background system. The foreground system includes the process-based model of dewatering, drying, pyrolysis and biochar utiliza-

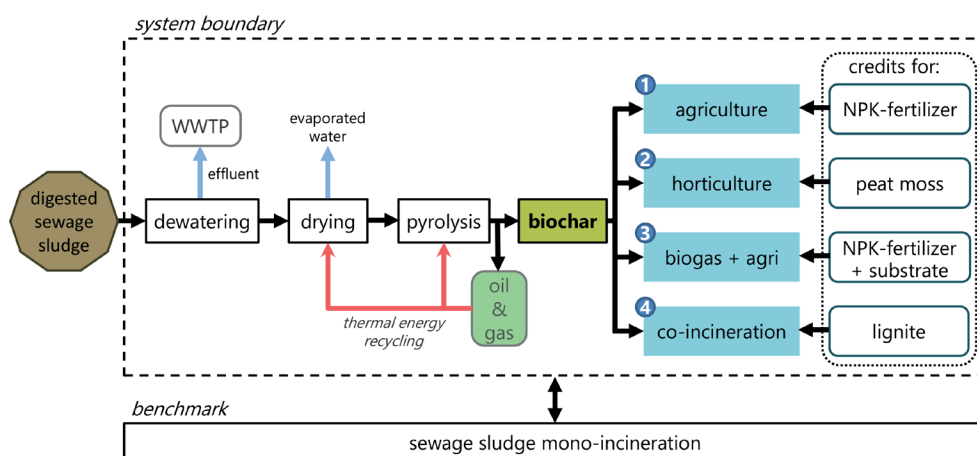


FIGURE 1: System boundary of the investigated sewage sludge to biochar process chains.

tion. Credits were accounted for cases of aggregated processes with substitution of commodities. The geographical framework of the LCA was the EU.

2.2.4 LCA-software and Life Cycle Inventory (LCI) data

The processes were modeled with the LCA software GaBi ts (Version 10, sphaera solutions GmbH, Leinfelden-Echterdingen, Germany). Life cycle inventory (LCI) datasets provided by GaBi and ecoinvent (v3.6) (Wernet et al., 2016) were used as data background. Some data concerning the dewatering, drying, pyrolysis and some auxiliary flows were either estimated, calculated or taken from the literature (see Table 1). The biochar characteristics for the LCI were adopted using the values of Table 2. Additional information on LCI data can be found in the supplementary material.

2.2.5 Life Cycle Impact Assessment (LCIA)

Life Cycle Impact Assessment (LCIA) was performed using the ReCiPe 2016 midpoint methodology, as implemented in GaBi ts. In this paper the focus is on GWP measured in kg CO₂ eq. (incl. biogenic carbon) with a Hierarchist (H) perspective, which is based on the most common policy principles and uses a medium time frame of 100 years (Huijbregts et al., 2017). In order to obtain a complete picture of the environmental impacts of sewage sludge pyrolysis, further LCIA categories were evaluated according to the

ReCiPe method: Stratospheric Ozone Depletion, Ionizing radiation, Fine Particulate Matter Formation, Freshwater Eutrophication, Freshwater Ecotoxicity, Marine Eutrophication, Marine Ecotoxicity, Terrestrial Acidification, Terrestrial Ecotoxicity, Fossil depletion and Human toxicity (cancer and non-cancer).

2.2.6 Assumptions and limitations

Due to the lack of data from users of sewage sludge-based biochar in an industrial scale, the material flows including transport routes, the weighting and use of modifications from generic data were determined on the basis of reasonable assumptions, data from pilot plants and literature. In addition, the geographical scope only includes energy mix data from the European Union and only four scenarios were modeled for the use of biochar and one scenario for the benchmark process of mono-incineration and ash landfilling without P recycling. The system boundary is limited to the treatment process after the anaerobic digestion and includes the construction and decommissioning of the pyrolysis plant, the actual pyrolysis process with the incineration of the gas and liquid phase and subsequent heat recovery for sludge drying and linked additional energy supply. Sludge generation processes in WWTP and subsequent sludge digestion were not in the scope of the study. The storage and transport of biochar by truck in the four different scenarios as well as the handling and credits

TABLE 2: Biochar characteristics.

Biochar Characteristics	Unit	Value	Source
C content	[kg kg ⁻¹]	0,134	(Breulmann et al., 2017; Paneque et al., 2017)
C _{labile} content	[%]	2	(Breulmann et al., 2017)
bulk density	[Mg m ⁻³]	0,2	(Breulmann et al., 2017)
calorific value	[MJ kg ⁻¹]	8,6	(Tomasi Morgano et al., 2018)
P content	[kg kg ⁻¹]	0,061	(Breulmann et al., 2017)
K content	[kg kg ⁻¹]	0,012	(Breulmann et al., 2017)
N content	[kg kg ⁻¹]	0,009	(Breulmann et al., 2017; Paneque et al., 2017)
Biochar application rate	[Mg ha ⁻¹]	20	estimated
As content	[mg kg ⁻¹]	14	(Song et al., 2014)
As leaching concentration	[mg kg ⁻¹]	3,2	(Song et al., 2014)
Zn content	[mg kg ⁻¹]	1784	(Song et al., 2014)
Zn leaching concentration	[mg kg ⁻¹]	6,4	(Song et al., 2014)
Pb content	[mg kg ⁻¹]	95,7	(Song et al., 2014)
Pb leaching concentration	[mg kg ⁻¹]	1,8	(Song et al., 2014)
Ni content	[mg kg ⁻¹]	61,5	(Song et al., 2014)
Ni leaching concentration	[mg kg ⁻¹]	0,3	(Song et al., 2014)
Cd content	[mg kg ⁻¹]	3,3	(Song et al., 2014)
Cd leaching concentration	[mg kg ⁻¹]	0,07	(Song et al., 2014)
Cr content	[mg kg ⁻¹]	58	(Song et al., 2014)
Cr leaching concentration	[mg kg ⁻¹]	0,2	(Song et al., 2014)
Cu content	[mg kg ⁻¹]	329	(Song et al., 2014)
Cu leaching concentration	[mg kg ⁻¹]	0,7	(Song et al., 2014)
PAH (sum)	[µg kg ⁻¹]	665	(Zielińska et al., 2016)

are included in the system. Where the handling of biochar was not the only activity associated with a process, e.g. the manufacturing of a tractor for use on a farm, the corresponding flows were either allocated (e.g. tractor) or neglected (e.g. potential adjustments to the biogas infrastructure). In general, it was estimated that 98% of the material and 95% of energy flows were captured in the model. Since sewage sludge is a very inhomogeneous material whose chemical and physical characteristics can vary greatly depending on regional, technical, and seasonal conditions (Twardowska et al., 2004), the most average possible values for the various material and energy flows as well as the biochar and by-products produced were used based on an extensive literature and industrial data research.

Therefore, the uncertainty for that kind of substrate is generally high. Since there is a large variety within the parameters, depending on the technical conditions in the wastewater treatment plant (high substrate diversity), the geographical conditions and the lack of data on the application of sewage sludge biochar on a large scale, the uncertainty is high in comparison to a specific (future) case, where sludge, pyrolysis and biochar parameters are well defined through industrial data and a pyrolysis treatment and a biochar utilization route are established. For the approach in this particular study where the goal was to cover a general European scope and not a specific WWTP and pyrolysis configuration, values out of many studies were conducted to specific aspects of the biochar and technical properties. Thus, the results of the LCA will also be subject to a high degree of uncertainty, which is immanent due to the different conditions and the chosen frame of reference. In addition, many of the generic inventories from the databases are representative of Global or German rather than European conditions, which, in turn decreases the certainty of model outcomes.

3. RESULTS AND DISCUSSION

3.1 Energy and material flows

The material flows of the entire process chain of treatment of digested sewage sludge and the thermal energy

flows of the pyrolysis process with thermal energy recovery were investigated to identify the most important processes and to determine possible options for their optimization. Regarding material flows, the largest mass loss was observed in the thickening process, where about 80% of the sludge mass can be reduced. In general, only very little of the initial sludge mass is treated by pyrolysis due to the high water content and the necessary pre-treatment for the pyrolysis process, which results in a total solids contents of over 80% in the dried sludge. About 2,3% of the input sludge mass ends up in the biochar and 3% in the oil and gas phase (Figure 2). Therefore a suitable pre-treatment leading to high total and volatile solids loads should be applied (Skinner et al., 2015) to achieve a good energetic performance of the pyrolysis and high biochar yields (Barry et al., 2019; Cao & Pawłowski, 2012). The treatment of the process water from the thickening process also requires an appropriate process to reduce the chemical oxygen demand (COD) and nitrogen load in the effluent with the aim to improve the environmental performance of the entire process chain (Gourdet et al., 2017). In general, a sludge mass reduction of 97% can be achieved over the entire process chain, which underlines its application as an efficient treatment process for volume reduction and increasing the transportability of the sewage sludge.

The analysis of the thermal energy flows of the pyrolysis process with energy recycling in the process itself and the upstream drying process shows that 86% of the thermal energy is used for water evaporation in the drying process (Figure 3). Around 52% of the total thermal energy required can be supplied by the combustion of the pyrolysis oils and gases, while 48% is supplied externally from biogas generated by the WWTP, which is also reflected in the results of Salman et al. (2019). Drying of the sludge can therefore be supported by the downstream treatment process with additional energy from the upstream digestion process. As the energy recovery potential is strongly influenced by the content of volatile solids in the sludge raw material, it would make sense to use primary and secondary sludge as substrate, but in general the combination of anaerobic

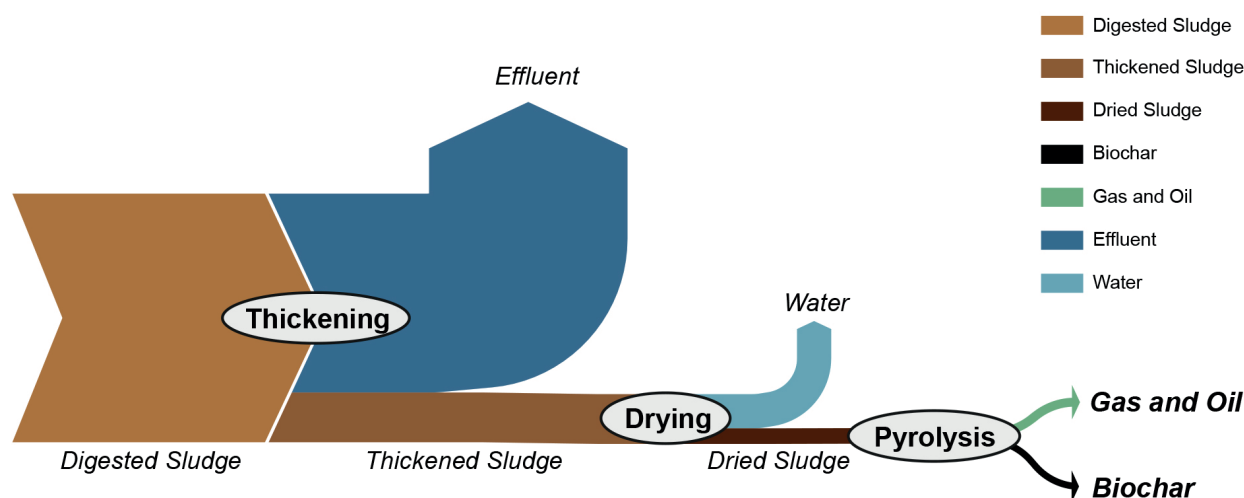


FIGURE 2: Material flows of sewage sludge thickening, drying and pyrolysis.

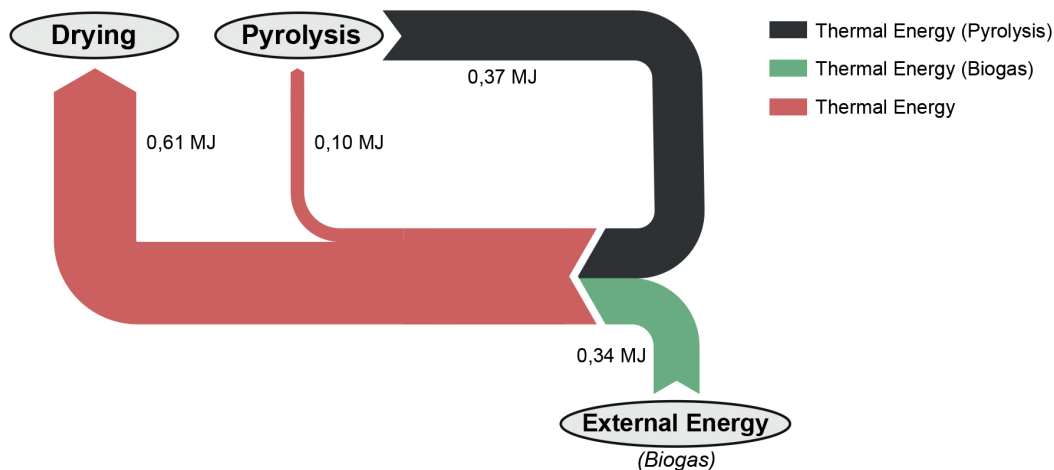


FIGURE 3: Thermal energy flows for the drying and pyrolysis of sewage sludge with an initial total solids content of 5%.

digestion and pyrolysis could achieve a higher energy efficiency compared to pyrolysis of untreated sludge (Cao & Pawłowski, 2012).

3.2 Benchmark process of sewage sludge mono-incineration

The benchmark process of sewage sludge digestate mono-incineration was based on a process from the ecoinvent database: [Jungbluth, N., treatment of digester sludge, municipal incineration, future, CH, Substitution, consequential, long-term]. The functional unit of the process refers to the mono-incineration of 1 kg of wet sludge with 5% dry solids and is therefore comparable to the results of the pyrolysis model. As commercial pyrolysis of sewage sludge has not yet reached a significant market share, a process adapted by ecoinvent with future emission reductions was chosen as a benchmark process. For the GWP this benchmarking process led to emissions of 7,5 g CO₂ eq./kg sewage sludge.

3.3 Overall GWP of sewage sludge pyrolysis and biochar application

The distributions of emissions for the sewage sludge treatment process with subsequent utilization scenarios of the biochar were analyzed to identify their environmental impact based on the GWP (Figure 4). Regarding the four biochar scenarios studied, horticultural use of biochar had the lowest net greenhouse gas (GHG) emissions of 1,6 g CO₂ eq./kg sewage sludge. The lignite-fired power plant scenario led to net emissions of 4,2 g CO₂ eq./kg sewage sludge and the scenario with cascade use of biochar resulted in total net emissions of 4,9 g CO₂ eq./kg sewage sludge. All these three scenarios had a lower GWP than the benchmark process of mono-incineration. The scenario of agricultural use of biochar had total emissions of 19,8 g CO₂ eq./kg sewage sludge. Credits for agricultural use of biochar are the lowest of all scenarios due to the relatively low impact of fossil-based fertilizers and the carbon sequestration potential of biochar compared to the substitution of fossil-based materials such as lignite or peat. In contrast to the findings, Mills et al. (2014) calculated a total

saving of 30,5 g CO₂ eq./kg sewage sludge with a slightly different system configuration and system boundary, mainly due to electricity generation credits from the pyrolysis process, whereas Li & Feng (2018) illustrated positive net emissions for a comparable system. Overall, the treatment of digested sewage sludge with dewatering, drying and pyrolysis resulted in emissions of around 25 g CO₂ eq./kg sewage sludge. The contribution of dewatering to the total emissions of the treatment was 29% and that of drying accounted for 57%. Emissions resulting from the pyrolysis process and the use of the generated liquids and gases for sludge drying contributed 14% of total treatment emissions. The emissions occurring during drying and dewatering underline the importance of the sludge water content for optimizing the environmental impact of the treatment process. The energy consumption for drying the dewatered sludge generates the greatest contribution to the energy demand of the whole process chain (Table 1) and to the CO₂ eq. emissions (Figure 4). As a wide range of energy consumption of dewatering technologies can be observed (Yoshida et al., 2013), an energetic optimisation option of the sludge pyrolysis process chain would be to increase the dry solids and carbon content of the digested sewage sludge with the most energy efficient dewatering technology before the drying process. Another option for further process improvements would be the co-pyrolysis of carbon-rich waste streams such as biowaste. Miller-Robbie et al. (2015) showed that combining agricultural application of sewage sludge with the addition of yard trimmings-biochar could reduce GHG emissions by sequestering carbon in the soil and avoiding fertilizer requirements.

In comparison to the mono-incineration of sewage sludge, the co-incineration of biochar in lignite power plants has a slightly lower emission potential of 4,2 g CO₂ eq./kg sewage sludge. However, due to the imminent phase-out of lignite-based electricity generation in the future and the associated reduction in co-combustion capacities, as well as the high emissions of the burned lignite, it does not make sense to pursue this utilization path further. In addition, the P concentration in the co-incineration ash would be further diluted and P could not be recycled as with material biochar use.

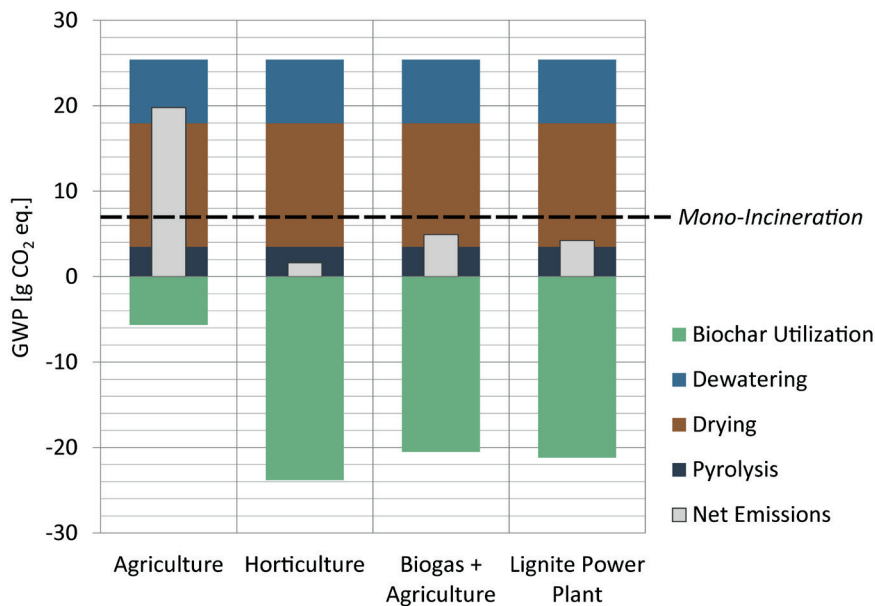


FIGURE 4: Global warming potential (GWP) of the four investigated scenarios of sewage sludge pyrolysis in comparison to the benchmark process.

3.4 GHG savings through biochar as a carbon sequestrator and nutrient recycler

Figure 5 shows the GHG emissions of the scenarios resulting from the application of biochar and the generated credits. The greatest amount of GHG reduction (19 g CO₂ eq./kg sewage sludge) was observed for the substitution of peat in horticulture. In the case of cascade use in a biogas plant and in agriculture, the substitution of maize silage due to the higher digestion performance (Yue et al., 2019) of 1% could achieve a saving of 15 g CO₂ eq./kg sewage sludge.

The carbon sequestration potential of biochar when used in agriculture or horticulture is relatively low at

2 g CO₂ eq./kg sewage sludge, as the stable carbon content of biochar from sewage sludge is also very low at around 13%. The carbon sequestration capacity of biochar could be increased by broadening the substrate spectrum, for example by using activated sludge for pyrolysis instead of digested sludge (Cao & Pawłowski, 2012). With around 4 g CO₂ eq./kg sewage sludge, the substitution of fossil-based NPK fertilizers contributed to the emission savings, mainly due to the P content of the biochar.

For the scenario of co-incineration of biochar in lignite-fired power plants, savings of 21 g CO₂ eq./kg sewage sludge were observed when energy from fossil lignite was substituted. In general, the contributions to emission re-

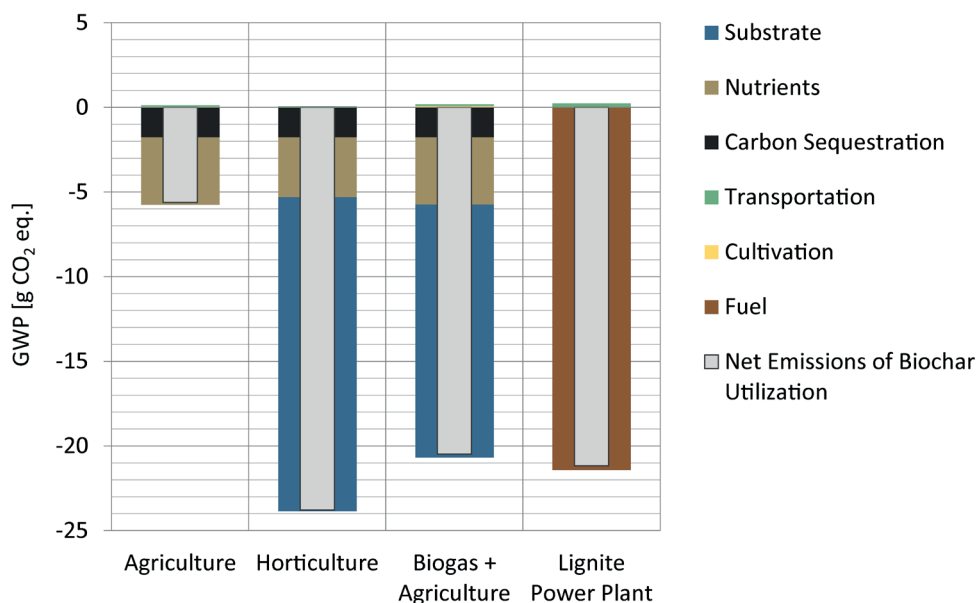


FIGURE 5: GHG emissions of different applications of biochar produced from 1 kg digested sewage sludge.

duction through carbon sequestration and P recycling of biochar are below the credits derived from replacing fossil materials such as lignite and peat. In all scenarios, the emissions caused by the transport and handling of biochar were comparably low. Furthermore, the results show that cascade use of biochar could increase the benefits compared to single use.

3.5 Results of other LCIA categories

To evaluate the overall environmental performance of the sewage sludge-to-biochar system, several LCIA categories in addition to GWP were evaluated and compared to the benchmark process. The net emissions for each scenario (S1-S4) are shown in Table 3 and the comparison with the benchmark process (100%) is illustrated in Figure 6.

Figure 6 shows the percentage of net emissions of the different scenarios compared to the benchmark. For all scenarios (S1-S4), results for impact categories regarding (terrestrial, freshwater and marine) ecotoxicity and (freshwater and marine) eutrophication were all lower than the benchmark impacts (0,1% to 40%), although nutrient flows and potential toxic contaminants like heavy metals and polycyclic aromatic hydrocarbons (PAH) were included in the model. In contrast, impacts on terrestrial acidification, ionizing radiation and stratospheric ozone depletion exceeded benchmark emissions up to 190%. Compared to the benchmark scenario, each scenario resulted in very low human toxicity (cancer), freshwater ecotoxicity and marine ecotoxicity potential, regardless of whether the biochar was used as a material or as an energy source (2-3%). The emissions contributing to this impact category depend mainly on the heavy metal content of the biochar and its re-solubility into the environment, but also on the relatively high loads of heavy metals (e.g. chromium) of the generic benchmark process in comparison. Non-cancer human toxicity results were also lower than the benchmark emissions in all scenarios. The category with the greatest differences within the scenarios was fossil depletion. For the substitu-

tion of lignite overall savings of -30% could be accounted while for the agricultural use (S1) and the combined biogas and agricultural use (S3) fossil depletion were higher than the baseline (170% and 157%) which was mainly due to the higher consumption of fossil fuels by agricultural activity (S1 and S3) and the substitution of lignite (S4). For terrestrial acidification, only S3 had lower emissions compared to the benchmark (71%) which can be explained with the credits from the saved maize cultivation. A similar pattern is also evident for stratospheric ozone depletion, where the biogas and agriculture scenario had a lower impact compared to the benchmark (62%). Only in this category the horticultural scenario (S2) performed the worst, resulting in the highest emissions of 146% compared to the benchmark.

In general, the cascade use of biochar in biogas plants and agriculture (S3) resulted in the lowest impact in most categories, with exception of GWP, ionizing radiation and fossil depletion. The horticulture scenario (S2) was the best in terms of GWP impacts and due to peat substitution, the fossil depletion potential was very low. Even the co-incineration scenario in lignite power plants (S4) in some categories can lead to lower impacts compared to the benchmark. This can be explained by the very poor environmental performance of lignite combustion for power generation compared with the European grid mix. However, the material use of biochar showed no environmental hotspot in critical categories for agricultural use such as eutrophication or ecotoxicity compared to the benchmark, although all potentially critical substance flows such as heavy metals and PAH were represented in the model. For example, the innovative use of biochar in a cascade to exploit multiple positive effects can achieve nutrient recycling while keeping the environmental impacts low.

3.6 Sensitivity analysis

Sensitivity analyses were conducted for (1) the electricity and thermal energy consumptions of the pyrolysis

TABLE 3: LCIA emissions of the investigated scenarios (S1-S4).

LCIA Category (ReCiPe, 2016)	Unit	Scenario				Benchmark
		Agri (S1)	Horti (S2)	Biogas + Agri (S3)	Lignite (S4)	Mono-Incineration
Global Warming Potential	[kg CO ₂ eq.]	1,98E-02	1,62E-03	4,91E-03	4,23E-03	7,45E-03
Fine Particulate Matter Formation	[kg PM _{2.5} eq.]	2,79E-05	2,52E-05	1,87E-05	2,83E-05	2,64E-05
Fossil Depletion	[kg oil eq.]	4,84E-03	6,73E-05	4,48E-03	-8,43E-04	2,85E-03
Freshwater Ecotoxicity	[kg 1,4 DB eq.]	8,46E-05	6,10E-05	3,92E-06	8,37E-05	2,81E-03
Freshwater Eutrophication	[kg P eq.]	1,01E-05	9,66E-06	8,11E-06	2,69E-05	6,69E-05
Ionizing Radiation	[Bq. Co-60 eq. to air]	7,45E-04	6,60E-04	7,14E-04	7,47E-04	3,94E-04
Marine Ecotoxicity	[kg 1,4 DB eq.]	1,10E-04	7,91E-05	1,52E-05	1,08E-04	3,39E-03
Marine Eutrophication	[kg N eq.]	5,51E-05	5,51E-05	4,42E-05	5,50E-05	1,56E-04
Stratospheric Ozone Depletion	[kg CFC-11 eq.]	1,10E-07	1,15E-07	4,86E-08	1,05E-07	7,86E-08
Terrestrial Acidification	[kg SO ₂ eq.]	1,07E-04	1,03E-04	5,06E-05	1,04E-04	7,17E-05
Terrestrial Ecotoxicity	[kg 1,4 DB eq.]	1,18E-02	8,15E-03	7,58E-03	7,19E-03	2,53E-02
Human Toxicity, cancer	[kg 1,4 DB eq.]	1,53E-04	1,17E-04	1,05E-04	1,52E-04	5,09E-03
Human Toxicity, non-cancer	[kg 1,4 DB eq.]	2,16E-02	2,06E-02	9,62E-03	1,37E-02	2,89E-02

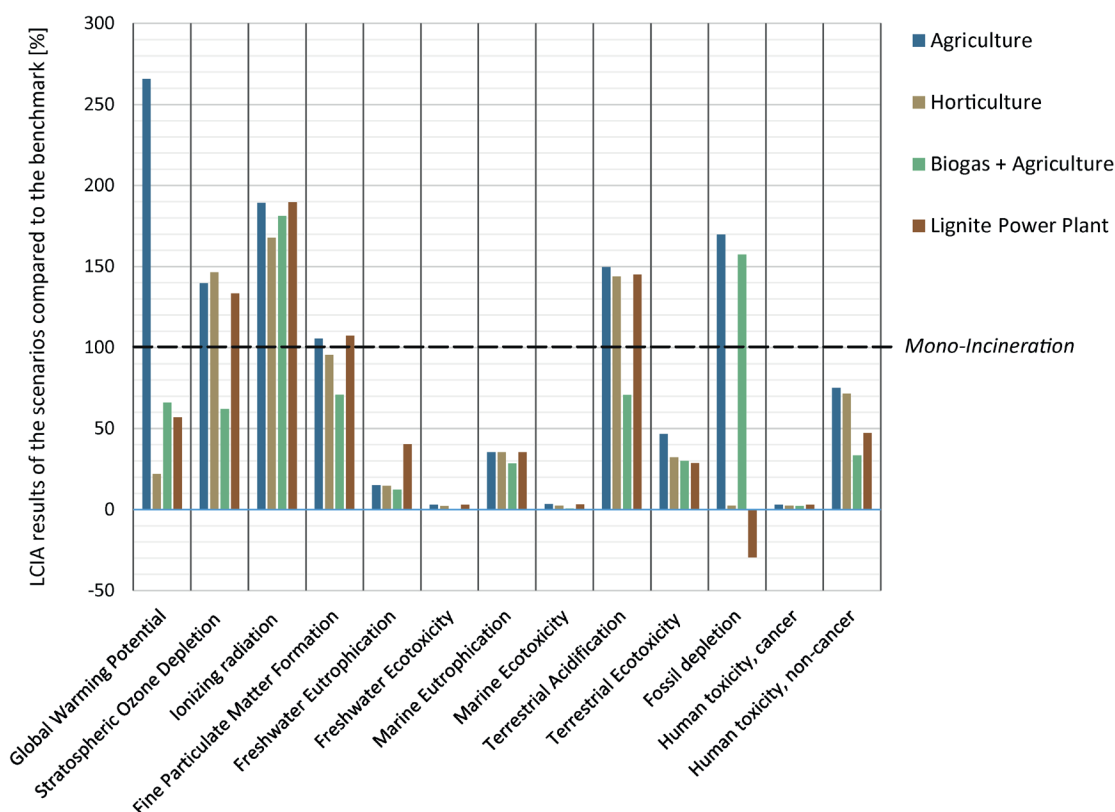


FIGURE 6: LCIA results of different biochar applications compared to the benchmark scenario of mono-incineration.

process, the drying step and the dewatering process, (2) the nutrients (N, P, and K), Carbon and heavy metals (Pb, Cd and Cr) contents of the biochar for the scenarios with material use of biochar (S1-S3) and (3) the calorific value of the biochar for scenario S4. Within the parameter variation, all other parameter values were the same as in the reference scenario or as in the baseline values in the scenarios S1-S4. Sensitivity of parameters changes ($\pm 10\%$) to LCIA results was conducted by comparing LCIA results with and without parameter changes. If the ratios are positive, the environmental impact increases with an increase in the parameter value and vice versa (see Supplementary Material, Table A.3, Table A.4, Table A.5, Table A.6 and Table A.7). Parameters with an absolute LCIA category change of less than 2,5% are considered insensitive. For the sake of clarity, only the results for the most sensitive parameters were explained further. Regarding the influence of the increased electricity demand of the pretreatment steps and pyrolysis, a small net emission increase of about 2,5% in the pyrolysis process and 3,3% in the drying process could only be found for fossil depletion and ionizing radiation, resulting from the generic electricity mix based on partially nuclear and fossil fuels electricity. The sensitivity of heat demand for the drying process indicates, that a minute variation can have a major effect on the resulting impacts, which was also revealed by Cao & Pawłowski (2013). For the GWP an increase of 8,4% and for fossil depletion an increase of 3,9% were determined for an heat demand increase of 10%. Other categories with a notable increase were marine ecotoxicity and marine

eutrophication (13,8% and 3,5%), freshwater eutrophication (3%), stratospheric ozone depletion (14,3%), fine particulate matter formation (13,9%) and terrestrial acidification (13,4%). In general, higher electricity and thermal energy demands resulted in higher emissions in the respective categories due to the associated emissions within the generic processes. In particular, the model is quite sensitive to the thermal energy input of the drying process. These results are consistent with earlier work from Li & Feng (2018), which found that the dewatering and drying processes also played a key role in the determination of the assessment results.

Results for the biochar characteristics variation (2) showed that only the C and P concentrations affected the categories GWP and fossil depletion in nearly all scenarios. In general, it was found that an increase in nutrient and carbon levels caused a reduction in emissions. This can be explained by the credits from the avoided product systems and the C sequestration properties of the biochar, although the C sequestration potential is highly variable and depends on the particular soil conditions and biochar substrates (Schmidt et al., 2018) and in some cases an increase in the C content of the biochar may even result in a lower C sequestration potential (Santín et al., 2017). In addition, Li & Feng (2018) showed that varying the VS/TS ratio, and thus the carbon content, in the feedstock sludge can lead to very different environmental impact profiles. An increase or decrease in leachable heavy metal contents had no significant effect on any category, also not to the toxicity-relevant.

The sensitivity regarding the calorific value of the biochar was high for GWP, fossil depletion, terrestrial acidification, terrestrial ecotoxicity and particulate matter formation where a 10% increase had a decrease in emissions of -56% to 56,0%, -8% to -8,0% and -3% to -3,0%. The main reason for that was the substitution of fossil-based energy from lignite. Since the modeled emissions from biochar are based on carbon content and not calorific value, there is greater uncertainty in the model regarding the energy use of biochar. For this reason, energy use was evaluated as a possible exception to the material utilization of biochar.

Other important assumptions concern substitution of products and processes, because avoided impacts often had a significant effect. Different choices concerning fertilizing properties or the mix and amount of electricity and thermal energy would have led to different results. In particular, the model is sensitive to the thermal energy input of the drying process and the C and especially P content of the biochar.

4. CONCLUSIONS

Energy and nutrient recovery from sewage sludge represents an important strategic lever for sustainable management of sewage sludge in an emerging bioeconomy. In this study, a LCA was conducted to determine whether pyrolysis is more sustainable than mono-incineration and whether biochar can be a sustainable form of fertilizer that simultaneously sequesters carbon. The results of the LCA show that substituting fossil based material and fuel (peat and lignite) with biochar has the highest potential to reduce the climate change impact of sewage sludge treatment. In comparison to the benchmark process of mono-incineration, the scenarios of biochar application in horticulture, biochar in cascade use in anaerobic digestion and agriculture and the energetic use in lignite power plant has lower emissions. The analyses of the material flows show that the main flows, which consist mainly of water, are separated before the pyrolysis process. Thus, the pyrolysis process can reduce the original sludge mass by 97%. It was also revealed that the energy flows of the pyrolysis process chain can achieve higher energy efficiency and lower emissions if thermal energy from the pyrolysis process can be recycled and biogas from the upstream anaerobic digestion process can be used in the sludge drying process. For the environmental performance exemplified in the GWP, the use of biochar as a material has a similar GHG saving potential than its use in existing fossil fuel based power plants. Especially if the biochar can be used in a cascade (S3), first in anaerobic digestion to improve process parameters and then in agriculture to sequester carbon and close the nutrient cycle, GHG savings can be generated. Remarkably, the use of biochar in agriculture without an additional utilization step (S1) has a lower GHG savings potential than the use in lignite-fired power plants (S4) and in horticulture (S2). The overall environmental impacts determined from the results of the other LCIA categories indicate that no potential hot spots were detected. In particular, for critical categories directly affected by biochar material use, such as ecotoxicity to environmental compartments, human tox-

icity or eutrophication, the analysis showed that all biochar use scenarios perform better than the benchmark. However, six categories perform worse than the benchmark for some scenarios: global warming potential, fossil depletion, terrestrial acidification, ionizing radiation, and stratospheric ozone depletion.

In general, improvements in LCIA methodology are needed in order to evaluate future benefits of the sludge treatment process and biochar utilization, such as recycling of nutrients and soil improvement aspects and general improvements like pathogen reduction. For biochar as a carbon sequestrator, a high carbon content in the untreated sludge is needed with suitable process settings of the pyrolysis. Further LCA studies should therefore be carried out with different input sludges and various volatile solids concentrations. With regard to the recyclability of P through the pyrolysis process, it was determined that almost the entire P content of the sludge is accumulated in the biochar. This could ensure an effective nutrient recycling without any further downstream treatment. Overall, the results show that in some cases, compared to the incineration of sewage sludge, it is possible to reduce GHG emissions while at the same time closing the P and (partially) the C cycles and minimizing environmental risks of potentially toxic substances like heavy metals or PAH.

ACKNOWLEDGEMENTS

This work was funded with federal state resources from the Ministry of Science and Culture of Lower Saxony in the framework of the program "Niedersächsisches Vorab". We would also like to thank Tobias Roether from the "3N Competence Center Lower Saxony Network Renewable Resources and Bioeconomy e.V." for the intensive and inspiring discussions during the development of the LCA model and the reviewers of this paper for their constructive comments, which helped to improve the quality of the paper.

REFERENCES

- Agrafioti, E., Bouras, G., Kalderis, D. & Diamadopoulos, E. (2013). Biochar production by sewage sludge pyrolysis. *Journal of Analytical and Applied Pyrolysis*, 101, 72–78. <https://doi.org/10.1016/j.jaap.2013.02.010>
- Alhashimi, H. A. & Aktas, C. B. (2017). Life cycle environmental and economic performance of biochar compared with activated carbon: A meta-analysis. *Resources, Conservation and Recycling*, 118, 13–26. <https://doi.org/10.1016/j.resconrec.2016.11.016>
- Bauer, T., Andreas, L., Lagerkvist, A. & Burgman, L. E. (2020). EFFECTS OF THE DIFFERENT IMPLEMENTATION OF LEGISLATION RELATING TO SEWAGE SLUDGE DISPOSAL IN THE EU. *Detritus*(10), 92–99. <https://doi.org/10.31025/2611-4135/2020.13944>
- Barry, D., Barbiero, C., Briens, C. & Berruti, F. (2019). Pyrolysis as an economical and ecological treatment option for municipal sewage sludge. *Biomass and Bioenergy*, 122, 472–480. <https://doi.org/10.1016/j.biombioe.2019.01.041>
- Breulmann, M., van Afferden, M., Müller, R. A., Schulz, E. & Fühner, C. (2017). Process conditions of pyrolysis and hydrothermal carbonization affect the potential of sewage sludge for soil carbon sequestration and amelioration. *Journal of Analytical and Applied Pyrolysis*, 124, 256–265. <https://doi.org/10.1016/j.jaap.2017.01.026>
- Bridle, T. R. & Pritchard, D. (2004). Energy and nutrient recovery from sewage sludge via pyrolysis. *Water Science and Technology*, 50(9), 169–175. <https://doi.org/10.2166/wst.2004.0562>

- Cao, Y. & Pawłowski, A. (2012). Sewage sludge-to-energy approaches based on anaerobic digestion and pyrolysis: Brief overview and energy efficiency assessment. *Renewable and Sustainable Energy Reviews*, 16(3), 1657–1665. <https://doi.org/10.1016/j.rser.2011.12.014>
- Cao, Y. & Pawłowski, A. (2013). Life cycle assessment of two emerging sewage sludge-to-energy systems: evaluating energy and greenhouse gas emissions implications. *Bioresource Technology*, 127, 81–91. <https://doi.org/10.1016/j.biortech.2012.09.135>
- Christodoulou, A. & Stamatelatos, K. (2016). Overview of legislation on sewage sludge management in developed countries worldwide. *Water science and technology: a journal of the International Association on Water Pollution Research*, 73(3), 453–462. <https://doi.org/10.2166/wst.2015.521>
- Cordell, D. & White, S. (2011). Peak Phosphorus: Clarifying the Key Issues of a Vigorous Debate about Long-Term Phosphorus Security. *Sustainability*, 3(12), 2027–2049. <https://doi.org/10.3390/su3102027>
- Denkert, R., Kopp, J., Meyer, H., Wolf, S., Ewert, W., Lou, U., Melsa, A., Roediger, M. & Sievers, M. (2013). Merkblatt DWA-M 366: Maschinelle Schlammbehandlung (2013. Aufl.). DWA-Merkblatt: M 366. Deutsche Vereinigung für Wasserwirtschaft Abwasser und Abfall.
- Deutsches Institut für Normung. (2009). Umweltmanagement - Ökobilanz - Grundsätze und Rahmenbedingungen: (ISO 14040:2006); deutsche und englische Fassung EN ISO 14040:2009 (Deutsche Norm DIN EN ISO 14040). Berlin.
- Egle, L., Rechberger, H., Krampe, J. & Zessner, M. (2016). Phosphorus recovery from municipal wastewater: An integrated comparative technological, environmental and economic assessment of P recovery technologies. *The Science of the total environment*, 571, 522–542. <https://doi.org/10.1016/j.scitotenv.2016.07.019>
- ELIQUO. (2020). ELoDry® sewage sludge drying technology. Retrieved from <https://www.eliquo-we.com/en/elodry.html>
- Elser, J. & Bennett, E. (2011). Phosphorus cycle: A broken biogeochemical cycle. *Nature*, 478(7367), 29–31. <https://doi.org/10.1038/478029a>
- Ennis, C. J., Evans, A. G., Islam, M., Ralebitso-Senior, T. K. & Senior, E. (2012). Biochar: Carbon Sequestration, Land Remediation, and Impacts on Soil Microbiology. *Critical Reviews in Environmental Science and Technology*, 42(22), 2311–2364. <https://doi.org/10.1080/10643389.2011.574115>
- Frísták, V., Pipiška, M. & Soja, G. (2018). Pyrolysis treatment of sewage sludge: A promising way to produce phosphorus fertilizer. *Journal of Cleaner Production*, 172, 1772–1778. <https://doi.org/10.1016/j.jclepro.2017.12.015>
- Gievers, F., Loewen, A. & Nelles, M. (2019). Hydrothermal Carbonization (HTC) of Sewage Sludge: GHG Emissions of Various Hydrochar Applications. In: L. Schebek, C. Herrmann, F. Cerdas (eds), *Sustainable Production, Life Cycle Engineering and Management. Progress in Life Cycle Assessment* (Bd. 142, P. 59–68). Springer International Publishing. https://doi.org/10.1007/978-3-319-92237-9_7
- Glaser, B. & Lehr, V.-I. (2019). Biochar effects on phosphorus availability in agricultural soils: A meta-analysis. *Scientific reports*, 9(1), 9338. <https://doi.org/10.1038/s41598-019-45693-z>
- Gourdet, C., Girault, R., Berthault, S., Richard, M., Tosoni, J. & Pradel, M. (2017). In quest of environmental hotspots of sewage sludge treatment combining anaerobic digestion and mechanical dewatering: A life cycle assessment approach. *Journal of Cleaner Production*, 143, 1123–1136. <https://doi.org/10.1016/j.jclepro.2016.12.007>
- Haupt, M. & Hellweg, S. (2019). Measuring the environmental sustainability of a circular economy. *Environmental and Sustainability Indicators*, 1–2, 100005. <https://doi.org/10.1016/j.indic.2019.100005>
- Huijbregts, M. A. J., Steinmann, Z. J. N., Elshout, P. M. F., Stam, G., Veronesi, F., Vieira, M., Zijp, M., Hollander, A. & van Zelm, R. (2017). ReCiPe2016: A harmonised life cycle impact assessment method at midpoint and endpoint level. *The International Journal of Life Cycle Assessment*, 22(2), 138–147. <https://doi.org/10.1007/s11367-016-1246-y>
- Jacobs, U., Fehr, G., Geyer, J., Heindl, A., Husmann, M., Kellermann, H.-G., Lehrmann, F., Ritterbusch, S., Schönfeld, R., Tomalla, M., Beatt, B., Hanßen, H., Haselwimmer, T., Hochsgürtel, H., Hüppe, P., Jasper, M., Kappa, S., Kristkeitz, R., Ludwig, P., Maurer, M., Pietsch, B.; Schmitt, P.; Six, J.; Stamer, F., Werther, J. (2019). Merkblatt DWA-M 379 Klärschlamm-trocknung (Entwurf) (2019. Aufl.). DWA-Regelwerk: Bd. 379. Deutsche Vereinigung für Wasserwirtschaft, Abwasser und Abfall.
- Leinweber, P., Bathmann, U., Buczko, U., Douhaire, C., Eichler-Löbermann, B., Frossard, E., Ekardt, F., Jarvie, H., Krämer, I., Kabbe, C., Lennartz, B., Mellander, P.-E., Nausch, G., Ohtake, H. & Tränckner, J. (2018). Handling the phosphorus paradox in agriculture and natural ecosystems: Scarcity, necessity, and burden of P. *Ambio*, 47(Suppl 1), 3–19. <https://doi.org/10.1007/s13280-017-0968-9>
- Li, H. & Feng, K. (2018). Life cycle assessment of the environmental impacts and energy efficiency of an integration of sludge anaerobic digestion and pyrolysis. *Journal of Cleaner Production*, 195, 476–485. <https://doi.org/10.1016/j.jclepro.2018.05.259>
- Marazza, D., Macrelli, S., D'Angeli, M., Righi, S., Hornung, A. & Contin, A. (2019). Greenhouse gas savings and energy balance of sewage sludge treated through an enhanced intermediate pyrolysis screw reactor combined with a reforming process. *Waste management*, 91, 42–53. <https://doi.org/10.1016/j.wasman.2019.04.054>
- Mayer, B. K., Baker, L. A., Boyer, T. H., Drechsel, P., Gifford, M., Hanjra, M. A., Parameswaran, P., Stoltzfus, J., Westerhoff, P. & Rittmann, B. E. (2016). Total Value of Phosphorus Recovery. *Environmental science & technology*, 50(13), 6606–6620. <https://doi.org/10.1021/acs.est.6b01239>
- Méndez, A., Terradillos, M. & Gascó, G. (2013). Physicochemical and agronomic properties of biochar from sewage sludge pyrolysed at different temperatures. *Journal of Analytical and Applied Pyrolysis*, 102, 124–130. <https://doi.org/10.1016/j.jaap.2013.03.006>
- Miller-Robbie, L., Ulrich, B. A., Ramey, D. F., Spencer, K. S., Herzog, S. P., Cath, T. Y., Stokes, J. R. & Higgins, C. P. (2015). Life cycle energy and greenhouse gas assessment of the co-production of biosolids and biochar for land application. *Journal of Cleaner Production*, 91, 118–127. <https://doi.org/10.1016/j.jclepro.2014.12.050>
- Mills, N., Pearce, P., Farrow, J., Thorpe, R. B. & Kirkby, N. F. (2014). Environmental & economic life cycle assessment of current & future sewage sludge to energy technologies. *Waste management*, 34(1), 185–195. <https://doi.org/10.1016/j.wasman.2013.08.024>
- Paneque, M., Knicker, H., Kern, J. & La Rosa, J. M. de (2019). Hydrothermal Carbonization and Pyrolysis of Sewage Sludge: Effects on Lolium perenne Germination and Growth. *Agronomy*, 9(7), 363. <https://doi.org/10.3390/agronomy9070363>
- Paneque, M., La Rosa, J. M. de, Kern, J., Reza, M. T. & Knicker, H. (2017). Hydrothermal carbonization and pyrolysis of sewage sludges: What happen to carbon and nitrogen? *Journal of Analytical and Applied Pyrolysis*, 128, 314–323. <https://doi.org/10.1016/j.jaap.2017.09.019>
- Paz-Ferreiro, J., Nieto, A., Méndez, A., Askeland, M. P. J. & Gascó, G. (2018). Biochar from Biosolids Pyrolysis: A Review. *International journal of environmental research and public health*, 15(5). <https://doi.org/10.3390/ijerph15050956>
- Peccia, J. & Westerhoff, P. (2015). We Should Expect More out of Our Sewage Sludge. *Environmental science & technology*, 49(14), 8271–8276. <https://doi.org/10.1021/acs.est.5b01931>
- PYREG. (2020). sewage sludge. Retrieved from https://www.pyreg.de/wp-content/uploads/2020_pyreg_brochure_sludge_EN.pdf
- Salman, C. A., Schwede, S., Thorin, E., Li, H. & Yan, J. (2019). Identification of thermochemical pathways for the energy and nutrient recovery from digested sludge in wastewater treatment plants. *Energy Procedia*, 158, 1317–1322. <https://doi.org/10.1016/j.egypro.2019.01.325>
- Samolada, M. C. & Zabaniotou, A. A. (2014). Comparative assessment of municipal sewage sludge incineration, gasification and pyrolysis for a sustainable sludge-to-energy management in Greece. *Waste management (New York, N.Y.)*, 34(2), 411–420. <https://doi.org/10.1016/j.wasman.2013.11.003>
- Santín, C., Doerr, S. H., Merino, A., Bucheli, T. D., Bryant, R., Ascough, P., Gao, X. & Masiello, C. A. (2017). Carbon sequestration potential and physicochemical properties differ between wildfire charcoals and slow-pyrolysis biochars. *Scientific reports*, 7(1), 11233. <https://doi.org/10.1038/s41598-017-10455-2>
- Schmidt, H.-P., Anca-Couce, A., Hagemann, N., Werner, C., Gerten, D., Lucht, W. & Kammann, C. (2018). Pyrogenic carbon capture and storage. *GCB Bioenergy*, 38(1), 215. <https://doi.org/10.1111/gcbb.12553>
- Schoumans, O. F., Bouraoui, F., Kabbe, C., Oenema, O. & van Dijk, K. C. (2015). Phosphorus management in Europe in a changing world. *Ambio*, 44 Suppl 2, 92. <https://doi.org/10.1007/s13280-014-0613-9>
- Skinner, S. J., Studer, L. J., Dixon, D. R., Hillis, P., Rees, C. A., Wall, R. C., Cavalida, R. G., Usher, S. P., Stickland, A. D. & Scales, P. J. (2015). Quantification of wastewater sludge dewatering. *Water research*, 82, 2–13. <https://doi.org/10.1016/j.watres.2015.04.045>

- Song, X. D., Xue, X. Y., Chen, D. Z., He, P. J. & Dai, X. H. (2014). Application of biochar from sewage sludge to plant cultivation: Influence of pyrolysis temperature and biochar-to-soil ratio on yield and heavy metal accumulation. *Chemosphere*, 109, 213–220. <https://doi.org/10.1016/j.chemosphere.2014.01.070>
- Teoh, S. K. & Li, L. Y. (2020). Feasibility of alternative sewage sludge treatment methods from a lifecycle assessment (LCA) perspective. *Journal of Cleaner Production*, 247, 119495. <https://doi.org/10.1016/j.jclepro.2019.119495>
- Tomasi Morgano, M., Leibold, H., Richter, F., Stapf, D. & Seifert, H. (2018). Screw pyrolysis technology for sewage sludge treatment. *Waste management (New York, N.Y.)*, 73, 487–495. <https://doi.org/10.1016/j.wasman.2017.05.049>
- Twardowska, I., Schramm, K.-W. & Berg, K. (2004). Sewage sludge. In I. Twardowska (Hg.), *Waste Management Series. Solid Waste: Assessment, Monitoring and Remediation* (Bd. 4, S. 239–295). Elsevier. [https://doi.org/10.1016/S0713-2743\(04\)80013-8](https://doi.org/10.1016/S0713-2743(04)80013-8)
- van Wesenbeeck, S., Prins, W., Ronsse, F. & Antal, M. J. (2014). Sewage Sludge Carbonization for Biochar Applications. *Fate of Heavy Metals. Energy & Fuels*, 28(8), 5318–5326. <https://doi.org/10.1021/ef500875c>
- Wernet, G., Bauer, C., Steubing, B., Reinhard, J., Moreno-Ruiz, E. & Weidema, B. (2016). The ecoinvent database version 3 (part I): Overview and methodology. *The International Journal of Life Cycle Assessment*, 21(9), 1218–1230. <https://doi.org/10.1007/s11367-016-1087-8>
- Yoshida, H., Christensen, T. H. & Scheutz, C. (2013). Life cycle assessment of sewage sludge management: a review. *Waste management & research: the journal of the International Solid Wastes and Public Cleansing Association, ISWA*, 31(11), 1083–1101. <https://doi.org/10.1177/0734242X13504446>
- Yue, X., Arena, U., Chen, D., Lei, K. & Dai, X. (2019). Anaerobic digestion disposal of sewage sludge pyrolysis liquid in cow dung matrix and the enhancing effect of sewage sludge char. *Journal of Cleaner Production*, 235, 801–811. <https://doi.org/10.1016/j.jclepro.2019.07.033>
- Zielińska, A. & Oleszczuk, P. (2016). Effect of pyrolysis temperatures on freely dissolved polycyclic aromatic hydrocarbon (PAH) concentrations in sewage sludge-derived biochars. *Chemosphere*, 153, 68–74. <https://doi.org/10.1016/j.chemosphere.2016.02.118>

POTENTIALS AND COSTS OF VARIOUS RENEWABLE GASES: A CASE STUDY FOR THE AUSTRIAN ENERGY SYSTEM BY 2050

Daniel C. Rosenfeld *, Johannes Lindorfer, Hans Böhm, Andreas Zauner and Karin Fazeni-Fraisl

Energieinstitut an der Johannes Kepler Universität Linz, Altenberger Straße 69, 4040 Linz, Austria

Article Info:

Received:
24 March 2021
Revised:
3 August 2021
Accepted:
23 August 2021
Available online:
30 September 2021

Keywords:

Anaerobic digestion
Power-to-gas
Gas greening
Biomass gasification
Technoeconomic analysis

ABSTRACT

This analysis estimates the technically available potentials of renewable gases from anaerobic conversion and biomass gasification of organic waste materials, as well as power-to-gas (H₂ and synthetic natural gas based on renewable electricity) for Austria, as well as their approximate energy production costs. Furthermore, it outlines a theoretical expansion scenario for plant erection aimed at fully using all technical potentials by 2050. The overall result, illustrated as a theoretical merit order, is a ranking of technologies and resources by their potential and cost, starting with the least expensive and ending with the most expensive. The findings point to a renewable methane potential of about 58 TWh per year by 2050. The highest potential originates from biomass gasification (~49 TWh per year), while anaerobic digestion (~6 TWh per year) and the power-to-gas of green CO₂ from biogas upgrading (~3 TWh per year) demonstrate a much lower technical potential. To fully use these potentials, 870 biomass gasification plants, 259 anaerobic digesters, and 163 power-to-gas plants to be built by 2050 in the full expansion scenario. From the cost perspective, all technologies are expected to experience decreasing specific energy costs in the expansion scenario. This cost decrease is not significant for biomass gasification, at only about 0.1 €-cent/kWh, resulting in a cost range between 10.7 and 9.0 €-cent/kWh depending on the year and fuel. However, for anaerobic digestion, the cost decrease is significant, with a reduction from 7.9 to 5.6 €-cent/kWh. It is even more significant for power-to-gas, with a reduction from 10.8 to 5.1 €-cent/kWh between 2030 and 2050.

1. INTRODUCTION

The major challenge of this century is climate change. To tackle this challenge, it is necessary to find measures to limit the temperature rise to a maximum of 2°C, or even 1.5°C in an optimal case (Gao et al., 2017). Therefore, it is necessary to significantly reduce global CO₂ emissions and reach, at a minimum, carbon neutrality within the next 20 to 30 years.

On a European scale, in 2011, the European Union published a "roadmap for moving to a competitive low-carbon economy in 2050." This roadmap aims for a greenhouse gas emission reduction of 80% to 95% by 2050 (European Commission, 2011). In 2019, the European Union published "new green deal" priority energy efficiency measures. However, these measures further include the substitution of 72% of current fossil-based energy by renewable energy since this amount cannot be reduced by efficiency measures (European Commission, 2019). This goal could be reached by either electrification using renewable electricity

or substitution with a renewable alternative such as fossil natural gas with synthetic natural gas (SNG). This action plans to reach net carbon neutrality by 2050 are mainly being carried out on a national basis.

The objective of the current program of the Austrian Federal Government is to provide 100% of Austria's electricity supply from renewable energy sources by 2030. Doing so requires an increase in renewable electricity generation of 27 TWh in total (11 TWh photovoltaic, 10 TWh wind power, 5 TWh hydropower, and 1 TWh biomass). Regarding gas supply, an expansion and support program is planned to promote the production of renewable gas (i.e., biomethane, green hydrogen, and SNG based on renewable electricity) by 2030. The aim is to feed 5 TWh of "green gas" into the natural gas grid by 2030. A full decarbonization of the Austrian economy, aiming for carbon neutrality, should be reached by 2040 (Republik Österreich, 2020). Therefore, the Austrian natural gas demand – 87.2 TWh in 2018 (British Petroleum p.l.c, 2019) – must be reduced and fully substituted by renewables.

* Corresponding author:
Daniel C. Rosenfeld
email: rosenfeld@energieinstitut-linz.at

However, as of today only 3,000 Nm³/h biomethane from 15 biomethane plants is fed into the gas grid (Kompost & Biogas Verband Österreich, 2021). With annual full load hours of 8,000 h per year and a lower heating value (LHV) of 9.944 kWh/Nm³, this would correspond to about 239 GWh/a. Therefore, only about 0.2% of today's natural gas demand can be provided from biomethane. This example shows that fossil energy carriers must be reduced drastically, while renewable ones must be used in larger quantities. This means that the electrification rate of the industrial, household, and mobility sectors should be increased while simultaneously reducing dependency on fossil energy carriers (Schiffer & Manthiram, 2017). Furthermore, renewable methane could serve as a bridge to the full electrification of private households. Nevertheless, some industries rely on carbon-containing energy carriers such as natural gas as part of their processes; an example is the chemical industry (Lechtenböhmer et al., 2016). Therefore, it is necessary to produce renewable methane to fulfill the need for carbon in industrial routes or for high energy density demands, such as in aviation.

This results in many studies focusing on the potential of bioenergy and renewable methane. Mostly on a national scale. (Steubing et al., 2010) conducted, that about 7 % of the Switzerland energy demand could be covered by bioenergy. Another study, focusing on Swiss manure potentials stated that about 250 GJ gross biogas per year (corresponding to about 69 MWh per year) could be produced resulting in a GHG reduction of 159 kt of CO₂,eq. (Burg et al., 2018). A study for turkey has shown that about 2.14 billion Nm³ per year (corresponding to about 21 TWh per year) of biomethane could be produced from cattle and sheep manure till 2026 (Melikoglu & Menekse, 2020). Many similar studies for different other countries were conducted in the past years. (Wang et al., 2018) analyzed the biomethane potential from slaughterhouse wastes in the US. (O'Shea, Wall, McDonagh, et al., 2017) is one of only a few studies that has not focused on one source in detail, but combined industries, waste water treatment and power-to-gas for renewable methane production in Ireland. Another study of the same year (O'Shea, Wall, Kilgallon, et al., 2017) focused on the theoretical potential of biomethane from different biogenic sources and combined the potential study with an economic analysis. Another study for Ireland has focused on the bio-SNG potential from waste and residues. It was conducted that about 10.18 PJ Bio-SNG per year (corresponding to about 2.8 TWh per year) could be produced in Ireland (Singlitico et al., 2018).

For Austria there are several recent studies focusing on the renewable methane potentials. (Daniel C Rosenfeld et al., 2020) stated a theoretical production potential of 900 million Nm³ per year (corresponding to about 8.9 TWh) of biomethane from anaerobic digestion of organic waste materials and also includes the potential recovery of P and N. (Dißbauer et al., 2019) focused on renewable methane production of woody biomass and organic wastes via biomass gasification. For the year 2050 the study has shown a theoretical potential of renewable methane of 10 billion Nm³ per year (corresponding to 99 TWh per year). The realizable potential was calculated with 4 billion Nm³ per

year (corresponding to 40 TWh per year). Furthermore, the study included a cost perspective for renewable methane from gasification showing specific production costs of 4.3 to 5.5 €-cent per kWh.

As shown by this overview most studies either focus only on the potential or the cost analysis. If in only a few cases the cost perspective is combined with a potential analysis, the study focuses only on one technology. Furthermore, studies like (Dißbauer et al., 2019) and (O'Shea, Wall, Kilgallon, et al., 2017) have shown that currently the most relevant hurdles for renewable energy systems are their corresponding costs, which is one reason for the slow transition from fossil to sustainable energy. Therefore, studies that investigate future potentials must include cost structures and the economic impact of renewable energy systems. Furthermore, for a better understanding of the energy sector transition studies that evaluate the combination of different technologies to fully use the potential for renewable methane production are beneficial.

Within this work the technically available potentials for green gases from anaerobic conversion and biomass gasification of organic waste materials, and power-to-gas (H₂ and SNG based on renewable electricity) for Austria, as well as their approximate energy production costs, and quantifies their economic effects on the Austrian energy system were analyzed. Aim of the work is therefore to provide a broad overview of potential renewable gas production routes. Furthermore, to have a sustainable system, the substrates for gasification and anaerobic digestion are limited to waste streams. This allows for a sustainable and future fit overview of renewable methane potentials till 2050.

To do so this work includes three types of analyses. First, a potential analysis was carried out for the methane production potential from anaerobic digestion and biomass gasification from organic waste materials, as well as power-to-gas. Subsequently, a technoeconomic analysis was conducted to gather information about the costs of the different potential types. Finally, an expansion scenario for the plants was created to fully exploit all potentials by 2050.

2. METHODOLOGY

2.1 Description of the Analyzed System

This work focuses on the renewable methane generation potential of biogenic (waste) streams in Austria. For this analysis, data concerning the anaerobic digestion potential of residual and waste materials and biomass for dual fluidized gasification were extracted from existing literature (Bundesanstalt für Agrarwirtschaft, 2016; Bundesministerium Nachhaltigkeit und Tourismus, 2019; FNR, 2013; Reisinger, 2012; Universität Rostock, 2007).

Three technology pathways were investigated for the purpose of developing a full renewable methane generation potential. Waste streams with high moisture content that are well suited for anaerobic digestion should be used for biomethane generation. The biogenic CO₂ that is separated from the biogas as part of the gas cleaning (including also cleaning steps like moisture and H₂S separation) to reach biomethane in grid quality (CH₄ ≥ 96% (ÖVGW, 2011)) should be further processed with a power-to-gas approach.

In general, the separation step could be avoided by adding the cleaned biogas (that only includes CH₄ and CO₂) directly to the power-to-gas plant. However, e.g. higher volume flows or the operational systems linkage are potential associated problems to solve. While it is expected, that efficient biomethane plants are operated with more than 8,000 hours per year, power-to-gas plants utilizing fluctuating renewable electricity production typically would operate with only about 3,500 hours per year. Therefore, a storage of either the biogas or only the CO₂ is necessary for optimal operation. Since it is desirable to have the highest possible baseload capacity for renewable methane, this work considers a CO₂ storage instead of a biogas storage. This allows production of the maximum amount of renewable methane from organic waste. Furthermore, lignocellulosic biomass streams should be used for conversion to SNG, with a dual fluidized bed gasifier coupled with a methanation unit for syngas upgrading. Figure 1 shows the analyzed technology pathways as well as their potential fields of application.

2.2 Potential Analysis

According to (Batidzirai et al., 2012), the theoretical, technical, economic, and sustainable potential (see Fig-

ure 2) can be differentiated. The highest potential comes from the theoretical potential since it includes all available quantities without considering technical or economic feasibilities of exploitation (Thrän et al., 2013). The technical potential is reduced by technical constraints such as salvage rates and technical restrictions (Brosowski et al., 2015). The economic potential is further decreased since it only includes the economically feasible potential (Umweltveränderungen, 2009). In this work, the technical potential of biomethane production from the organic waste fraction and its synergy with power-to-gas technology is evaluated, as well as the SNG production potential from biomass gasification, as described in the previous section.

An overview of the reduction factors for calculating the technical potential is shown in Table 1.

The technical potential ($P_{\text{technical}}$) is calculated by applying the ratio of technical to theoretical potential (p) to the theoretical potential ($P_{\text{theoretical}}$) as described in Equation 1. The index n represents the substrate category that is calculated.

$$P_{\text{technical},n} = P_{\text{theoretical},n} * p_n \quad (1)$$

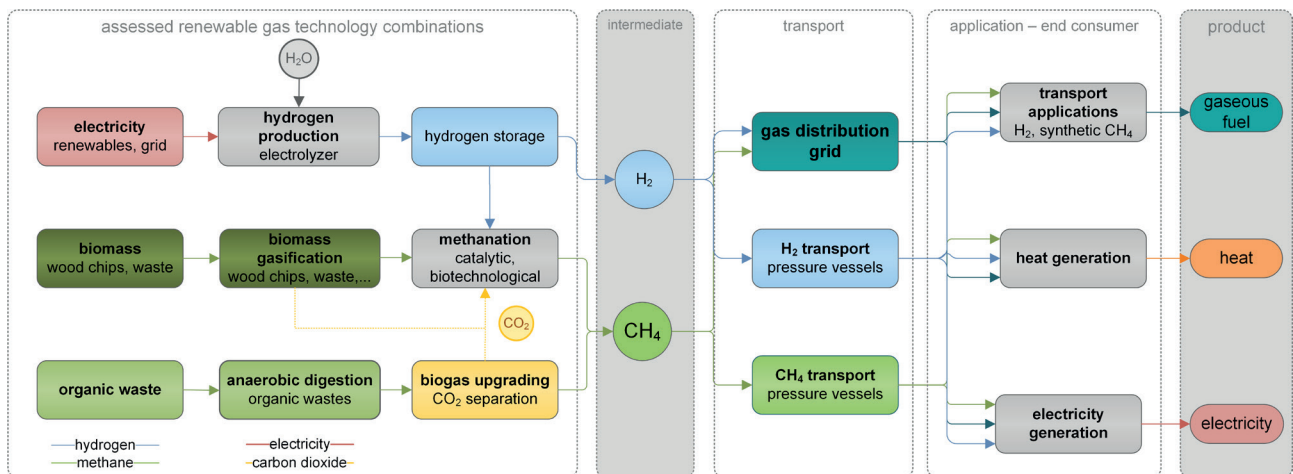


FIGURE 1: Renewable gas pathways (Daniel C. Rosenfeld, 2020).

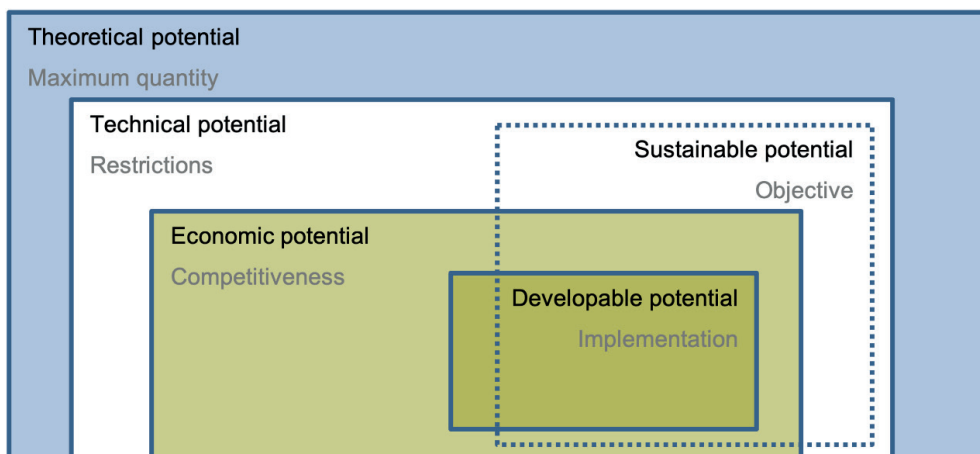


FIGURE 2: Schematic overview of types of potentials (Steubing et al., 2010).

TABLE 1: Technical potential characteristics for biomethane from organic waste.

Substrate	Ratio of technical to theoretical potential	Source
Farm manure ^a	70%	(Erler et al., 2013)
Straw ^b	30%	(Erler et al., 2013)
Beet leaves ^c	20%	(Erler et al., 2013)
Biowaste from households ^d	90%	(Erler et al., 2013)
Bush, grass and tree cuttings ^e	90%	(Erler et al., 2013)
Sewage sludge ^f	50%	Own assumption
Food fats and oils ^g	60%	Own assumption
Garden composting ^h	0%	Own assumption

^a The share of technical potential considers storage and withdrawal losses as well as livestock housing rates. In addition, only farms with more than 50 life stock unit (LSU) were considered.

^b The share of technical potential takes into account the long-term preservation of soil fertility, salvage quotas, and existing straw uses in livestock farming and horticulture.

^c Technical potential is equal to salvage quota.

^d Technical potential takes into account storage and transport losses; this fraction is additionally subtracted from the theoretical potential.

^e For the quantities of green waste already collected today, 90% is also assumed for the technical potential, based on the biowaste material.

^f It one assumes that about 50% of the sewage sludge from wastewater treatment plants with a capacity greater than a population equivalent of 60 is available as the technical potential.

^g The survey includes the quantities that are already collected today.

^h It is assumed that the connection rate to the organic waste collection in the municipalities will increase by 2040. In the long term, home garden composting will therefore be merged with biogenic waste, and, by 2040, this biogenic waste will also gradually become usable for anaerobic digestion. However, the potential is still theoretical.

2.2.1 Biomethane Potential

To estimate the technical biomethane yield potential, as a first step, all usable residue flows in Austria were identified. Subsequently, the theoretical biomethane yield potential for Austria was calculated on the basis of biomethane yield factors for the different waste fractions. The exact values that were used in the calculation can be found in the supplementary materials.

The selected waste streams that were considered were manure, straw, waste from food production, biowaste from households, green cuttings, food and kitchen waste, and sewage sludge. Waste food in residual waste and garden composting was considered as well but assumed to be zero for the technical potential since these categories cannot be gathered technically. In terms of agricultural facilities, it was assumed that cow, poultry, pig, and horse manure without straw could be gathered only during winter months since in summer months animals are likely held outside and gathering is not feasible. Furthermore, only agricultural facilities with more than 50 livestock animals were considered in this study since it is difficult to collect manure at sites with fewer livestock animal. In terms of straw, only cereal, maize, and rape straw, as well as beet leaves, were considered since other types of straw do not exist in sufficient amounts in Austria.

These waste streams are then fed to a biomethane plant based on anaerobic digestion. Depending on the waste stream, different biomethane yields can be attained via this biochemical process. As depicted in Table 2, sewage sludge has the highest biomethane production value,

TABLE 2: Methane and biogas production rates.

Substrate	Methane production rate	Biogas production rate	Methane share	Source
Manure				
Cow dung		60 Nm ³ / t _{DM}	60 vol.-%	(LFL, 2019)
Pig dung		60 Nm ³ / t _{DM}	60 vol.-%	(LFL, 2019)
Pig manure		20 Nm ³ / t _{DM}	60 vol.-%	(LFL, 2019)
Poultry manure		80 Nm ³ / t _{DM}	60 vol.-%	(LFL, 2019)
Horse manure w/o straw		60 Nm ³ / t _{DM}	60 vol.-%	(LFL, 2019)
Straw				
Cereal straw		331 Nm ³ / t _{DM}	51 vol.-%	(LFL, 2019)
Maize straw		331 Nm ³ / t _{DM}	51 vol.-%	(LFL, 2019)
Rape straw		187 Nm ³ / t _{DM}	52 vol.-%	(LFL, 2019)
Beet leaves	105 Nm ³ / t _{DM}			(FNR, 2013)
Waste from food production	145 Nm ³ / t _{DM}			(Reisinger, 2012; Universität Rostock, 2007)
Other biogenic waste				
Municipal garden and park waste	105 Nm ³ / t _{DM}			(FNR, 2013)
Cemetery waste	105 Nm ³ / t _{DM}			(FNR, 2013)
Roadside vegetation	105 Nm ³ / t _{DM}			(FNR, 2013)
Kitchen and food waste	164 Nm ³ / t _{DM}			(Alibardi & Cossu, 2015)
Biowaste from households	185 Nm ³ / t _{DM}			(KTBL, 2008)
Bush, grass, and tree cuttings	105 Nm ³ / t _{DM}			(FNR, 2013)
Sewage sludge	312 Nm ³ / t _{DM}			(Kuo & Dow, 2017)

while manure has the lowest value, depending on the category.

To calculate the biomethane potential ($P_{m,x}$), the production rates for biomethane ($pr_{\text{biomethane}}$) are applied to the substrate potentials ($P_{s,x}$) where x stands either for the theoretical or technical potential (see Equation 2).

$$P_{m,x,n} = pr_{\text{biomethane},n} * P_{s,x,n} \quad (2)$$

The production rates for biomethane are substrate depending and can be calculated by combining the production rate of biogas (pr_{biogas}) with its biomethane content ($x_{\text{biomethane}}$) as shown in Equation 3.

$$pr_{\text{biomethane},n} = pr_{\text{biogas},n} * x_{\text{biomethane},n} \quad (3)$$

2.2.2 Power-to-Gas

Another potential resource available for biochemical methane production is CO_2 from biogenic sources. This potential resource can be used for a power-to-gas approach. Here, H_2 is produced from renewable electricity via electrolysis to further methanate H_2 with CO_2 to produce SNG. Therefore, this form of sector coupling is perfectly suited to further increasing methane yields from biogenic waste. To accomplish this, 2.75 kg of CO_2 and 0.5 kg of H_2 are needed for the production of 1 kg of SNG. For a more detailed overview of power-to-gas technology, see (Götz et al., 2016; Steinmüller et al., 2014).

2.2.3 Biomass Gasification

In the field of thermochemical conversion of biomass (gasification), residues mainly from the categories of firewood, bark, sawmill byproducts, and woodchips were considered for utilization in the thermochemical gasification process. The theoretical potential in the categories of firewood, woodchips, and bark comprises the total amount of biomass that grows annually in Austria (Dißauer et al., 2019). The theoretical potential in the sawmill byproducts category comprises 100% of the residual biomass stream generated in sawmills (Dißauer et al., 2019). Recovery pathways for wood are very well established in Austria, as is shown in the current wood flow diagram (Strimitzer & Höher, 2020). Therefore, estimation of a feasible potential of available wood for biomass gasification is mainly about avoiding competing uses. In determining the realizable potential, this study is guided by the assumptions from (Dißauer et al., 2019): the authors assume that 50% of the unused increment of biomass is available for gasification under the assumption that the structure of wood use in industrial sectors will remain constant in the future. The reason for the 50% reduction (apart from technical restrictions, which would result from complete utilization of the renewable volume and thus already lead to a reduction) is the idea of sustainability and possible further competing uses. Especially in terms of sustainability, not using the entire increment is important to, for example, preserve forest areas as carbon sinks (Bundesforschungszentrum für Wald, 2013). At the same time, with expected higher levels of damaged wood due to bark beetle infestation and weather extremes, demand for sawmill byproducts for pellets is expected to increase, and demand from wood heat-

ing systems is expected to decrease. Thus, based on this approximate approach, a total of about 1.6 million t-atro (a ton of absolute dry wood) of forest biomass (firewood and woodchips) is realistically available for thermochemical conversion. For sawmill byproducts (including bark), about 50% of sawmill byproducts can presumably be used for gasification in the future, even if this requires a redirection of wood flows. Thus, approximately 1 million t-atro of sawmill byproducts (including bark) is available (Dißauer et al., 2019).

This technoeconomic calculation did not include wood from short rotation coppice and miscanthus like some other studies, as these would require their own cropland. Thus, they cannot be seen as residuals and are therefore not within the scope of this work (Dißauer et al., 2019), especially because studies have found that this land use change is often at the expense of food or feed production (Xie et al., 2019). Therefore, these categories were not further investigated beyond their potential.

2.3 Technoeconomic Analysis

To categorize the different potentials in a theoretical merit order (see Section 12), a technoeconomic analysis was performed to calculate of the levelized costs of energy (LCOE). This analysis is based on the annuity method and applied as described by (Böhm et al., 2020).

2.3.1 Investment Costs

As a first step, the investment-based annuity was calculated. This was done using the values for capital expenditures (CAPEX) for different years on base-scale plants as listed in Table 3.

Additionally, the assessment considers increasing process efficiencies for the different observation periods as stated in Table 3. The efficiency of the methanation process is kept constant, presuming a complete conversion. However, based on the expected role of power-to-gas in the future energy system a CAPEX decrease was given by (Böhm et al., 2020). This cost reduction also applies to water electrolysis, as the key technology for all power-to-x applications.

For biomass gasification, the CAPEX reduction potential is expected to be much lower in comparison to the power-to-gas systems. This results from its availability on industrial scale. Since there are already realized projects as for example Senden in the Netherlands (Kern et al., 2013), GoBiGas in Gothenburg, Sweden (Thunman et al., 2018) or Güssing in Austria (Hofbauer et al., 2002), it is expected that additional CAPEX decrease from scaling is not as high as with the comparatively new power-to-gas technology.

For fixed plant scales (size), the investment cost part I_0 of the LCOE is calculate from specific CAPEX according to Equation 4 (Kotowicz et al., 2018).

$$I_0 = \text{CAPEX} * \text{size} \quad (4)$$

However, this calculation only describes the investment costs for the plant at reference scale (e.g. in terms of biomass gasification in this paper 25 MW). For differing scales the investment costs for the new scale can be cal-

TABLE 3: Data for investment cost modelling of the main components.

		Biomass gasification	Polymer electrolyte membrane (PEM) electrolyzer	Methanation	Anaerobic digester & gas upgrading
Base scale	MW	25	10	5	1–8
CAPEX 2020	€/kW	2,400 ^a	1,100 ^c	600 ^c	Ø 2,900 ⁱ
CAPEX 2030	€/kW	2,200 ^a	630 ^c	530 ^c	Ø 2,300 ⁱ
CAPEX 2050	€/kW	1,900 ^a	270 ^c	340 ^c	Ø 2,000 ⁱ
Efficiency 2020	% _{LHV}	69 ^b	61 ^e	83 ^c	40–60 ^h
Efficiency 2030	% _{LHV}	69 ^b	63 ^e	83 ^c	40–60 ^h
Efficiency 2050	% _{LHV}	69 ^b	68 ^e	83 ^c	40–60 ^h
Lifetime	years	20 ^a	20 ^e	15	15
OPEX _{pl} ^d	%	1.5 ^a	3–5 ^f	5 ^h	3

^a Values and assumptions were made according to the data of (Müller, 2013).

^b Values for biomass gasification coupled with catalytic methanation according to the data of (Dißauer et al., 2019).

^c Based on scaling effects given by (Böhm et al., 2020) for PEM electrolysis and catalytic methanation

^d Operational expenditures (OPEX) for operation, maintenance, taxes, etc. in percentage of investment costs

^e Based on (Smolinka et al., 2018)

^f Based on (Buttler & Spliethoff, 2018)

^g Based on (Gorre et al., 2019)

^h Based on (TNO, 2021) and (Boldrin et al., 2016)

ⁱ Based on (Biol, 2020; Kampman et al., 2020; Skovsgaard & Jacobsen, 2017; Vienna University of Technology, 2012)

culated using scaling factors as described in Equation 5 (Swanson et al., 2010).

$$I_{new} = I_0 \left(\frac{Scale_{new}}{Scale_0} \right)^{x_f} \quad (5)$$

Within this equation, the scaling factor x_f is 0.86 (Günther, 2014). Further factors influencing the investment costs are the building, and engineering costs, that are investment costs specific. These overhead costs are assumed to be 20% of I_0 for buildings, and 15% of I_0 for engineering (DACE Price Booklet, 2017) and are added on top of the investment costs. The resulting total investment costs are further referred to as I .

The capital-related annuity A_c is calculated as follows (Becker, 2013):

$$A_c = I * a$$

and

$$a = \frac{(1+i)^n * i}{(1+i)^n - 1}$$

where n describes the years of operation and i the interest rate. The interest rate used is 5% (Steinmüller et al., 2014).

2.3.2 Operational Costs

The operational costs (OPEX) are split into the operation-related annuity A_o and the variable costs C_{var} . The op-

eration-related annuity A_o includes operation, maintenance, tax, etc. This factor is included with the OPEX_{pl} values from Table 3 and calculated as following:

$$A_o = A_c * OPEX_{pl} \quad (6)$$

The variable costs C_{var} include demand related costs like electricity, biomass, and water costs, as shown in Table 4.

Substrate cost characteristics as input factors for the analysis are averaged based on the substrates in Table 2 and data from three disposal companies operating in Austria, whereas revenues from the disposal of organic wastes depend on the type of biowaste e.g., the disposal fee for organic household waste is approximately 55 €/tFM (Lindorfer & Schwarz, 2013). Substrates that contribute to the cost side are all categories for gasification as well as agricultural feedstocks like manure and straw for anaerobic digestion especially for transport expenses, while waste from food production and other organic wastes can be counted as revenues based on their representative disposal fee.

For agricultural residues, the energy density and specific methane yield determine the substrate costs e.g., substrate cost of approximately 90 €/tFM for straw, 35 €/t for grass silage; (Thrän et al., 2013).

2.3.3 Levelized Cost of Energy

To determine the levelized costs of the product, all

TABLE 4: Material costs for the investigated years.

		2020	2030	2050	Source
Electricity	€/MWh _{el}	50	70	80	(Marktstudie zur Strompreisentwicklung 2016 - 2050, 2016)
Water	€/m ³		1.15		averaged water charges in the nine provincial capitals in Austria based on data from January 2018
Woodchips, firewood	€/MWh _{th}	36	42	47	
Bark	€/MWh _{th}	27	32	35	(Landwirtschaftskammer Österreich, 2020)
Sawmill byproduct	€/MWh _{th}	28	33	37	

costs and revenues are related to the energy output of the process. According to VDI 2067 the total annuity A is calculated as follows:

$$A = A_p - (A_c + A_d + A_o + A_m) \quad (7)$$

Since the proceeds from by-product sales are treated together with the demand-related costs as actual annual costs in C_{var} (instead of attributing discount rate and price changes), the annuities of proceeds A_p and demands A_d can be omitted in Equation 7. Same accounts for the annuity of additional costs A_m representing the overhead costs for buildings and engineering, which are already included in A_c . Thus, Equation 7 is simplified to:

$$A = A_c + A_o \quad (8)$$

With the annuity and demand related variable costs, one can calculate the LCOE as described in Equation 9, with $P_{SNG,n}$ as the annual methane production (Böhm et al., 2020; Parra et al., 2017).

$$LCOE = \frac{-A + \sum_n C_{var,n}}{\sum_n P_{SNG,n}} \quad (9)$$

2.4 Theoretical Merit Order

In the energy economy, a theoretical merit order is a statistical tool to rank energy potentials from different sources by their costs. It is most commonly used in the electricity market to determine which power stations should run at what time to fulfill electricity demand with the lowest overall generation costs. The overall result is a ranking of technologies and resources by their potential and price, starting with the least expensive and ending with the most expensive (Cludius et al., 2014; Luňáčková et al., 2017; Sensfuß et al., 2008). Therefore, it is a popular method in many papers that focus on potential, costs, or both in terms of energy generation.

In this paper, a theoretical merit order is used to compare the costs of the potentials for biomass gasification, anaerobic digestion, and power-to-gas. This merit order

should allow for the quantification of which potential should be used first to meet demands.

3. RESULTS AND DISCUSSION

As part of this work, the described system was analyzed with a potential analysis and technoeconomic analysis approach. This permits us to describe the potential of renewable gas production from organic waste and biomass in a technology-coupled approach.

3.1 Anaerobic Digestion

For 2020 the theoretical potential from all residue flows in Austria results in 1,582 Mio. Nm³ biomethane from anaerobic digestion per year. This value is reduced to 1,533 Mio. Nm³ biomethane per year till 2050 due to the reduction of agricultural waste streams that current developments show. However, these values only represent the theoretical potential. More interesting is the technical potential, since it shows the potential cap of gatherable biomethane with available technologies.

This process can produce about 650 million Nm³ of biomethane per year in 2020, a value that will decrease slightly by 2050 to about 600 million Nm³ of biomethane. Most of it can be produced from agricultural residue and waste from food production. Furthermore, the calculations revealed that up to 450 million Nm³ CO₂ from biogas cleaning would be available for SNG production via power-to-gas. More detailed information on the calculations for the potential categories is provided in the supplementary material.

To develop this potential, facilities for this purpose must be constructed. Figure 3 illustrates a possible expansion scenario to tap into the full potential by 2050. In the beginning, many small biomethane plants will be expanded and will later be partially replaced by or upgraded into plants with much higher production volumes. In total, 259 plants will need to operate in 2050 to fully exploit the potential.

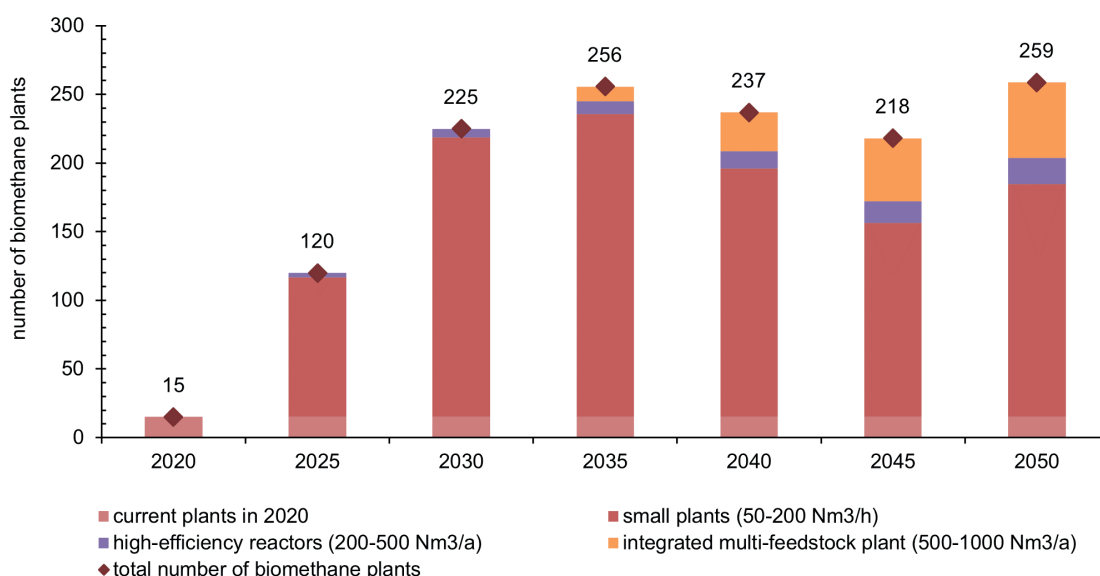


FIGURE 3: Expansion scenario for biomethane plants between 2020 and 2050.

However, the technical potential only includes current technical possibilities in gathering waste and not future developments. In the case of cuttings from bushes, grass, and trees and biowaste from households, future technologies will likely not substantially increase salvage rates. This differs for categories such as garden composting and straw. In terms of garden composting, the value of 0% of technical potential on the theoretical one will likely not increase, but regulative changes may move this category to biowaste from households, which already has a high technical potential. The idea is that people will stop composting waste privately and start to treat this waste like biowaste from households and therefore “activate” this category for anaerobic digestion. For straw, a higher gathering rate from fields may be possible with better developed tools for agriculture.

In the first stage of expansion (from today through 2030), new plants for the utilization of biogenic waste from the food industry, biowaste, food waste in residual waste, and sewage sludge will contribute to increasing resource efficiency. This prioritization was used since these categories are easily fermentable, more liquid biogenic residues in which they are easier for energetically utilization via anaerobic decomposition. Under this assumption, around 226 million Nm³/a of the technical methane potential can be realized in 2030. This corresponds to around 37% of the total potential.

In the second expansion stage (2030–2050), biogas will be produced from the more difficult-to-use residues from animal and plant production, and more synthetic methane will be produced. Further potentials, such as use of biogenic material from home garden composting, require a more in-depth system conversion and expansion of existing residue logistics and could therefore be realized from 2030 to 2050 at the earliest.

However, there are technical issues with this form of renewable energy, in addition to activating waste streams to increase the technical potential and the expansion of plants. The costs are another point that should be evaluated. As demonstrated in Figure 4, the costs for produc-

ing biomethane from organic waste are highly dependent on the plant size. With about 9 €-cent/kWh in 2020, small plants with a capacity of 50 to 200 Nm³/h are more cost intensive in comparison to high-efficiency reactors with a 200 to 500 Nm³/h capacity (~7 €-cent/kWh in 2020) and integrated multifeedstock plants with a capacity of 500 to 1,000 Nm³/h (~6 €-cent/kWh in 2020). The major share of the costs comes from building the biogas plant itself (62% to 64%). Another major cost component is the CH₄ processing that is necessary for feeding into the gas grid (25% to 27%), while substrate input has no significant influence on the cost. These costs are expected to decrease to 5 to 6 €-cent/kWh by 2050.

These costs as shown in Figure 4 are in a good range compared to other studies. (Nelissen et al., 2020) analyzed many studies that focused on anaerobic digestion and gasification of biomass. Within the study it was shown that LCOE for anaerobic digestion are in a range of 5.7 and 14.1 €-cent per kWh. This range is due to the wide variety of substrates and plant technologies (pretreatment, fermentation and upgrading) taken into account. The values are comparable with other analyses for central Europe e.g. (Kost et al., 2018) 5.4 - 6.9 or (European Commission, 2020) 4.1 - 8.0 €-cent per kWh recalculated from Levelized cost of electricity production.

Another issue is that the utilization of biogenic waste in anaerobic digestion plants can only be successfully established in the future if nutrient cycles are successfully closed at the same time. Anaerobic digestion is followed by composting of the digestate, and the resulting compost and the nutrients it contains are preserved for agriculture, horticulture, or private gardens. The liquid digestate can be used directly in agriculture. This could further increase the rentability of such plants, while also solving the issue of energy-intensive and resource-depleting fertilizer production.

3.2 Power-to-Gas

The CO₂ from biogas cleaning (see Section 3.1) is a suitable source for power-to-X applications (Götz et al., 2016;

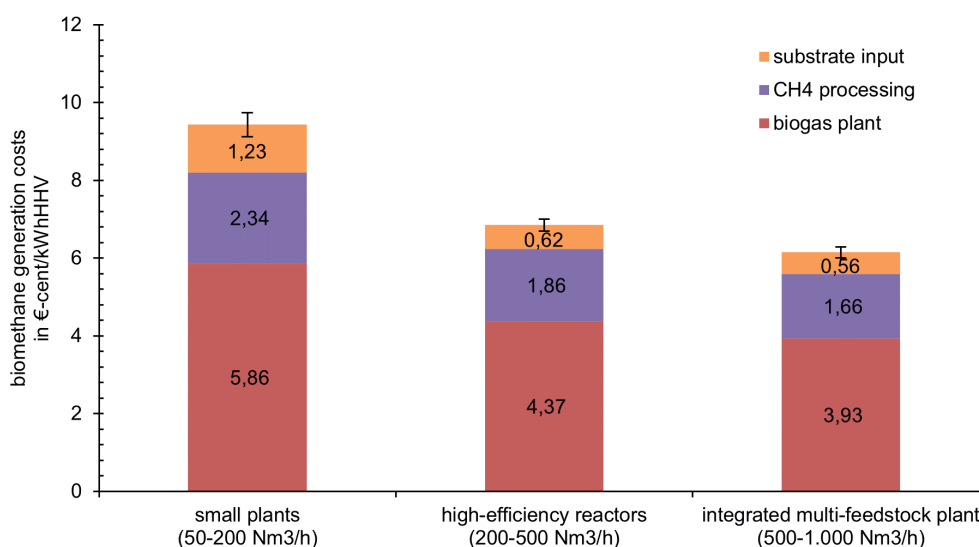


FIGURE 4: Costs for biomethane production via anaerobic digestion in 2020.

Rodin et al., 2020). Up to 330 million Nm³ SNG per year may be produced by using the technically available CO₂ from the biogas upgrading process. To provide sufficient H₂ for the methanation reaction, about 160 million Nm³ H₂ per year would be necessary, which correlates to about 9 GWh of electricity demand per year for the electrolyzer unit.

As illustrated in Figure 5, to provide sufficient hydrogen for methanation, 178 plants, mainly small plants in the size of 0.5 to 1 MW, must be built. This number must increase to 870 by 2050. Since the number of power-to-gas plants is much higher than the number of biomethane plants, a decentralized approach is possible. All values are based on an average operation time of 3,500 hours per year since this value would allow for cost-effective operation and fluctuations of the electricity grid could be used to produce hydrogen at peak times (Gorre et al., 2019).

In terms of specific costs, due to economies of scale and learning curve effects, significant cost reduction potentials likely exist for plant-specific investment costs. The CAPEX values in Section 2.3 illustrate this point.

Therefore, the investment costs of the LCOE for the production of SNG via power-to-gas shrink over time (see Figure 6). In addition, the operational costs in Figure 6 decrease over time since this category is mainly influenced by investment costs related to operational costs such as insurance, maintenance, and administration. For electricity-related costs (electricity costs and grid fees), the cost reduction is not as high as for investment-related costs. This effect stems from the fact that the overall electricity price is expected to rise by 2050 (enervis energy advisor GmbH, 2016). However, since the plant is expected to be operated at peak load hours (about 3,500 h/a), when electricity-related costs are low, a small reduction effect for electricity-related costs was investigated. In total, for SNG, costs are expected to decline from 29.3 €-cent per kWh in 2020 to 10.9 €-cent per kWh by 2050 (see Figure 6). However, under consideration of potential revenues from selling byproduct oxygen and heat, effective production costs could be reduced to 24.8 and 6.5 €-cent/kWh, respectively.

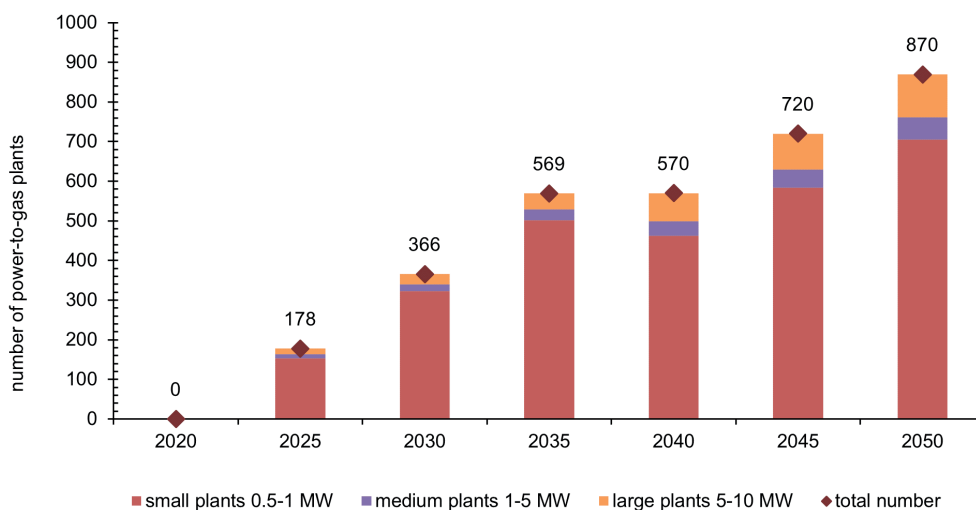


FIGURE 5: Expansion Scenario for Power-to-Gas Plants by 2050.

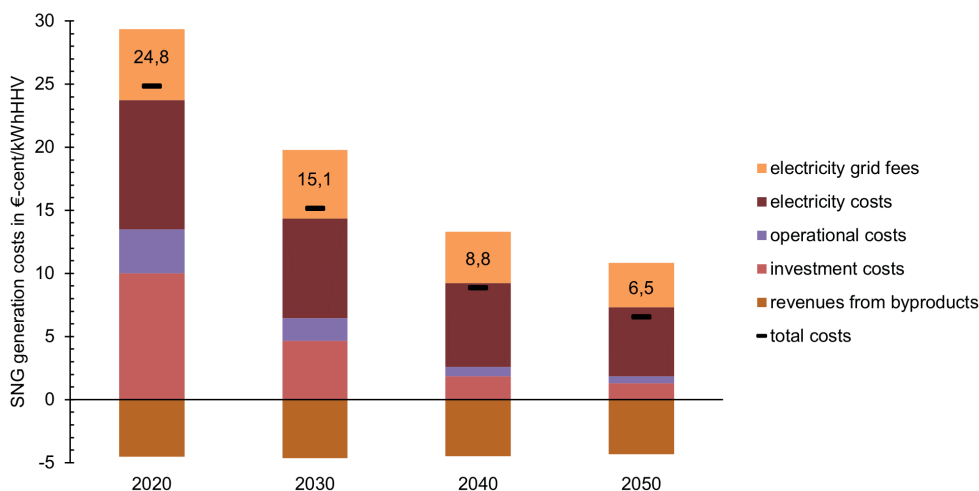


FIGURE 6: Synthetic natural gas generation costs for electrolyzers with 10–50 MWeL.

These cost ranges are comparable to the results gained by previous studies on power-to-gas production costs. (Gorre et al., 2020) calculated SNG production costs of 4.7 to 21 €-cent/kWh by optimizing hydrogen storage and methanation capacities. The costs evaluated by (Böhm et al., 2020) suggest that hydrogen could be produced at about 5 €-cent/kWh in 2050, presuming electricity costs similar to today. However, due to the strong dependencies of the power-to-gas process on external conditions, such as electricity costs, mode of operation, storage capacities, etc. as shown by (Gorre et al., 2019) a direct comparison of different applications is hardly possible.

The long-term use of existing gas infrastructure will depend heavily on the degree of integration of renewable gases. Thus, overall climate and energy policy objectives will also be supported by the existing gas infrastructure, which could ensure the long-term use of this infrastructure. As a consequence, enormous investments that have not yet been depreciated can still be realized, and massive opportunity costs or investments are not necessary; such investments would have a significant negative impact on

the national economy, with the exception of an interim investment impulse in alternative strategies. "Greening the gas" through hydrogen and synthetic methane from renewable energy sources as well as through biomethane from biogenic residues is thus a main component of the need for the sustainable further development of the energy system (Tichler & Zauner, 2018).

3.3 Biomass Gasification

In the course of the assessment of the potential for the production of green methane via the thermochemical conversion of biomass with a high lignin content, much higher technical potentials were identified than for biomethane production. As seen in Figure 7, the potential in 2030 amounts to about 3,300 million Nm³ per year and increases to just under 4,000 million Nm³ per year by 2050.

To exploit the full biomass gasification potential, 163 plants must be commissioned by 2050 (see Figure 8). The majority of these are plants should have a capacity of 35 MW. The other plants can be operated with up to 100 MW and will, despite their smaller numbers, produce the majority of bio SNG from biomass by 2050.

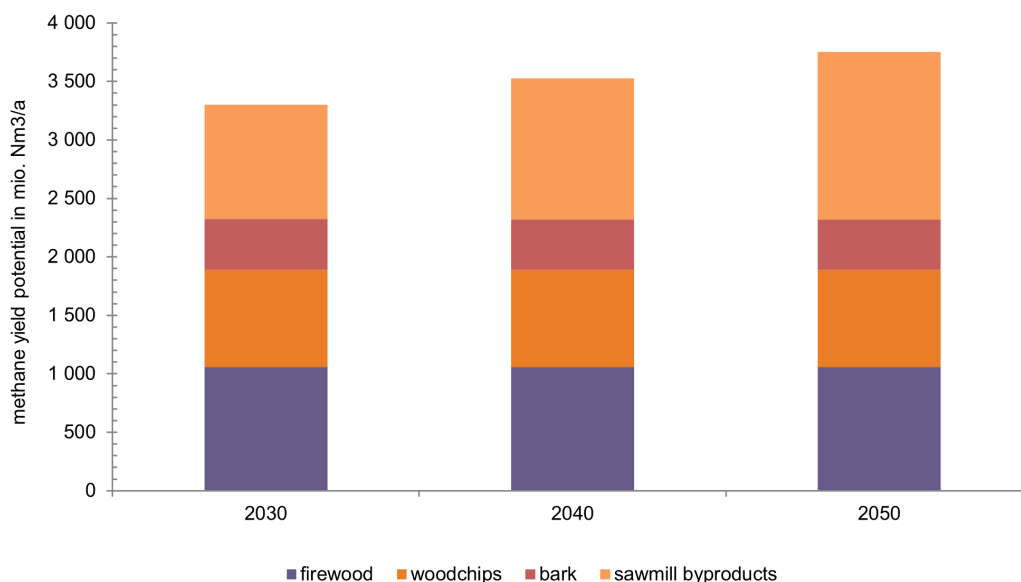


FIGURE 7: Potential for green methane from biomass gasification between 2030 and 2050.

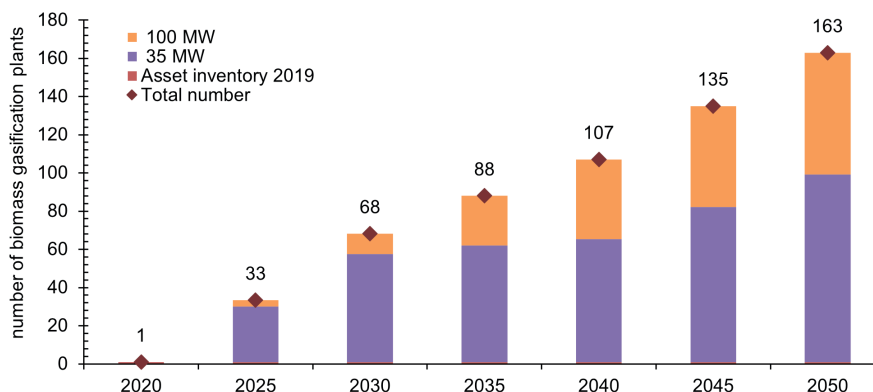


FIGURE 8: Expansion scenario for biomass gasification plants between 2020 and 2050.

As shown within this section, the power-to-gas plants outnumber the gasification and biomethane plants. The reason for the outnumbering of the power-to-gas plants in comparison to the gasification or biomethane plants originate from the different plant capacities. While the investigated gasification system is defined with a scaling of up to 100 MW based on the complex feedstock handling and gas cleaning, the investigated power-to-gas plants only reach up to a maximum of 10 MW per plant. Therefore, one power-to-gas plant can methanate the CO₂ from more than one biomethane plant (that can reach up to 1 MW within the investigated scope) but only a small percentage of the CO₂ from the 35 MW and 100 MW gasification plants.

To minimize transport costs and losses, a decentralized approach would be favorable, were several power-to-gas, biomethane and gasification plants are connected within a short geographical radius.

From the cost perspective, the 100 MW scale plant was specifically investigated. The results suggest that investment costs should decrease from 4.1 €-cent/kWh in 2020 to 3.2 €-cent/kWh by 2050 (see Table 5). Furthermore, the operation, maintenance, and other costs will decrease from 0.8 €-cent/kWh in 2050 to 0.7 €-cent/kWh by 2050. However, the most significant cost factor is the fuel price. Woodchips are particularly expensive, with a cost increase from 5.2 €-cent/kWh in 2050 to 6.8 €-cent/kWh by 2050. Bark (3.9 €-cent/kWh in 2020 and 5.1 €-cent/kWh in 2050), as well as sawmill byproducts (4.1 €-cent/kWh in 2020 and 5.4 €-cent/kWh in 2050), have increasing prices as well. Nevertheless, both bark and sawmill byproducts are less expensive than woodchips.

The costs are in a good range to other studies according to a review by (Nelissen et al., 2020). Within the study, LCOE for methane from gasification was given in a range of 6.9 and 17.71 €-cent per kWh for current technologies. This large range comes from the different plant sizes, that reaches up to 150 MW within the analyzed studies, and the different substrates. For future costs only one study is mentioned within the review. This study by (van Melle et al., 2018) shows LCOE of 3.7 €-cent per kWh for a about 50 MW plant. However, this low costs mainly occur from the used assumptions for the fuels. The fuels are mainly low-cost biomass including some substrate categories that in this study are used for anaerobic digestion. Furthermore, the costs for the fuels are assumed much lower in comparison to the values in this work. Within (van Melle et al., 2018) the fuel costs are not in detail mentioned experts assumption. Beside this methodological difference, geo-

TABLE 5: Specific costs for the production of 1 kWh of synthetic natural gas with biomass gasification for woodchips, bark, and sawmill byproducts as fuel – 100 MW plant.

In €-cent per kWh SNG	2020	2030	2050
Investment costs	4.1	3.8	3.2
Operation, maintenance, and other fuel	0.8	0.8	0.7
Woodchips	5.2	6.1	6.8
Bark	3.9	4.6	5.1
Sawmill byproducts	4.1	4.8	5.4

graphical factors etc. further have a large influence on the biomass prices. According to (Kraussler et al., 2018), the plant size on the other hand does not have a large cost reducing factor above 40 MW.

3.4 Merit Order

In total, up to 60 TWh of green gas can be produced from these three categories of potential as technical potential. Within the technoeconomic analysis, the costs of such an expansion of green gases were considered. Figure 9 shows the time course of production costs between 2030 and 2050; these include not only investment costs but also operating costs. For the three categories of biomass gasification (only the fuels, not the plants, being changed), costs remain relatively constant, ranging from 9.0 to 10.7 €-cent/kWh depending on the fuel and year. For SNG from power-to-gas, production costs will presumably decrease from an initial 10.8 €-cent/kWh in 2030 to 6.5 €-cent/kWh by 2050. For anaerobic digestion, the average production costs will likely decrease from 7.9 to 5.4 €-cent/kWh between 2030 and 2050.

Based on the production costs and potentials, forming a theoretical merit order curve was possible, as described in section 0. Figure 10 shows an example for 2030. The figure demonstrates that the biomethane potential from anaerobic digestion should be used first, followed by biomass gasification and power-to-gas. However, methane from power-to-gas is becoming increasingly important and will have similar production costs in 2050 as biomethane from anaerobic conversion.

In terms of investment costs, with the calculated costs and expansion scenarios for developing 17 TWh of biomethane from anaerobic fermentation, €3.3 billion would have to be invested by 2050. To develop the 52 TWh and 62 TWh gasification plants, €2.4 billion and €5.7 billion, respectively, would have to be invested by 2050.

Overall, the prime costs for green gas are higher than the average prices of natural gas (reference year 2019) for households (5 €-cent/kWh) and for industry (2.5 €-cent/kWh; (eurostat, 2020)). As a result, the promotion of green gas leads to additional costs for utilities.

4. CONCLUSIONS AND OUTLOOK

Natural gas is an energy source that currently plays an important role in many areas. Especially in some applications, it is costly or technologically complex to replace due to its technical and economic properties. Therefore, many actors are making an effort to replace the current fossil energy carriers of natural gas with gas from renewable sources. At the same time, assumptions differ regarding the domestic supply of renewable gases that will be available for these applications. The availability of renewable gas was determined in an Austrian case study based on the technical quantities of methane that can be produced from biogenic residues. The feasible quantities were estimated for 2040 with the assumption that value chains for the use of biogenic residues can be redesigned by then to maximize availabilities.

The potential analysis demonstrated a high potential

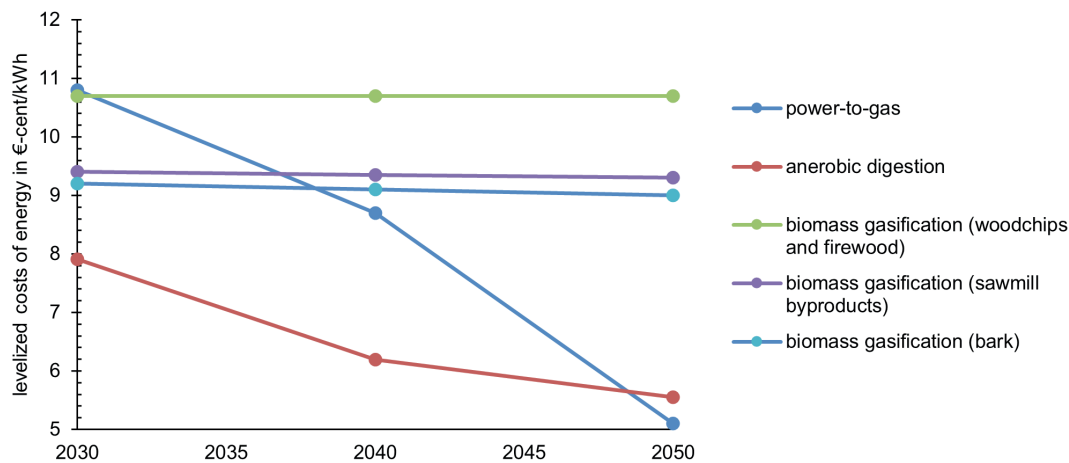


FIGURE 9: Timeline of the production costs for green gases.

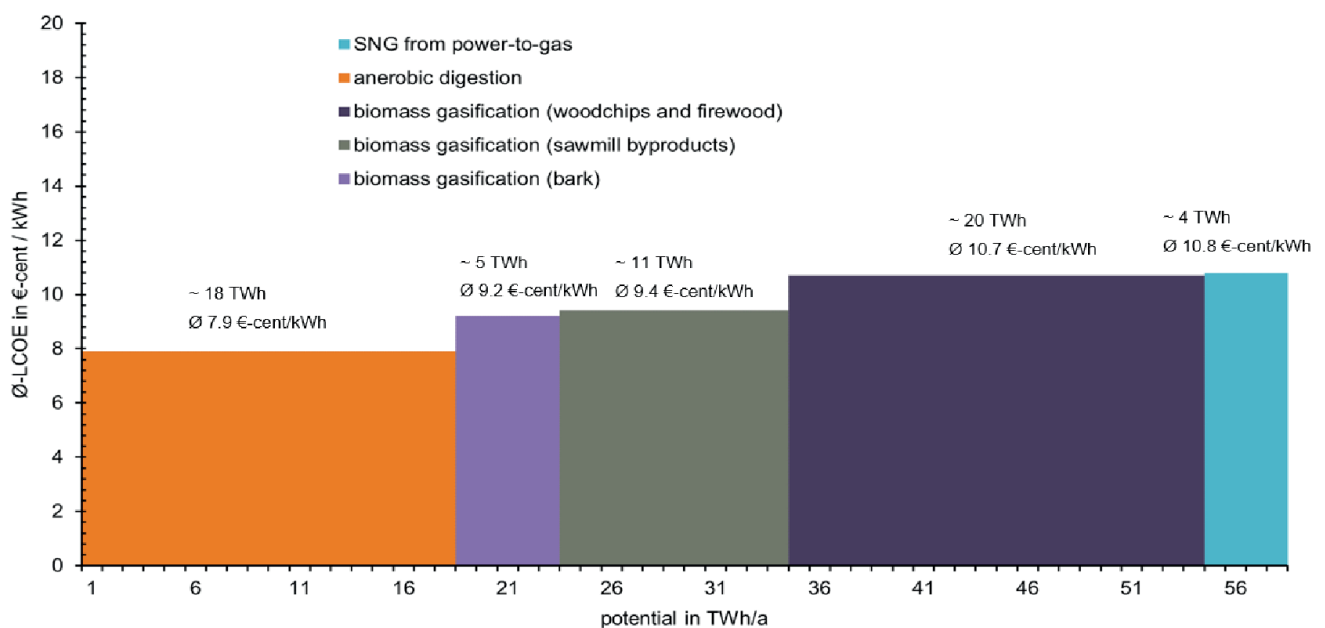


FIGURE 10: Theoretical merit order curve of the potential for 2030.

for renewable methane, with a production capacity of more than 50 TWh in 2030 increasing to more than 60 TWh in 2050 throughout all biogenic residue categories, synthetic renewable gas potentials, and conversion technologies. This could technically meet the Austrian natural gas demand by more than 50%. For the potential categories, the analysis outlined that biomass gasification of firewood and woodchips (e.g., from storm-damaged timber) and anaerobic digestion of the various streams provide the two largest quantitative contributions to the overall potential, while SNG from power-to-gas utilizing CO₂ from anaerobic digestion contributes the smallest amount. To increase the potential, future research and legislative actions need to focus on increasing the accessibility of the technical potential. Especially from an ecological point of view, the addressed residues (e.g., from wood) can play an important role as a primary raw material, and their use could reduce fossil energy and greenhouse gas emissions in many sec-

tors such as the paper and pulp industry or construction. Competing uses are to be predicted and, at any rate, prevented when a technical potential is realized.

However, even though renewable methane has a large energy potential, another point that must be critically reviewed is economic performance. From a technoeconomic perspective, the results revealed that the two categories with the highest potential are on the opposite ends of the merit order. While anaerobic digestion was expected to be the least cost-intensive renewable methane source of the study with about 7.9 €-cent per kWh, biomass gasification of firewood and woodchips has one of the highest costs of 10.7 €-cent per kWh. However, even anaerobic digestion resulted in much higher costs compared with the current industrial and household price for natural gas. Therefore, future work should focus on utilizing most byproducts of the various technologies to increase side revenues, which then should make the technologies more cost effective.

Furthermore, the framework conditions should change in an attempt to eliminate the cost difference between renewable and fossil energy carriers.

ACKNOWLEDGMENTS

This work was supported by the Austrian Research Promotion Agency [grant number 864876-ReNOx 2.0] and the Energieinstitut an der Johannes Kepler Universität Linz.

REFERENCES

- Alibardi, L., & Cossu, R. 2015. Composition variability of the organic fraction of municipal solid waste and effects on hydrogen and methane production potentials. *Waste Manag*, 36, 147-155. doi: <https://doi.org/10.1016/j.wasman.2014.11.019>
- Batidzirai, B., Smeets, E. M. W., & Faaij, A. P. C. 2012. Harmonising bioenergy resource potentials-Methodological lessons from review of state of the art bioenergy potential assessments. *Renewable & Sustainable Energy Reviews*, 16(9), 6598-6630. doi: <https://doi.org/10.1016/j.rser.2012.09.002>
- Becker, H. P. 2013. *Investition und Finanzierung (Investment and financing)*. Wiesbaden: Springer. ISBN: 978-3-658-00378-4
- Birol, F. 2020. Energy technology perspectives. cited in <https://www.iea.org/reports/energy-technology-perspectives-2020> consulted on the 09.09.2021
- Böhm, H., Zauner, A., Rosenfeld, D. C., & Tichler, R. 2020. Projecting cost development for future large-scale power-to-gas implementations. *Applied Energy*, 264, 114780. doi: <https://doi.org/10.1016/j.apenergy.2020.114780>
- Boldrin, A., Baral, K. R., Fitamo, T., Vazifehkhoran, A. H., Jensen, I. G., Kjaergaard, I., Lyng, K. A., Nguyen, Q. V., Nielsen, L. S., & Triolo, J. M. 2016. Optimised biogas production from the co-digestion of sugar beet with pig slurry: Integrating energy, GHG and economic accounting. *Energy*, 112, 606-617. doi: <https://doi.org/10.1016/j.energy.2016.06.068>
- British Petroleum p.l.c. 2019. BP statistical review of world energy. cited in <https://www.bp.com/content/dam/bp/business-sites/en/global/corporate/pdfs/energy-economics/statistical-review/bp-stats-review-2019-full-report.pdf> consulted on the 09.09.2021
- Brosowski, A., Adler, P., Erdmann, G., Thrän, D., Mantau, U., & Blanke, C. 2015. Biomassepotenziale von Rest- und Abfallstoffen – Status quo in Deutschland (Biomass potential of residue and waste streams - status quo in Germany). cited in <https://mediathek.fnr.de/band-36-biomassepotenziale-von-rest-und-abfallstoffen.html> consulted on the 09.09.2021
- Bundesanstalt für Agrarwirtschaft. 2016. Grüner Bericht 2016 (Green report 2016). cited in <https://gruenerbericht.at/cm4/jdownload/download/2-gr-bericht-terreich/1650-gb2016> consulted on the 03.09.2019
- Bundesforschungszentrum für Wald. 2013. Wald im Fokus (Forrest in focus). cited in https://www.google.com/url?sa=t&rct=j&q=&esrc=s&source=web&cd=&ved=2ahUKEwjJ1bbPifLyAhUrSaQKHUm8Bi4QFn0ECAUQA-Q&url=http%3A%2Fwww.bfw.ac.at%2Fwebshop%2Findex.php%3Fcontroller%3Dattachment%26id_attachment%3D151&usq=A0vVaw2KuXFKU5pkYNC4re2Sqqr consulted on the 09.09.2021
- Bundesministerium Nachhaltigkeit und Tourismus. 2019. Die Bestandsaufnahme der Abfallwirtschaft in Österreich - Statusbericht 2019 (The inventory of waste management in Austria - status report 2019). cited in https://www.arge.at/wp-content/uploads/2019/06/Die_Bestandsaufnahme_der_Abfallwirtschaft_in_%c3%96sterreich_web.pdf consulted on the 03.09.2019
- Burg, V., Bowman, G., Haubensak, M., Baier, U., & Thees, O. 2018. Valorization of an untapped resource: energy and greenhouse gas emissions benefits of converting manure to biogas through anaerobic digestion. *Resources Conservation and Recycling*, 136, 53-62. doi: <https://doi.org/10.1016/j.resconrec.2018.04.004>
- Buttler, A., & Spliethoff, H. 2018. Current status of water electrolysis for energy storage, grid balancing and sector coupling via power-to-gas and power-to-liquids: A review. *Renewable & Sustainable Energy Reviews*, 82, 2440-2454. doi: <https://doi.org/10.1016/j.rser.2017.09.003>
- Cludius, J., Hermann, H., Matthes, F. C., & Graichen, V. 2014. The merit order effect of wind and photovoltaic electricity generation in Germany 2008-2016: Estimation and distributional implications. *Energy Economics*, 44, 302-313. doi: <https://doi.org/10.1016/j.eneco.2014.04.020>
- DACE Cost and Value. 2017. DACE price booklet (32 ed.). Nijkerk: DACE Cost and Value. ISBN: 9463460039
- Dißbaur, C., Rehling, B., & Strasser, C. 2019. *Machbarkeitsuntersuchung Methan aus Biomasse (Feasibility study methane from biomass)*. cited in https://www.gruenes-gas.at/assets/Uploads/BioEnergy2020+_Machbarkeitsuntersuchung_Methan_aus_Biomasse.pdf consulted on the 01.03.2020
- enervis energy advisor GmbH. 2016. *Marktstudie zur Strompreisentwicklung 2016-2050 (Marketstudy on the electricity price development 2016-2050)*. cited in <https://enervis.de/leistung/euro-pean-power-market-outlook/> consulted on the 09.09.2021
- Erler, R., Hüttenrauch, J., Schuhmann, E., Graf, F., Kiefer, J., Ball, T., Fischer, T., Kappertsbusch, V., & Dresen, B. 2013. *Potenzialstudie zur nachhaltigen Erzeugung und Einspeisung gasförmiger, regenerativer Energieträger in Deutschland (Biogasatlas) (Potentialstudy on the sustainable production and feed in of gaseous, renewable energy carriers in Germany (Biogas atlas))*. cited in https://www.dvgw.de/medien/dvgw/forschung/berichte/gw2_01_10.pdf consulted on the 09.09.2021
- European Commission. 2011. A Roadmap for moving to a competitive low carbon economy in 2050. cited in <https://eur-lex.europa.eu/LexUriServ/LexUriServ.do?uri=COM:2011:0112:FIN:EN:PDF> consulted on the 09.09.2021
- European Commission. 2019. The European green deal. cited in <https://eur-lex.europa.eu/legal-content/EN/TXT/PDF/?uri=CELEX:52019DC0640&from=EN> consulted on the 09.09.2021
- European Commission. 2020. Final Report Cost of Energy (LCOE) - Energy costs, taxes and the impact of government interventions on investments. cited in <https://op.europa.eu/en/publication-detail/-/publication/76c57f2f-174c-11eb-b57e-01aa75ed71a1/language-en> consulted on the 09.09.2021
- eurostat. (2020). Natural gas price statistics. cited in https://ec.europa.eu/eurostat/statistics-explained/index.php/Natural_gas_price_statistics consulted on the 24.02.2021
- FNR. 2013. *Leitfaden Biogas: Von der Gewinnung zur Nutzung (Guideline biogas: from extraction to use)*. cited in https://www.fnr.de/fileadmin/allgemein/pdf/broschueren/Leitfaden_Biogas_web_V01.pdf consulted on the 09.09.2021
- Gao, Y., Gao, X., & Zhang, X. H. 2017. The 2 degrees C global temperature target and the evolution of the long-term goal of addressing climate change - from the United Nations framework convention on climate change to the Paris agreement. *Engineering*, 3(2), 272-278. doi: <https://doi.org/10.1016/J.Eng.2017.01.022>
- German Advisory Council on Global Change. 2009. *Welt im Wandel: Zukunftsfähige Bioenergie und nachhaltige Landnutzung (Future bioenergy and sustainable land use)*: WBGU. ISBN: 978-3-936191-21-9
- Gorre, J., Ortloff, F., & van Leeuwen, C. 2019. Production costs for synthetic methane in 2030 and 2050 of an optimized Power-to-Gas plant with intermediate hydrogen storage. *Applied Energy*, 253, 113594. doi: <https://doi.org/10.1016/j.apenergy.2019.113594>
- Gorre, J., Ruoss, F., Karjunen, H., Schaffert, J., & Tynjala, T. 2020. Cost benefits of optimizing hydrogen storage and methanation capacities for Power-to-Gas plants in dynamic operation. *Applied Energy*, 257, 113967. doi: <https://doi.org/10.1016/j.apenergy.2019.113967>
- Götz, M., Lefebvre, J., Mörs, F., McDaniel Koch, A., Graf, F., Bajohr, S., Reimert, R., & Kolb, T. 2016. *Renewable Power-to-Gas: A technological and economic review*. *Renewable Energy*, 85, 1371-1390. doi: <https://doi.org/10.1016/j.renene.2015.07.066>
- Günther, T. 2014. *Entwicklung einer Bewertungsmethodik zur Standortplanung und Dimensionierung von Wasserstoffanlagen (Development of an evaluation methodology for site planning and dimensioning of hydrogen plants)*. (Dr.Ing.). Brandenburgischen Technischen Universität Cottbus (Brandenburg University of Technology - Cottbus), cited in <https://opus4.kobv.de/opus4-btu/frontdoor/index/index/docId/2984> consulted on the 10.09.2021
- Hofbauer, H., Rauch, R., Bosch, K., Koch, R., & Aichernig, C. (2002). *Biomass CHP plant Guessing – a success story*. Paper presented at the Expert meeting on pyrolysis and gasification of biomass and waste. cited in <https://citeseerx.ist.psu.edu/viewdoc/download?doi=10.1.1.607.9078&rep=rep1&type=pdf> consulted on the 10.09.2021

- Kampman, B., Leguijt, C., Scholten, T., Tallat-Kelpsaite, J., Brückmann, R., Maroulis, G., Lesschen, J., Meesters, K., Sikirica, N., & Elbersen, B. 2020. Optimal use of biogas from waste streams. cited in https://ec.europa.eu/energy/sites/ener/files/documents/ce_delft_3g84_biogas_beyond_2020_final_report.pdf consulted on the 09.09.2021
- Kern, S., Pfeifer, C., & Hofbauer, H. 2013. Gasification of wood in a dual fluidized bed gasifier: Influence of fuel feeding on process performance. *Chemical Engineering Science*, 90, 284-298. doi: <https://doi.org/10.1016/j.ces.2012.12.044>
- Kompost & Biogas Verband Österreich. (2021). Biomethan in Österreich (Biomethane in Austria). cited in <https://www.kompost-biogas.info/biogas/biomethan/biomethan-in-oesterreich/> consulted on the 23.02.2021
- Kost, C., Shammugam, S., Jülch, V., Huyen-Tran, N., & Schlegl, T. 2018. Levelized cost of electricity renewable energy technologies. cited in https://www.ise.fraunhofer.de/content/dam/ise/en/documents/publications/studies/EN2018_Fraunhofer-ISE_LCOE_Renewable_Energy_Technologies.pdf consulted on the 09.09.2021
- Kotowicz, J., Węcel, D., & Jurczyk, M. 2018. Analysis of component operation in power-to-gas-to-power installations. *Applied Energy*, 216, 45-59. doi: <https://doi.org/10.1016/j.apenergy.2018.02.050>
- Kraussler, M., Pontzen, F., Muller-Hagedorn, M., Nanning, L., Luisser, M., & Hofbauer, H. 2018. Techno-economic assessment of biomass-based natural gas substitutes against the background of the EU 2018 renewable energy directive. *Biomass Conversion and Biorefinery*, 8(4), 935-944. doi: <https://doi.org/10.1007/s13399-018-0333-7>
- KTBL. 2008. Betriebsplanung Landwirtschaft 2008/09: Daten zu Schlachtabfällen und Schweinemist aus Genesys-Merkblatt M101 - Biogasausbeute von Hofdüngern und Co-Substraten (Farm planning for agriculture 2008/09: Data on slaughterhouse waste and pig manure from Genesys leaflet M101 - Biogas yield from farm manure and co-substrates). cited in https://www.ktbl.de/fileadmin/user_upload/Allgemeines/Download/Datensammlung/P_19491-small.pdf consulted on the 09.09.2021
- Kuo, J., & Dow, J. 2017. Biogas production from anaerobic digestion of food waste and relevant air quality implications. *J Air Waste Manag Assoc*, 67(9), 1000-1011. doi: <https://doi.org/10.1080/10962247.2017.1316326>
- Landwirtschaftskammer Österreich. 2020. Holzmarktbericht 2020 (Wood market report 2020). cited in <https://www.waldverband.at/holzmarktbericht-der-ikoe-september-2020-2/> consulted on the 09.09.2021
- Lechtenböhrer, S., Nilsson, L. J., Åhman, M., & Schneider, C. 2016. Decarbonising the energy intensive basic materials industry through electrification—Implications for future EU electricity demand. *Energy*, 115, 1623-1631. doi: <https://doi.org/10.1016/j.energy.2016.07.110>
- LFL. (2019). Biogasausbeute verschiedener Substrate (Biogas content from various substrates). cited in https://www.lfl.bayern.de/iba/energie/049711/?sel_list=20%2Cb&anker0=substratanker#substratanker consulted on the 04.09.2019
- Lindorfer, J., & Schwarz, M. M. 2013. Site-specific economic and ecological analysis of enhanced production, upgrade and feed-in of biomethane from organic wastes. *Water Sci Technol*, 67(3), 682-688. doi: <https://doi.org/10.2166/wst.2012.617>
- Luňáčková, P., Průša, J., & Janda, K. 2017. The merit order effect of Czech photovoltaic plants. *Energy Policy*, 106, 138-147. doi: <https://doi.org/10.1016/j.enpol.2017.02.053>
- Melikoglu, M., & Menekse, Z. K. 2020. Forecasting Turkey's cattle and sheep manure based biomethane potentials till 2026. *Biomass & Bioenergy*, 132, 105440. doi: <https://doi.org/10.1016/j.biombioe.2019.105440>
- Müller, S. 2013. Hydrogen from biomass for industry-Industrial application of hydrogen production based on dual fluid gasification. (Dr. techn.). Technical University of Vienna, Vienna. cited in <https://repositum.tuwien.at/handle/20.500.12708/14449> consulted on the 10.09.2021
- Nelissen, D., Faber, J., van der Veen, R., van Grinsven, A., Shanthy, H., & van den Toorn, E. 2020. Availability and costs of liquefied bio- and synthetic methane: The maritime shipping perspective. cited in https://cedelft.eu/wp-content/uploads/sites/2/2021/03/CE_Delft_190236_Availability_and_costs_of_liquefied_bio_and_synthetic_methane_Def.pdf consulted on the 09.09.2021
- O'Shea, R., Wall, D. M., Kilgallon, I., Browne, J. D., & Murphy, J. D. 2017. Assessing the total theoretical, and financially viable, resource of biomethane for injection to a natural gas network in a region. *Applied Energy*, 188, 237-256. doi: <https://doi.org/10.1016/j.apenergy.2016.11.121>
- O'Shea, R., Wall, D. M., McDonagh, S., & Murphy, J. D. 2017. The potential of power to gas to provide green gas utilising existing CO2 sources from industries, distilleries and wastewater treatment facilities. *Renewable Energy*, 114, 1090-1100. doi: <https://doi.org/10.1016/j.renene.2017.07.097>
- ÖVGW. 2011. ÖVGW Richtlinie G B220 Regenerative Gase - Biogas (ÖVGW Guideline G B220 renewable gases - biogas). cited in https://portal.ovgw.at/pls/f?p=101:203:::RP,203:P203_ID,P203_FROM_PAGE_ID:1075524,202 consulted on the 09.09.2021
- Parra, D., Zhang, X., Bauer, C., & Patel, M. K. 2017. An integrated techno-economic and life cycle environmental assessment of power-to-gas systems. *Applied Energy*, 193, 440-454. doi: <https://doi.org/10.1016/j.apenergy.2017.02.063>
- Reisinger, H. 2012. Rückstände aus der Nahrungs-und Genussmittelproduktion (Residues from food and luxury food production). cited in <https://www.umweltbundesamt.at/fileadmin/site/publikationen/REP0403.pdf> consulted on the 09.09.2021
- Republik Österreich. 2020. Aus Verantwortung für Österreich. Regierungsprogramm 2020-2024 (Out of responsibility for Austria. Governmental program 2020-2024). cited in https://www.dieneuevolkspartei.at/Download/Regierungsprogramm_2020.pdf consulted on the 09.09.2021
- Rodin, V., Lindorfer, J., Bohm, H., & Vieira, L. 2020. Assessing the potential of carbon dioxide valorisation in Europe with focus on biogenic CO2. *Journal of CO2 Utilization*, 41, 101219. doi: <https://doi.org/10.1016/j.jcou.2020.101219>
- Rosenfeld, D. C. 2020. Generation and application of renewable gases as sustainable energy carrier for industry and mobility. (Dr. Dissertation). University of Natural Resources and Life Sciences, Vienna, Austria. cited in https://forschung.boku.ac.at/fis/suchen.hochschulschriften_info?sprache_in=de&menue_id_in=107&id_in=&hochschulschrift_id_in=19542 consulted on the 10.09.2021
- Rosenfeld, D. C., Lindorfer, J., & Ellersdorfer, M. 2020. Valorization of organic waste fractions: a theoretical study on biomethane production potential and the recovery of N and P in Austria. *Energy Sustainability and Society*, 10(1), 1-11. doi: <https://doi.org/10.1186/s13705-020-00272-3>
- Schiffer, Z. J., & Manthiram, K. 2017. Electrification and decarbonization of the chemical industry. *Joule*, 1(1), 10-14. doi: <https://doi.org/10.1016/j.joule.2017.07.008>
- Sensfuß, F., Ragwitz, M., & Genoese, M. 2008. The merit-order effect: A detailed analysis of the price effect of renewable electricity generation on spot market prices in Germany. *Energy Policy*, 36(8), 3086-3094. doi: <https://doi.org/10.1016/j.enpol.2008.03.035>
- Singlitico, A., Goggins, J., & Monaghan, R. F. D. 2018. Evaluation of the potential and geospatial distribution of waste and residues for bio-SNG production: A case study for the Republic of Ireland. *Renewable & Sustainable Energy Reviews*, 98, 288-301. doi: <https://doi.org/10.1016/j.rser.2018.09.032>
- Skovsgaard, L., & Jacobsen, H. K. 2017. Economies of scale in biogas production and the significance of flexible regulation. *Energy Policy*, 101, 77-89. doi: <https://doi.org/10.1016/j.enpol.2016.11.021>
- Smolinka, T., Wiebke, N., Sterchele, P., Lehner, F., & Jansen, M. 2018. Studie_IndWEde-Industrialisierung der Wasserelektrolyse in Deutschland: Chancen und Herausforderungen für nachhaltigen Wasserstoff für Verkehr, Strom und Wärme (Industrialization of water electrolysis in Germany: Chances and challenges for sustainable hydrogen in mobility, electricity and heat). cited in <https://www.dwv-info.de/wp-content/uploads/2019/06/NOW-Elektrolysestudie-2018.pdf> consulted on the 09.09.2021
- Steinmüller, H., Reiter, G., Tichler, R., Friedl, C., Furtlehner, M., Lindorfer, J., Schwarz, M., Koppe, M., Biegger, P., & Felder, A. 2014. Power to Gas-eine Systemanalyse: Markt-und Technologiescouting und-analyse (Power to Gas - a system analysis: market and technology scouting and analysis). cited in https://www.ea.tuwien.ac.at/fileadmin/t/ea/projekte/PtG/Endbericht_-_Power_to_Gas_-_eine_Systemanalyse_-_2014.pdf consulted on the 10.09.2021
- Steubing, B., Zah, R., Waeger, P., & Ludwig, C. 2010. Bioenergy in Switzerland: Assessing the domestic sustainable biomass potential. *Renewable & Sustainable Energy Reviews*, 14(8), 2256-2265. doi: <https://doi.org/10.1016/j.rser.2010.03.036>

- Strimitzer, L., & Höher, M. 2020. Holzströme in Österreich (Wood streams in Austria). cited in https://www.klimaaktiv.at/erneuerbare/energieholz/holzstr_oesterr.html consulted on the 09.09.2021
- Swanson, R. M., Platon, A., Satrio, J. A., & Brown, R. C. 2010. Techno-economic analysis of biomass-to-liquids production based on gasification. *Fuel*, 89, S11-S19. doi: <https://doi.org/10.1016/j.fuel.2010.07.027>
- Thrän, D., Pfeiffer, D., Brosowski, A., Fischer, E., Herrmann, A., Majer, S., Oehmichen, K., Schmersahl, R., Schröder, T., & Stecher, K. 2013. *Methodenhandbuch Stoffstromorientierte Bilanzierung der Klimagaseffekte (Methods manual material flow-oriented balancing of greenhouse gas effects)*. cited in https://www.energetische-biomassenutzung.de/fileadmin/media/6_Publikationen/04_Methodenhandbuch_2013_final.pdf consulted on the 09.09.2021
- Thunman, H., Seemann, M., Vilches, T. B., Maric, J., Pallares, D., Strom, H., Berdes, G., Knutsson, P., Larsson, A., Breitholtz, C., & Santos, O. 2018. Advanced biofuel production via gasification - lessons learned from 200 man-years of research activity with Chalmers' research gasifier and the GoBiGas demonstration plant. *Energy Science & Engineering*, 6(1), 6-34. doi: <https://doi.org/10.1002/ese3.188>
- Tichler, R., & Zauner, A. 2018. Perspectives of the Gas Sector - GREENING THE GAS. *Renewable Energy Law and Policy Review*, 8(4), 42-48. doi: <https://doi.org/10.2307/26638285>
- TNO. (2021). Database for the physico-chemical composition of (treated) lignocellulosic biomass, micro- and macroalgae, various feedstocks for biogas production and biochar. cited in <https://phyllis.nl/> consulted on the 05.03.2021
- Universität Rostock, I. f. E. u. U. g., ; Bundesforschungsanstalt für Landwirtschaft, . 2007. Biogaserzeugung durch Trockenvergärung von organischen Rückständen, Nebenprodukten und Abfällen aus der Landwirtschaft (Biogas production via dry anaerobic digestion of organic residues, by-products and wastes from agriculture). cited in https://www.infothek-biomasse.ch/images/2007_FNR_Trockenvergaerung.pdf consulted on the 09.09.2021
- van Melle, T., Peters, D., Cherkasky, J., Wessels, R., Mir, G. R., & Hofsteenge, W. 2018. Gas for Climate: How gas can help to achieve the Paris Agreement target in an affordable way. cited in <https://gasforclimate2050.eu/> consulted on the 09.09.2021
- Vienna University of Technology. 2012. Biogas to biomethane. Technology review. cited in https://www.membran.at/downloads/2012_BioRegions_BiogasUpgradingTechnologyReview_ENGLISH.pdf consulted on the 09.09.2021
- Wang, S. L., Jena, U., & Das, K. C. 2018. Biomethane production potential of slaughterhouse waste in the United States. *Energy Conversion and Management*, 173, 143-157. doi: <https://doi.org/10.1016/j.enconman.2018.07.059>
- Xie, L., MacDonald, S. L., Auffhammer, M., Jaiswal, D., & Berck, P. 2019. Environment or food: Modeling future land use patterns of misanthus for bioenergy using fine scale data. *Ecological economics*, 161, 225-236. doi: <https://doi.org/10.1016/j.ecolecon.2019.03.013>

APPENDIX

TABLE A6: Substrate potential for the different Austrian states (Bundesanstalt für Agrarwirtschaft, 2016; Bundesministerium Nachhaltigkeit und Tourismus, 2019; FNR, 2013; Reisinger, 2012; Universität Rostock, 2007).

substrate potential [t/a]	Vienna	Lower Austria	Upper Austria	Styria	Salzburg	Tyrol	Carinthia	Burgenland	Vorarlberg	Austria
sewage sludge	71.000	44.500	37.000	21.200	13.200	17.200	12.500	8.800	10.800	236.200
bio waste from households	92.408	149.115	77.462	68.773	37.005	53.301	15.166	15.819	16.702	525.751
bush-, grass- and tree-cuts	11.550	134.904	162.670	44.161	22.398	51.193	13.528	22.679	13.469	476.552
straw	250	1.132.645	491.064	256.093	61.144	1.178	201.018	287.549	250	2.431.191
manure	728	1.854.860	2.548.075	1.581.797	344.251	382.069	546.984	100.962	142.270	7.501.996
waste from food production *	264.623	233.949	206.692	173.356	77.431	105.251	78.228	40.922	54.988	1.235.441
other biogenic wastes *	131.643	116.384	102.824	86.240	38.520	52.360	38.917	20.358	27.355	614.600
total	572.203	3.666.357	3.625.787	2.231.619	593.949	662.551	906.341	497.089	265.835	13.021.731

* cumulative value for Austria segmented according to the population share of the specific state

Extra contents
COLUMNS AND SPECIAL CONTENTS

Environmental Forensic

ANALYSIS OF MICROPLASTICS FOR ENVIRONMENTAL FORENSIC APPLICATIONS

Ashwini Suresh Kumar ¹, Alberto Pivato ², Claire Gwinnett ³ and George Varghese ¹

¹ NIT Calicut, Kozhikode, India

² University of Padova, Italy

³ Staffordshire University, United Kingdom

Introduction

The knowledge that microplastics (defined as plastics smaller than 5mm in size), a pollutant of emerging concern, can pose significant challenges to the ecosystem and human health due to its ubiquitous and persistent nature, calls for urgent measures for its control. Identifying the sources of pollutants and the extent of their contribution is one of the first steps in their management. However, the source apportionment is extremely challenging in microplastic pollution, due to diverse use of a single type of polymer, multiple manufacturing techniques, use of different additives in the same type of polymer by different industries, etc. (Kumar and Varghese 2021b). Use of robust environmental forensic techniques and protocols, both at the sampling and analysis stages can address this challenge to a great extent.

Gwinnett et. al (2021), in an earlier edition of this column had explained the different sampling methods adopted for microplastics with emphasis on the special considerations required when sampling is carried out for forensic purposes. Just as sampling for forensic purposes demands certain procedures to be followed, so does its subsequent analysis. Once the microplastic is sampled and brought to the laboratory, it goes through distinct phases of analysis, namely, drying of the samples (if the sample is wet), separating the microplastics from the matrix, classification, microscopic observations, polymer identification and interpretations regarding the sources. Brief explanations of these phases are given below for the analysis of microplastics from sand/sediment.

Drying of samples

When extracting microplastics from soil/sand/sediment samples, these matrices regularly have high moisture content and thus drying prior to microplastic separation is required. Drying is also required for preserving the samples for future analysis. Depending on how wet the sample is, the duration of drying can vary. For moderately wet beach sediment samples, 6 hrs drying at 60°C was found to be suitable (Kumar and Varghese 2021a). When

the purpose of the analysis is to know the abundance of microplastics or its impact on the ecosystem, keeping the physical properties of the microplastic intact may not be important. However, when the sampling is for forensic application, this is not the case. Heating at higher temperatures is found to disfigure and change the colour of microplastic, resulting in the loss of characteristics which are vital for forensic examination.

Separating microplastics from the sand matrix

There are different techniques followed for separation of microplastics, based on the objective and the type of environmental matrix (Figure 1). The most commonly used separation technique is density separation explained in the manual by NOAA (Masura et al., 2015). A major problem with this method is the possibility to leave out the denser plastics, and also those with biofilms present on the surface. Missing a particular type of microplastic from the chain of analyses can prove costly, especially when the analyses are for forensic applications. Sieving and separating the microplastics (Hidalgo-Ruz et al. 2012) is reported to be useful in overcoming this problem when the matrix is fine beach sediments and the microplastics targeted are more than 1 mm in size (Kumar and Varghese, 2021a). Although the method is cumbersome, involving manual sorting of microplastics, it was seen to give good results for forensic applications. If the focus of study is microplastics below 1mm in size which are difficult to be handpicked, density separation followed by filtration of the supernatant and observation under a microscope is a possible technique (Windsor et al. 2019; Urban-Malinga et al. 2020). Microplastics may be freshly formed from the fragmentation of accumulated macro plastics, rather than transported to the sampling location as microplastics. Therefore, plastics above 5mm, though not considered as microplastic, should be preserved after separating it out from the matrix as they could be of use in identifying the source if a matching part is retrieved from the samples (Ashwini and Varghese, 2020).



FIGURE 1: Microplastics separated out from Beypore beach, Kerala, India.

Classification

After separating the microplastics from the environmental matrix, it is classified under various morphological categories to draw useful conclusions regarding its source, fate and effects. A frequently used classification scheme classifies microplastics into fragments, film and fibre (Karbalaee et al. 2019). However, this scheme of classification does not differentiate the regular 3D shaped fragments from the irregular. Regular shapes for microplastics, like spherical, cylindrical, etc., are indicative of specific sources and cannot be missed when the purpose of analysis is source apportionment. Moreover, studies have also shown that there is a significant effect for the shape on the transport of microplastics in the environment (Jahnke et al., 2017; Harrison et al., 2018). Hence, there needs to be a classification scheme which distinguishes the regular shaped 3D microplastics from the irregular shaped ones. Another criteria for classification can be the colour. Classifying microplastics based on colour may lead to sources in some cases. Kumar and Varghese (2021a) were able to use colour among other characteristics to identify the source of the polyethylene fibres sampled from the Calicut beach as fishing nets.

Microscopic observations

Microscopical observations of microplastics may encompass the morphological and optical properties of the samples. Many microplastic studies limit their observations to colour, size and classification of the sample set as a whole rather than fully characterizing each microplastic as seen in forensic examinations (Gwinnett et al., 2021). Much can be learnt from forensic fibre analysis, where polymer fibres are examined for their colour, width, cross-sectional shape, presence of inclusions and optical properties such as its birefringence and sign of elongation (Robertson et al., 2018). The latter can also provide an initial polymer identification (Johri and Jatar, 1979). Gwinnett et al. (2021) have proposed a new workflow for the recovery and analysis of microplastics, particularly fibres for plastic pollution monitoring using forensic approaches. This new workflow

allows greater differentiation between samples and aids in source identification.

Observing degradation patterns of microplastics under an optical microscope can provide a basic idea on the resident time of microplastics in the environment (Kumar and Varghese, 2021a). Such observation will help in answering the questions if the microplastics are recently formed or are quite old. Sharp edges of a fragment indicate freshly formed microplastic when compared to a microplastic with blunt edges. Also, crack formation, loss of material from the surface, etc. are indications of longer residence time in the environment (Figure 2).

Polymer identification

One of the important steps in microplastic analysis is the identification of the polymer type. The most common polymer types noticed are polyethylene (PE), polypropylene (PP), polystyrene (PS), and polyethylene terephthalate (PET), the polymers of common commodity plastics used for packing, containers, carry bags, fishing nets, etc. Some plastics may have a combination of polymers like polyethylene and polypropylene. Fourier Transform Infrared Spectroscopy (FTIR) is the most widely used technique for polymer identification (Figure 3). Micro-Fourier transform infrared (μ FTIR) microscopy, which is also an FTIR technique, uses a microscope to analyse smaller samples, some set-ups also automatically detect and count the microplastics of different polymer types (Li et al., 2021). A particle finder software identifies particles which is followed by the generation of IR spectra of all the identified particles. This method is suitable for smaller microplastics that do not cover the diamond aperture of the FTIR with Attenuated Total Reflection (ATR) mode in the sample holder. Not covering the diamond aperture in the instrument results in obtaining an IR spectrum with high background noise. Once the spectrum of the polymer is obtained, polymer spectral libraries can be used to match and identify the polymer analyzed. Other popular methods for polymer identification include Raman spectroscopy (Frère et al, 2016) and pyrolysis-gas chromatography with and without mass spectrometry (Jung et al, 2021).

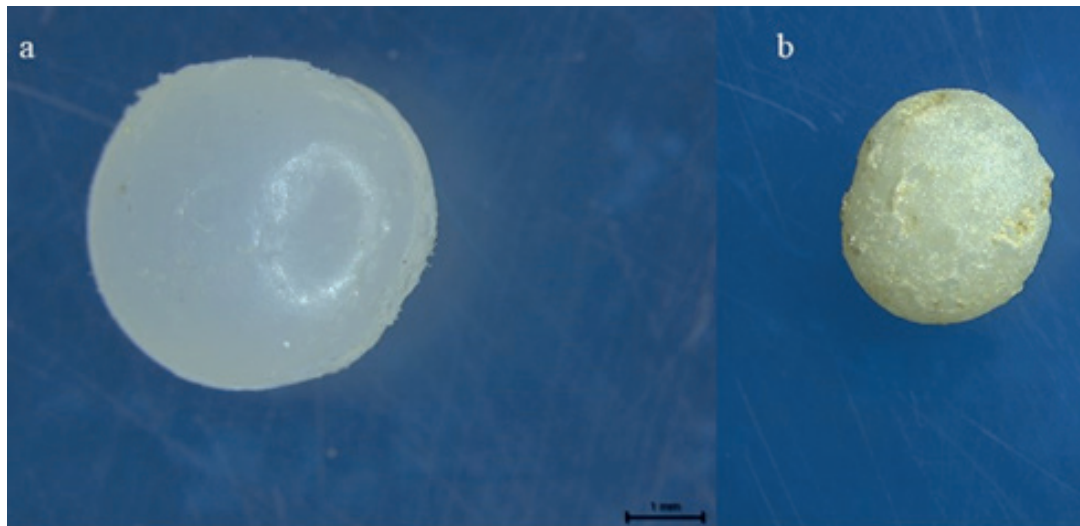


FIGURE 2: a) Low residence time plastic pellet, b) Higher residence time plastic pellet.

Procedural Contamination Prevention

It is standard practice in forensic examinations to include strict anti-contamination protocols when handling small particulates. This is also true for microplastic analysis although many studies still only report crude or limited procedures far less comprehensive than those that would be used in criminal investigations. The potential for contamination of samples is high though, therefore protocols which limit exposure of the sample to the air and sources of plastic should be incorporated in all of the

stages described above. Prata et al. (2021) describe the protocols that should be in place during the analysis stages of microplastic studies, these include; comprehensive washing of equipment before and between samples, controlled air flow in the laboratory and wearing of non-synthetic clothing during analysis. Protocols adapted from those used for the forensic examination of fibres, such as those developed by Woodall et al. (2015), are likely to be the most effective as they must stand up to the scrutiny of the courts.

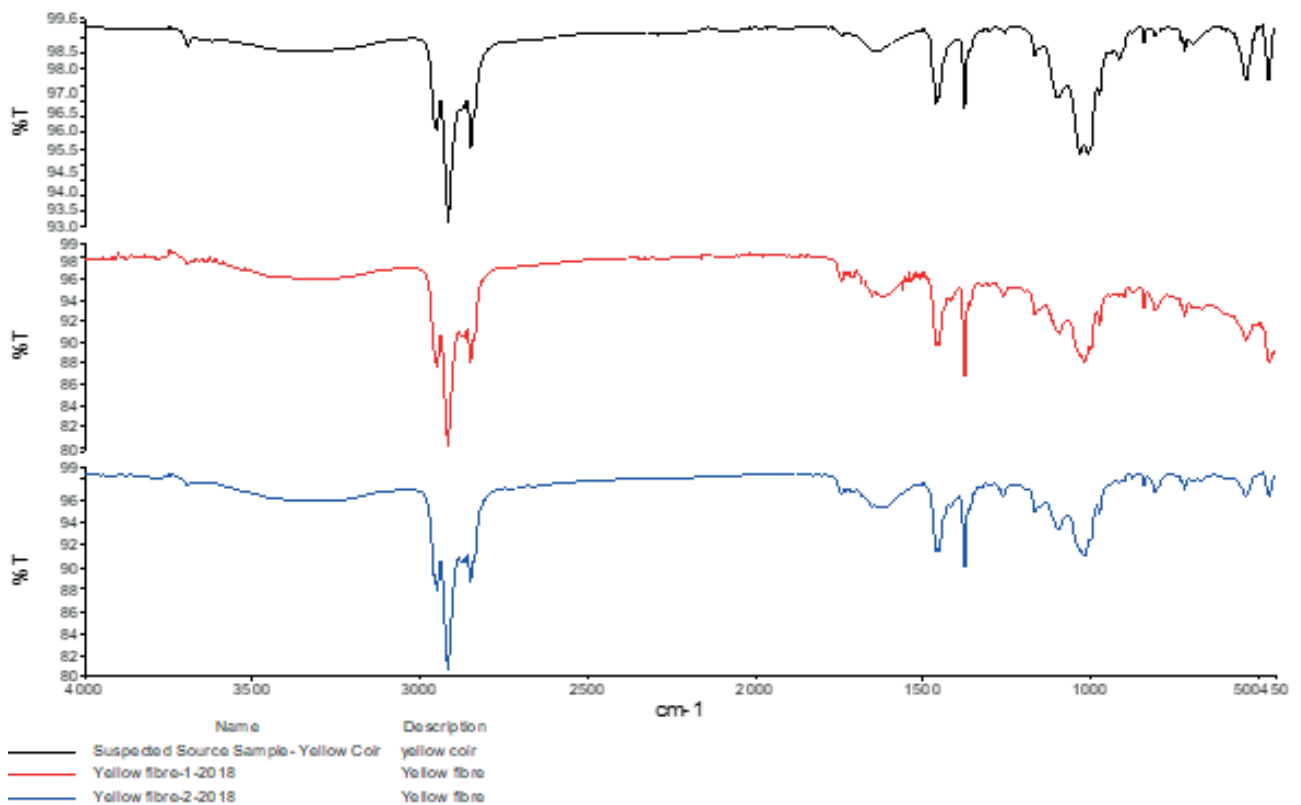


FIGURE 3: Example of FTIR spectra of suspected source and sample.

Interpreting source

This is the phase in forensic analysis, where the information generated in the previous phases are used to identify the possible sources and pathways of the microplastics sampled from the site. Along with analysis data, information collected during sampling such as geographical features, proximity of harbor, influence of river, type of beach activities, etc. (Lippiatt et al., 2013) are also used to identify the source. Kumar and Varghese (2020) have proposed a forensic framework for the source apportionment of microplastic in beach sediments that utilizes the information collected during the sampling and the data generated in the various stages of analyses. The framework was used to reach different levels of conclusion regarding the source of microplastics; in some cases it was possible to identify the exact source, whereas in other cases only the pathway through which the microplastic reached the marine environment could be identified.

Concluding Remarks

Environmental forensic investigations leading to the identification of the source of contamination requires robust protocols starting from the sampling stage to the analysis stage. Based on the information acquired during sampling and analyses, different degrees of confirmation about the source of microplastics are possible. Though the scientific literature is scarce on the analysis of microplastics for environmental forensic applications, the current understanding is that analyses for forensic applications demand special considerations such as those mentioned above. More studies are needed and the ultimate aim of such studies should be the development of a comprehensive forensic analysis protocol for microplastics.

REFERENCES

- Frère, L., Paul-Pont, I., Moreau, J., Soudant, P., Lambert, C., Huvet, A., Rinnert, E., 2016. A semi-automated Raman micro-spectroscopy method for morphological and chemical characterizations of microplastic litter, *Marine Pollution Bulletin*, 113 (1–2), pp. 461–468
- Gwinnett, C., Harrison, E., Osborne, A., Pivato, A. and Varghese, G., 2021. Environmental Forensic: Sampling microplastics for Environmental Forensic applications. *Detritus*, 14, pp. I–III.
- Gwinnett, C., Osborne, A.O., Jackson, A.R.W., 2021. The application of tape lifting for microplastic pollution monitoring, *Environmental Advances*, 5.
- Harrison, J.P., Hoellein, T.J., Sapp, M., Tagg, A.S., Ju-Nam, Y., Ojeda, J.J., 2018. Microplastic-associated biofilms: a comparison of freshwater and marine environments, *Handbook of Environmental Chemistry*. doi:https://doi.org/10.1007/978-3-319-61615-5_9
- Hidalgo-Ruz, Valeria, Lars Gutow, Richard C. Thompson, and Martin Thiel. 2012. "Microplastics in the Marine Environment: A Review of the Methods Used for Identification and Quantification." *Environmental Science & Technology* 46 (6): 3060–75. https://doi.org/10.1021/es2031505.
- Jahnke, A., Arp, H.P.H., Escher, B.I., Gewert, B., Gorokhova, E., Kühnel, D., Ogonowski, M., Potthoff, A., Rummel, C., Schmitt-Jansen, M., Toorman, E., MacLeod, M., 2017. Reducing uncertainty and confronting ignorance about the possible impacts of weathering plastic in the marine environment. *Environ. Sci. Technol. Lett.* 4, 85–90. https://doi.org/10.1021/acs.estlett.7b00008.
- Johri, M.C and Jatar, D.P., 1979, Identification of some Synthetic Fibres by their Birefringence, *Journal of Forensic Science*, 24 (3), pp. 692–697
- Masura, J., et al. 2015. Laboratory methods for the analysis of microplastics in the marine environment: recommendations for quantifying synthetic particles in waters and sediments. NOAA Technical Memorandum NOS-OR&R-48
- Jung, S., Cho, S-H., Kim, K-H., Kwon, E.E., 2021, Progress in quantitative analysis of microplastics in the environment: A review, *Chemical Engineering Journal*, 422.
- Karbalaei, Samaneh, Abolfazl Golieskardi, Hazilawati Binti Hamzah, Samiaa Abdulwahid, Parichehr Hanachi, Tony R. Walker, and Ali Karami. 2019. "Abundance and Characteristics of Microplastics in Commercial Marine Fish from Malaysia." *Marine Pollution Bulletin* 148 (July): 5–15. https://doi.org/10.1016/j.marpolbul.2019.07.072.
- Kumar, A.S., Varghese, G.K., 2021a. Microplastic Pollution of Calicut Beach - Contributing Factors and Possible Impacts. *Marine Pollution Bulletin* 169 (May): 112492. https://doi.org/10.1016/j.marpolbul.2021.112492.
- Kumar, A.S., Varghese, G.K., 2021b. "Source Apportionment of Marine Microplastics: First Step Towards Managing Microplastic Pollution." *Chemical Engineering and Technology* 44 (5): 906–12. https://doi.org/10.1002/ceat.202000482.
- Kumar, A.S., Varghese, G.K., 2020. Environmental Forensic Analysis of the Microplastic Pollution at 'Nattika' Beach, Kerala Coast, India. *Environmental Forensics* 21 (1): 21–36. https://doi.org/10.1080/15275922.2019.1693442.
- Li, Siyang, Yilin Wang, Lihong Liu, Houwei Lai, Xiancan Zeng, Jianyu Chen, Chang Liu, and Qijin Luo. 2021. "Temporal and Spatial Distribution of Microplastics in a Coastal Region of the Pearl River Estuary, China." *Water* 13 (12): 1618. https://doi.org/10.3390/w13121618.
- Lippiatt, Sherry, Sarah Opfer, and Courtney Arthur. 2013. "Marine Debris Monitoring and Assessment: Recommendations for Monitoring Debris Trends in the Marine Environment." NOAA Technical Memorandum NOS-OR&R-46. http://marinedebris.noaa.gov/sites/default/files/Lippiatt_et_al_2013.pdf.
- Prata, J.C., Reis, V., Da Costa, J.P., Mouneyrac, C., Duarte, A.C., Rocha-Santos, T. 2021. Contamination issues as a challenge in quality control and quality assurance in microplastics analytics, *Journal of Hazardous Materials*, 403.
- Robertson, J., Roux, C., Wiggins, K., 2018. *Forensic Examination of Fibres* (3rd edn.), CRC Press, Boca Raton.
- Urban-Malinga, Barbara, Mariusz Zalewski, Aneta Jakubowska, Tycjan Wodzinowski, Maja Malinga, Barbara Pałys, and Agnieszka Dąbrowska. 2020. "Microplastics on Sandy Beaches of the Southern Baltic Sea." *Marine Pollution Bulletin* 155 (April): 111170. https://doi.org/10.1016/j.marpolbul.2020.111170.
- Windsor, Fredric M., Isabelle Durance, Alice A. Horton, Richard C. Thompson, Charles R. Tyler, Steve J. Ormerod, Alethia Vazquez, et al. 2019. "Standardised Protocol for Monitoring Microplastics in Seawater." *Marine Pollution Bulletin* 90 (February): 96. https://doi.org/10.13140/RG.2.2.14181.45282.
- Woodall, L. C., Gwinnett, C., Packer, M. P., Thompson, R. C., Robinson, L. F. & Paterson, G. L. J. 2015. Using a forensic science approach to minimize environmental contamination and to identify microfibrils in marine sediments. *Marine Pollution Bulletin*. 95 (1). pp. 40–46.

DETRITUS & ART / A personal point of view on Environment and Art by Rainer Stegmann

Artists seldom provide an interpretation of their own work; they leave this to the observer. Each of us will have his/her own individual view of a specific piece of art, seeing different contents and experiencing a range of own feelings and emotions. Bearing this in mind, I created this page where you will find regularly selected masterpieces from different epochs and I express my thoughts on what the work conveys to me personally. My interpretation will refer specifically to the theme "Environment". Any comments or suggestions regarding this column should be addressed to stegmann@tuhh.de.



FABRICE MONTEIRO AND DOULSY JAH GAL / The Prophecy #1, 2013 (© VG Bild-Kunst, Bonn 2021).

Fabrice Monteiro was born in 1972 in Belgium and lives in Dakar, Senegal; he has a Benin father and a Belgium mother. Doulsy Jah Gal, is a young African stylist and fashion designer of Senegalese origin born in the 1980s and lives in Dakar.

"We live in this hyper-consumerist system where profit comes first, and the links to our origins and the ancestral source of life is slowly being dissipated. While making this work, I tried to rebuild and strengthen that link" – Fabrice Monteiro.

This quote says a lot about the artist and helps understanding his art work. He also notes that the indigenous people he met in Australia and Texas *"are the ones who are truly grounded and respectful of nature."* He hopes that his work connects art with culture and politics and *"a sense of awareness and collective ethical concern will be ignited"*.

When I first this photo I was quite excited, this photo cast a spell over me, it got my immediate attention. There is a magic in this picture.

We often talk at conferences about the disastrous situation of open dumps in Africa with people on site searching for goods, that can be sold. Scavengers are exposed to dust, toxic gases and fumes, and come in contact with

hazardous waste, syringes, broken glass etc. In addition, unwritten hierarchies among the scavengers on the dump often cause conflicts. Since decades the problematic of open dumps and scavengers is well known but not much has happened.

Complete remediation of dumps is technically demanding and costly. As immediate actions the main emissions gas and leachate should be captured and treated. Scavengers should not be any longer present in the unhealthy atmosphere of the waste dump, and should work on a controlled site to recover reusable materials from the incoming waste before it is dumped. By these means they may still make their living from recovered materials but in a healthier more organized way. But I get lost in details.

Now coming back to the photo or better to the photo installation of the two artists: the oversized magic and mystical woman beautifully dressed in colorful plastic waste pieces on a dump. The dress merges with the plastic on the surface of the dump and shows the beauty and value of the discarded plastic as a symbol for other dumped reusable waste components. The woman seems to "grow" out of the dump, as being a part of it, bringing displaced plastic to the surface. It shows the beauty and the ugly; on one side the abundance of plastic production but also – looking at the mystical woman – the potential for plastic recovery. The woman moves upright and self-confident to the edge of the dump ...



In the background we see fumes from fires inside the dump that escape into the sky, the landscape is getting dark while the sun goes down. By these means the bright colors of the mystic dump scene become even brighter. As Fabrice Monteiro indicated the African culture plays an important role in this photo installation e.g., looking at the hair arrangement of the woman. We should highlight Doulsy (Jah Gal) who took care of this phantastic fashion arrangements designed from discarded plastic.

So let your mood sink in, internalize the clear message, but also enjoy the atmosphere, the special beauty and the spirit that emanates from this picture.

The next art work I will present is "The Bride of Beirut" which was created by sculptor, Engineer Hani Tabsharani, in Gemmayzeh, Lebanon. This statue is made from rubble and broken glass as left overs from the August 4 2020 explosion in the harbor of Beirut.



HANI TABSHARANI / The Bride of Beirut (2020).

CONTENTS

Editorial

- A NEW DISCIPLINE: WASTE PREVENTION MANAGEMENT
R. Stegmann 1

Waste characterization

- WASTE HAZARD PROPERTIES HP 4 'IRRITANT' AND HP 8
'CORROSIVE' BY PH, ACID/BASE BUFFER CAPACITY AND
ACID/BASE CONCENTRATION
P. Hennebert 5

- THE SUBSTITUTION OF REGULATED BROMINATED FLAME
RETARDANTS IN PLASTIC PRODUCTS AND WASTE AND THE
DECLARED PROPERTIES OF THE SUBSTITUTES IN REACH
P. Hennebert 16

Circular Economy

- IMPLEMENTATION STAGE FOR CIRCULAR ECONOMY IN THE
DANISH BUILDING AND CONSTRUCTION SECTOR
L.M. Ottosen, L.B. Jensen, T.F. Astrup, T.C. McAloone,
M. Ryberg, C. Thuesen, S. Lütken, S. Christiansen,
A.J. Damø and M.H. Odgaard 26

- EFFICIENT AND SAFE SUBSTRATES FOR BLACK SOLDIER FLY
BIOWASTE TREATMENT ALONG CIRCULAR ECONOMY PRIN-
CIPLES
M. Gold, D. Ileri, C. Zurbrügg, T. Fowles and
A. Mathys 31

Recycling of PV panels

- INNOVATIVE RECYCLING OF END OF LIFE SILICON PV
PANELS: RESIELP
P. Cerchier, K. Brunelli, L. Pezzato, C. Audoin, J. Patrice
Rakotoniaina, T. Sessa, M. Tammara, G. Sabia,
A. Attanasio, C. Forte, A. Nisi, H. Suitner and
M. Dabalà 41

- PHOTOVOLTAIC MODULE RECYCLING: THERMAL TREAT-
MENT TO DEGRADE POLYMERS AND CONCENTRATE VAL-
UABLE METALS
P.S. Silveira Camargo, A. da Silva Domingues, J.P. Guê
Palomero, A.C. Kasper, P. Ribeiro Dias and
H. Marcelo Veit 48

Thermal Treatment

- WOOD GASIFICATION. INFLUENCE OF PROCESS PARAME-
TERS ON THE TAR FORMATION AND GAS CLEANING
M. Dudyński 63

- ANTIMONY AND VANADIUM IN INCINERATION BOTTOM ASH
–LEACHING BEHAVIOR AND CONCLUSIONS FOR TREATMENT
PROCESSES
F.-G. Simon, C. Vogel and U. Kalbe 75

Sludge management

- PHOSPHATE SLUDGE: OPPORTUNITIES FOR USE AS A FER-
TILIZER IN DEFICIENT SOILS
A. Haouas, C. El Modafar, A. Douira, S. Ibnsouda-Koraichi,
A. Filali-Maltouf, A. Moukhli and S. Amir 82

- LIFE CYCLE ASSESSMENT OF SEWAGE SLUDGE PYROLY-
SIS: ENVIRONMENTAL IMPACTS OF BIOCHAR AS CARBON
SEQUESTRATOR AND NUTRIENT RECYCLER
F. Gievers, A. Loewen and M. Nelles 94

Renewable energy

- POTENTIALS AND COSTS OF VARIOUS RENEWABLE GAS-
ES: A CASE STUDY FOR THE AUSTRIAN ENERGY SYSTEM
BY 2050
D.C. Rosenfeld, J. Lindorfer, H. Böhm, A. Zauner and
K. Fazeni-Fraisl 106

Columns

- ENVIRONMENTAL FORENSIC
Analysis of Microplastics for Environmental Forensic
Applications I

- DETRITUS & ART / A personal point of view on Environment
and Art
Fabrice Monteiro and Doulsy Jah Gal / The Prophecy #1,
2013 (© VG Bild-Kunst, Bonn 2021) V